MATHEMATICAL MODELING OF ATMOSPHERIC AEROSOL EQUILIBRIA AND DYNAMICS

Thesis by

Mark Elliott Bassett

In Partial Fulfullment of the Requirements

for the Degree of

Doctor of Philosophy

California Institute of Technology

Pasadena, California

1984

(Submitted September 28, 1983)

ACKNOWLEDGEMENT

Looking back on my time at Cal Tech, I am struck by the number of people who have helped me grow during the past few years. While is is impossible to mention everyone, I would like to mention some of those who have been the most notable.

First, I would like to thank Dr. John Seinfeld, my advisor for his guidance in my research. Helpful contributions were also made by Dr. Richard Flagan and Dr. Glen Cass. Dr. Herb Keller provided useful insights on the homotopy method used in this work.

In addition to the faculty, many co-workers provided help, especially Art Stelson, Fred Gelbard and Jim Crump.

A special note of appreciation is due to Lenore Kerner who typed the manuscript.

I am grateful for financial support provided by the U. S. Environmental Protection Agency and the Environmental Quality Laboratory of the California Institute of Technology.

I would like to thank those who provided encouragement when things got tough. Particular thanks go to Dan Hanle, Russell Sharer, Roger Jensen, Dean Hardi, Don Schroeder and Tim Sisemore. We had many memorable adventures together. In addition, thanks to my roommates Bill Kath, John Torczynski and Mike Templeton for many interesting discussions.

Finally, I would like to thank my family, especially my parents, for their constant love and encouragement.

ABSTRACT

Atmospheric aerosols consist of submicron-sized particles occurring at number concentrations of the order of 10^5 cm^{-3} and mass concentrations of the order of 100 μg m^{-3}. These aerosols, when occurring in urban areas, consist of aqueous solutions of sulfate, nitrate, ammonium, organic constituents, and certain metals. This thesis is a contribution toward our ability to describe mathematically the formation and growth of such atmospheric aerosols. Since a substantial fraction of the mass of urban aerosols consists of sulfate, nitrate, ammonium and water (Stelson and Seinfeld, 1981), the description of the dynamics of such an aerosol is an important place to initiate the development of aerosol models. The size and composition distribution of atmospheric aerosols are governed by a combination of thermodynamics and kinetics. A detailed treatment of the thermodynamics of the atmospheric sulfate/nitrate/ammonium/water system is presented. Based on this treatment, models are developed to predict the equilibrium quantity, composition, state, and size of the aerosol given gas phase properties. Aerosol kinetics are approached by solution of the General Dynamic Equation for the aerosol sized distribution using the sectional method of Gelbard and Seinfeld. In the most general kinetic model presented, the evolution of the size and composition of an atmospheric sulfate aerosol is predicted under power plant plume conditions. Users manuals for the computer codes comprising the models developed here are given in the Appendix.

TABLE OF CONTENTS

CHAPTER 1

INTRODUCTION

Introduction

1 Background

Several mathematical models have been developed to describe aerosol dynamics and chemistry based on a theoretical description of the governing processes. These models are summarized in Table 1. They may be grouped in four main categories:

(1) Models that describe the evolution of the aerosols size distribution by coagulation and condensation of one or more gaseous species

(2) Models that describe aerosol growth by condensation of one or more gaseous species

(3) Models that describe the evolution of the aerosols size and chemical composition by coagulation and condensation of one or more gaseous species and by aerosol-phase chemical reaction.

(4) Models that describe the thermodynamic equilibrium of the aerosol with the surrounding gas phase.

Models that describe aerosol dyanmics are based in one form or another on the solution of the General Dynamic Equation (GDE) that includes coagulation, condensation, and nucleation for a continuous size distribution. For the aerosol number distribution, n(v,t) the GDE is expressed as follows

$$\frac{\partial n(v,t)}{\partial t} = -\frac{\partial}{\partial v}\left(n(v,t)\,\frac{dv}{dt} \right) + \frac{1}{2}\int_0^v \beta(v-\tilde{v},\tilde{v})n(v-\tilde{v},t)n(\tilde{v},t)\,d\tilde{v}$$

$$- \int_0^\infty \beta(v,\tilde{v})n(v,t)n(\tilde{v},t)\,d\tilde{v} + J(v_0)$$

where v is the aerosol volume or mass, t the time, β the coagulation coefficient and J the nucleation rate. The first term on the right hand side represents condensation, the second and third terms represent coagulation, and the last term represents nucleation.

Table 1

Summary of some recently developed aerosol models

Model	Size Distribution	Coagulation	Condensation/Evaporation	New Particle Formation	Aerosol Chemistry and Thermodynamics
Middleton and Brock (1976); Middleton and Kiang (1978)	Continuous representation	Evaluation of integrals	Growth law from H_2SO_4 and H_2O concentrations	Classical nucleation theory	None
Gelbard and Seinfeld (1978,1979)	Continuous representation with discrete representation of molecular clusters	Evaluation of integrals	Growth law from H_2SO_4 and H_2O concentrations	Monomer balance theory	None
Tsang and Brock (1982a, 1982b); Brock (1983)	Continuous representation	Evaluation of integrals	Growth law from gas-phase concentration	Monomer balance theory	None
Gelbard, Tambour and Seinfeld (1980) ; Gelbard and Seinfeld (1980) Bassett, Gelbard and Seinfeld (1981)	Continuous representation	Inter- and intra-sectional coagulation	Growth law from H_2SO_4 concentration and aerosol/gas-phase equilibrium	None	Aqueous chemistry (sulfate) Bassett, Gelbard and Seinfeld (1981)
Seigneur (1982)	Sectional representation	Inter and intra-sectional coagulation	Growth law from H_2SO_4 $(NH_4)_2SO_4$ and NH_4NO_3 condensation	Parameterized monomer balance theory	None
Whitby (1978)	Trimodal representation	Parameterized	Parameterized	Parameterized	None
Eltgroth and Hobbs (1979)	Trimodal log-normal representation	Inter- and intra-modal coagulation	Growth law from H_2SO_4 concentration	Monomer balance theory	None

Table 1 (continued)

Model	Size Distribution	Coagulation	Condensation/Evaporation	New Particle Formation	Aerosol Chemistry and Thermodynamics
Orel and Seinfeld (1977); Peterson and Seinfeld (1979, 1980)	Normalized size distribution	None	Growth law from H_2SO_4 concentration and aerosol/gas-phase equilibrium	None	Aqueous phase (sulfate, nitrate)
Middleton, Kiang and Mohnen (1980)	Sectional representation	None	Growth law from H_2SO_4 concentration and aerosol/gas-phase equilibrium	None	Aqueous phase (sulfate)
Saxena, Seigneur and Peterson (1983)	None	None	Growth law from H_2SO_4 concentration and aerosol/gas-phase equilibrium	None	Aqueous phase chemistry, simple treatment of gas/aqueous/solid phase equilibrium (sulfate, nitrate)
Bassett and Seinfeld (1983)	None	None	No dynamic treatment	None	Detailed treatment of gas/aqueous/solid phase equilibrium

Let us now summarize the methods in Table 1 in terms of the categories given above.

(1) Models that describe the evolution of the aerosol size distribution by coagulation and condensation of one or more gaseous species.

Models that describe the evolution of the aerosol size distribution by coagulation and condensation are based on the solution of the GDE given above. The solution of the GDE is difficult because both n and v vary over several orders of magnitude. The numerical solution approaches have generally followed one of two techniques, one based on the use of spline or collocation methods, e.g.

Middleton and Brock (1976)

Gelbard and Seinfeld (1978, 1979)

Middleton and Kiang (1979)

Suck and Brock (1979)

Tsang and Brock (1982a,b)

and the other based on dividing the size regime into sections, e.g.,

Gelbard, Tambour and Seinfeld (1980)

Gelbard and Seinfeld (1980)

Seigneur (1982)

These two approaches have common roots. In fact, the sectional approach can be viewed as simply the first level of approximation in a hierarchy of methods, such as splines or orthogonal collocation on finite elements. The above models work well for coagulation processes, based on a comparison of the numerical solutions with exact solutions. However, condensation, which is represented by the first term on the right hand side of the GDE, leads to numerical difficulties. This is a result of the

first-order nature of the term, which is identical to the advection term in transport-diffusion models. Brock (1982) has suggested the use of recently developed finite-element techniques to minimize the numerical diffusion that results from this term.

In a regional air quality simulation, the models summarized above would have to be used at every grid point. As a result, the time required to run such a model may become prohibitive. In an effort to avoid this difficulty, Whitby (1981, 1983) proposed a three-mode parameterization of the coagulation, condensation and nucleation processes. Thus, Whitby's model provides an approximate solution to the evolution of the aerosol size distribution which requires less computer time to run.

(2) Models that describe aerosol growth by the condensation of one or more gaseous species.

The second group of models neglects coagulation. Thus, they are based, in essence, on solving

$$\frac{\partial n(v)}{\partial t} = - \frac{\partial}{\partial v} n(v) \frac{dv}{dt} + J(v_o)$$

where growth, dv/dt, may occur by condensation of one or more species. Most of the models developed have focused on sulfate and nitrate aerosols. These include:

Orel and Seinfeld (1977)

Peterson and Seinfeld (1979, 1980)

Middleton, Kiang, and Mohnen (1980)

Brock (1982)

Saxena, Seigneur, and Peterson (1983)

Each of these models included aqueous-phase chemistry and thermodynamic equilibrium in addition to growth by condensation of gaseous species.

When coagulation can be neglected, a considerable simplification results. This is because the presence of coagulation imposes limitations on the method to be used. For example, in the sectional approach, there is the geometric constraint which limits the number of sections that can be used. When coagulation can be neglected, these problems will not arise. Then, in general, there will be no major difficulties in simulating gas-to-particle conversion and aerosol-phase chemical reactions in a multi-component system.

(3) Models that describe the evolution of the aerosol size and chemical composition by coagulation and condensation of one or more gaseous species and by aerosol-phase chemical reaction.

The only model that combines size distribution evolution by coagulation and condensation with aerosol-phase chemical reaction is that of Bassett, Gelbard and Seinfeld (1981) which is Chapter 6 of this thesis. The model was developed specifically to simulate plume aerosols, where both coagulation and aerosol-phase chemistry might be expected to be of importance. The model is based on the sectional approach to solving the GDE. It also includes some simple aerosol thermodynamics. This model demonstrates the way in which type (1) and (4) models can be combined to produce a complete model of an aerosol. However, further work is required, especially in the incorporation of more sophisticated thermodynamics.

(4) Models that describe the thermodynamic equilibrium of the aerosol with the surrounding gas phase.

It has become apparent that thermodynamic equilibrium plays a key role in determining the quantity and composition of atmospheric aerosols (Stelson, Friedlander, and Seinfeld, 1979; Stelson and Seinfeld, 1982a,b,c). The models in category (1) assume that condensation is essentially irreversible. That is, no account is taken of equilibrium processes. However, the concentration of water, a major component in many aerosols, is determined by equilibrium. Thus, it is clear that proper prediction of particle size for these aerosols requires that equilibrium be taken into account. Models in categories (2) and (3) have attempted to do this by continually adjusting the particle size so that equilibrium is maintained.

In Chapter 3 we present a model that predicts the quantity, composition and physical state (liquid or solid) of a sulfate/nitrate/ammonium/water aerosol at equilibrium given the total concentrations, present, and the temperature and relative humidity. Thus, this model provides information that is fundamentally different from models directed towards describing the evolving size distributions. This model can then be incorporated into those of classes (1) and (2) to provide a complete description of aerosol behavior.

2 Overview of this Work

The models discussed in the previous section may be broken down into two broad areas, thermodynamic models and kinetic models. This work contains contributions to both of these areas.

Chapters 2, 3 and 4 discuss the development of a detailed thermodynamic model for the atmospheric sulfate/nitrate/ammonium/water system. The first step in this development is the determination of correlations for the chemical potentials of the various species involved. Chemical potentials for several of these species had been available previously (Stelson and Seinfeld 1982a,b,c). In Chapter 2, correlations are developed for the remaining species. In addition, the results obtained using these correlations are checked against experimental data.

The next step in the model development is the construction of a computer program to calculate the equilibrium of the system. The construction of such a code is detailed in Chapter 3. The code developed here uses the expressions for the chemical potential developed previously. It accepts as inputs the total concentrations of the various components, as well as the temperature and relative humidity. Using these, the program then calculates the total amount of aerosol present, its composition, and physical state (solid or liquid).

In the course of developing a temperature-dependent model, it was necessary to develop correlations for the dependence of the chemical potentials on temperature. These are presented in an appendix.

Chapter 4 describes the development of a generalized code to handle the case where the effect of particle curvature on vapor pressure, the so-called Kelvin effect, is important. Using this code, it is possible to

explain quantitatively for the first time the observation that nitrate tends to be found in larger particles than sulfate (Appel et al., 1978).

The next two chapters, Chapters 5 and 6 describe a study of aerosol kinetics. Chapter 5 deals with growth by gas-to-particle, condensation or intra-particle chemical reaction, when coagulation is negligible. Thus, for this case, the GDE becomes

$$\frac{\partial n(v,t)}{\partial t} = - \frac{\partial}{\partial v} \left(n(v,t) \frac{dv}{dt} \right)$$

Thus, in this case, the GDE is linear, so that the method of characteristics may be used to solve it. As a result of this study, it is shown that one can use the evolution of an aerosol distribution to infer the mechanism of sulfate production.

Chapter 6 describes a model for the evolution of an aerosol size and chemical composition by coagulation and condensation of one or more gaseous species and by aerosol-phase chemical reaction. Thus, it fits into category (3) of Section 1. This model uses the sectional method. In addition, it also includes a simplified thermodynamic calculation. Future work would involve inclusion of more sophisticated thermodynamic data into such a model.

During the course of this study, two large computer codes were developed to predict the thermodynamics of the atmospheric sulfate/nitrate/ammonium/water system. Users manuals for these codes are presented in Appendices A and B. These manuals are for the codes described in Chapters 3 and 4, respectively.

REFERENCES

Bassett M., Gelbard F. and Seinfeld J.H. (1981) Mathematical model for multicomponent aerosol formation and growth in plumes. Atmospheric Environment 15, 2395-2406.

Bassett M. and Seinfeld J.H. (1983) Atmospheric equilibrium model of sulfate and nitrate aerosols. Atmospheric Environment 17, XXX-XXX.

Brock J. R. (1983) Simulation of aerosol dynamics in Theory of Dispersed Multiphase Flow (Edited by R. E. Meyer) Academic Press, New York.

Eltgroth M. W. and Hobbs P. V. (1979) Evolution of particles in the plume of coal-fired power plants - II. A numerical model and comparisons with field measurements. Atmospheric Environment 13, 953-976.

Gelbard F. and Seinfeld J. H. (1978) Numerical solution of the dynamic equation for particulate systems J. Comput. Phys. 28, 357-375.

Gelbard F. and Seinfeld J. H. (1979) Exact solution of the general dynamic equation for aerosol growth by condensation. J. Colloid Interface Sci. 68, 173-183.

Gelbard F. and Seinfeld J. H. (1980) Simulation of multicomponent aerosol dynamics. J. Colloid Interface Sci. 78, 485-501.

Gelbard F., Tambour Y. and Seinfeld J. H. (1980) Sectional representation for simulating aerosol dynamics. J. Colloid Interface Sci. 76, 541-556.

Middleton P. and Brock J. (1976) Simulation of aerosol kinetics. J. Colloid Interface Sci. 54, 249-264.

Middleton P., Kiang C. S. and Mohnen V. A. (1980) Theoretical estimate of the relative importance of various sulfate aerosol production mechanisms. Atmospheric Environment 14, 463-472.

Middleton P. and Kiang C. S. (1978) A kinetic aerosol model for the formation and growth of secondary sulfuric acid particles. J. Aerosol Sci. 9, 359-385.

Orel A. E. and Seinfeld J. H. (1977) Nitrate formation in atmospheric aerosols. Environ. Sci. Technol. 11, 1000-1007.

Peterson T. W. and Seinfeld J. H. (1979) Calculation of sulfate and nitrate levels in a growing, reacting aerosol. AIChE J. 25, 831-838.

Peterson T. W. and Seinfeld J. H. (1980) Heterogeneous condensation and chemical reaction in droplets- application to the heterogeneous atmospheric oxidation of SO2 in Advances in Environmental Science and Technology Vol. 10 (Edited by J. N. Pitts and R. L. Metcalf) Wiley-Interscience New York.

Saxena P., Seigneur C. and Peterson T. W. (1983) Modeling of multiphase atmospheric aerosols. Atmospheric Environment 17, 1315-1329.

Seigneur C. (1982) A model of sulfate aerosols in atmospheric plumes. Atmospheric Environment 16, 2207-2228.

Stelson A. W. and Seinfeld J. H. (1981) Chemical mass accounting of urban aerosol. Environ. Sci. Technol. 15, 671-679.

Stelson A. W. and Seinfeld J. H. (1982a) Relative humidity and temperature dependence of the ammonium nitrate dissociation constant. Atmospheric Environment 16, 983-992.

Stelson A. W. and Seinfeld J. H. (1982b) Relative humidity and pH dependence of the vapor pressure of ammonium nitrate-nitric acid solutions at 25°C. Atmospheric Environment 16, 993-1000.

Stelson A. W. and Seinfeld J. H. (1982c) Thermodynamic prediction of the water activity, NH_4NO_3 dissociation constant, density and refractive index for the NH_4NO_3-$(NH_4)_2SO_4$-H_2O system at 25°C Atmospheric Environment 16, 2507-2514.

Stelson A. W., Friedlander S. K. and Seinfeld J. H. (1979) A note on the equilibrium relationship between ammonia and nitric acid and particulate ammonium nitrate. Atmospheric Environment 13, 369-371.

Suck S. H. and Brock J. R. (1979) Evolution of atmospheric aerosol particle size distributions via Brownian coagulation: numerical simulation. J. Aerosol Sci. 10, 581-590.

Tsang T. H. and Brock J. R. (1982a) Effect of coagulation on extinction in an aerosol plume propigating in the atmosphere. Applied Optics 21, 1588-1592.

Tsang T. H. and Brock J. R. (1982b) Aerosol coagulation in the plume from a cross-wind line source. Atmospheric Environment 16, 2229-2235.

Whitby K. T. (1978) The physical characteristics of sulfur aerosols. Atmospheric Environment 12, 135-159.

CHAPTER 2

THERMODYNAMIC EQUILIBRIUM PROPERTIES OF AQUEOUS SOLUTIONS OF NITRATE, SULFATE AND AMMONIUM

to appear in

"Chemistry of Particles, Fogs and Rain"

J. L. Durham, Editor
Ann Arbor Science Publishers

THERMODYNAMIC EQUILIBRIUM PROPERTIES OF AQUEOUS SOLUTIONS OF NITRATE, SULFATE AND AMMONIUM

Arthur W. Stelson,* Mark E. Bassett, and John H. Seinfeld
Department of Chemical Engineering
California Institute of Technology
Pasadena, California 91125

for publication in

"Chemistry of Particles, Fogs and Rain"

J. L. Durham, Editor
Ann Arbor Science Publishers

Expected 1983

*Current address: Exxon Research and Engineering Co.
Box 101
Florham Park, N.J. 07932

INTRODUCTION

Knowledge of the thermodynamic equilibrium properties of aqueous solutions is required in virtually any calculation associated with particle and droplet acidification. For example, prediction of the equilibrium vapor pressures of dissolved solutes and water is necessary when predicting the rate of uptake of pollutant gases into cloud and rain drops and aerosol particles. In addition, evidence indicates that atmospheric aerosols and small droplets are frequently in chemical equilibrium with the local surrounding air. In such a situation, given the ambient gaseous concentrations of pollutant species, and the temperature and relative humidity, it is desired to determine the physical state (liquid or solid) and the chemical composition of the particle or drop in equilibrium with the air.

To motivate the material to be presented in this chapter, consider for a moment predicting the rate of uptake of a species i into an atmospheric particle of radius r. The rate of change of the mass of species i in a particle or droplet due to transfer of that species to or from the vapor phase can be expressed as

$$\frac{dm_i}{dt} = f_i(r)(p_{i_\infty} - p_{i_s})$$

where p_{i_∞} and p_{i_s} are the partial pressures of species i far from the particle and just above the particle surface, respectively, and $f_i(r)$ is a function of particle size that depends on the mechanism of transport of i from the bulk gas to the particle surface (e.g. molecular or turbulent diffusion depending on the particle size).

The partial pressure of component i in equilibrium with a particle of radius r is given by

$$p_{i_s} = p^{\circ}_{i_s} \exp\left(\frac{2\sigma \bar{V}_i}{rRT}\right)$$

where $p^{\circ}_{i_s}$ is the partial pressure of species i over a solution having a flat surface and having the composition of the particle. For particles of radius larger than about 1 μm, the Kelvin correction for curvature effects on vapor pressure is negligible and $p_{i_s} = p^{\circ}_{i_s}$.

The vapor pressure $p^{\circ}_{i_s}$ depends on the composition of the solution, m_1, $m_2, \ldots, m_n$. Therefore, to calculate the rate of uptake of each of n dissolving species it is necessary to know how the equilibrium vapor pressure of each species depends on the composition of the mixture.

We noted above that atmospheric particles and drops are frequently in chemical equilibrium with the surrounding air. In connection with this statement, let us estimate the characteristic time τ for approach to equilibrium of a particle of radius 1 μm. If the particle consists of a single component, then the characteristic time for growth of a particle of such size is

$$\tau = \frac{\rho r^2 RT}{3DM(p_{i_\infty} - p_{i_s})}$$

Let us take the particle density $\rho = 1$ g cm^{-3}, the diffusivity of the transferring species, $D = 0.14$ cm^2 sec^{-1}, the value for SO_2 in air at room temperature, $M = 98$, the molecular weight of sulfuric acid, and $p_{i_\infty} - p_{i_s} = 1$ ppm. Based on these values, $\tau = 6$ sec. The time scale over which other phenomena influencing the particle, such as transport or chemical reaction, occur will generally be on the order of minutes or hours. Thus, most small particles may be assumed to be at equilibrium with the local ambient air. This assumption will hold regardless of the presence of chemical reactions in the gas phase or in the particle.

For a particle or droplet at equilibrium with its surroundings,

$$p_{i_\infty} = p_{i_s}(m_1, m_2, \ldots, m_n)$$

$$i = 1,2,\ldots, n$$

and the particle composition, indicated here by the n masses, $m_1, m_2, \ldots, m_n$, must obey these n relations. Generally, p_{i_∞} will be known either from measurements or gas-phase model predictions. Thus, the equilibrium condition may be viewed as n simultaneous algebraic equations for the n compositions. In virtually all atmospheric situations the component that contributes most to the total particle mass is water. Consequently, determination of the amount of water associated with a particle is a critical part of calculating its equilibrium composition (and size). Another important inference from the equilibrium conditions is the physical state of the particle. For example, ammonium nitrate exists as a solid at low relative humidities and as an aqueous solution at high relative humidities. In fact, in a multicomponent system some components may exist in solution whereas others may be in solid form at a given relative humidity.

In short, the ability to calculate the equilibrium properties of mixtures characteristic of atmospheric particles and droplets is essential to predicting rates of growth (and acidification). Unfortunately, the calculation of equilibrium properties is frequently not straightforward because the solutions typical of atmospheric particles and droplets often lie in the concentration range where solutions are strongly nonideal. For example, Stelson and Seinfeld[1] have shown that Los Angeles aerosols consist of concentrated solutions in the range 8 to 26 molar.

This chapter summarizes the results of a comprehensive effort aimed at providing a basis for determining the equilibrium properties of atmospheric droplets and aerosols. We begin the chapter with a concise review of nonideal solution theory.

Four principal components of atmospheric particles and drops are sulfates, nitrates, ammonia and water. The relative amounts of these species will, of course, vary, however valuable insight into the equilibrium behavior of such solutions can be gained by considering three idealized cases. This chapter will focus on the following three cases.

The first case is one in which the solution consists of nitric acid, ammonium nitrate and water. The presence of ammonium nitrate in atmospheric aerosols has been confirmed by a number of investigators. Doyle et al.[2] and Stelson et al.[3] have inferred the existence of an equilibrium between ammonium nitrate precursors, ammonia and nitric acid, and solid particulate ammonium nitrate. Using the ambient ammonia and nitric acid data of Spicer[4] at West Covina, CA, Stelson et al.[3] showed that the measured and predicted concentration products, $[NH_3][HNO_3]$, were in essential agreement. Doyle et al.[2] demonstrated the same phenomenon at Riverside, CA based on FT-IR ammonia and nitric acid measurements. Thus, the case of an ammonium nitrate, nitric acid, water system is one with practical importance in its own right as well as serving as an approximation for the situation when nitrates dominate sulfates.

Case two is that in which there is an abundance of ammonium and where the ammonium ion can be assumed to be the only cation present. The solution is treated as containing only ammonium sulfate, ammonium nitrate, and water. This system is of great practical interest, since, for typical urban situations, the ammonium concentration is often greater than that of unneutralized protons.

The final case is one devoid of nitrate, namely containing ammonium sulfate, sulfuric acid and water. This situation is of interest in power plant and smelter plumes where sulfates dominate nitrates.

REVIEW OF NONIDEAL SOLUTION THERMODYNAMICS

Consider the chemical equilibrium in a closed system at constant temperature T and pressure p. The condition for equilibrium is that the total Gibbs free energy of the system G is a minimum. That is, dG must be non-negative for any possible change in the system,

$$0 \leq dG = -SdT + Vdp + \sum_i \mu_i dn_i \tag{1}$$

where $\mu_i = (\partial G/\partial n_i)_{T,p}$ is the chemical potential of the ith component. At constant T and p,

$$dG = -\sum \mu_i dn_i \geq 0 \tag{2}$$

Consider the process $A_j \rightarrow A_k$, where A_j and A_k denote components j and k, respectively, representing either a chemical reaction or a phase change. If $d\alpha$ moles undergo the transformation,

$$\begin{aligned} dG &= -\mu_j(-d\alpha) - \mu_k(d\alpha) \geq 0 \\ &= (\mu_j - \mu_k)d\alpha \geq 0 \end{aligned} \tag{3}$$

Since $d\alpha$ may be positive or negative, the inequality holds only if $\mu_j = \mu_k$. In a similar manner, for a chemical reaction of the form,

$$\sum_j \nu_j^r A_j \rightleftharpoons \sum_k \nu_k^p A_k \tag{4}$$

where ν_j^r and ν_k^p are the stoichiometric coefficients of the reactants and products, respectively, the equilibrium condition is

$$\sum_j \nu_j^r \mu_j = \sum_k \nu_k^p \mu_k \tag{5}$$

Note that both G and n_i are extensive properties, whereas μ_i is intensive, i.e. if the number of moles of all components in the system is multiplied by a factor α, G and n_i each increase by a factor of α, while μ_i does not change.

Consider (2) in the case $dn_i = n_i\, d\alpha$. Then

$$dG = -\left(\sum_i n_i\, \mu_i\right) d\alpha \tag{6}$$

Integrate (6) with respect to α from $\alpha = 0$ to $\alpha = 1$ noting that the μ_i are constant along the path to obtain

$$G = -\sum_i n_i\, \mu_i \tag{7}$$

Take the differential of (7),

$$dG = -\sum_i n_i d\mu_i - \sum_i \mu_i dn_i \tag{8}$$

Subtracting (8) from (2) gives

$$\sum_i n_i d\mu_i = 0 \tag{9}$$

known as the Gibbs-Duhem equation.

Having derived conditions for the equilibrium of a system in terms of the chemical potentials μ_i, it is now necessary to relate the μ_i to the composition of the system. Consider first the determination of the chemical potential of a gas phase component. At a total pressure of one atmosphere, the gas phase can be taken as ideal. The chemical potential of an ideal gas is

$$\mu_i = \mu_i^o + RT\, \ell n(p_i/p_o) \tag{10}$$

where p_o is customarily taken as one atmosphere, and p_i is the partial pressure of component i.

An ideal liquid solution may be defined as one in which

$$\mu_i = \mu_i^o + RT \ln m_i \tag{11}$$

where m_i is the molality (moles of i/kg of water) of component i.* The assumptions underlying the ideal solution are of two types. The first is that the energy of interaction of all molecules is the same, whereas the second is that the solute does not dissociate. The systems of interest in atmospheric particles and droplets, consisting of concentrated electrolyte solutions, do not obey the assumptions of an ideal solution.

Activity Coefficients

To account for nonideality due to different energies of interaction, it is customary to define

$$\mu_i = \mu_i^o + RT \ln \gamma_i m_i \tag{12}$$

where the activity coefficient γ_i accounts for intermolecular forces. Methods of calculating the γ_i will be discussed shortly. Equation (12) is sometimes expressed in terms of the activity $a_i = \gamma_i m_i$ as

$$\mu_i = \mu_i^o + RT \ln a_i \tag{13}$$

Before proceeding further, it is necessary to discuss the convention used to define μ_i^o. First consider the solvent, in this case water. For water, μ_i^o is chosen so that $a_w = 1$ for pure water, i.e.

$$a_w = 1 \text{ as } x_w \to 1 \tag{14}$$

where x_w is the mole fraction of water. For water the symbol μ_i^o will be replaced by μ_w^o, the standard Gibbs free energy of formation of water, $\Delta G_{f_w}^o$.

*Henceforth, m_i will denote the molality of species i in solution.

Now consider the reference chemical potential for each of the solutes, μ_i° . Although there are several conventions on defining μ_i° , the one to be used here is that the activity coefficient of component i equals unity as the solution approaches infinite dilution,

$$\gamma_i = 1 \text{ as } m_j \to 0 \text{ all } j \tag{15}$$

There are two items to note about the convention. First, all solutes must become infinitely dilute simultaneously. Second, and most important, μ_i° does not correspond to a physically attainable state. For this reason, it is customary to use for it a different symbol, μ_i^*.

Having discussed nonideality due to intermolecular forces, it is now possible to treat nonidealities due to dissociation. When a solute dissociates, the total activity is the sum of the activities of the products of dissociation. For an ammonium nitrate solution, for example, assuming total dissociation, the chemical potential of NH_4NO_3 is

$$\mu_{NH_4NO_3} = \mu^*_{NH_4NO_3} + RT \ln \left(\gamma_{NH_4^+} \gamma_{NO_3^-} m_{NH_4^+} m_{NO_3^-} \right) \tag{16}$$

For ammonium sulfate, assuming total dissociation,

$$\mu_{(NH_4)_2SO_4} = \mu^*_{(NH_4)_2SO_4} + RT \ln \left(\gamma^2_{NH_4^+} \gamma_{SO_4^{2-}} m^2_{NH_4^+} m_{SO_4^{2-}} \right) \tag{17}$$

Because of the form of these expressions, the only quantity that can be measured experimentally is the product of the activity coefficients. Thus, it is convenient to introduce the mean activity coefficient $\gamma_\pm$, defined as the geometric mean of the activity coefficients, e.g. for NH_4NO_3, $\gamma_\pm^2 = \gamma_{NH_4^+}\gamma_{NO_3^-}$ while for $(NH_4)_2SO_4$, $\gamma_\pm^3 = \gamma^2_{NH_4^+} \gamma_{SO_4^{2-}}$.

A correlation for the mean activity coefficient in dilute one-component systems is

$$\ell n\ \gamma_{\pm} = \frac{A|z_+z_-|}{1+b\sqrt{I}}\sqrt{I} \tag{18}$$

where I is the ionic strength,

$$I = \frac{1}{2}\sum_i z_i^2 m_i \tag{19}$$

and where z_i is the charge on an ion of type i, z_+ and z_- being the charges on the positive and negative ions. The quantity A is a constant for each solvent at a given temperature, equal to 1.17625 for water at 298 K. The constant b depends on the size of the ions. When b = 0, (18) is called the Debye-Huckel limiting law. Although (18) represents data well at low ionic strengths, it is necessary to add additional terms in I to correlate data at higher ionic strengths,

$$\ell n\ \gamma_{\pm} = -\frac{A|z_+z_-|\sqrt{I}}{1+b\sqrt{I}} + \sum_{\ell}\alpha_{\ell}\ I^{\ell} \tag{20}$$

Here, b and the α_{ℓ} are empirical constants.

Finally, it is possible to use the Gibbs-Duhem equation (9) to calculate the water activity of a one-solute (binary) solution. Let ν_+ and ν_- be the numbers of moles of cations and anions produced by the dissociation of one mole of solvent and $\nu = \nu_+ + \nu_-$ be the total number of moles produced. Let m be the molality of the solution and n_w and n be the numbers of moles of water and solute present. Then (9) becomes

$$0 = n_w\ d\ell na_w + \nu_+ n\ d\ell n(\gamma_{\pm}\nu_+ m) + \nu_- n\ d\ell n(\gamma_{\pm}\nu_- m) \tag{21}$$

On a basis of 1 kg of water,

$$-\ n_w\ d\ell na_w = \nu m\ d\ell n\gamma_{\pm} + \nu m\ d\ell n\ m \tag{22}$$

Integrating with respect to m from zero to m gives

$$\ln a_w = -\frac{\nu M_w}{10^3} \int_0^m m' d\ln\gamma_{\pm} - \frac{\nu M_w}{10^3} m \tag{23}$$

where M_w is the molecular weight of water. The water activity a_w is related to the relative humidity RH in percent by

$$RH = 100\, a_w \tag{24}$$

Experimental values of a_w are commonly tabulated in terms of the molal osmotic coefficient ϕ, defined by

$$\phi = -\frac{10^3}{\nu m M_w} \ln a_w \tag{25}$$

Thus, (23) can be expressed in terms of ϕ as

$$\phi = 1 + \frac{1}{m} \int_0^m m' d\ln\gamma_{\pm} \tag{26}$$

Activity Coefficients for Multicomponent Solutions

Having found the chemical potential for the case of a binary solutions, we now proceed to the general case of a multicomponent solution. A rigorous theory would include the effects of all possible interactions, for example not only solvent-solute interactions but also all interactions between ion pairs, ion triplets, etc. The expression could then be truncated when the interaction effects become sufficiently small. The drawback of this approach is that even for solutions containing only a few electrolytes, the number of parameters that must be known as functions of ionic strength is large. Furthermore, most of these parameters cannot be measured directly. As a new ion is added to a system, all the parameters need to be redetermined. Thus, we must generally resort to empirically based approaches that do not involve as many unknown parameters as the rigorous theory.

In the approach we will follow, the Bronstead principle of specific interaction will be used. Physically, the principle is based on considering only interactions between pairs of oppositely charged ions. Ions with charges of similar sign repel each other, and because of their mutual repulsion, the distances between them are greater than those between ions of opposite sign. Based on this assumption , Kusik and Meissner[5] proposed the following empirical mixing rule for activity coefficients in multicomponent systems,

$$\ln \gamma_{12} = \frac{z_2}{z_1+z_2}\left[m_2\left(\frac{z_1+z_2}{2}\right)^2 \ln \gamma^\circ_{12} + m_4\left(\frac{z_1+z_4}{2}\right)^2 \ln \gamma^\circ_{14} + \ldots\right] I^{-1}$$
$$+ \frac{z_1}{z_1+z_2}\left[m_1\left(\frac{z_1+z_2}{2}\right)^2 \ln \gamma^\circ_{12} + m_3\left(\frac{z_3+z_2}{2}\right)^2 \ln \gamma^\circ_{32} + \ldots\right] I^{-1} \qquad (27)$$

where the odd and even subscripts refer to cations and anions, respectively, γ°_{ij} is the mean activity coefficient for a binary solution containing only ions i and j, and m_i is the molality of species i. Note that the only empirical data required for this approach are binary solution activity coefficients.

Having found the solute activity coefficients, the water activity follows from the Gibbs-Duhem equation,

$$\ln a_w = \sum_{ij} \frac{m_{ij}}{I} \frac{\nu_{ij} z_i z_j}{z_i+z_j}\left[z_j \sum_{\substack{k \\ \text{even}}} \left(\frac{z_i+z_k}{2}\right)^2 \frac{m_k}{I} \ln a^\circ_{w_{ik}} + z_i \sum_{\substack{k \\ \text{odd}}} \left(\frac{z_j+z_k}{2}\right)^2 \frac{m_k}{I} \ln a^\circ_{w_{kj}}\right]$$
$$+ \frac{M_w}{10^3} \sum_{ij} \frac{\nu_{ij} m_{ij}}{z_i+z_j}\left[z_i\left(\sum_{\substack{k \\ \text{even}}} \left(\frac{z_i+z_k}{2}\right)^2 \frac{m_k}{I} - 1\right) + z_j\left(\sum_{\substack{k \\ \text{odd}}} \left(\frac{z_j+z_k}{2}\right)^2 \frac{m_k}{I} - 1\right)\right] \qquad (28)$$

where $a^{\circ}_{w_{ij}}$ is the binary water activity for electrolyte pair, i, j, m_{ij} is the molality of this electrolyte, ν_{ij} is the number of moles of ions each mole of ij dissociates into, and m_k is the total molality of ion k.

THERMODYNAMICS OF THE ATMOSPHERIC AMMONIUM NITRATE, NITRIC ACID, AMMONIA SYSTEM

Relative Humidity and pH Dependence of the Vapor Pressure of Ammonium Nitrate - Nitric Acid Solutions at 25°C[53]

Ammonia-Nitric Acid Equilibrium Product Over Solid and Aqueous Ammonium Nitrate

Below 62% relative humidity at 25°C, ammonium nitrate should be present as a solid and above this value it should be in solution. * Recent available free energy data for the NH_3-HNO_3-H_2O system are given in Table 1, from which the equilibrium constants for the NH_3-HNO_3-H_2O system in Table 2 can be calculated. The equilibrium constants in Table 2 are thermodynamic equilibrium constants where pressure is referenced to one atmosphere and aqueous solute concentration to unit molality.

For ammonium nitrate at 25°C below 62% relative humidity, the equilibrium product is K_1. Above 62% the equilibrium product is given by

$$P_{NH_3} P_{HNO_3} = K_2 \gamma_{NH_4} \gamma_{NO_3} m_{NH_4} m_{NO_3}$$
$$= K_2 (\gamma_{\pm})^2_{NH_4NO_3} m^2_{NH_4NO_3} \qquad (29)$$

where P_{NH_3}, P_{HNO_3} = the partial pressures of ammonia and nitric acid; γ_{NH_4}, γ_{NO_3} = the molal activity coefficients of the NH_4^+ and NO_3^- ions; m_{NH_3}, m_{NO_3}, $m_{NH_4NO_3}$ = the molalities of NH_4^+, NO_3^- and NH_4NO_3 and $(\gamma_{\pm})_{NH_4NO_3}$ = the mean molal activity coefficient for NH_4NO_3. Using the NH_4NO_3 solution activity coefficient data from Hamer and Wu[7], the equilibrium product can be calculated as a function of NH_4NO_3 molality. The relative humidity, R.H., over the solution can be calculated as a function of NH_4NO_3 molality from the molal osmotic coefficients in Hamer and Wu[7],

*Although recent work of Tang[6] indicates ammonium nitrate does not exhibit traditional deliquescence but is hygroscopic at relative humidities greater than about 30%, we will assume ammonium nitrate deliquesces at 62% relative humidity for the purpose of this work.

Table 1. Free Energy Data for the NH_3-HNO_3-H_2O System at 298 K

Species	$\Delta G/R, K^{-1}$	Reference
$NH_3(g)$	- 1,977	8
$HNO_3(g)$	- 8,903	9
$NH_4NO_3(c, IV)$	-22,220	8
$NH_4NO_3(aq.\ m = 1)$	-22,940	10
$NO_3^-(aq, m = 1)$	-13,410	8
$H^+(aq, m = 1)$	0	8
$NH_4^+(aq, m = 1)$	- 9,558	8
$H_2O(\ell)$	-28,530	8
$NH_3 \cdot H_2O(aq)$	-31,730	10
$OH^-(aq, m = 1)$	-18,925	8

Table 2. Equilibrium Constants for the NH_3-HNO_3-H_2O System at 298 K

	Reaction	Equilibrium Constant*,†
1.	$NH_4NO_3(c,IV) \rightleftarrows NH_3(g) + HNO_3(g)$	3.03×10^{-17}
2.	$NH_4NO_3(aq) \rightleftarrows NH_3(g) + HNO_3(g)$	2.71×10^{-18}
3.	$NO_3^-(aq) + H^+(aq) \rightleftarrows HNO_3(g)$	2.72×10^{-7}
4.	$NH_3 \cdot H_2O(aq) \rightleftarrows H_2O(\ell) + NH_3(g)$	1.65×10^{-2}
5.	$NH_4^+(aq) + OH^-(aq) \rightleftarrows NH_3 \cdot H_2O(aq)$	5.37×10^{4}
6.	$H^+(aq) + OH^-(aq) \rightleftarrows H_2O(\ell)$	9.79×10^{13}

*Values calculated from the free energy data of Table 1. The equilibrium constants listed here can be tested for internal consistency in two ways. First, K_2 should equal $K_5K_4K_3/K_6$. Based on the values given, $K_5K_4K_3/K_6 = 2.46 \times 10^{-18}$ vs. $K_2 = 2.71 \times 10^{-18}$, an error of 9.2%. Second, K_1 should equal $K_2\, a_{NH_4NO_3}$, where $a_{NH_4NO_3}$ = saturated ammonium nitrate solution activity. Using the value of $a_{NH_4NO_3}$ of Hamer and Wu , $K_1 = 3.14 \times 10^{-17}$, which agrees well with $K_1 = 3.03 \times 10^{-17}$ as calculated and given here.

†The differences between the values for reactions 4-6 and those of Tang are < 6%. A 21% difference exists between the equilibrium constant used for reaction 3 by Tang[11] and the value here.

$$\text{R.H.} = 100\, a_w = 100 \exp\left(-3.6031 \times 10^{-2}\, m_{NH_4NO_3} \phi_m\right), \qquad (30)$$

where ϕ_m = the molal osmotic coefficient at $m_{NH_4NO_3}$. Since the equilibrium product and the relative humidity over solution are both solely dependent on $m_{NH_4NO_3}$, the equilibrium product - $m_{NH_4NO_3}$ functionality can be replaced by a function relating the equilibrium product directly to the relative humidity, as in Figure 1. Note that the product, $p_{NH_3} p_{HNO_3}$, is expressed in units of $(ppb)^2$ in Fig. 1 for convenience in atmospheric applications. The effect of non-ideality can be examined by assuming ϕ_m and $(\gamma_\pm)_{NH_4NO_3}$ are unity. (See the curve labelled ideal solution in Fig. 1). The ideal solution curve ends at $m_{NH_4NO_3} = 25.954$, saturated NH_4NO_3 solution at 25°C, which shows the ideal solution approach grossly mispredicts the deliquiescence relative humidity.

The solid NH_4NO_3 vapor pressure product calculated using a least squares fit of the data of Brandner, et al.[12] and the thermodynamic prediction of Stelson et al.[3] are also shown in Fig. 1. The new solid vapor pressure product prediction and the non-ideal NH_4NO_3 solution curve at saturation join closely, indicating the improved quality of this prediction for the NH_4NO_3 solid vapor pressure product at 25°C over that of Stelson et al.[3]

Ammonium Nitrate-Nitric Acid Mixtures.

Consider now a solution containing both ammonium nitrate and nitric acid. Let 1, 2, and 3 denote the H^+, NO_3^- and NH_4^+ ions, respectively. Then, by equations (27) and (28)

$$\ln \gamma_{12} = \frac{1+x}{2} \ln \gamma^\circ_{12} + \frac{1-x}{2} \ln \gamma^\circ_{32} \qquad (31)$$

$$\ln \gamma_{32} = \frac{x}{2} \ln \gamma^\circ_{12} + \frac{2-x}{2} \ln \gamma^\circ_{32} \qquad (32)$$

$$\ln a_w = x \ln a^\circ_{w_{12}} + (1-x) \ln a^\circ_{w_{14}} \qquad (33)$$

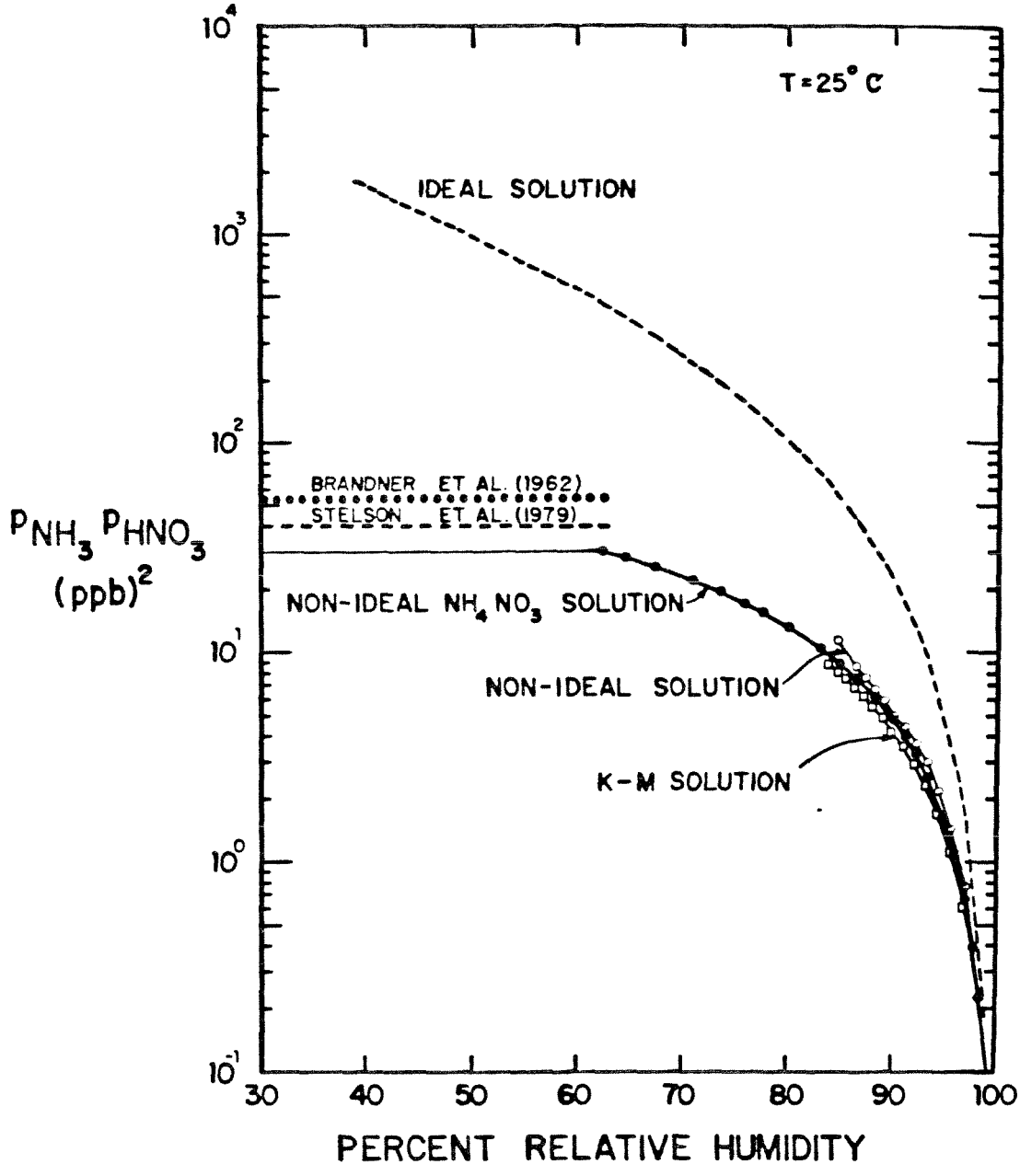

Figure 1

Effect of relative humidity on ammonia-nitric acid partial pressure product.[53]

where $x = m_1/m_2$. Using these equations we will now show how the partial pressures of nitric acid and ammonia over the solution are calculated.

The nitric acid partial pressure is determined from the equilibrium of reaction 3 in Table 2,

$$P_{HNO_3} = K_3 \gamma_{12}^2 m_1 m_2 \tag{34}$$

Using equation (31) and the value for K_3 determined from the thermodynamic data in Table 1,

$$P_{HNO_3} = 272(\gamma_{\pm})_{H,NO_3}^{1+x} (\gamma_{\pm})_{NH_4NO_3}^{1-x} x\, m_{NO_3}^2 \quad \text{(in ppb)} \tag{35}$$

By specifying m_H, m_{NO_3}, and m_{NH_4}, the ionic strength is determined by $I = m_{NO_3} = m_{NH_4} + m_H$, and only $(\gamma_{\pm})_{H,NO_3}$ needs to be evaluated to calculate P_{HNO_3}. The ionic strength functional dependence of $(\gamma_{\pm})_{H,NO_3}$ must be calculated by an indirect method which is different from the usual experimental activity coefficient determination methods, vapor pressure, freezing point depression or electrochemical, since nitric acid does not totally dissociate in water.

The degree of dissociation of nitric acid in water as a function of acid concentration can be determined using the approach of Högfeldt[13], in which the dissociation of nitric acid is represented by three equilibria;

$$HNO_3(H_2O)_3(aq) \rightleftarrows H^+(aq) + NO_3^-(aq) + 3H_2O(\ell)$$

$$K_a = \frac{[HNO_3(H_2O)_3]}{\{H^+\}\{NO_3^-\}\{H_2O\}^3}$$

$$HNO_3(H_2O)(aq) \rightleftarrows H^+(aq) + NO_3^-(aq) + H_2O(\ell)$$

$$K_b = \frac{[HNO_3(H_2O)]}{\{H^+\}\{NO_3^-\}\{H_3O\}}$$

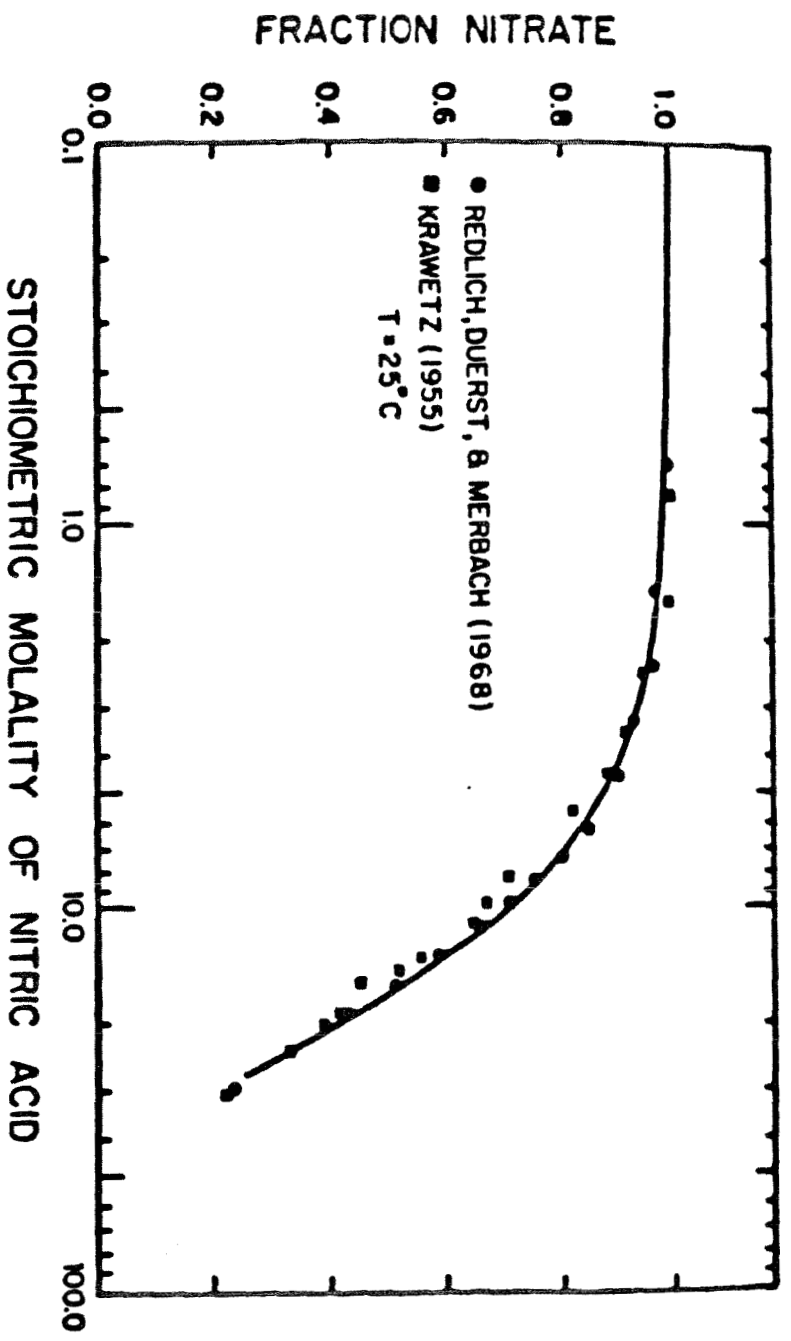

Figure 2

Ionization of nitric acid.[53]

$$HNO_3(aq) \rightleftarrows H^+(aq) + NO_3^-(aq)$$

$$K_c = \frac{[HNO_3]}{\{H^+\}\{NO_3^-\}}$$

where [ ] represents molar concentration and { } refers to the activity. K_a, K_b and K_c are 3.63×10^{-2}, 8.13×10^{-3} and 1.66×10^{-4}, respectively[13]. Högfeldt[13] assumes the molar activity coefficients of the undissociated aqueous nitrate species to be unity. When converting to a molal basis, the undissociated nitric acid species molal activity coefficient, γ_u is not unity, but rather is given by

$$\gamma_u = \frac{1000d}{d_o(1000+M_{HNO_3} m_s)} \tag{36}$$

where d and d_o are the nitric acid solution and pure water densities in g ml^{-1}, respectively, M_{HNO_3} = the molecular weight of nitric acid, and m_s = stoichiometric nitric acid molality. Using Högfeldt's equilibria and equation (36), the fraction of nitric acid that is dissociated, α, can be calculated from

$$\alpha = 1 - \frac{d_o \gamma_s^2 m_s}{\gamma_u} (K_a a_w^3 + K_b a_w + K_c) \tag{37}$$

where γ_s = the stoichiometric molal nitric acid activity coefficient. The dissociation of nitric acid can be calculated using the stoichiometric molal nitric acid activity and water activity data fit of Hamer and Wu[7], pure water density and nitric acid molecular weight of Weast[14], and the nitric acid solution density interpolation formula of Granzhan and Laktionova[15]. The dissociation calculated from equation (37) is compared to the dissociation data of Krawetz[16] and Redlich, et al.[17] in Fig. 2. The agreement, especially with the data of Redlich et al.[17], is good.

The total nitric acid dissociation constant can be expressed in terms of K_a, K_b and K_c by

$$K_N = \frac{1}{K_a a_w^3 + K_b a_w + K_c} \tag{38}$$

Using Högfeldt's[13] equilibrium constants and noting that $a_w = 1.0$ at infinite dilution, $K_N = 22.4$, which compares favorably with values of 15.4, 20.0 and 26.8 from Davis and De Bruin[18], Redlich et al.[17] and Young et al.[19], respectively.

The mean molal ionic activity coefficients for the H^+ and NO_3^- ions, $(\gamma_\pm)_{H,NO_3}$, can be found from

$$(\gamma_\pm)_{H,NO_3} = \gamma_s/\alpha. \tag{39}$$

Using equations (36), (37) and (39), $(\gamma_\pm)_{H,NO_3}$ can be calculated as a function of ionic strength. The maximum ionic strength is about 8.3 m and occurs between 17 and 21 stoichiometric nitric acid molality. The mean molal ionic activity coefficient polynomial regression up to 7.5 m is

$$\begin{aligned} \ln(\gamma_\pm)_{H,NO_3} = {} & \frac{-1.17625\sqrt{I}}{1+1.44\sqrt{I}} + 2.260 \times 10^{-1} I \\ & - 4.722 \times 10^{-2} I^2 \\ & + 1.656 \times 10^{-2} I^3 - 2.396 \times 10^{-3} I^4 \\ & + 1.384 \times 10^{-4} I^5, \end{aligned} \tag{40}$$

where the standard deviation is ±0.0022. Although $(\gamma_\pm)_{H,NO_3}$ should also be a function of the undissociated nitric acid concentration, the effect of undissociated nitric acid will be shown to be negligible up to 7.0 ionic strength.

Ammonia Partial Pressure.

Now we may use the results of the previous section to find the partial pressure of ammonia over the solution. Dividing equation (29) by (34) gives

$$p_{NH_3} = \frac{K_2}{K_3} \frac{\gamma_{32}^2}{\gamma_{12}^2} \frac{m_3}{m_1} \tag{41}$$

Using equations (31) and (32) and the values for the equilibrium constants from Table 2 gives

$$p_{NH_3} = 9.05 \times 10^{-3} \frac{\gamma_{32}^{\circ}}{\gamma_{12}^{\circ}} \frac{1-x}{x} \qquad \text{(in ppb)} \tag{42}$$

where K_2 has been replaced by $K_5K_4K_3/K_6$.

Variation of Ammonia and Nitric Acid Partial Pressures as a Function of pH

The variation of the ammonia and nitric acid partial pressures as a function of pH can be evaluated using the expression for $(\gamma_{\pm})_{NH_4NO_3}$ from Hamer and Wu[7] and equations (35),(40) and (42). The water activity of the NH_4NO_3-HNO_3 solution $(a_w)_{MIX}$, is given by

$$(a_w)_{MIX} = (a_w^{o})^{x}_{H,NO_3} (a_w^{o})^{1-x}_{NH_4NO_3}, \tag{43}$$

where the superscript ^{o} denotes activities in a binary solution and where $(a_w^{o})_{H,NO_3}$ is obtained from equation (40) and the Gibbs-Duhem relationship[5]. The variation of p_{NH_3} and p_{HNO_3} with pH is shown in Fig. 3 for a relative humidity of 94.5%.

The product of the ammonia and nitric acid partial pressures calculated from equations (35) and (42) as a function of relative humidity is compared to the equilibrium product calculated using ammonium nitrate activities in Fig. 1. By comparing the curves labelled K-M solution and non-ideal NH_4NO_3 solution, the agreement is shown to be good. The major source of disagreement between the K-M solution and the non-ideal NH_4NO_3 solution curves is the 9.2%

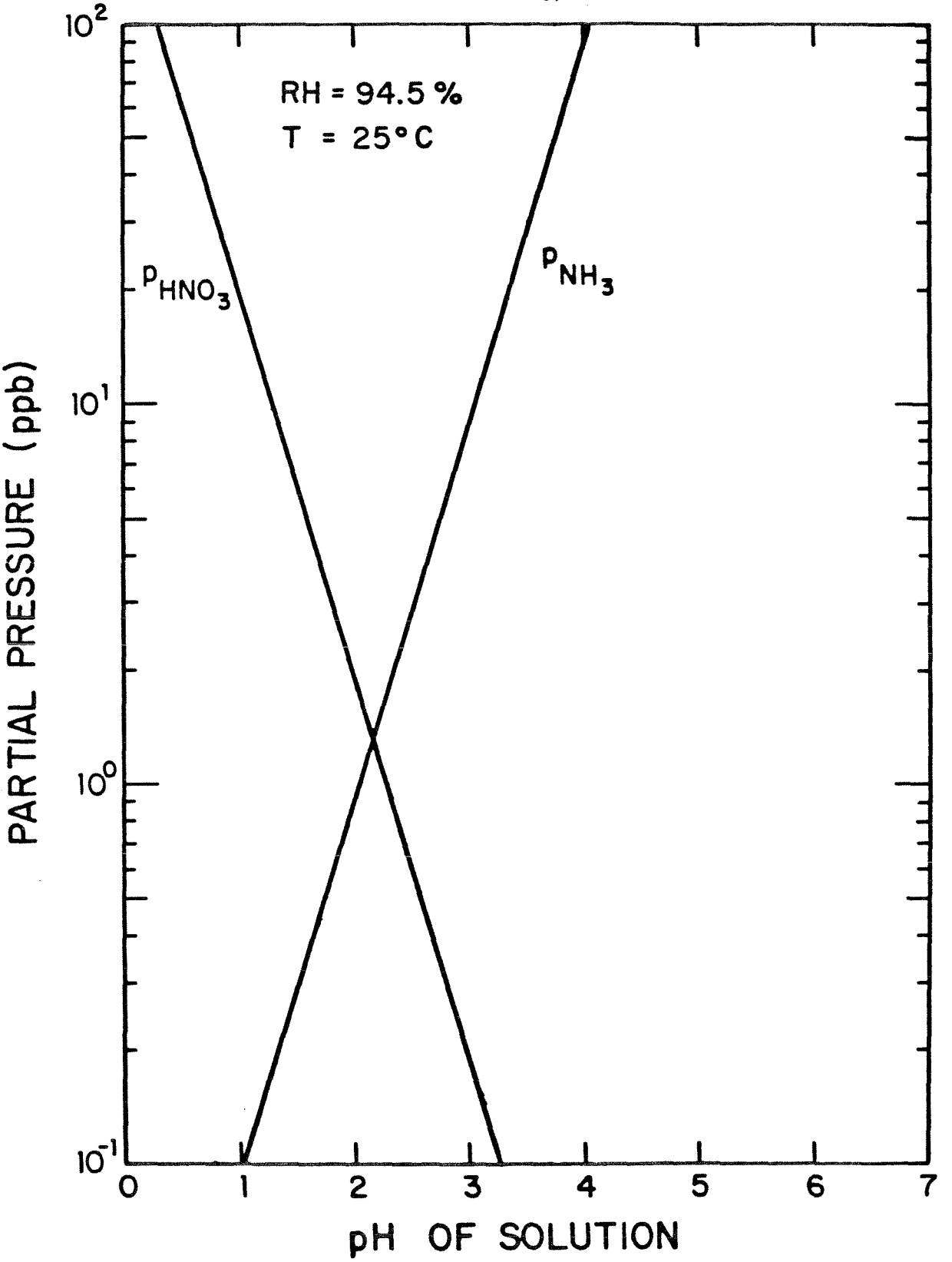

Figure 3

Effect of pH on the ammonia and nitric acid partial pressures.[53]

difference between $K_5K_4K_3/K_6$ and K_2. The insensitivity of $p_{NH_3}p_{HNO_3}$ to pH can be seen in the range of relative humidity variation by multiplying equations (35) and (42),

$$p_{NH_3}p_{HNO_3} = 2.46(\gamma_{\pm}^{\circ})^{x}_{H,NO_3}(\gamma_{\pm}^{\circ})^{2-x}_{NH_4NO_3}(1-x)m^2_{NO_3} \text{ (in ppb}^2\text{)} \tag{44}$$

As the relative humidity decreases, the maximum x, which occurs at pH = 1, becomes smaller. Thus, the difference between an acidic ammonium nitrate solution (pH > 1) and a pure ammonium nitrate solution partial pressure product decreases with relative humidity.

Effect of Neglecting Undissociated Nitric Acid and Ion-Pairing

In developing quantitative expressions for the ammonia and nitric acid partial pressures, two assumptions were invoked. First, the effect of undissociated nitric acid on the $(\gamma_{\pm})_{H,NO_3}$, ionic strength functionality is small, below 7.0 m. Second, ion-pairing of NH_4^+ and NO_3^- ions has a minimal effect on the ammonia partial pressures predicted. Equation (44) requires as $x \to 0$, the solute activity approaches $(\gamma_{\pm})^2_{NH_4NO_3}m^2_{NH_4NO_3}$. Similarly, equation (31) requires $\gamma_H\gamma_{NO_3}$ to approach $(\gamma_{\pm})^2_{H,NO_3}$ as $x \to 1$. Inherent in equations (31) and (44) are the correct limits but neither equation gives insight into the effect of these two assumptions. This effect will be examined in this section.

The ammonium to hydrogen ion activity coefficient ratio, in a mixture, γ_{NH_4}/γ_H, can be evaluated from mean molal activity coefficients of an ammoniated salt NH_4X and the acid with the same univalent ion, HX, provided the acid completely dissociates. The activity coefficients of the two species are given by

$$\ln \gamma_{NH_4X} = \frac{2-x}{2} \ln \gamma^{\circ}_{NH_4X} + \frac{x}{2} \ln \gamma^{\circ}_{HX} \tag{45}$$

$$\ln \gamma_{HX} = \frac{1-x}{2} \ln \gamma^{\circ}_{NH_4X} + \frac{1+x}{2} \ln \gamma^{\circ}_{HX} \tag{46}$$

where $x = m_H/m_X$. Subtracting these two equations yields

$$\ln \frac{\gamma_{NH_4X}}{\gamma_{HX}} = \frac{1}{2} \ln \frac{\gamma^{\circ}_{NH_4X}}{\gamma^{\circ}_{HX}} \tag{47}$$

Then, since $\gamma^2_{NH_4X} = \gamma_{NH_4}\gamma_X$, etc.,

$$\frac{\gamma_{NH_4}}{\gamma_H} = \frac{\gamma^{\circ}_{NH_4X}}{\gamma^{\circ}_{HX}} = \left(\frac{\gamma^{\circ}_{NH_4}}{\gamma^{\circ}_{H}}\right)^{\frac{1}{2}} \tag{48}$$

Thus, if the approach is correct, the right hand side of equation (48) should be identical for all anions. This hypothesis was tested with five different anions, Cl^-, NO_3^-, I^-, Br^- and ClO_4^- (see Fig. 4). The assumption that HCl, HBr, HI and $HClO_4$ totally dissociated in solutions below 7m or saturation is appropriate since the dissociation constants are very large, $> 10^7$ [20,21]. It is incorrect to assume that HNO_3 completely dissociates, so the NO_3^- curve was calculated using $(\gamma_{\pm})_{H,NO_3}$ as previously derived.

Lee and Wilmshurst[22] have shown that a 5 m NH_4Cl solution forms ion-pairs. The observed mean molal activity coefficient, $(\gamma_{\pm})_{NH_4X}$, must be corrected as follows[21],

$$(\gamma_{\pm})_{NH_4X} = \frac{(\gamma_{\pm})_{NH_4X}}{1-\theta} \tag{49}$$

where $(\gamma_{\pm})_{NH_4X}$ = the corrected mean molal activity coefficient for salt NH_4X and θ = the fraction of NH_4 and X ions forming ion-pairs. Equation (5) assumes the ion-pairs are symmetric[23]. Also, the ionic strength would be corrected to $(1-\theta)m_{NH_4X}$. The net effect of ion-pairing on the curves in Fig. 4 is not

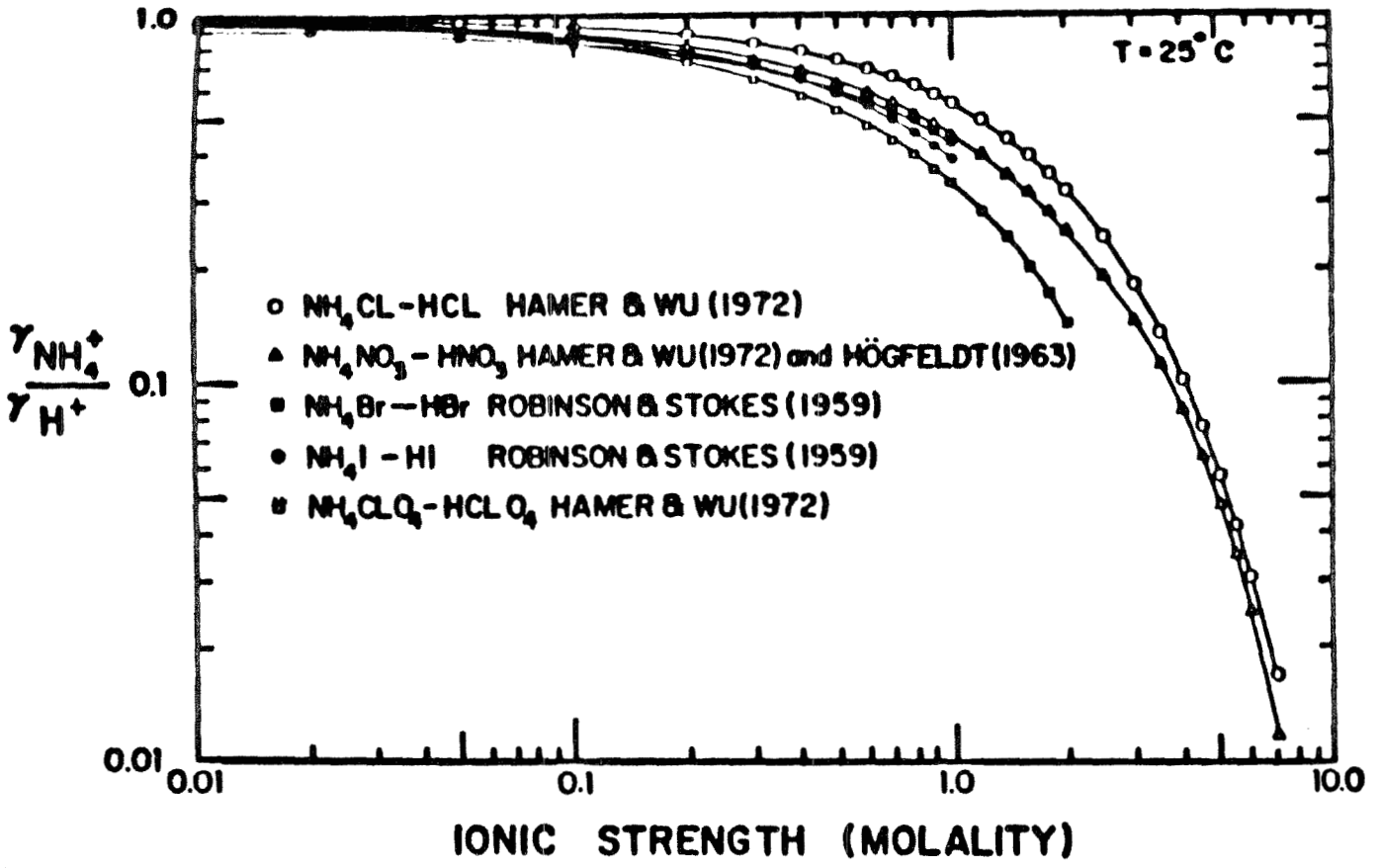

Figure 4

Effect of ionic strength on calculated ammonium/hydrogen ion mean molal activity coefficient ratio[53]

obvious since the NH_4X mean molal activity coefficient would increase and the ionic strength would decrease. Using density data of Pearce and Pumplin[24], a 5-M NH_4Cl solution is approximately 6.25 m. The NH_4Cl-HCl ammonium to hydrogen ion activity coefficient ratio is used to represent γ_{NH_4}/γ_H to 7.0 m. Thus, some NH_4Cl ion-pairing must be present above 6.25 m. From (48)

$$\left(\gamma^{\circ}_{NH_4NO_3}\right)^2 = \left(\frac{\gamma^{\circ}_{NH_4}}{\gamma^{\circ}_{H}}\right)\left(\gamma^{\circ}_{HNO_3}\right)^2 \qquad (50)$$

Thus, (50) allows $\gamma^{\circ}_{NH_4NO_3}$ to be calculated independent of ammonium nitrate data.

With (29), (40) (48) and (50) and replacing K_2 by $K_5K_4K_3/K_6$, the effect of ion-pairing and the undissociated nitric acid can be ascertained. We refer the reader to the curve labelled non-ideal solution in Fig. 1. The water activity was calculated from (30). The agreement between the non-ideal, non-ideal NH_4NO_3, and K-M solution curves supports the assumptions of neglecting both the influence of undissociated nitric acid on the mean molal activity coefficient of dissociated nitric acid $(\gamma_{\pm})_{H,NO_3}$, and the presence of ion-pairing in calculating γ_{NH_4}/γ_H. By comparing the K-M and non-ideal solution curves, the maximum possible error in the individual partial pressures can be ascertained as about 30%.

Assuming $\gamma_H\gamma_{NO_3} = (\gamma_{\pm})^2_{H,NO_3}$ and (48) holds, the $\gamma_H\gamma_{NO_3}$ product and the γ_{NH_4}/γ_H ratio calculated cannot be used for calculating the individual partial pressures of ammonia and nitric acid because $\gamma_H\gamma_{NO_3}$ goes to the wrong limit as $x \to 0$ and γ_{NH_4}/γ_H goes to the wrong limit as $x \to 1$. Even though these expressions cannot be used for the individual partial pressures, they can be multiplied together to check the ammonia-nitric acid partial pressure product calculated from (29) and (44) and the possible significance of ion-pairing and the undissociated nitric acid in calculating $(\gamma_{\pm})_{H,NO_3}$.

Discussion

This approach gives theoretical justification for the results of Forrest et al.[25] and Appel et al.[26]. As the relative humidity approaches 100%, the equilibrium vapor pressure product sharply decreases by several orders of magnitude. At 98% relative humidity and 25°C, the mass concentration of NH_3 plus HNO_3 (equimolar basis) in the gas in equilibrium with an aqueous ammonium nitrate solution is about 1.9 μg m^{-3} vs. 17.9 μg m^{-3} needed if ammonium nitrate is present as a solid. Thus, the observation[25] that greatest ammonium nitrate filter losses occurred at relative humidities below 60%, and no losses occurred at 100% relative humidity, and the observations[26] that nitrate aerosol is present even though the equilibrium product of ammonia and nitric acid is much less than the solid equilibrium product are consistent with this work.

The ammonia-nitric acid equilibrium product relative humidity functionality does not significantly change when the pH is varied between 1 and 7. The insensitivity of the ammonia-nitric acid equilibrium product with pH variation results from the ammonia-nitric acid equilibrium product being dominantly dependent on ionic strength. As the pH decreases below 1, the approach used in this work is not applicable since the role of undissociated nitric acid becomes significant and similarly for high pH undissociated dissolved ammonia would appear. From the electroneutrality balance and the average aerosol water data in Stelson and Seinfeld [1], a range of possible mass distribution averaged pH's between 2 and 12 is calculable for several locations in the Los Angeles Basin. Since the atmospheric aerosol is often a mixture of acidic and basic particles, a distribution of aerosol pH would exist, the basic particles existing predominantly in the coarse mode (> 1 μm) and the acidic particles in the fine mode (< 1 μm). Thus, these results have limited applicability to the possible range of existing ambient aerosol acidity.

Qualitatively, the result of adding an unreactive solute on the vapor pressure product-relative humidity curve can be discussed. The unreactive solute would lower the water vapor pressure but would not affect the ammonia-nitric acid vapor pressure product. Thus, the resulting situation would be a measured vapor pressure product and relative humidity location lying below the NH_4NO_3 non-ideal vapor pressure product-relative humidity curve in Fig. 1.

The presence of a saturated ammonium nitrate solution around a solid ammonium nitrate aerosol core can be examined. Since the saturated solution must be in equilibirum with solid ammonium nitrate, the vapor pressure product must be the same over the saturated solution as for the solid ammonium nitrate. Thus, the presence of a saturated aqueous layer around a solid ammonium nitrate core at relative humidities below 62% would not affect the equilibrium vapor pressure product prediction.

THERMODYNAMICS OF THE ATMOSPHERIC AMMONIUM NITRATE, AMMONIUM SULFATE, WATER SYSTEM[54]

Now we consider the second system, the atmospheric ammonium nitrate, ammonium sulfate, water system. Since the ammonium, nitrate and sulfate ions occur in particles of similar size, a thermodynamic study of the interaction between ammonium nitrate and ammonium sulfate provides a foundation for understanding atmospheric processes involving these species.

The relative humidity of air in equilibrium with a saturated solution of ammonium sulfate is relatively high, eighty percent. Thus, for a given situation, it is important to consider whether or not a solid phase is present. If a solid phase is present, it is further necessary to determine which species it contains. This question will be dealt with in the following section. We will then proceed to discuss the thermodynamics of the aqueous phase.

NH_4NO_3-$(NH_4)_2SO_4$-H_2O Phase Diagram

The NH_4NO_3-$(NH_4)_2SO_4$-H_2O phase diagram can be constructed from the data in Silcock[27] and Emons and Hahn[28] and is shown in Figure 5. The phase diagram shows several interesting items. By equating chemical potentials at eutonic points, E_1 and E_2, the NH_4NO_3 chemical potential can be shown to be constant along the solubility curve between pure NH_4NO_3 in water and E_3 and in the regions I, I & II, II, II & III, III and III & IV. If the NH_4NO_3 chemical potential is constant throughout these regions, then the NH_4NO_3 dissociation constant must be invariant. Similarly, the $(NH_4)_2SO_4$ chemical potential must be constant along the solubility curve between pure $(NH_4)_2SO_4$ in water and E_1 and in the regions IV, III & IV, III, II & III, II and I & II. If the chemical form of the aqueous solutes is the same along the solubility curve between E_1 and E_3, then by equating chemical potentials and by using the Gibbs-Duhem equation, the solution relative humidity should be constant. In Table 3, relative humidity measurements of saturated aqueous NH_4NO_3-$(NH_4)_2SO_4$ solutions

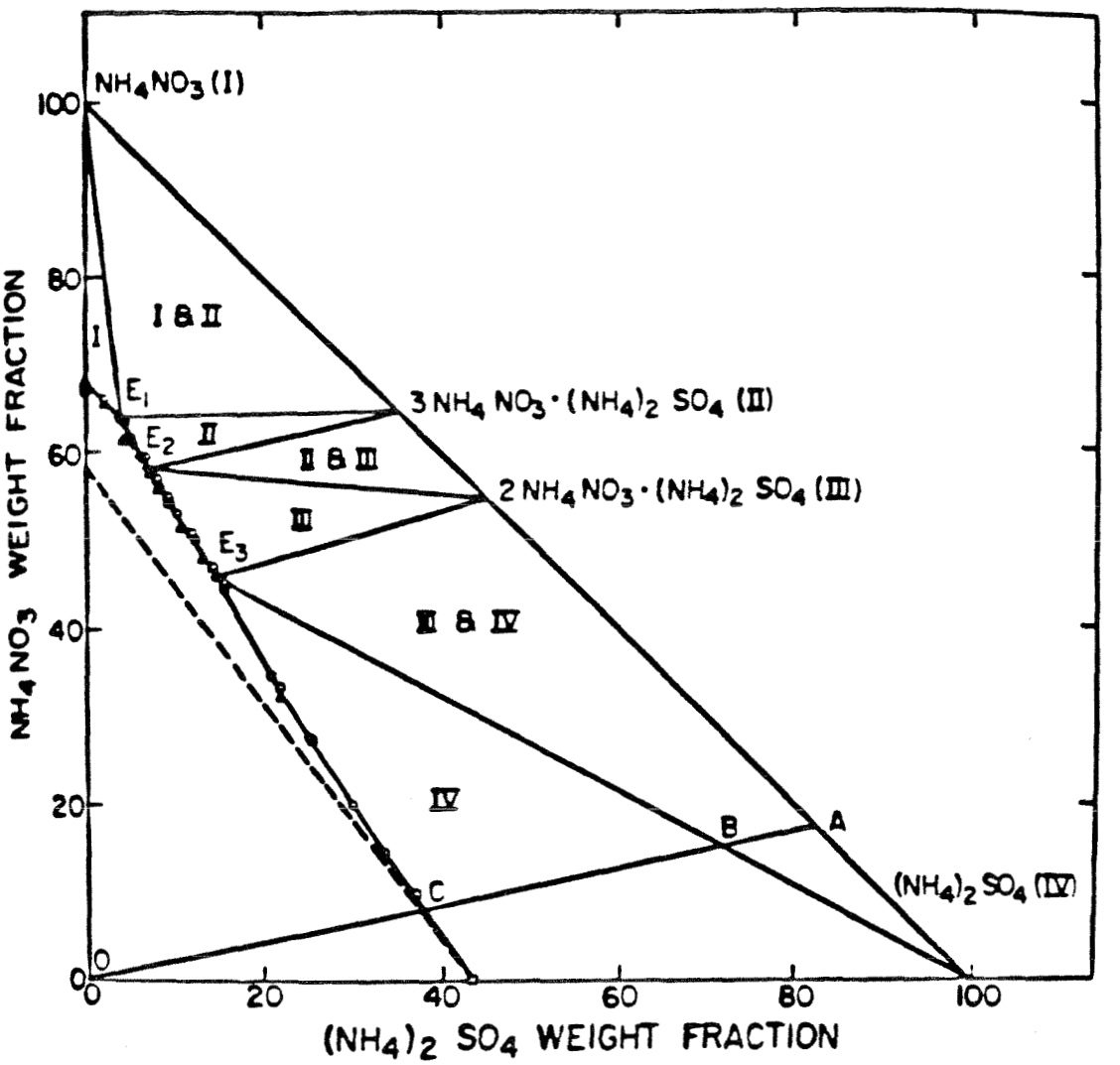

Figure 5

NH_4NO_3-$(NH_4)_2SO_4$-H_2O phase diagram at 25°C □ Emons and Hahn
0,+,Δ Silcock[54]

from Emons and Hahn[28] are shown. Their data show that the relative humidity varies between E_1 and E_3, indicating a new dissolved species must be formed. Finally, Figure 5 illustrates a problem when attempting to describe multicomponent aqueous mixtures up to saturation. Since $(NH_4)_2SO_4$ precipitates at a lower ionic strength than NH_4NO_3, there is a problem in describing the region of the phase diagram where the ionic strength is greater than the maximum ionic strength of the least soluble species. For the NH_4NO_3-$(NH_4)_2SO_4$-H_2O system, this region lies between the solubility curve and the dashed line in Fig. 5. In the next section, this problem will be discussed in more detail.

Estimation of the Water Activity and the NH_4NO_3 Dissociation Constant

Equations (27) and (28) can be used to estimate the water activity and the solute activity coefficients for the NH_4NO_3-$(NH_4)_2SO_4$-H_2O system. The NH_4NO_3 activity, a_{12}, is given by

$$\ln a_{12} = \frac{2+4Y}{3} \ln \gamma_{12}^{o} + \frac{3-3Y}{4} \ln \gamma_{14}^{o} + \ln \left(\frac{2+Y}{3} \right) YI^2 \tag{51}$$

where γ_{12}^{o}, γ_{14}^{o} = the activity coefficients of NH_4NO_3 or $(NH_4)_2SO_4$ alone in water at I, Y = the ionic strength fraction of NH_4NO_3,

$$Y = \frac{m_{NH_4NO_3}}{m_{NH_4NO_3} + 3\, m_{(NH_4)_2SO_4}} \tag{52}$$

and I = the total solution ionic strength. The $(NH_4)_2SO_4$ activity, a_{14}, is

$$\ln a_{14} = 2Y \ln \gamma_{12}^{o} + \frac{12-3Y}{4} \ln \gamma_{14}^{o} + \ln (2+Y)^2 \left(\frac{1-Y}{27} \right) I^3. \tag{53}$$

From equation (28), the water activity can be calculated as

$$\ln a_w = \left(\frac{2+Y}{3}\right) Y \ln a^{\circ}_{w_{12}} + \left(\frac{2+Y}{2}\right) (1-Y) \ln a^{\circ}_{w_{14}} - \frac{Y M_w I}{6000} (1-Y) \qquad (54)$$

where $a^{\circ}_{w_{12}}$, $a^{\circ}_{w_{14}}$ = the water activities of NH_4NO_3 or $(NH_4)_2SO_4$ aqueous solutions at I, and M_w = the molecular weight of water.

Equations (51), (53) and (54) can be used to evaluate the activities up to an ionic strength of 17.5 molal, the solubility of $(NH_4)_2SO_4$ in water at 25°C. Expressions for the ionic strength dependences of the NH_4NO_3 activity coefficient and water activity were obtained from Hamer and Wu[7]. The expressions used for the $(NH_4)_2SO_4$ activity coefficient and water activity ionic strength dependences were based on the isopiestic measurements of Wishaw and Stokes[29]. The solution osmotic coefficients were calculated using the method outlined in Staples and Nuttall[30] and referenced to the ionic strength dependence of the NaCℓ osmotic coefficient of Hamer and Wu[7]. The more recent NaCℓ expression of Gibbard et al.[31] was not used since it is in good agreement with the work of Hamer and Wu[7]. The resulting $(NH_4)_2SO_4$ osmotic coefficient data were fit to a polynomial and, with the Gibbs-Duhem equation, the following ionic strength dependence for the $(NH_4)_2SO_4$ activity was obtained,

$$\ln \gamma^{o}_{14} = \frac{-2.3525\sqrt{I}}{1+1.02\sqrt{I}} - 8.369\times10^{-2} I + 7.635\times10^{-3} I^2 - 3.307\times10^{-4} I^3 + 5.783\times10^{-6} I^4 \qquad (55)$$

where the standard deviation of the original regression was 7.55×10^{-4}. Still unresolved is how to predict the activity coefficient of $(NH_4)_2SO_4$ in the region of the phase diagram between the dashed line and the solubility curve.

The activity coefficient of $(NH_4)_2SO_4$ at ionic strengths greater than its solubility in water can be approximated four ways from existing data. First, Emons and Hahn[28] measured the water activity along the solubility curve for the NH_4NO_3-$(NH_4)_2SO_4$-H_2O system. From equation (54), the data of Emons and Hahn[28] and the NH_4NO_3 water activity ionic strength dependence, the hypothetical $(NH_4)_2SO_4$ water activity can be calculated to 26.0 molal, the solubility of NH_4NO_3 in water. By using the Gibbs-Duhem equation, the $(NH_4)_2SO_4$ activity coefficient can be obtained. Second, the dissolved ammonium sulfate activity must be constant along the solubility curve between $(NH_4)_2SO_4$ in pure water and E_1. Thus, the hypothetical $(NH_4)_2SO_4$ activity coefficient ionic strength dependence can be calculated from the solubility data in Silcock[27], the NH_4NO_3 activity coefficient ionic strength dependence, the activity of a saturated aqueous $(NH_4)_2SO_4$ solution and equation (53). Third, the $(NH_4)_2SO_4$ activity coefficient data below 17.5 molal can be linearly extrapolated to higher ionic strengths. Fourth, equation (55) could be used above 17.5 molal.

The results of the four techniques were compared. The second method exhibits a higher ionic strength dependence than the other three. The first method results scattered about the predictions of the third and fourth with neither method showing better agreement. Thus, equation (55) was used to represent the ionic strength dependence of the $(NH_4)_2SO_4$ activity coefficient above as well as below 17.5 molal.

Using equation (54), the water activities of NH_4NO_3-$(NH_4)_2SO_4$ solutions were predicted and compared to the data of Emons and Hahn[28] and Thudium [32] in Tables 3 and 4. The agreement between the predictions and data is good even though the data were taken using distinctly different experimental techniques. The maximum error was 3.7%. Table 3 and Table III of Saxena

Table 3. Comparison of Calculated and Measured Water Activities Along the NH_4NO_3-$(NH_4)_2SO_4$ Aqueous Solubility Curve

I	Y	a_w (Calc.)	a_w (Meas.)†	% Error	Solid Phase*
17.46	0.000	0.800	0.801	- 0.12	$(NH_4)_2SO_4$
18.06	0.126	0.775	0.767	1.04	$(NH_4)_2SO_4$
19.64	0.371	0.725	0.727	- 0.28	$(NH_4)_2SO_4$
20.76	0.457	0.701	0.700	0.14	$(NH_4)_2SO_4$
23.25	0.614	0.655	0.655	0.00	$(NH_4)_2SO_4$
23.84	0.640	0.645	0.662	- 2.57	$2NH_4NO_3 \cdot (NH_4)_2SO_4$
24.54	0.697	0.634	0.657	- 3.50	$2NH_4NO_3 \cdot (NH_4)_2SO_4$
25.02	0.758	0.627	0.651	- 3.69	$2NH_4NO_3 \cdot (NH_4)_2SO_4$
25.91	0.793	0.616	0.625	- 1.44	$2NH_4NO_3 \cdot (NH_4)_2SO_4$
25.30	1.000	0.626	0.615	1.79	NH_4NO_3

†Emons and Hahn[28]

*Silcock[27]

Table 4. Comparison of Calculated and Measured Water Activities for Dilute NH_4NO_3-$(NH_4)_2SO_4$

I	Y	a_w (Calc.)	a_w^* (Meas.)	% Error
1.288	0.25	0.9791	0.9788	0.03
0.882	0.25	0.9852	0.9852	0.00
0.597	0.25	0.9897	0.9896	0.01
0.289	0.25	0.9947	0.9948	-0.01

*Thudium[32]

and Peterson[33] are directly comparable. Saxena and Peterson[33] used Bromley's model with higher order coefficients. Their maximum error was 12.3%. Thus, the approach of Kusik and Meissner[5] is better suited for NH_4NO_3-$(NH_4)_2SO_4$ mixtures.

Finally, the influence of $(NH_4)_2SO_4$ on the NH_4NO_3 dissociation constant can be calculated. The appropriate equilibria for the NH_4NO_3-$(NH_4)_2SO_4$-H_2O system are listed in Table 5. As stated in the phase diagram discussion, the NH_4NO_3 dissociation constant would be invariant along the solubility curve between pure NH_4NO_3 in water and E_3 and in the regions I, I & II, II, II & III, III and III & IV and is given by the equilibrium constant of Reaction 1 in Table 5 and is independent of relative humidity. Within the aqueous solution region of the phase diagram, the NH_4NO_3 dissociation constant varies and is a function of Y and the ionic strength. From equations (51) and (54) and the equilibrium constant for Reaction 2 in Table 5, the water activity or relative humidity and the Y dependence of the NH_4NO_3 dissociation constant can be evaluated and are shown in Fig. 6. The dashed curve is obtained by calculating the relative humidity and the NH_4NO_3 dissociation constant along the solubility curve between E_3 and pure $(NH_4)_2SO_4$ in water. A striking feature of Fig. 6 is the insensitivity of the NH_4NO_3 dissociation constant to the ionic fraction of nitrate. For example, the NH_4NO_3 dissociation constant for Y = 0.5 varies from that of pure NH_4NO_3 in water by only 40%.

In addition to the NH_4NO_3 dissociation constant, the $(NH_4)_2SO_4$ dissociation constant relative humidity dependence can be evaluated from equations (53) and (54) and Reactions 3 and 4 of Table 5. Evaluation of the $(NH_4)_2SO_4$ dissociation constant is generally not merited because the dissociation

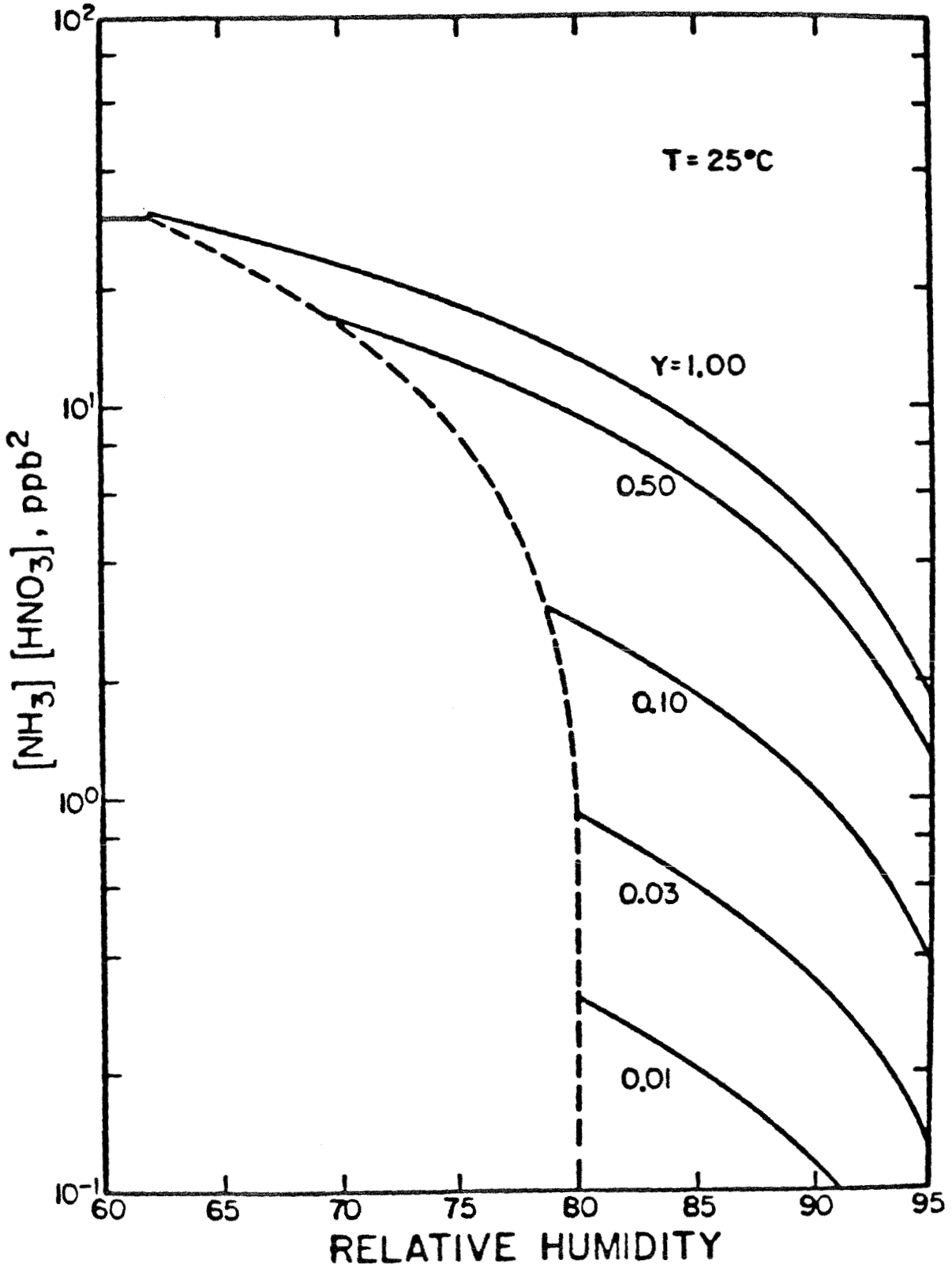

Figure 6

The effect of $(NH_4)_2SO_4$ on the relative humidity dependence of the NH_4NO_3 dissociation constant.[54]

Table 5. Equilibrium Constants for the NH_4NO_3-$(NH_4)_2SO_4$-H_2O System at 298 K.

Reaction	Equilibrium Constant*
1. $NH_4NO_3(c,IV) \rightleftarrows NH_3(g) + HNO_3(g)$	3.03×10^{-17}
2. $NH_4NO_3(aq) \rightleftarrows NH_3(g) + HNO_3(g)$	2.71×10^{-18}
3. $(NH_4)_2SO_4(c) \rightleftarrows 2NH_3(g) + H_2SO_4(g)$	2.33×10^{-38}
4. $(NH_4)_2SO_4(aq) \rightleftarrows 2NH_3(g) + H_2SO_4(g)$	2.62×10^{-38}

Free Energy Data Sources:

$NH_3(g)$, $NH_4NO_3(c,IV)$	Parker et al.[8]
$HNO_3(g)$, $H_2SO_4(g)$	JANAF[9]
$NH_4NO_3(aq,m=1)$, $(NH_4)_2SO_4(aq,m=1)$	Wagman et al.[10]

*Thermodynamic equilibrium constants - pressures in atmospheres, aqueous concentration in molality.

constant is small at 25°C. The amount of $(NH_4)_2SO_4$ precursor in the gas phase, the cubic root of the equilibrium constant for Reaction 3 expressed as $(NH_4)_2SO_4$, is about 0.002 μg m^{-3}. Thus, the relative humidity dependence of the $(NH_4)_2SO_4$ dissociation constant is not presented in detail.

THERMODYNAMICS OF THE ATMOSPHERIC SULFURIC ACID AMMONIUM SULFATE, WATER SYSTEM

All of the preceding systems have involved nitrate. Now, consider the system without nitrate, i.e. containing only sulfate. This system may be considered as a mixture of sulfuric acid and ammonium sulfate. The problem we are interested in is the following; given the temperature T, the relative humidity RH, and the background pressure of ammonia, determine the droplet composition, and the equilibrium pressure of sulfuric acid. That is, determine m_1, m_2, m_3, m_4, and $p_{H_2SO_4}$ where 1, 2, 3, 4 represent H^+, HSO_4^-, NH_4^+ and SO_4^{2-}, respectively. This system can be represented by the equilibria shown in Table 6. The constants were calculated from the free energy data shown in Table 7.

The equilibrium expressions may be written as,

$$K_1 = \frac{p_{H_2SO_4}}{a_1 a_2} \tag{56}$$

$$K_2 = \frac{a_1^2 a_4}{a_1 a_2} \tag{57}$$

$$K_3 = \frac{p_{H_2SO_4} p_{NH_3}}{a_3 a_2} \tag{58}$$

$$K_4 = \frac{p_{NH_3}^2 p_{H_2SO_4}}{a_3^2 a_4} \tag{59}$$

$$K_5 = \frac{p_{H_2O}}{a_w} \tag{60}$$

where a_i is the activity of the i-th species. Note that $K_5 = 1/p^o_{H_2O}$ where $p^o_{H_2O}$ is the vapor pressure of pure water. Thus, (60) may be rewritten as

$$a_w = RH \tag{61}$$

Making use of the mean molal activity coefficients previously defined $a_1a_2 = \gamma_{12}^2 m_1 m_2$ etc. Then (56)-(60) become

$$K_1 = \frac{P_{H_2SO_4}}{\gamma_{12}^2 m_2 m_1} \tag{62}$$

$$K_2 = \frac{\gamma_{14}^3 m_1^2 m_4}{\gamma_{12}^2 m_1 m_2} \tag{63}$$

$$K_3 = \frac{P_{NH_3} P_{H_2SO_4}}{\gamma_{32}^2 m_3 m_2} \tag{64}$$

$$K_4 = \frac{P_{NH_3}^2 P_{H_2SO_4}}{\gamma_{34}^3 m_3^2 m_4} \tag{65}$$

The activity coefficients as computed using the approach of Kusik and Meissner[5],

$$\ln \gamma_{12} = \frac{z_2}{(z_1+z_2)I}\left[m_2\left(\frac{z_1+z_2}{2}\right)^2 \ln \gamma_{12}^o + m_4\left(\frac{z_1+z_4}{2}\right)^2 \ln \gamma_{14}^o\right] + \frac{z_1}{(z_1+z_2)I}\left[m_1\left(\frac{z_1+z_2}{2}\right)^2 \ln \gamma_{12}^o + m_3\left(\frac{z_3+z_2}{2}\right)^2 \ln \gamma_{32}^o\right] \tag{66}$$

$$\ln \gamma_{32} = \frac{z_2}{(z_3+z_2)I}\left[m_2\left(\frac{z_3+z_2}{2}\right)^2 \ln \gamma_{32}^o + m_4\left(\frac{z_3+z_4}{2}\right)^2 \ln \gamma_{34}^o\right] + \frac{z_3}{(z_3+z_2)I}\left[m_3\left(\frac{z_3+z_2}{2}\right)^2 \ln \gamma_{32}^o + m_1\left(\frac{z_1+z_2}{2}\right)^2 \ln \gamma_{12}^o\right] \tag{67}$$

$$\ln \gamma_{14} = \frac{z_4}{(z_1+z_4)I}\left[m_4\left(\frac{z_1+z_4}{2}\right)^2 \ln \gamma_{14} + m_2\left(\frac{z_1+z_2}{2}\right)^2 \ln \gamma_{12}^o\right] + \frac{z_1}{(z_1+z_4)I}\left[m_1\left(\frac{z_1+z_4}{2}\right)^2 \ln \gamma_{14}^o + m_3\left(\frac{z_3+z_4}{2}\right)^2 \ln \gamma_{34}^o\right] \tag{68}$$

Table 6. Equilibrium Constants for the $(NH_4)_2SO_4$ - H_2SO_4-H_2O System at 298K

	Reaction	Equilibrium Constant
1.	$H^+ + HSO_4^- \rightleftarrows H_2SO_{4(g)}$	3.28×10^{-18}
2.	$H^+ + HSO_4^- \rightleftarrows 2H^+ + SO_4^{2-}$	1.03×10^{-2}
3.	$NH_4^+ + HSO_4^- \rightleftarrows H_2SO_{4(g)} + NH_{3(g)}$	3.00×10^{-29}
4.	$2NH_4^+ + SO_4^{2-} \rightleftarrows H_2SO_{4(g)} + 2NH_{3(g)}$	2.67×10^{-38}
5.	$H_2O_{(\ell)} \rightleftarrows H_2O_{(g)}$	3.11×10^{-2}

Table 7. Free Energy Data for the $(NH_4)_2SO_4$-H_2SO_4-H_2O System at 298 K

Species	G/RT	Reference
H^+	0	8
NH_4^+	-32.05	8
HSO_4^-	-304.93	8
SO_4^{2-}	-300.35	8
$H_2O_{(\ell)}$	- 95.684	8
$H_2SO_{4(g)}$	-264.67	9
$NH_{3(g)}$	- 6.632	8
$H_2O_{(g)}$	- 92.213	8

Table 8. Binary Activity Coefficients Required

			Reference
γ^{o}_{12}	NH_4^+	HSO_4^-	This work
γ^{o}_{14}	NH_4^+	SO_4^{2-}	Stelson & Seinfeld[54]
γ^{o}_{32}	H^+	HSO_4^-	This work
γ^{o}_{34}	H^+	SO_4^{2-}	This work

$$\ln \gamma_{34} = \frac{z_4}{(z_3+z_4)I}\left[m_4\left(\frac{z_3+z_4}{2}\right)^2 \ln \gamma^o_{34} + m_2\left(\frac{z_3+z_2}{2}\right)^2 \ln \gamma^o_{32}\right]$$
$$+ \frac{z_3}{(z_3+z_4)I}\left[m_3\left(\frac{z_3+z_4}{2}\right)^2 \ln \gamma^o_{34} + m_1\left(\frac{z_1+z_4}{2}\right)^2 \ln \gamma^o_{14}\right] \quad (69)$$

where z_1 is the magnitude of the charge on the i-th ion, i.e. $z_1=z_2=z_3=1$, $z_4=2$. Water activity can be computed from the Gibbs-Duhem equation (9) as follows. From (9) and (13)

$$- n_w d \ln a_w = \sum_i n_i \, d \ln a_i \quad (70)$$

where the sum is over all ions present. Take as the basis one kilogram of water. Use the definition of the mean molal activity coefficient to express the activities in terms of the activity coefficients. In order to do this, it is necessary to replace the sum over all ions i, by a sum over all molecules i-j. Doing this and integrating holding composition constant gives

$$- \frac{10^3}{M_w} \ln a_w = \sum_{ij}\left[m_{ij} + \int_0^I m_{ij} d \ln \gamma_{ij}\right] \quad (71)$$

Table 8 lists the sources of the various activity coefficients. The quantities $\ln \gamma^o_{12}$, $\ln \gamma^o_{32}$ and $\ln \gamma^o_{34}$ will be calculated in the following sections. Once these are known, equations (61)-(65) can be solved numerically as a system of five equations in five unknowns, m_1, m_2, m_3, m_4 and $P_{H_2SO_4}$.

Calculation of Activity Coefficients

Any solution containing bisulfate ions will contain sulfate ions formed by dissociation as well. However the quantities γ^o_{H,HSO_4} and $\gamma^o_{NH_4,HSO_4}$ refer to hypothetical solutions containing only bisulfate ions. Thus, they cannot be measured directly. Instead, they must be inferred by other means. The simplest system which can help us in our quest for these activity coefficients is the sulfuric acid-water system.

The amount of undissociated sulfuric acid in aqueous solution is negligible below 40 molal,[19,34] which corresponds to a relative humidity of less than one percent. Thus, sulfuric acid will be treated as a ternary system of sulfate, bisulfate and water. For this system, equation (27) gives

$$\ln a_{12} = \frac{2}{3}(1+2Y)\ln \gamma^{\circ}_{12} + \frac{3}{4}(1-Y)\ln \gamma^{\circ}_{14} + \ln \frac{(2+Y)YI^2}{3} \qquad (72)$$

$$\ln a_{14} = 2Y \ln \gamma^{\circ}_{12} + \frac{3}{4}(4-Y)\ln \gamma^{\circ}_{14} + \ln \frac{(2+Y)^2(1-Y)}{27} I^3 \qquad (73)$$

where 1, 2 and 4 represent H^+, HSO_4^- and SO_4^{2-}, respectively, and

$$Y = \frac{m_{HSO_4}}{m_{HSO_4} + 3m_{SO_4}} \qquad (74)$$

Consider now the equilibrium between sulfate and bisulfate,

$$H^+ + HSO_4^- \rightleftarrows 2H^+ + SO_4^{2-}$$

The equilibrium constant can be expressed as

$$\ln K_2 = \ln a_{14} - \ln a_{12} \qquad (75)$$

Substituting (56) and (57) in (59) gives

$$\ln K_2 = \frac{2}{3}(Y-1)\ln \gamma^{\circ}_{12} + \frac{9}{4}\ln \gamma^{\circ}_{14} + \ln \frac{(2+Y)(1-Y)}{9Y} I \qquad (76)$$

Also, the Gibbs-Duhem equation is

$$-n_w d\ell n a_w = n_{12}\, d\ell n a_{12} + n_{14}\, d\ell n a_{14} \tag{77}$$

where n_{12} and n_{14} are the numbers of moles of bisulfate and sulfate, respectively.

Now use (72) and (73) in (77) and integrate over I holding Y constant to obtain

$$\begin{aligned} - n_w \ell n a_w = {} & \frac{2Y}{3}(2+Y) I\, \ell n\, \gamma_{12}^{\circ} - \frac{2Y}{3}(2+Y) \int_0^I \ell n\, \gamma_{12}^{\circ}\, dI' \\ & + \frac{(1-Y)}{2}(2+Y) I \ell n\, \gamma_{14}^{\circ} - \frac{(1-Y)}{2}(2+Y) \int_0^I \ell n\, \gamma_{14}^{\circ}\, dI' + (1+Y)I \end{aligned} \tag{78}$$

Then $\ell n\, \gamma_{12}^{\circ}$ and $\ell n\, \gamma_{14}^{\circ}$ are found by solving the system of coupled ordinary differential equations corresponding to equations (76) and (78), that is

$$\begin{aligned} & \frac{2Y}{3}(2+Y) \frac{dU}{dI} + \frac{(1-Y)}{2}(2+Y) \frac{dV}{dI} \\ & = -\left(\frac{n_w}{I} \ell n\, a_w + 1 + Y \right) + \frac{2Y}{3I}(2+Y)U + \frac{(1-Y)}{2I}(2+Y)V \end{aligned} \tag{79}$$

$$\frac{2}{3}(Y-1) \frac{dU}{dI} + \frac{9}{4} \frac{dV}{dI} = \ell n\, (K_2/Q) \tag{80}$$

$$U(0) = V(0) = 0 \tag{81}$$

where

$$U(I) = \int_0^I \ell n\, \gamma_{12}^{\circ}\, dI'' \qquad V(I) = \int_0^I \ell n\, \gamma_{14}^{\circ}\, dI'' \tag{82}$$

and where the dissociation quotient Q is given by

$$Q = \frac{m_H m_{SO_4}}{m_{HSO_4}}$$

$$= \frac{(2+Y)(1-Y)I}{9Y} \qquad (83)$$

The quantity Y can then be calculated from Q by

$$Y = -\frac{1}{2}\left(1 + \frac{9Q}{I}\right) + \frac{1}{2}\left[\left(1 + \frac{9Q}{I}\right)^2 + 8\right]^{\frac{1}{2}} \qquad (84)$$

Away from I = 0 these two ordinary differential equations can be numerically integrated readily. The desired quantities, $\ell n\ \gamma^{\circ}_{12}$ and $\ell n\ \gamma^{\circ}_{14}$, are obtained as dU/dI and dV/dI, respectively. At I = 0, from the properties of activity coefficients, dU/dI and dV/dI are both zero.

The dissociation quotient Q has been measured by many investigators.[19,34-37] These values are shown in Figure 7. Also shown is a least squares fit to the data given by

$$\ell n\ Q = -4.5740 + 4.0071\sqrt{I} - 0.99893\ I + 0.13250\ I^{3/2} - 0.010675\ I^2 \qquad (85)$$

The water activity is based on the fit given by Rard et al.[38] Using equation (85), equations (79) and (80) were numerically integrated. The results of this integration are shown in Fig. 8. A comparison between the activity coefficient for H/HSO_4 and the activity coefficients of a number of other univalent acids is shown in Figure 9. Note the qualitative agreement between the activity coefficient of the bisulfate ion compared with the other acids.

Sulfuric Acid-Ammonium Sulfate System

Consider a system containing both ammonia and sulfuric acid. Examples of such systems are ammonium bisulfate and letovicite. This system will be modeled as a mixture of $2H/SO_4$, H/HSO_4, $2NH_4/SO_4$ and NH_4/HSO_4. The activity coefficients

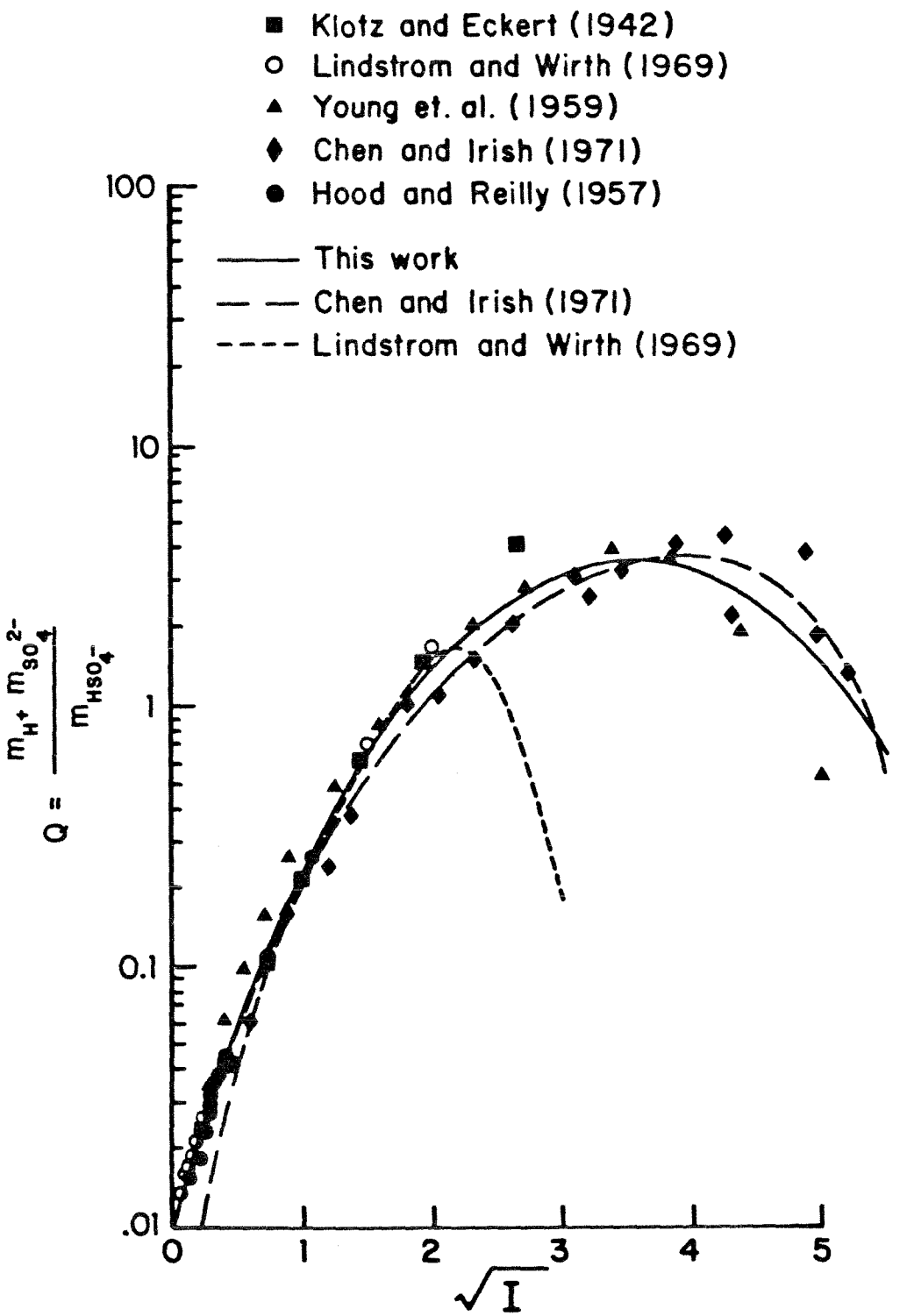

Figure 7

Bisulfate dissociation quotient as a function of ionic strength in aqueous sulfuric acid solutions.

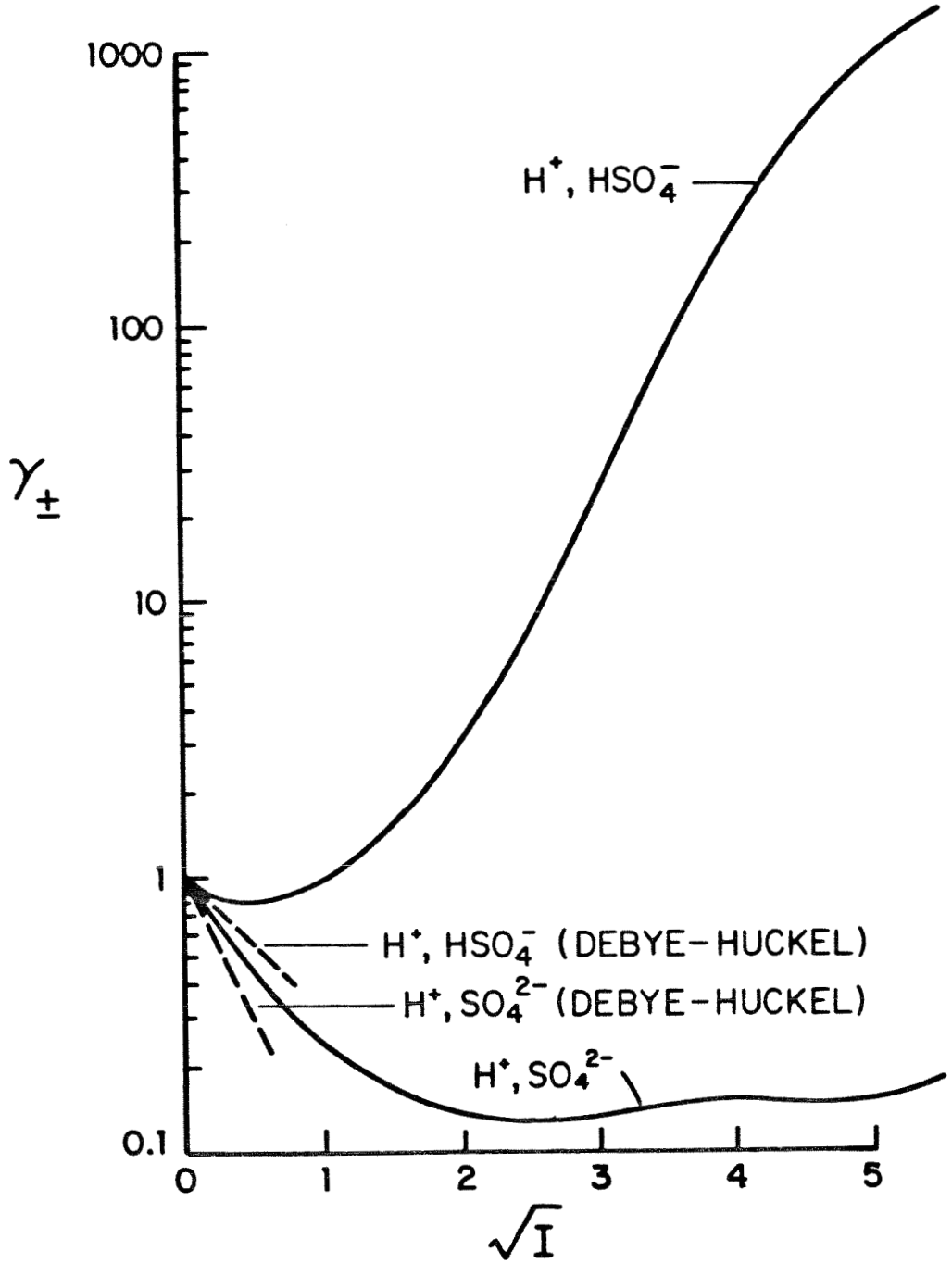

Figure 8

H^+/HSO_4^- and H^+/SO_4^{2-} activity coefficients as functions of ionic strength.

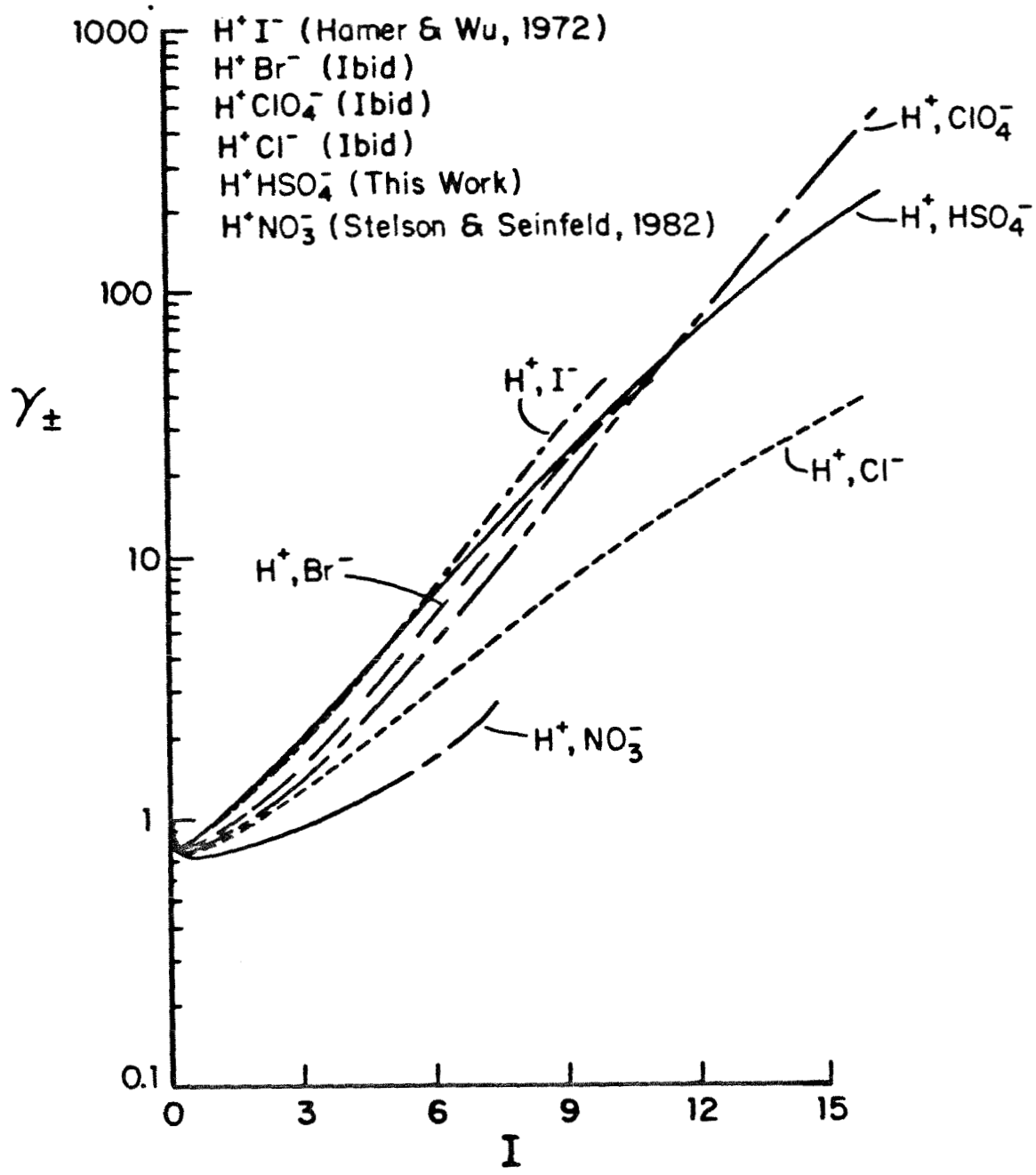

Figure 9

Comparison of the H^+ / HSO_4^- activity coefficient with those for other univalent acids.

of the first two species are known from the previous sections. The activity coefficient of the third was given by equation (55). Thus, the only remaining unknown is the activity coefficient for NH_4/HSO_4.

The activity coefficient for NH_4/HSO_4 will be assumed to be the same as for NH_4/Cl. This assumption is analogous to the approach adopted by Lee and Brosset[39] for the sulfuric acid system. A problem arises in that a solution of ammonium cloride is saturated at 7.4 molal. Thus, it is necessary to extrapolate to higher concentrations. The activity coefficient is linear in ionic strength for moderate concentrations. Thus, it will be linearly extrapolated to higher strengths.

Using these activity coefficients a series of runs were made for the ammonium bisulfate system. This system is derived from the original system by replacing reactions 3 and 4 by reaction 6 where

$$\text{reaction 6} = (\text{reaction 3}) - \frac{1}{2}(\text{reaction 1} + \text{reaction 4})$$

i.e.

$$NH_4^+ + HSO_4^- \rightleftarrows NH_4^+ + H^+ + SO_4^{2-}$$

$$K_6 = \frac{\left(\gamma_{14}\gamma_{34}\right)^{3/2} m_1 m_3 m_4}{\gamma_{32}^2 m_3 m_2}$$

$$K_6 = 1.03 \times 10^{-2}$$

The results are shown in Figure 10. The agreement with the experimental results of Tang and Munkelwitz[40] is seen to be good.

Conclusions

The ammonium sulfate-sulfuric acid system has been studied. Activity coefficients have been obtained for the various species present. The agreement between the activity coefficient of H/HSO_4^- and other univalent acids is good.

Calculations of the water activity over these solutions have been performed. The agreement with experimental data is good.

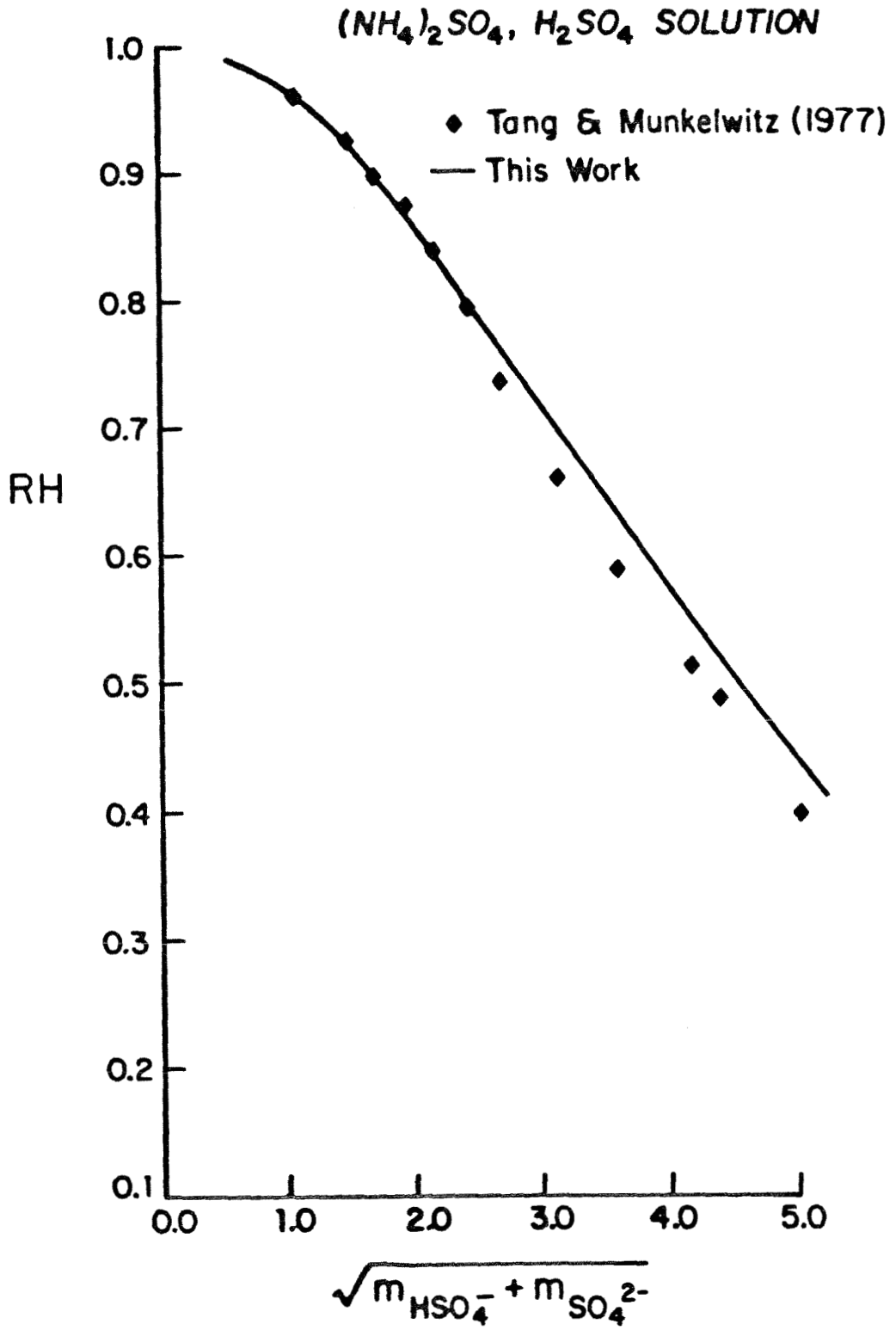

Figure 10

Comparison of experimental and predicted water activities as a function of molality for ammonium sulfate/sulfuric acid solutions.

RELATIVE HUMIDITY AND TEMPERATURE DEPENDENCE OF THE AMMONIUM NITRATE DISSOCIATION CONSTANT[55]

Up to this point we have restricted our attention to systems at 25°C. We now address the issue of extrapolating the thermodynamic results to other temperatures. For this extrapolation it will be necessary to have access to enthalpy and heat capacity data. This section will illustrate the calculation of thermodynamic properties for one particular system, the aqueous ammonium nitrate system.

Theory and Thermodynamic Data for the Ammonium Nitrate System

Solid NH_4NO_3 dissociation constant

At temperatures below 170°C, solid ammonium nitrate exists in equilibrium with ammonia and nitric acid:

$$NH_4NO_3(s) \rightleftarrows NH_3(g) + HNO_3(g).$$

The equilibrium constant for this reaction, K_p', is related to the partial pressures of NH_3 and HNO_3 by $K_p' = p_{NH_3} p_{HNO_3}$, and K_p' is related to the standard Gibbs free energy change for reaction, ΔG_T°, by

$$\Delta G_T^\circ = - RT \ln K_p' \tag{86}$$

Since the thermodynamic data for NH_4NO_3 are limited, an extrapolation formula for the equilibrium constant as a function of temperature can be derived as follows. Start with the van't Hoff equation,

$$\frac{d \ln K_p}{dT} = \frac{\Delta H}{RT^2} \tag{87}$$

where ΔH is the change in enthalpy of the reaction at temperature T. By definition,

$$\frac{d\Delta H}{dT} = C_{p_{NH_3}} + C_{p_{HNO_3}} - C_{p_{NH_4NO_3}} \tag{88}$$

$$\Delta V \approx V_{gas} \approx \frac{RT}{p} \tag{93}$$

Using equation (93) in (92) gives

$$\frac{dp}{dT} = \frac{Lp}{RT^2} \tag{94}$$

Equation (94) may be integrated, assuming L is constant, to give

$$\ln \frac{p_1}{p_o} = \frac{-L}{R}\left(\frac{1}{T_1} - \frac{1}{T_o}\right) \tag{95}$$

Now, p is proportional to the relative humidity of deliquescence. Thus,

$$\ln (RHD) = \ln (RHD)_{298} - \frac{L}{R}\left(\frac{1}{T} - \frac{1}{298}\right) \tag{96}$$

where RHD is the percent relative humidity of deliquescence.

Using the water heat of fusion from Weast[14] and the relative humidity of a saturated NH_4NO_3 solution at 298.15 K from Hamer and Wu[7],

$$\ln (RHD) = \frac{723.7}{T} + 1.7037 \tag{97}$$

Equation (97) agrees well with the least square expression derived from the data of Dingemans[42],

$$\ln (RHD) = \frac{856.23 \pm 13.25}{T} + 1.2306 \pm 0.0439 \tag{98}$$

Equations (97) and (98) are shown with experimental data in Fig. 11.

We estimate the effect of temperature on solubility as follows. The van't Hoff equation is

$$\frac{\bar{H}_s - h_s}{RT^2} = \left(\frac{\partial \ln K_p}{\partial T}\right) = \left(\frac{\partial \ln (\gamma^2_{NH_4NO_3} m^2)}{\partial T}\right) \tag{99}$$

where $\bar{H}_s$ and h_s are the partial molal enthalpies in the saturated solution and crystal phase respectively. This relation becomes

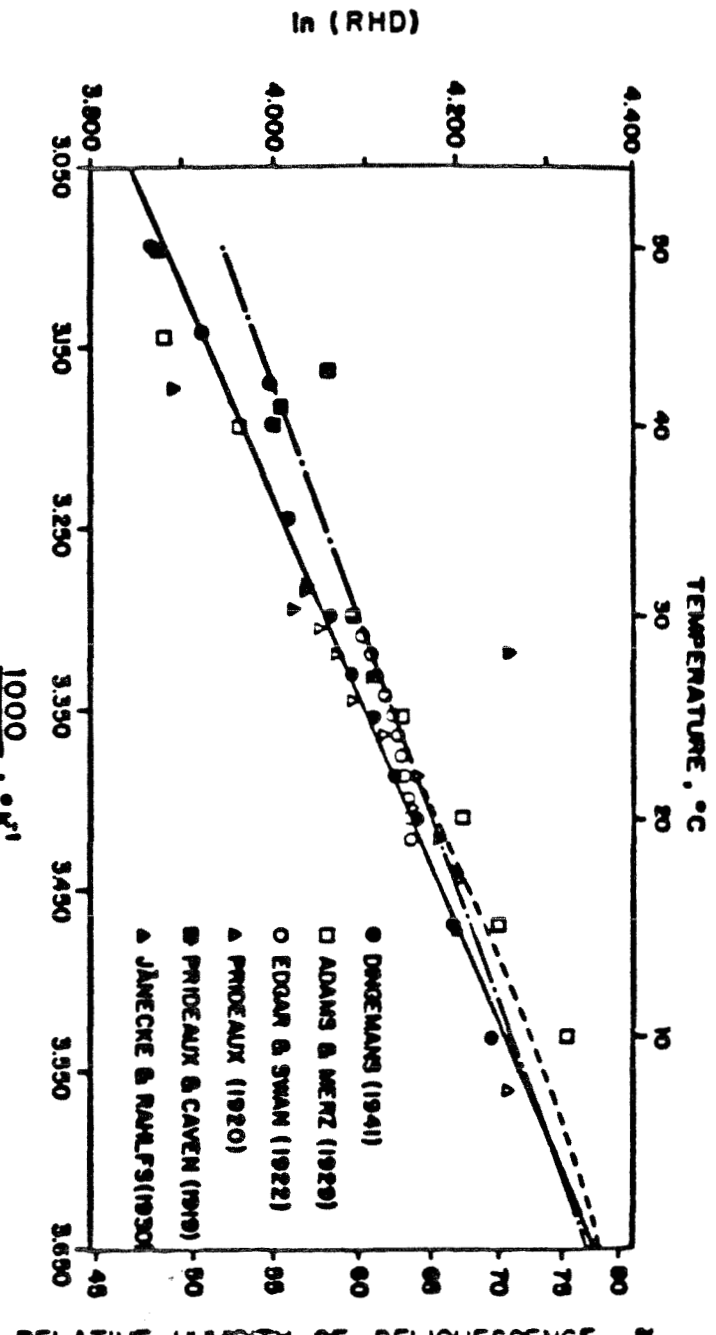

Figure 11

Temperature dependence of the NH_4NO_3 relative humidity of deliquescence (·---·) Equation (97); (——) Equation (98);--- Equations (105), (111), (117) and (118).[55]

where $C_{p_{NH_3}}$, $C_{p_{HNO_3}}$, and $C_{p_{NH_4NO_3}}$ are the heat capacities of $NH_{3(g)}$, $HNO_{3(g)}$ and $NH_4NO_{3(s)}$, respectively. Integrating equation (88) gives

$$\Delta H = \Delta H_o + \int_{298}^{T'} \left(C_{p_{NH_3}} + C_{p_{HNO_3}} - C_{p_{NH_4NO_3}} \right) dT' \qquad (89)$$

where ΔH_o is the change in enthalpy at 298K. Using equation (89) in the van't Hoff equation and integrating gives

$$\ell n\ K_p' = \ell n\ K_{p_{298}} - \frac{\Delta H_o}{R} \left(\frac{1}{T} - \frac{1}{298} \right) + \int_{298}^{T} \frac{1}{RT''^2} \int_{298}^{T'} \left(C_{p_{NH_3}} + C_{p_{HNO_3}} - C_{p_{NH_4NO_3}} \right) dT' dT'' \qquad (90)$$

Using the data in Table 9 and assuming the heat capacities are independent of temperature, we obtain from equation (90),

$$\ell n\ K_p' = 84.6 - \frac{24220}{T} - 6.1\ \ell n \left(\frac{T}{298} \right) \qquad (91)$$

where K_p' is the equilibrium constant in units of ppb^2.

Relative humidity of deliquescence and solubility

Now, consider the saturated solution relative humidity. Start with the Clausius-Clapeyron equation

$$\frac{dp}{dT} = \frac{L}{T\Delta V} \qquad (92)$$

where L is the latent heat of vaporization of water, and ΔV is the change in volume during vaporization. The left hand side represents the change in pressure required to maintain equilibrium when the temperature changes by dT. Now, consider the volume change during vaporization. The volume of the liquid is negligible compared to that of the gas. Thus, using the ideal gas law

$$\frac{\overline{H}_s - h_s}{RT^2} = \left(\frac{\partial \ell n m^2}{\partial T}\right) + \left(\frac{\partial \ell n \gamma^2}{\partial T}\right) + \left(\frac{\partial m}{\partial T}\right)\left(\frac{\partial \ell n \gamma^2}{\partial m}\right) \tag{100}$$

$$\left(\frac{\partial \ell n m^2}{\partial T}\right) = \frac{\overline{H}^\circ - h_s}{RT^2} - \left[\frac{\overline{H}^\circ - \overline{H}_s}{RT^2} + \frac{\partial \ell n \gamma^2}{\partial T} + \frac{\partial m}{\partial T}\frac{\partial \ell n \gamma^2}{\partial m}\right] \tag{101}$$

where H° is the partial molal enthalpy at infinite dilution. The terms in the brackets on the right hand side of (101) give the effects of nonidealities. In order to obtain a rough estimate of the behavior of $\ell n m^2$, we will assume that these terms are negligible. There results

$$\frac{\partial \ell n m^2}{\partial T} = \frac{\overline{H}^\circ - h_s}{RT^2} \tag{102}$$

By integrating equation (86),

$$\ell n\ m = -\frac{(\overline{H^\circ} - h_s)}{2R}\left(\frac{1}{T} - \frac{1}{298}\right) + \ell n(m)_{298} \tag{103}$$

is obtained. Using the thermodynamic data in Table 6 and noting that $(m)_{298} = 25.954$ from Hamer and Wu[7],

$$\ell n\ m = -\frac{1600}{T} + 8.6228 \tag{104}$$

Equation (104) agrees well with the least squares expression for the data of Stephen and Stephen[43],

$$\ell n\ m = -\frac{1837.3 \pm 18.0}{T} + 9.4235 \pm 0.0602 \tag{105}$$

Equations (104) and (105) are shown with the data of Stephen and Stephen[43] in Fig. 12.

Figures 11 and 12 show the strong temperature dependence of the relative humidity of deliquescence and the solubility of ammonium nitrate. This temperature dependence is an unfortunate complication when attempting to

Table 9. Thermodynamic Data for the Ammonium Nitrate System at 298 K

Species	$\frac{\Delta G}{R}(K^{-1})$	$\frac{\Delta H}{R}(K^{-1})$	$\frac{C_p}{T}$	Reference
$NH_3(g)$	-1977	-5526	4.285	8,9
$HNO_3(g)$	-8903	-16,155	6.416	9
$NH_4NO_3(c,IV)$	-22,220	-44,080	16.8	8,10
$NH_4NO_3(aq,m = 1)$	-22,940	-40,880	-0.505	10,41

ΔG = Standard free energy of formation

ΔH = Heat of formation

C_p = Heat capacity.

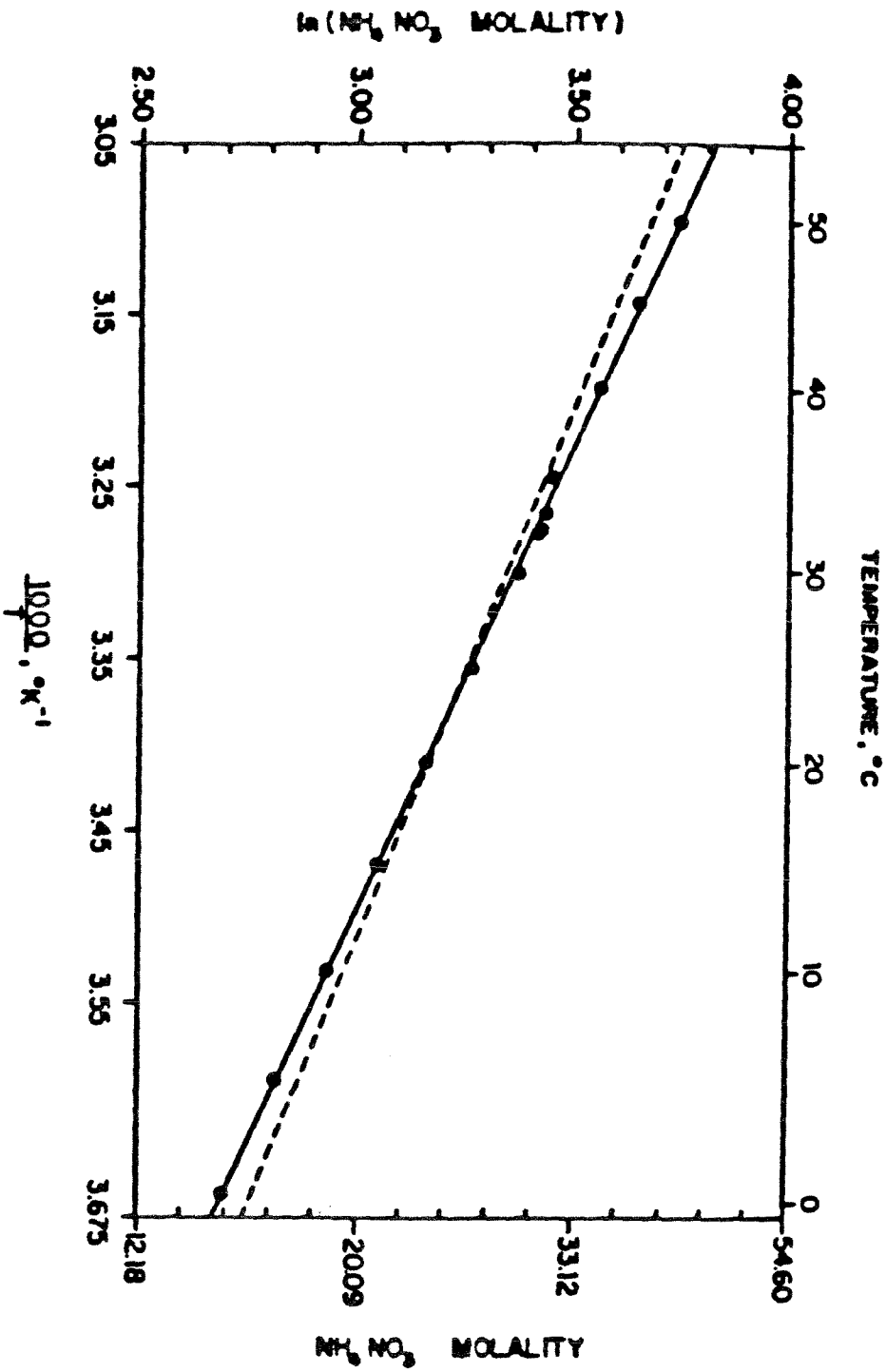

Figure 12

Temperature dependence of the NH_4NO_3 solubility:[55] (——) Equation (105) (--) Equation (104) Data[3] from Stephen and Stephen[43]

extrapolate aqueous ammonium nitrate thermodynamic data to temperatures above 25°C.

Aqueous NH_4NO_3 dissociation constant

Analogous to the solid NH_4NO_3 dissociation constant derivation, an expression for the equilibrium constant over aqueous NH_4NO_3 can be derived,

$$\ln K_p^* = \alpha - \frac{\Delta H_o}{RT} + \int_{298}^{T} \frac{1}{RT''^2} \int_{298}^{T''} \left(C_{PNH_3} - C_{p_{HNO_3}} - \overline{C_p^o} \right) dT' dT'' \qquad (106)$$

where $K_p^* = p_{NH_3} p_{HNO_3} / a_{NH_4NO_3} = K_p' / a_{NH_4NO_3}$, $a_{NH_4NO_3} = \gamma^{\pm 2}_{NH_4NO_3} m^2$, $\overline{C_p^o}$ = NH_4NO_3 partial molal heat capacity at infinite dilution, and $\gamma^{\pm}_{NH_4NO_3}$ = mean molal ionic activity coefficient of dissolved NH_4NO_3. Using the data in Table 9 and assuming the heat capacities are independent of temperature, we obtain from equation (106)

$$\ln K_p^* = \ln \frac{K_p'}{a_{NH_4NO_3}} = 54.18 - \frac{15,860}{T} + 11.206 \ln \left(\frac{T}{298} \right) \qquad (107)$$

where K_p^* has units of ppb^2 $molal^{-2}$. The temperature variation of $\gamma^{\pm}_{NH_4NO_3}$ can be calculated as follows:

$$\left(\frac{\partial \ln \gamma^{\pm}_{NH_4NO_3}}{\partial T} \right)_p = \frac{\overline{H^o} - \bar{H}}{2RT^2} \qquad (108)$$

The temperature variation of $\gamma^{\pm}_{NH_4NO_3}$ can be calculated as follows. Start with the expression for the chemical potential for ammonium nitrate (16)

$$\mu_{NH_4NO_3} = \mu^{\circ}_{NH_4NO_3} + RT \ln \left(\gamma^{2\pm}_{NH_4NO_3} m^2_{NH_4NO_3} \right) \tag{109}$$

Divide by RT and differentiate with respect to temperature at constant molality,

$$\frac{\bar{H}^* - \bar{H}}{RT^2} = \left(\frac{\partial \ln \gamma^2_{NH_4NO_3}}{\partial T} \right)_p \tag{110}$$

where H* is the partial molal enthalpy at the hypothetical standard state. However, H* must equal H°. This is because (110) must hold at all values of molality. As the molality approaches zero, $\ln \gamma_{NH_4NO_3}$ approaches zero. Thus, the right hand side approaches zero, assuming that $\ln \gamma_{NH_4NO_3}$ is a smooth function. Thus, the left hand side must also approach zero. This means that $\bar{H}$ approaches $\bar{H}^*$ as the molality approaches zero. However, the value of $\bar{H}$ at infinite dilution has been defined as $\bar{H}^\circ$. Thus,

$$\left(\ln \gamma^{\pm}_{NH_4NO_3} \right)_T = \left(\ln \gamma^{\pm}_{NH_4NO_3} \right)_{298} + \left(\frac{\bar{H} - \bar{H}^\circ}{2R} \right)_{298}$$

$$\cdot \left(\frac{1}{T} - \frac{1}{298} \right) - \left(\frac{\bar{C}_p - \bar{C}^\circ_p}{2R} \right) \left(\ln \frac{T}{298} + \frac{298}{T} - 1 \right) \tag{111}$$

is obtained, where $\bar{C}^\circ_p$, $\bar{C}_p$ = NH_4NO_3 partial molal heat capacities at infinite dilution and m, respectively, and $\left(\frac{\bar{H} - \bar{H}^\circ}{R} \right)_{298}$ = the normalized NH_4NO_3 relative partial molal enthalpy difference between infinite dilution and m at 298.15 K. To evaluate $(\ln \gamma^{\pm}_{NH_4NO_3})_T$, the concentration dependence of $\left(\ln \gamma^{\pm}_{NH_4NO_3} \right)_{298}$, $\left(\frac{\bar{H} - \bar{H}^\circ}{R} \right)_{298}$ and $\left(\frac{\bar{C}_p - \bar{C}^\circ_p}{R} \right)$ must be known. The expression of Hamer and Wu[7] can be used to represent the concentration dependence of $\left(\ln \gamma^{\circ}_{NH_4NO_3} \right)_{298}$ to 25.954 molal. Obtaining expressions for $\left(\frac{\bar{H} - \bar{H}^\circ}{R} \right)_{298}$ and $\left(\frac{\bar{C}_p - \bar{C}^\circ_p}{R} \right)$ is more complicated.

Relative apparent molal heat content data can be obtained from Wagman et al.[10] and Vanderzee et al.[44] . Since the data of Vanderzee et al.[44] are more recent and span a larger concentration range, they will be used to represent the variation in enthalpy with concentration. A polynomial regression can be calculated using ideal gas constant normalized relative apparent molal heat content data of Vanderzee et al.[44] between 0.1 and 25 molal. The partial molal enthalpy was derived using equation (8-2-7) from Harned and Owen[45], as

$$(\bar{H}-\bar{H}^{\circ}) = \phi_L + m\frac{\partial(\phi_L)}{\partial m} \qquad (112)$$

where ϕ_L = relative apparent molal heat content at m. The resulting polynomial regression is

$$\left(\frac{\bar{H}-\bar{H}^{\circ}}{R}\right)_{298} = 297.85\ m^{1/2} - 983.98\ m + 508.08\ m^{3/2} - 133.86\ m^2 + 19.328\ m^{5/2} - 1.2071\ m^3 \qquad (113)$$

where the standard deviation for the normalized relative apparent molal heat content polynomial regression is $\pm 3.54\ K^{-1}$. The error in the relative partial molal enthalpy polynomial regression is unknown since it was obtained using the normalized relative apparent molal heat content polynomial regression and (112).

Roux et al.[43] measured the apparent molal heat capacity, ϕ_{C_p}, of aqueous ammonium nitrate at 25°C to 22.4 molal. Their expression for their data,

$$\frac{\phi_{C_p}}{R} = -0.505 + 3.482\ m^{1/2} + 3.159\ m - 1.605\ m^{3/2} + 0.274\ m^2 - 0.0161\ m^{5/2}\ , \qquad (114)$$

agrees well with the measurements of Gucker et al.[46] and Sorina et al.[47] . Using equation (8-4-7) from Harned and Owen[45],

$$\bar{C}_p = \phi_{C_p} + m \frac{\partial \phi_{C_p}}{\partial m} \tag{115}$$

the partial molal heat capacity can be calculated from (98) as,

$$\frac{\bar{C}_p}{R} = -0.505 + 5.223\, m^{1/2} + 6.318\, m - 4.013\, m^{3/2} + 0.822\, m^2 - 0.0564\, m^{5/2} \tag{116}$$

The data of Sorina et al.[47] extend to 50 molal, supersaturation at 25°C. With relative apparent molal heat content and solute activity data to 50 molal, the temperature extrapolation of $\gamma^{\pm}_{NH_4NO_3}$ could be performed to saturation at 50°C. Unfortunately, the relative apparent molal heat content data are limited to 25 molal[44]. Even though (116) is based on data to 22.4 molal, it will be used to 25 molal. Within the region 22.4-25 molal, (116) is a smoothly continuous extrapolation of the data below 22.4 molal and represents the data of Gucker et al.[46] and Sorina et al.[47] fairly well.

Once $(\ell n\ \gamma^{\pm}_{NH_4NO_3})_T$ has been calculated, the osmotic coefficient of the solution, ϕ , can be derived from the Gibbs-Duhem equation,

$$\phi = 1 + \frac{1}{m} \int_0^m m d(\ell n\ \gamma^{\pm}_{NH_4NO_3})_T \cdot \tag{117}$$

The per cent relative humidity at temperature T, RH , can be calculated from

$$RH = 100 \exp\left(- \frac{\nu m M \phi_T}{1000} \right) \tag{118}$$

where ν = the number of moles of ions formed by the ionization of one mole of solute and M = molecular weight of water.

Results

By using appropriate expressions for the temperature dependence of solid or aqueous phase NH_4NO_3 thermodynamic properties, the dissociation constant can be calculated at a specific temperature and relative humidity. With (98), the form of ammonium nitrate, solid or aqueous, can be determined. At a specific temperature the NH_4NO_3 dissociation constant is invariant below the relative humidity of deliquescence and can be obtained from (91). Above the relative humidity of deliquescence, the NH_4NO_3 dissociation constant relative humidity dependence can be calculated from (107), (111), (117) and (118) to 25 molal. Equation (105) is used to calcualte the solubility temperature dependence. Figure 13 has been constructed using the previously mentioned techniques. Notice discontinuities exist between the solid NH_4NO_3 dissociation constant and the dissociation constant for a saturated solution at 25°C and below.

The possible sources of these discontinuities at temperatures below 25°C are manifold and the relative error from each source is difficult to evaluate. First, the temperature extrapolations for the solid NH_4NO_3 and the aqueous NH_4NO_3 dissociation constants are based on different thermodynamic data sets so an inconsistent value in one data set can cause discontinuity. Second, the relative humidity of deliquescence is obtained by different methods for solid NH_4NO_3 and aqueous NH_4NO_3. The relative humidity of deliquescence for solid NH_4NO_3 was calculated from (98) and aqueous NH_4NO_3 from (105), (110), (117) and (118). The relative error can be seen by comparing the solid and dashed curves in Fig. 11. Third, error is introduced by differentiating the polynomial regressions obtained for the relative apparent molal heat content and the apparent molal heat capacity to get expressions for the partial molal enthalpy and heat capacity. The amount of error is known for the original polynomial regressions but not for the derived regressions. Finally, the error must be introduced by the enthalpy, heat capacity, relative humidity of deliquescence or solubility

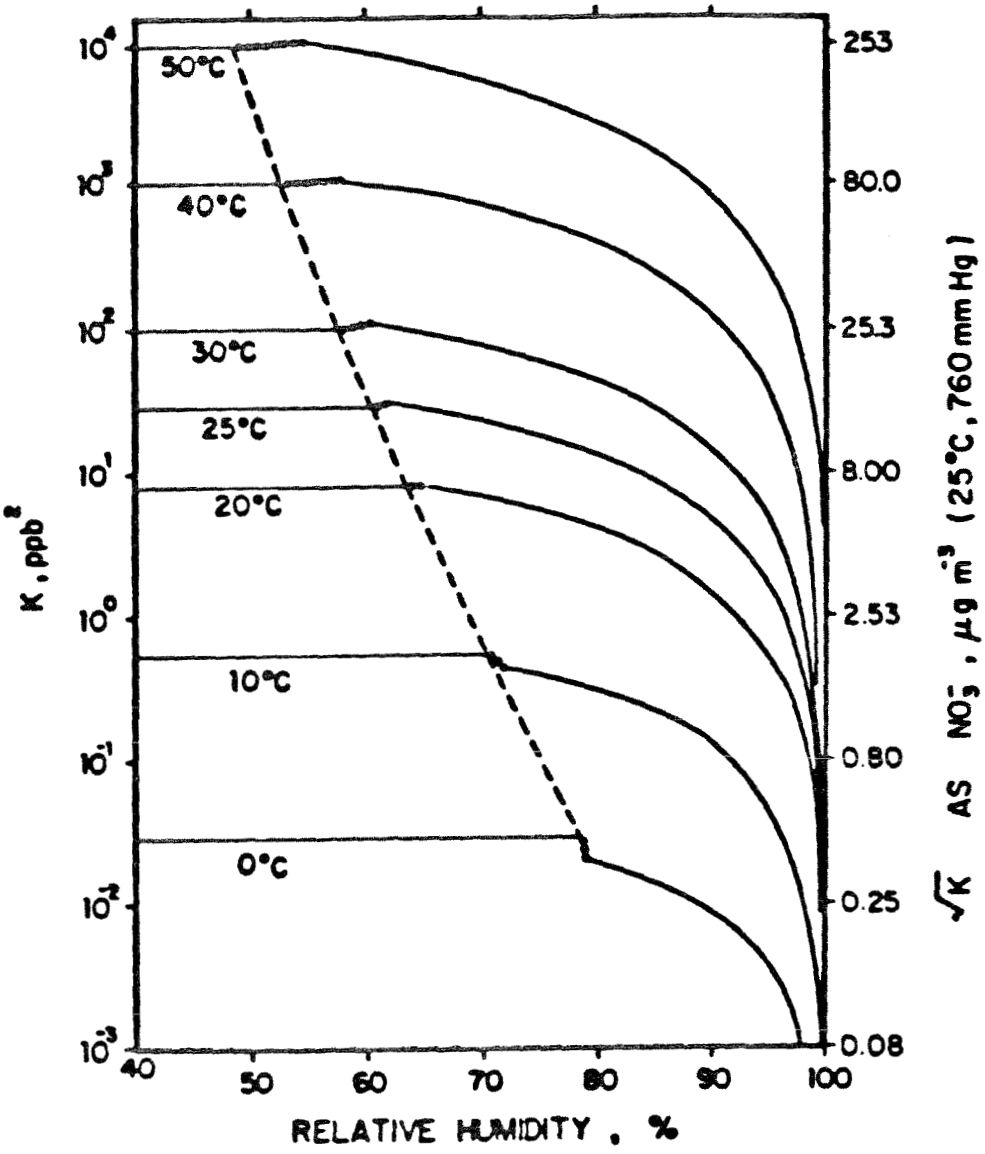

Figure 13

Temperature and relative humidity dependence of the NH_4NO_3 dissociation constant (---) solid NH_4NO_3 to aqueous NH_4NO_3 solution transition predicted from Equation (104);(—) Isothermal prediction of NH_4NO_3 dissociation constant for solid NH_4NO_3 and non-ideal NH_4NO_3 solutions at indicated temperatures (•••••) Extrapolation between predicted solid and maximum calculable aqueous NH_4NO_3 dissociation constant.[55]

data or the temperature extrapolation technique, since the free energy data are consistent at 298 K.

Above 25°C, an interpolation must be performed between the relative humidity corresponding to 25 molal and saturation. Since the curves are fairly flat in the region between 25 molal and saturation, a linear interpolation between the dissociation constant at 25 molal and at saturation should approximate the dissociation constant in this region.

The temperature dependence of the saturated solution relative humidity can be calculated using (105), (111), (117) and (118) for temperatures below 25°C. A curve calculated using this method is shown in Fig. 14.

Data for the molal variation of the solution relative humidity at various temperatures are shown in Fig. 14.[48-52] The data scatter is considerable and shows no definite temperature variation trend. Curves for the relative humidity concentration dependence were calculated at 0, 25 and 50°C using (111), (117) and (118) and are shown in Fig. 14. The predictions coincide with the general area of the data but do not show agreement with any particular data set. Also shown in Fig. 14 is the relative humidity concentration dependence for an ideal NH_4NO_3 solution which poorly predicts the non-ideal NH_4NO_3 behavior.

Figure 14 illustrates the infeasibilty of attempting to use water activities at higher temperatures, 25-50°C, and the Gibbs-Duhem equation to calculate solute activities. The data have too much scatter and are too sparse at any particular temperature. Furthermore, the maximum concentration of existing water activity data is 29.2 molal and saturation is 42 molal at 50°C.

Effect of an Unreactive Solute

The effect of an unreactive solute in solution with ammonium nitrate on the ammonia-nitric acid partial pressure can be evaluated qualitatively. From the Gibbs-Duhem equation,

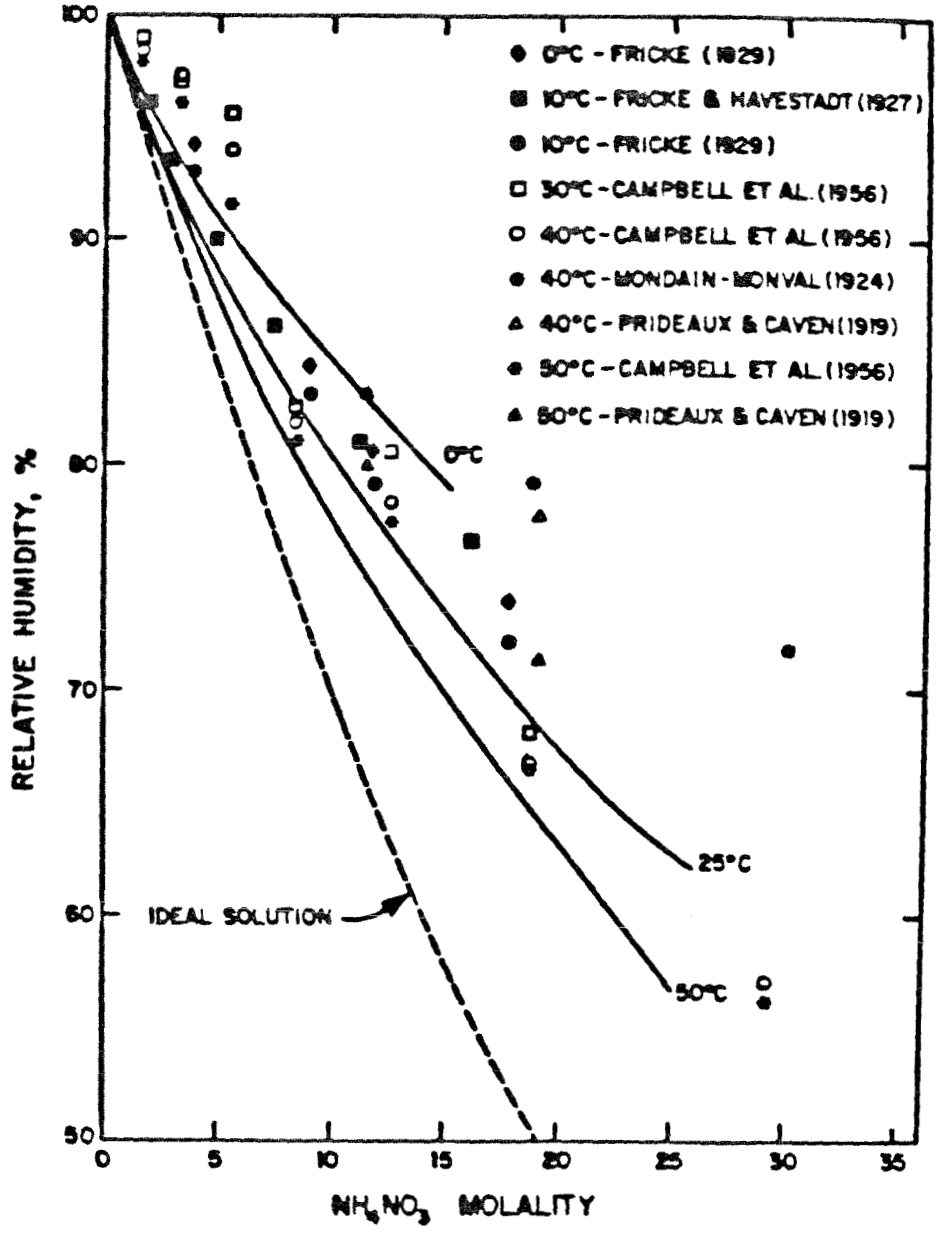

Figure 14

Temperature and concentration dependence of NH_4NO_3 solution relative humidity (----) ideal solution prediction; (——) non-ideal solution predictions at 0, 25, and 50°C.[35]

$$RH = 100 \exp\left(\frac{-M}{1000}\left[\int_0^m m \, d \, \ell n a_{NH_4NO_3} + \int_0^{m_1} m_1 \, d \, \ell n a_1\right]\right) \quad (119)$$

where m_1 = molality of inert solute and a_1 = activity of inert solute. Assuming the inert solute is ideal and undissociated,

$$RH = 100 \exp\left(\frac{-M}{1000}\left[\int_0^m m \, d \, \ell n a_{NH_4NO_3} + m_1\right]\right) \quad (120)$$

Equation (120) shows the addition of an ideal inert solute would decrease the relative humidity above an ammonium nitrate solution for a specific ammonium nitrate molality. Since the additional solute is assumed not to interact with the dissolved ammonium nitrate, the ammonia-nitric acid partial pressure product would be the same as in the situation without any inert solute. Thus, the presence of an inert solute results in an ammonia-nitric acid partial pressure product being observed at a lower relative humidity than would be predicted from the pure ammonium nitrate-water system.

CONCLUSIONS

The thermodynamic properties of three aqueous systems systems have been considered in detail:

(1) $NH_4NO_3/HNO_3/H_2O$

(2) $NH_4NO_3/(NH_4)_2SO_4/H_2O$

(3) $(NH_4)_2SO_4/H_2SO_4/H_2O$

The theory and techniques presented in this chapter enable one to calculate the vapor pressure and thermodynamic properties of any aqueous system of nitrate, sulfate, ammonium, nitric and sulfuric acids. For example, all the activity coefficients required to study the full NH_4NO_3-HNO_3-$(NH_4)_2SO_4$-H_2SO_4- H_2O system are now known. In addition, techniques for estimating the temperature dependence can be applied to the other systems considered here.

ACKNOWLEDGMENT

This work was supported by U.S. Environmental Protection Agency grant R806844.

NOTATION

a_i	activity of the i-th species, mol (kg water)$^{-1}$
a_{ij}	activity of the dissociated molecule ij, mol(kg water)$^{-1}$
a_w	total water activity
$(a_w^o)_{ij}$	water activity in a binary solution of ij
$(a_w)_{mix}$	water activity in a mixture (dimensionless)
A	constant in equations (18) and (20), equal to 1.17625 (kg water)$^{\frac{1}{2}}$ mole$^{-\frac{1}{2}}$ for water at 25°C
A_j,A_k	designations for various species
b	constant in equations (18) and (19), (kg water)$^{\frac{1}{2}}$ mol$^{-\frac{1}{2}}$
$C_{p_{NH_3}}$,$C_{p_{HNO_3}}$, $C_{p_{NH_4NO_3}}$	heat capacities of $NH_{3(g)}$, $HNO_{3(g)}$, and $NH_4NO_{3(g)}$ respectively, cal/mol K
$\overline{C}_p^{\circ}$ C_p	partial molal heat capacities of NH_4NO_3 at infinite dilution and molality m respectively, cal/mol K
d	density of the solution, g/cm^3
d_o	density of pure water, g/cm^3
$d\alpha$	number of moles undergoing a transformation,mol
D	molecular diffusivity, cm^2/s
$f_i(r)$	growth coefficient for component i, µg/s ppb
G	total Gibbs free energy, kcal
h_s	partial molal enthalpy of $NH_4NO_{3(s)}$, kcal/mol
$\overline{H}_s$	partial molal enthalpy of $NH_4NO_{3(aq)}$ in a saturated solution, kcal/mol
$\overline{H}^{\circ}$,$\overline{H}$	partial molal enthalpy of $NH_4NO_{3(aq)}$ at infinite dilution and molality m, respectively, kcal/mol
$\overline{H}^*$	partial molal enthalpy of $NH_4NO_{3(aq)}$ at the hypothetical standard state kcal/mol

I ionic strength, mol (kg water)$^{-1}$

K_a, K_b, K_c equilibrium constants for the formation of various undissociated nitric acid species

K_N total nitric acid dissociation constant, mol/ℓ

K'_p equilibrium constant for the reaction $NH_4NO_{3(s)} \rightleftarrows NH_{3(g)} + HNO_{3(g)}$ at a temperature T

$K'_{p_{298}}$ equilibrium constant for the reaction $NH_4NO_{3(s)} \rightleftarrows NH_{3(g)} + HNO_{3(g)}$ at 25°C, atm^2

K^*_p equilibrium constant for the reaction $NH_4NO_{3(aq)} \rightleftarrows NH_{3(g)} + HNO_{3(g)}$ at a temperature T, atm^2 (kg water)/mol

$K_1, K_2, K_3, K_4, K_5, K_6$ equilibrium constants given in Tables 2, 5 and 6

L latent heat of vaporization, kcal/mol

m molality of solute, mol (kg water)$^{-1}$

m_i molality of the i-th species, mol (kg water)$^{-1}$

m_{ij} molality of component i-j, mol (kg water)$^{-1}$

m_s stoichiometric molality of nitric acid , total moles nitrate per kg water

M molecular weight, g/mol

n number of molecules of solute

n_i number of moles of the i-th component in the system, mol

n_w number of moles of water in the system, mol

p_o reference pressure .1 atm

p_i partial pressure of the i-th component, atm

p_{i_s} partial pressure of the i-th component in equilibrium with a particle, ppb

$p^\circ_{i_s}$ partial pressure of the i-th component in equilibrium with a solution having the same composition as the particle but having a flat interface, ppb

p_{i_∞}	partial pressure of the i-th component far from the particle (ppb)
Q	dissociation quotient for HSO_4^-, mol (kg water)$^{-1}$
r	particle radius, μm
R	gas law constant, atm cm^3/K mol
RH	relative humidity
RHD	relative humidity of deliquescence
S	entropy, cal/K
t	time, s
T	absolute temperature, K
U(I)	auxiliary function in (79)-(82), mol (kg water)$^{-1}$
$\bar{V}_i$	partial molar volume of the i-th species, cm^3/mol
V	total volume, cm^3
V_{gas}	specific volume of water vapor, cm^3/mol
V(I)	auxiliary function in (79)-(82), mol (kg water)$^{-1}$
x	$m_{H^+}/m_{NO_3^-}$
x_w	mole fraction of water
Y	Ionic strenth fraction of univalent anion (NO_3^- or HSO_4^-)
z_i	magnitude of the charge on the i-th ion
z_+, z_-	magnitude of the charge on the cation and anion, respectively.

Greek

α	factor used in deriving (9) (dimensionless)
α	degree of dissociation (dimensionless)
α_ℓ	empirical constant in (20) (mol/kg water)$^{-\ell}$
γ_i	activity coefficient for the i-th species
γ_{ij}	mean molal activity coefficient of component i-j
γ°_{ij}	mean molal activity coefficient of component ij in a binary solution

γ_s stoichiometric mean molal nitric acid activity coefficient

γ_u mean molal activity coefficient for undissociated nitric acid

$\gamma_\pm$ mean molal activity coefficient

$(\gamma_\pm)_{H,NO_3}, (\gamma_\pm)_{NH_4NO_3}$ mean molal activity coefficients for nitric acid and ammonium nitrate, respectively

$\Delta G^\circ_{f_w}$ standard Gibbs free energy of formation of water, kcal/mol

ΔG_T Gibbs free energy change for a reaction, kcal/mol

ΔH enthalpy change during a reaction at a temperature T, kcal/mol

ΔH° enthalpy change during a reaction at 25°C, kcal/mol

ΔV volume change during the vaporization of water, cm^3/mol

θ fraction of NH_4 and x ions forming ion pairs

μ_i partial molar Gibbs free energy of the i-th component, kcal/mol

μ_i° partial molar Gibbs free energy of the reference state of the i-th component, kcal/mol

μ_i^* partial molar Gibbs free energy of the hypothetical reference state of the i-th component, kcal/mol

ν_{ij} total number of moles of ions a mole of component ij dissociate into

ν_{ij}^r, ν_k^p stoichiometric coefficients of the reactants and products, respectively in a chemical reaction

ν_+, ν_-, ν number of moles of cations, anions, and total ions a mole of solute dissociates into, eg. for $(NH_4)_2SO_4$ $\nu_+ = 2$, $\nu_- = 1$, $\nu = 3$

ρ particle density, g/cm^3

σ surface tension, dyne/cm

τ time constant for growth by condensation, s

ϕ osmotic coefficient (dimensionless)

ϕ_{cp} apparent molal heat capacity at a temperature T, cal/mol K

ϕ_L apparent molal enthalpy at a temperature T, kcal/mol

Symbols

[ ] concentration - mol/ℓ for liquids, ppb for gases

{ } activity in molar units, mol/ℓ

REFERENCES

1. Stelson, A. W. and J. H. Seinfeld, "Chemical Mass Accounting of Urban Aerosol," Envir. Sci. Technol. 15, 671-679 (1981).

2. Doyle, G. J., E. C. Tuazon, R. S. Graham, T. M. Mischke, A. M. Winer and J. N. Pitts, Jr. "Simultaneous Concentrations of Ammonia and Nitric Acid in a Polluted Atmosphere and Their Equilibrium Relationship to Particulate Ammonium Nitrate," Envir. Sci. Technol. 13, 1416-1419 (1979).

3. Stelson, A. W., S. K. Friedlander, and J. H. Seinfeld, "A Note on the Equilibrium Relationship Between Ammonia and Nitric Acid and Particulate Ammonium Nitrate," Atmospheric Environment 13, 369-371 (1979).

4. Spicer, C. W. "The Fate of Nitrogen Oxides in the Atmosphere." Batelle Columbus Rep. to Coordinating Res. Council and U.S. Environ. Protection Agency Rep. 600/3-76-030. (1974).

5. Kusik, C. L. and H. P. Meissner "Electrolyte Activity Coefficients in Inorganic Processing, A.I.Ch.E. Symp. Ser. 173, 14-20 (1978)

6. Tang, I. N. "Deliquescence Properties and Particle Size Change of Hygroscopic Aerosols," In Generation of Aerosols, (Edited by K. Willeke) Ch. 7, Ann Arbor Science Publisher, Ann Arbor, Michigan (1980).

7. Hamer, W. J. and Y. C. Wu "Osmotic Coefficients and Mean Activity Coefficients of Uni-univalent Electrolytes in Water at 25°C," J. Phys. Chem. Ref. Data 1, 1047-1099 (1972).

8. Parker, V. B., D. D. Wagman and D. Garvin "Selected Thermochemical Data Compatible with the CODATA Recommendations" NBSIR 75-968.

9. JANAF Thermochemical Tables, 2nd edition (1971), NSRDS-NBS 37.

10. Wagman, D. D., W. H. Evans, V. B. Parker, I. Harlow, S. M. Baily and R. H. Schumm "Selected Values of Chemical Thermodynamic Properties; Tables for the First Thirty-Four Elements in the Standard Order of Arrangement," NBS Technical Note 270-3. (1968).

11. Tang, I. N. "On the Equilibrium Partial Pressures of Nitric Acid and Ammonia in the Atmosphere," Atmospheric Environment 14, 819-828 (1980).

12. Brandner, J. D., N. M. Junk, J. W. Lawrence and J. Robins, "Vapor Pressure of Ammonium Nitrate," J. Chem. Engng Data 7, 227-228 (1962).

13. Högfeldt, E. "The Complex Formation Between Water and Strong Acids," Acta. Chem. Scand. 17, 785-796 (1963).

14. Weast, R. C. Handbook of Chemistry and Physics, 54th edition, CRC Press, Cleveland (1973).

15. Granzhan, V. A. and S. K.Laktionova "The Densities, Viscosities and Surface Tensions of Aqueous Nitric Acid Solutions," Russ. J. Phys. Chem. 49, 1448 (1975).

16. Krawetz, A. A. "A Raman Spectral Study of Equilbria in Aqueous Solutions of Nitric Acid," PhD Thesis, University of Chicago, IL (1955).

17. Redlich, O., R. W. Duerst and A. Merbach "Ionization of Strong Electrolytes. XI The Molecular States of Nitric Acid and Perchloric Acid," J. Chem. Phys. 49, 2986-2994 (1968).

18. Davis, W. Jr. and H. J. De Bruin "New Activity Coefficients of 0-100 Percent Aqueous Nitric Acid," J. Inorg. Nucl. Chem. 26, 1069-1083 (1964).

19. Young, T. F.,L. F. Maranville and H. M. Smith "Raman Spectral Investigation of Ionic Equilibria in Solutions of Strong Electrolytes." In The Structure of Electrolytic Solutions, (Edited by W. J. Hamer) Ch. 4, John Wiley, New York (1959).

20. McCoubrey, J. C. "The Acid Strength of the Hydrogen Halides," Trans. Faraday Soc. 51, 743-747 (1955).

21. Bockris, J. O'M. and A. K. N. Reddy Modern Electrochemistry, An Introduction to an Interdisciplinary Area, Vol. 1 (Plenum Press, New York, 1970).

22. Lee, H. and J. K. Wilmshurst "Observation of Ion-pairs in Aqueous Solutions by Vibrational Spectroscopy," Aust. J. Chem. 17, 943-945 (1964).

23. Robinson, R. A. and R. H. Stokes Electrolyte Solutions, The Measurement and Interpretation of Conductance, Chemical Potential and Diffusion in Solutions of Simple Electrolytes, 2nd ed, Butterworths, London (1959).

24. Pearce, J. N. and G. G. Pumplin "The Apparent and Partial Molal Volumes of Ammonium Chloride and of Cupric Sulfate in Aqueous Solution at 25°C," J. Am. Chem. Soc. 59, 1221-1222 (1937).

25. Forrest, J., R. L. Tanner, D. Spandau, T. D'Ottavio and L. Newman "Determination of Total Inorganic Nitrate Utilizing Collection of Nitric Acid on NaCl-impregnated Filters," Atmospheric Environment 14, 137-144 (1980).

26. Appel, B. R., S. M. Wall, Y. Tokiwa and M. Haik, "Simultaneous Nitric Acid, Particulate Nitrate and Acidity Measurements in Ambient Air," Atmospheric Environment 14, 549-554 (1980).

27. Silcock, H. L. Solubilities of Inorganic and Organic Compounds, Vol. 3 (New York: Pergamon Press, 1979). Part 2, p. 157-159.

28. Emons, H. H. and W. Hahn "Dampdruckmessungen in system ammonnitrat-ammonsulfat-wasser. Leuna Technischen Hochschule fur Chemie. Wissenschaftliche Zeitschrift 12, 129-132 (1970).

29. Wishaw, B. F. and R. H. Stokes "Activities of Aqueous Ammonium Sulphate Solutions at 25°C," Trans. Faraday Soc. 50, 952-954 (1954).

30. Staples, B. R. and R. L. Nuttall "The Activity and Osmotic Coefficients of Aqueous Calcium Chloride at 298.15 K." J. Phys. Chem. Ref. Data 6, 385-407 (1977).

31. Gibbard, H. F. Jr., G. Scatchart, R. A. Rousseau and J. L. Creek "Liquid-Vapor Equilibrium of Aqueous Sodium Chloride, From 298 to 373K and from 1 to 6 mol kg^{-1}, and Related Properties," J. Chem. Engng. Data 19, 281-288 (1974).

32. Thudium J. "Water Uptake and Equilibrium Sizes of Aerosol Particles at High Relative Humidities: Their Dependence on the Composition of the Water-Soluble Material," Pageoph 116, 130-148 (1978).

33. Saxena, P. and T. W. Peterson "Thermodynamics of Multicomponent Electrolytic Aerosols," J. Coll. Int. Sci. 79, 496-510 (1981).

34. Hood, G. C. and C. A. Reilly "Ionization of Strong Electrolytes. II. Proton Magnetic Resonance in Sulfuric Acid," J. Chem. Phys. 27, 1126-1128 (1957).

35. Lindstrom, R. E. and H. E. Wirth "Estimation of the Bisulfate Ion Dissociation in Solutions of Sulfuric Acid and Sodium Bisulfate," J. Phys. Chem. 73, 218-223 (1969).

36. Chen, H. and D. E. Irish, "A Raman Spectral Study of Bisulfate-Sulfate Systems. II. Constitution, Equilibria and Ultrafast Proton Transfer in Sulfuric Acid," J. Phys. Chem. 75, 2672-2684. (1971)

37. Klotz, J. M. and C. F. Eckert,"The Apparent Molal Volumes of Aqueous Solutions of Sulfuric Acid at 25°C," J. Am. Chem. Soc. 64, 1878-1880 (1942).

38. Rard, J. A., A Habenschuss and F. H. Spedding "A Review of the Osmotic Coefficients of Aqueous H_2SO_4 at 25°C," J. Chem. Engng Data 21, 374-379 (1976).

39. Lee, Y. H. and C. Brosset, "Interaction of Gases with Sulfuric Acid Aerosol in the Atmosphere," WMO Symposium on the Long-range Transport of Pollutants and its Relation to General Circulation Including Stratospheric/Tropospheric Exchange Processes, Sofia, Bulgaria 1-5 October, 1979.

40. Tang, I. N. and H. R. Munkelwitz, "Aerosol Growth Studies. III. Ammonium Bisulfate Aerosols in a Moist Atmosphere," J. Aero Sci. 8, 321-330 (1977).

41. Roux, A., G. M. Musbally, G. Perron, J. E. Desnoyers, P. P. Singh, E. M. Woolley, and L. G. Hepler "Apparent Molal Heat Capacities and Volumes of Aqueous Electrolytes at 25°C: $NaClO_3$, $NaClO_4$, $NaNO_3$, $NaBrO_3$, $NaIO_3$, $KClO_3$, $KBrO_3$, KIO_3, NH_4NO_3, NH_4Cl, and NH_4ClO_4." Can J. Chem. 56, 24-28 (1978).

42. Dingemans, P. "The Vapor Pressure of Saturated Solutions of Ammonium Nitrate," Recl. Trav. Chim pays-Bas Belg. 60, 317-328 (1941).

43. Stephen, H. and T. Stephen. Solubilities of Inorganic and Organic Compounds. Vol. 1 (New York: Macmillan, 1963) Part I, p. 217.

44. Vanderzee, C. E., D. H. Waugh and N. C. Haas "Enthalpies of Dilution and Relative Apparent Molar Enthalpies of Aqueous Ammonium Nitrate. The Case of a Weakly Hydrolysed (Dissociated) Salt," J. Chem. Thermodynamics 12, 21-25. (1980).

45. Harned, H. S. and B. B. Owen The Physical Chemistry of Electrolytic Solutions, ACS Monograph Series No. 137, 3rd Edn. Chap 8, Reinhold, New York.

46. Gucker, F. T. Jr., F. D. Ayers and T. R. Rubin "A Differential Method Employing Variable Heaters for the Determination of the Specific Heats of Solutions, with Results for Ammonium Nitrate at 25°C." J. Am. Chem. Soc. 58, 2118-2126 (1936).

47. Sorina, G. A., G. M. Kozlovskaya, Y. V. Tsekhanskaya, L. I. Bezlyudova and N. G. Shmakov, "The Specific Heats of Ammonium Nitrate Solutions and the Partial Specific Heats of their Components," Russ. J. Phys. Chem. 51, 1226-1227 (1977).

48. Fricke, R. "The Thermodynamic Behavior of Concentration Solutions" Z. Elektrochem. 35, 631-640 (1929).

49. Fricke, R. and L. Havestadt, "Work of Dilution and Heat of Dilution in the Sphere of Concentrated Solutions," Z. Electrochem angew. phys. Chem. 33, 441-455 (1927).

50. Campbell, A. N., J. B. Fishman, G. Rutherford, T. P. Schaefer and L. Ross "Vapor Pressures of Aqueous Solutions of Silver Nitrate, of Ammonium Nitrate, and of Lithium Nitrate," Can. J. Chem. 34, 151-159 (1956).

51. Mondain-Monval, P. "Law of the Solubility of Salts," Compt. rend. 178, 1164-1166 (1924).

52. Prideaux, E. B. R. and R. M. Caven, "The Evaporation of Concentrated and Saturated Solutions of Ammonium Nitrate, Vapour Pressures, Heats of Solution, and Hydrolysis," J. Soc. Chem. Ind. 38, 353-355T (1919).

53. Stelson, A. W. and J. H. Seinfeld, "Relative Humidity and pH Dependence of the Vapor Pressure of Ammonium Nitrate-Nitric Acid Solutions at 25°C," Atmospheric Environment 16, 993 (1982)

54. Stelson, A. W. and J. H. Seinfeld, "Thermodynamic Prediction of the Water Activity, NH_4NO_3 Dissociation Constant, Density and Refractive Index for the NH_4NO_3-$(NH_4)_2SO_4$-H_2O System at 25°C" Atmospheric Environment 16, (1982)

55. Stelson, A. W. and J. H. Seinfeld, "Relative Humidity and Temperature Dependence of the Ammonium Nitrate Dissociation Constant," Atmospheric Environment 16, 983-992 (1982).

CHAPTER 3

ATMOSPHERIC EQUILIBRIUM MODEL OF SULFATE AND NITRATE AEROSOLS

Accepted for publication in Atmospheric Environment

ATMOSPHERIC EQUILIBRIUM MODEL OF SULFATE AND NITRATE AEROSOLS

Mark Bassett and John H. Seinfeld
Department of Chemical Engineering
California Institute of Technology
Pasadena, California 91125

ABSTRACT

Given local rates of production of gas-phase sulfate and nitrate, ammonia concentration, relative humidity and temperature, a model is presented that enables calculation of the quantity of sulfate/nitrate/ammonium/water aerosol, its precise chemical composition and physical state. The model is based on a complete thermodynamic chemical and phase equilibrium calculation for the sulfate/nitrate/ammonium system. Detailed simulations of sulfate/nitrate/ammonium aerosol evolution are presented, and recent ambient data of Tanner (1983) are interpreted. Some new results on temperature variation of activity coefficients are presented in the Appendix.

1. INTRODUCTION

Sulfate and nitrate are ubiquitous components of atmospheric aerosols, having been observed in New York City (Leaderer, 1978; Tanner et al., 1979), Denver (Countess et al., 1980, 1981), Los Angeles (Appel et al., 1978; South Coast Air Quality Management District, 1982), St. Louis (Alkezweeny, 1978), the Great Smoky Mountains (Stevens et al., 1980), The Southwestern U.S. (Macias et al., 1981), and in the background troposphere (Brosset, 1978; Charlson et al., 1978; Tanner et al., 1981). Thus, a mathematical model for predicting ambient particulate sulfate and nitrate levels is an essential ingredient of a comprehensive description of atmospheric aerosols.

A major advance in our understanding of atmospheric aerosols has been achieved by considering the chemical and phase equilibria existing between gaseous species and the corresponding aerosol-phase ionic or molecular species. On the basis of a reasonable quantity of ambient data and extensive thermodynamic predictions, the hypothesis that equilibrium generally exists between gaseous and aerosol phases appears to be largely substantiated (Stelson et al., 1979; Stelson and Seinfeld, 1982a; Tanner, 1983). It may be anticipated that the ambient gas-aerosol system will be at equilibrium if the rates of change of the concentrations of gaseous species such as HNO_3, H_2SO_4, NH_3 and H_2O are slow compared with the characteristic times for diffusion of these species to the particles and for equilibration within the particle. In most ambient situations it is expected that the assumptions required for equilibrium to hold are valid since the characteristic time for mass transfer to and from an aerosol particle is of the order of a fraction of a second (Seinfeld, 1980; Schwartz and Freiberg, 1981).

Because of the frequent predominance of sulfate, nitrate, ammonium, and water by total aerosol mass, ambient atmospheric aerosol can often be characterized as consisting of a concentrated aqueous solution of ammonium nitrate, ammonium bisulfate and sulfate, nitric and sulfuric acids and two mixed salts of ammonium sulfate and nitrate. (Which of these species predominate depends of course on ambient conditions.) To predict the quantity and composition of such an aerosol, a gas-phase air quality model that predicts the rate of formation of nitric acid and sulfuric acid from SO_2 and NO_x precursors must be coupled to an equilibrium description of the aerosol. Knowledge of temperature, relative humidity and gaseous ammonia concentration is assumed. The first effort at coupling a gas-phase air quality model to an aerosol equilibrium calculation is that of Russell et al. (1983) who considered ammonium nitrate aerosol.

The sulfate/nitrate/ammonium system is of course an idealized one for representing actual ambient aerosols. The presence of other species such as those in the gaseous HCℓ-particulate chloride system can be expected to alter the sulfate/nitrate equilibria. Also, the existence of a stable organic (surfactant) film on aerosol particles would reduce the rate of mass transfer between the gas and liquid phases and might even affect the position of equilibrium through solvation and solution activity effects. Similar comments apply in the case of the existence of a solid elemental carbon or mixed elemental-organic carbon core. Nevertheless, the sulfate/nitrate/ammonium system is of such importance, an equilibrium model of that system will be quite valuable in analyzing ambient data and as a component of urban- and regional-scale air quality models.

A gas-phase air quality model provides a prediction of the spatial and temporal distributions of primary and secondary gaseous species resulting from emissions, advection, diffusion, dry deposition, and chemical reaction. Given the local rates of production of nitric acid and sulfuric acid, the resulting concentration of aerosol, its composition and physical state, can be calculated from fundamental thermodynamic principles. It is that calculation that constitutes the subject of this work. Thus, the basic problem addressed here is - Given the rates of generation of ambient gaseous nitric acid and sulfuric acid, the temperature and relative humidity, and the ammonia concentration, determine the physical state (liquid or solid) and the chemical composition of the particles, including the amounts of the phases present, and their compositions existing in equilibrium with the gas. When aerosol size-related effects, such as visibility reduction, are of interest, it will be necessary to predict size distributions. In the present work we do not address predicting size distributions of sulfate/nitrate/ammonium aerosols.

Because the recent work of Saxena et al. (1983) addresses essentially the same topic as the present paper, it is worthwhile to comment on the two studies. In their analysis of aerosol equilibria, Saxena et al. (1983) neglect the presence of mixed sulfate-nitrate salts, such as $(NH_4)_2SO_4 \cdot 3NH_4NO_3$, and the presence of bisulfate ion. The importance of including mixed salts is evident from the results of simulation of situations with high ammonia concentrations and low relative humidity, such as Case 4 to be presented subsequently. If mixed salts are not considered, the condensed phase is predicted to contain no nitrate, an erroneous conclusion. With respect to the presence of bisulfate ion, by considering the second dissociation constant for sulfuric acid,

$$K = \frac{\gamma^3_{2H^+,SO_4^{2-}} \, m_{H^+} m_{SO_4^{2-}}}{\gamma^2_{H^+,HSO_4^-} \, m_{HSO_4^-}}$$

which has the value 0.0103 mol kg^{-1} at 25°C (Readnour and Cobble, 1969), we can show that $m_{HSO_4^-} > m_{H^+}$. For example, at RH = 80 percent, when m_{H^+} = 0.3 mol kg^{-1}, $m_{HSO_4^-}$ = 3.9 mol kg^{-1} and $m_{HSO_4^-}/(m_{HSO_4^-} + m_{SO_4^{2-}}) = 0.61$, whereas when m_{H^+} = 0.1 mol kg^{-1}, $m_{HSO_4^-}$ = 0.92 mol kg^{-1} and $m_{HSO_4^-}/(m_{HSO_4^-} + m_{SO_4^{-2}}) = 0.15$. Whenever there is an excess of ammonia present, it is sufficient to assume that only $(NH_4)_2SO_4$ and NH_4NO_3 are in the liquid phase, and estimate m_{H^+} subsequently. However, when it is necessary to include H^+ explicitly in the equilibrium calculation, it is also necessary to include HSO_4^-.

2. FORMULATION OF THE EQUILIBRIUM MODEL

The essential element of the equilibrium model of sulfate and nitrate aerosols is a complete phase and chemical equilibrium calculation for the system. The condition for chemical equilibrium in a closed system at constant temperature T and pressure p is that the total Gibbs free energy of the system, G, is a minimum. The Gibbs free energy is a function of T, p, and the number of moles of the components in the system, n_i. Thus, determination of the equilibrium composition of the system is a minimization problem:

$$\min_{n_i} G(T,p,n_i)$$

subject to T, p constant, $n_i \geq 0$, and conservation of mass. If one deals with the extents of reaction, ξ_j, j = 1,2,... instead of the n_i, then the equilibrium determination problem is:

$$\min_{\xi_j} G(T,p,\xi_j)$$

subject to

$$n_i^o + \sum_j \nu_{ij}\xi_j \geq 0$$

where n_i^o is the initial number of moles of component i and ν_{ij} is the stoichiometric coefficient for species i in reaction j. The condition for a minimum of G,

$$\left(\frac{\partial G}{\partial \xi_j}\right)_{T,p,\xi_k} = 0 \qquad (1)$$

is equivalent to

$$\sum_i \nu_{ij}\mu_i = 0 \qquad \text{all } j \qquad (2)$$

where $\mu_i = (\partial G/\partial n_i)_{T,p,n_k}$ is the chemical potential of species i.

2.1 Chemical Potentials of Atmospheric Species

The determination of the equilibrium state of a system requires that one solve Equation (2). To do so, we need explicit expressions for the chemical potentials, μ_i. For solid phases the chemical potential depends only on temperature,

$$\mu_i = \mu_i^\circ(T) \tag{3}$$

where $\mu_i^\circ(T)$ is the standard Gibbs free energy of formation of the solid species.

For gases at atmospheric pressure, ideality may be assumed, so

$$\mu_i = \mu_i^\circ + RT \ln \frac{p_i}{p_i^\circ} \tag{4}$$

where p_i° is the pressure at which the standard state chemical potential is defined, by convention equal to one atmosphere. Equation (4) may be re-expressed as

$$\mu_i = \mu_i^\circ + RT \ln \left[n_i \frac{RT}{p_i^\circ} \right] \tag{5}$$

For species i in solution, the chemical potential is defined as

$$\mu_i = \mu_i^\circ + RT \ln a_i \tag{6}$$

where a_i is the activity of species i. For electrolytes, the activity is related to concentration by

$$a_i = \gamma_i^{\nu} m_+^{\nu_+} m_-^{\nu_-} \tag{7}$$

where the species i dissociates into ν_+ moles of cations and ν_- moles of anions of molalities m_+ and m_-, and $\nu = \nu_+ + \nu_-$. γ_i is the activity coefficient of species i.

The activity of water a_w is related to the activities of the solutes by the Gibbs-Duhem equation,

$$n_w \, d\ell n \, a_w = -\sum_i n_i \, d\ell n \, a_i \qquad (8)$$

The chemical potential of water then follows from (6), with the value of μ_w° chosen so that $a_w = 1$ for pure water. Equation (8) can be integrated to give a_w once the activities of the solutes are known.

2.2 Activity Coefficients of Aerosol Electrolytes

Stelson and Seinfeld (1981) have shown that solution concentrations of 8 to 26 M can be expected in wetted aerosol particles. At such concentrations, the solutions are strongly nonideal, and appropriate thermodynamic activity coefficient correlations have only recently been developed. In particular, Tang (1980), Stelson and Seinfeld (1982abc) and Stelson et al. (1983) have developed activity coefficient expressions for aqueous systems of nitrate, sulfate, ammonium, nitric and sulfuric acids at concentrations exceeding 1 M.

It is useful at this point to note that the direct dissolution of SO_2 in solutions of the type we are considering here can be neglected. To see this, note that the Henry's law constant for SO_2 at 25°C is 1.24 mole ℓ^{-1} atm^{-1}. At SO_2 concentration of 1 ppm, the liquid phase concentration of dissolved SO_2 is 1.24×10^{-6} mol ℓ^{-1}, far less than those of the major components. Thus, dissolved SO_2, and HSO_3^- and SO_3^{2-}, can be neglected in the basic thermodynamic calculation. Although we do not consider the

oxidation of S(IV) in the present work, it is straightforward to do so once the ionic strength and pH have been established.

In principle, each activity coefficient γ_i depends on the concentrations of all the other species in the solution. However, for the systems of interest here, Stelson and Seinfeld (1982abc) have shown that the empirical mixing rule of Kusik and Meissner (1978) adequately correlates experimental data. This rule can be expressed as

$$\ln \gamma_{12} = \frac{z_2}{I(z_1+z_2)}\left[m_2\left(\frac{z_1+z_2}{2}\right)^2 \ln \gamma^\circ_{12} + m_4\left(\frac{z_1+z_4}{2}\right)^2 \ln \gamma^\circ_{14} + \cdots\right] \qquad (9)$$

$$+ \frac{z_1}{I(z_1+z_2)}\left[m_1\left(\frac{z_1+z_2}{2}\right)^2 \ln \gamma^\circ_{12} + m_3\left(\frac{z_3+z_2}{2}\right)^2 \ln \gamma^\circ_{32} + \cdots\right]$$

where the odd and even subscripts refer to cations and anions, respectively, γ°_{ij} is the activity coefficient for a binary solution containing only ions i and j at the same ionic strength I, where

$$I = \frac{1}{2}\sum_i z_i^2 m_i \qquad (10)$$

z_i being the absolute value of the charge on species i and m_i its molality. Note that the only empirical data required to calculate all the paired activity coefficients are the binary solution activity coefficients γ°_{ij}. However, note also that data are required for all possible pairs of ions.

Finally, using (7) and (9) in (8) and integrating gives

$$\ln a_w = \sum_{ij} \frac{m_{ij}}{2I} \frac{n_{ij} z_i z_j}{z_i + z_j} \left[\sum_{\substack{k \\ \text{even}}} \left(\frac{z_i + z_k}{2} \right)^2 z_k \frac{m_k}{I} \ln a^{\circ}_{w_{ik}} + \sum_{\substack{k \\ \text{odd}}} \left(\frac{z_j + z_k}{2} \right)^2 z_k \frac{m_k}{I} \ln a^{\circ}_{w_{kj}} \right]$$

$$+ \frac{M_w}{10^3} \sum_{ij} \frac{n_{ij} m_{ij}}{z_i + z_j} \left[z_i \left(\sum_{\substack{k \\ \text{even}}} \left(\frac{z_i + z_k}{2} \right)^2 \frac{m_k}{I} - 1 \right) + z_j \left(\sum_{\substack{k \\ \text{odd}}} \left(\frac{z_j + z_k}{2} \right)^2 \frac{m_k}{I} - 1 \right) \right] \tag{11}$$

where $a^{\circ}_{w_{ij}}$ is the water activity for a solution containing only ions ij, m_{ij} is the molality of electrolyte i,j, n_{ij} is the number of moles of ions into which each mole of i,j dissociates, and m_k is the molality of ion k.

2.3 Chemical Potential of Water

A simplification is possible in the expression for the chemical potential of water vapor. Since water is by far the most plentiful gaseous species of those involved in the equilibrium, the change in the vapor pressure of water from that in the ambient air will be negligible. Thus, the relative humidity can be treated as constant and known for the calculation. Consider the expressions for the chemical potentials of gaseous and liquid water,

$$\mu_{H_2O\ (g)} = \mu^{\circ}_{H_2O(g)} + RT \ln \frac{p_w}{p^{\circ}_w} \tag{12}$$

$$\mu_{H_2O(\ell)} = \mu^{\circ}_{H_2O(\ell)} + RT \ln a_w \tag{13}$$

For pure water in equilibrium with its vapor, $a_w = 1$, $p_w = p^{sat}_w$. Thus,

$$\mu^{\circ}_{H_2O(\ell)} - \mu^{\circ}_{H_2O(g)} = RT \ln \left(\frac{p_w^{sat}}{p_w^{\circ}} \right) \tag{14}$$

Using (14) in (12) and replacing $\frac{p_w}{p_w^{sat}}$ by $\frac{RH}{100}$ yields

$$\mu_{H_2O(g)} = \mu^{\circ}_{H_2O(\ell)} + RT \ln \left(\frac{RH}{100} \right) \tag{15}$$

where RH is relative humidity in percent.

3. THE SULFATE/NITRATE/AMMONIUM SYSTEM

The system we are considering consists of the following components:

liquid phase: NH_4^+, H^+, HSO_4^-, SO_4^{2-}, NO_3^-, H_2O

solid phases: NH_4HSO_4, $(NH_4)_2SO_4$, NH_4NO_3, $(NH_4)_2SO_4 \cdot 2NH_4NO_3$, $(NH_4)_2SO_4 \cdot 3NH_4NO_3$, $(NH_4)_3 H(SO_4)_2$

gas phase: NH_3, HNO_3, H_2SO_4, H_2O

In this system there are 13 reactions involving 17 species. The reactions are listed in Table 1. To evaluate the chemical potentials in terms of the extents of reaction we have four additional mass balance equations for the total amount of ammonia, nitrate, sulfate and water in the system.

The conservation of mass constraint consists of one linear equation for each component initially present. For example, for a system consisting only of water and nitric acid, conservation of mass can be expressed as

$$\begin{aligned} n_{HNO_3(aq)} + n_{HNO_3(g)} &= (n_{HNO_3})_T \\ n_{H_2O(\ell)} + n_{H_2O(g)} &= (n_{H_2O})_T \end{aligned} \tag{16}$$

It is easiest to incorporate the conservation of mass constraint through the use of the extents of reaction, ξ_j. For the HNO_3/H_2O system, for example, we have

$$HNO_3(g) \rightleftarrows HNO_3(aq)$$
$$H_2O(g) \rightleftarrows H_2O(\ell)$$

Table 1. Chemical Reactions Occurring in the Sulfate/Nitrate/Ammonium System

Reaction	Equilibrium constant expression	Equilibrium constant value
$H_2SO_4(g) \rightleftarrows H^+ + HSO_4^-$	$\frac{\gamma^2_{H^+,HSO_4^-}\, m_{H^+}\, m_{HSO_4^-}}{p_{H_2SO_4}}$	$3.038\times10^{17}\ exp\left[60.59\left(\frac{T_o}{T}-1\right)+26.1\left(1+ln\frac{T_o}{T}-\frac{T_o}{T}\right)\right]mol^2kg^{-2}atm^{-1}$
$H_2SO_4(g) \rightleftarrows 2H^+ + SO_4^{2-}$	$\frac{\gamma^3_{2H^+,SO_4^{2-}}\, m^2_{H^+}\, m_{SO_4^{2-}}}{p_{H_2SO_4}}$	$3.131\times10^{15}\ exp\left[68.18\left(\frac{T_o}{T}-1\right)+44.925\left(1+ln\frac{T_o}{T}-\frac{T_o}{T}\right)\right]mol^3kg^{-3}\ atm^{-1}$
$HNO_3(g) \rightleftarrows H^+ + NO_3^-$	$\frac{\gamma^2_{H^+,NO_3^-}\, m_{H^+}\, m_{NO_3^-}}{p_{HNO_3}}$	$3.638\times10^{6}\ exp\left[29.47\left(\frac{T_o}{T}-1\right)+16.555\left(1+ln\frac{T_o}{T}-\frac{T_o}{T}\right)\right]mol^2kg^{-2}\ atm^{-1}$
$NH_3(g) + H_2SO_4(g) \rightleftarrows NH_4^+ + HSO_4^-$	$\frac{\gamma^2_{NH_4^+,HSO_4^-}\, m_{NH_4^+}\, m_{HSO_4^-}}{p_{NH_3}\, p_{H_2SO_4}}$	$3.339\times10^{28}\ exp\left[95.818\left(\frac{T_o}{T}-1\right)+20.77\left(1+ln\frac{T_o}{T}-\frac{T_o}{T}\right)\right]mol^2kg^{-2}\ atm^{-2}$
$2NH_3(g) + H_2SO_4(g) \rightleftarrows 2NH_4^+ + SO_4^{2-}$	$\frac{\gamma^3_{2NH_4^+,SO_4^{2-}}\, m^2_{NH_4^+}\, m_{SO_4^{2-}}}{p^2_{NH_3}\, p_{H_2SO_4}}$	$3.782\times10^{37}\ exp\left[138.636\left(\frac{T_o}{T}-1\right)+34.265\left(1+ln\frac{T_o}{T}-\frac{T_o}{T}\right)\right]mol^3kg^{-2}\ atm^{-2}$
$NH_3(g) + HNO_3(g) \rightleftarrows NH_4^+ + NO_3^-$	$\frac{\gamma^2_{NH_4^+,NO_3^-}\, m_{NH_4^+}\, m_{NO_3^-}}{p_{NH_3}\, p_{HNO_3}}$	$3.999\times10^{17}\ exp\left[64.698\left(\frac{T_o}{T}-1\right)+11.505\left(1+ln\frac{T_o}{T}-\frac{T_o}{T}\right)\right]mol^2kg^{-2}\ atm^{-2}$
$NH_3(g) + H_2SO_4(g) \rightleftarrows NH_4HSO_4(S)$	$\frac{1}{p_{NH_3}\, p_{H_2SO_4}}$	$1.975\times10^{26}\ exp\left[95.818\left(\frac{T_o}{T}-1\right)-6.22\left(1+ln\frac{T_o}{T}-\frac{T_o}{T}\right)\right]atm^{-2}$

Table 1. Chemical Reactions Occurring in the Sulfate/Nitrate/Ammonium System (Continued)

Reaction	Equilibrium constant expression	Equilibrium constant value
$2NH_3(g) + 2H_2SO_4(g) \rightleftharpoons (NH_4)_3H(SO_4)_2(S)$	$\frac{1}{P_{NH_3}^3 P_{H_2SO_4}^2}$	$4.079\times10^{65} \exp\left[237.084\left(\frac{T_o}{T}-1\right) - 191685\left(1+\ln\frac{T_o}{T}-\frac{T_o}{T}\right)\right] atm^{-5}$
$2NH_3(g) + H_2SO_4(g) \rightleftharpoons (NH_4)_2SO(S)$	$\frac{1}{P_{NH_3}^2 P_{H_2SO_4}}$	$3.782\times10^{37} \exp\left[141.266\left(\frac{T_o}{T}-1\right) - 6.22\left(1+\ln\frac{T_o}{T}-\frac{T_o}{T}\right)\right] atm^{-3}$
$NH_3(g) + HNO_3(g) \rightleftharpoons NH_4NO_3(S)$	$\frac{1}{P_{NH_3} P_{HNO_3}}$	$3.349\times10^{16} \exp\left[75.108\left(\frac{T_o}{T}-1\right) - 6.06\left(1+\ln\frac{T_o}{T}-\frac{T_o}{T}\right)\right] atm^{-2}$
$5NH_3(g) + 3HNO_3(g) + H_2SO_4(g) \rightleftharpoons (NH_4)_2SO_4 \cdot 3NH_4NO_3(S)$	$\frac{1}{P_{NH_3}^5 P_{HNO_3}^3 P_{H_2SO_4}}$	$9.035\times10^{87} \exp\left[366.59\left(\frac{T_o}{T}-1\right) - 31.645\left(1+\ln\frac{T_o}{T}-\frac{T_o}{T}\right)\right] atm^{-9}$
$4NH_3(g) + 2HNO_3(g) + H_2SO_4(g) \rightleftharpoons (NH_4)_2SO_4 \cdot 2NH_4NO_3(g)$	$\frac{1}{P_{NH_3}^4 P_{HNO_3}^2 P_{H_2SO_4}}$	$2.209\times10^{71} \exp\left[291.482\left(\frac{T_o}{T}-1\right) - 25.585\left(1+\ln\frac{T_o}{T}-\frac{T_o}{T}\right)\right] atm^{-7}$
$H_2O(g) \rightleftharpoons H_2O(\ell)$	$\frac{a_w}{\frac{RH}{100}}$	1.

If the vector $\underset{\sim}{n}$ is defined as

$$\underset{\sim}{n} = \begin{bmatrix} n_{HNO_3(aq)} \\ n_{H_2O(\ell)} \\ n_{HNO_3(g)} \\ n_{H_2O(g)} \end{bmatrix}$$

and the matrix of stoichiometric coefficients as

$$\underset{\sim}{\nu} = \begin{bmatrix} 1 & 0 \\ 0 & 1 \\ -1 & 0 \\ 0 & -1 \end{bmatrix}$$

then $\underset{\sim}{n} = \underset{\sim}{n}^\circ + \underset{\sim}{\nu}\underset{\sim}{\xi}$, where $\underset{\sim}{\xi} = [\xi_1, \xi_2]$, the extent of the two reactions, and $\underset{\sim}{n}^\circ$ is the initial value of $\underset{\sim}{n}$. If, for example, the system is initially all gaseous,

$$n_{HNO_3(aq)} = \xi_1 \qquad n_{HNO_3(g)} = (n_{HNO_3})_T - \xi_1$$

$$n_{H_2O(\ell)} = \xi_2 \qquad n_{H_2O(g)} = (n_{H_2O})_T - \xi_2$$

The expressions for the chemical potentials of the species in Table 1 are given in Table 2. We note that because the mixing rule (9) requires activity coefficient data on the binary solutions of all possible pairs of ions for the purpose of calculating activity coefficients, the aqueous phase is considered as a mixture of the six possible species:

1. H^+ HSO_4^-
2. $2H^+$ SO_4^{2-}
3. H^+ NO_3^-
4. NH_4^+ HSO_4^-
5. $2NH_4^+$ SO_4^{2-}
6. NH_4^+ NO_3^-

Table 2. Chemical Potentials in the Sulfate/Nitrate/Ammonium/Water System

Species	Chemical potential
H^+,HSO_4^-	$\mu^o_{H^+,HSO_4^-} + RT\ \ell n\ m_{H^+}\, m_{HSO_4^-} + \frac{RT}{I}\left[\left(m_{H^+} + m_{HSO_4^-}\right)\ell n\ \gamma^o_{H^+,HSO_4^-} + \frac{9}{4}\, m_{SO_4^{2-}}\, \ell n\ \gamma^o_{2H^+,SO_4^{2-}} + m_{NO_3^-}\, \ell n\gamma^o_{H^+,NO_3^-} + m_{NH_4^+}\, \ell n\gamma^o_{NH_4^+,HSO_4^-}\right]$
$2H^+,SO_4^{2-}$	$\mu^o_{2H^+,SO_4^{2-}} + RT\ \ell n\ m_{M^+}^2\, m_{SO_4^{2-}} + \frac{RT}{I}\left[2m_{HSO_4^-}\, \ell n\gamma^o_{H^+,HSO_4^-} + \frac{9}{4}\left(m_{H^+} + 2m_{SO_4^{2-}}\right)\ell n\ \gamma^o_{2H^+,SO_4^{2-}} + 2m_{NO_3^-}\, \ell n\gamma^o_{H^+,NO_3^-} + \frac{9}{4}\, m_{NH_4^+}\, \ell n\gamma^o_{2NH_4^+,SO_4^{2-}}\right]$
H^+,NO_3^-	$\mu^o_{H^+,NO_3^-} + RT\ \ell n\ m_{H^+}\, m_{NO_3^-} + \frac{RT}{I}\left[m_{HSO_4^-}\, \ell n\gamma^o_{H^+,HSO_4^-} + \frac{9}{4}\, m_{SO_4^{2-}}\, \ell n\gamma^o_{2H^+,SO_4^{2-}} + \left(m_{H^+} + m_{NO_3^-}\right)\ell n\gamma^o_{H^+,NO_3^-} + m_{NH_4^+}\, \ell n\gamma^o_{NH_4^+,NO_3^-}\right]$
NH_4^+,HSO_4^-	$\mu^o_{NH_4^+,HSO_4^-} + RT\ \ell n\ m_{NH_4^+} m_{HSO_4^-} + \frac{RT}{I}\left[\left(m_{NH_4^+} + m_{HSO_4^-}\right)\ell n\gamma^o_{NH_4^+,HSO_4^-} + \frac{9}{4}\, m_{SO_4^{2-}}\, \ell n\gamma^o_{2NH_4^+,SO_4^{2-}} + m_{NO^-}\, \ell n\gamma^o_{NH_4^+,NO_3^-} + m_{H^+}\, \ell n\gamma^o_{H^+,HSO_4^-}\right]$

Table 2. Chemical Potentials in the Sulfate/Nitrate/Ammonium/Water System (Continued)

Species	Chemical potential
$2NH_4,SO^{2-}_4$	$\mu^o_{2NH_4^+,SO_4^{2-}} + RT\ \ell n\ m^2_{NH_4^+}\ m_{SO_4^{2-}}$ $+ \frac{RT}{I}\left[2m_{HSO_4^-}\ \ell n\gamma^o_{NH_4^+,HSO_4^-} + \frac{9}{4}\left(m_{NH_4^+} + 2m_{SO_4^{2-}}\right)\ell n\gamma^o_{2NH_4^+SO_4^{2-}}\right.$ $\left. + 2\ m_{NO_3^-}\ \ell n\gamma^o_{NH_4^+,NO_3^-} + \frac{9}{4}\ m_{H^+}\ \ell n\gamma^o_{2H^+,SO_4^{2-}}\right]$
NH_4^+,NO_3^-	$\mu^o_{NH_4^+,NO_3^-} + RT\ \ell n\ m_{NH_4^+}\ m_{NO_3^-}$ $+ \frac{RT}{I}\left[m_{HSO_4^-}\ \ell n\gamma^o_{NH_4^+,HSO_4^-} + \frac{9}{4}\ m_{SO_4^{2-}}\ \ell n\gamma^o_{2NH_4^+,SO_4^{2-}}\right.$ $\left. + m_{H^+}\ \ell n\gamma^o_{H^+,NO_3^-} + \left(m_{NH_4^+} + m_{NO_3^-}\right)\ell n\gamma^o_{NH_4^+,NO_3^-}\right]$
$NH_4HSO_4(s)$	$\mu^o_{NH_4HSO_4(s)}$
$(NH_4)_3H(SO_4)_2(s)$	$\mu^o_{(NH_4)_3H(SO_4)_2(s)}$
$(NH_4)_2SO_4(s)$	$\mu^o_{(NH_4)_2SO_4(s)}$
$NH_4NO_3(s)$	$\mu^o_{NH_4NO_3(s)}$
$(NH_4)_2SO_4 \cdot 3NH_4NO_3(s)$	$\mu^o_{(NH_4)_2SO_4 \cdot 3NH_4NO_3(s)}$
$(NH_4)_2SO_4 \cdot 2NH_4NO_3(s)$	$\mu^o_{(NH_4)_2SO_4 \cdot 2NH_4NO_3(s)}$

Table 2. Chemical Potentials in the Sulfate/Nitrate/Ammonium/Water System (Continued)

Species	Chemical potential
$H_2O(\ell)$	$\mu^o_{H_2O(aq)} + RT\left[\frac{1}{2I^2}\left[m_{H^+} m_{HSO_4^-} \ell n\, a^o_{w\,H^+,HSO_4^-} + 9\left(m_{H^+} - m_{2H^+,SO_4^{2-}}\right) m_{SO_4^{2-}} \ell n\, a^o_{w\,2H^+,SO_4^{2-}} + m_{H^+} m_{NO_3^-} \ell n\, a^o_{w\,H^+,NO_3^-} + m_{NH_4^+} m_{HSO_4^-} \ell n\, a^o_{w\,NH_4^+,HSO_4^-} + 9\left(m_{NH_4^+} - m_{2NH_4^+,SO_4^{2-}}\right) m_{SO_4^{2-}} \ell n\, a^o_{w\,2NH_4^+,SO_4^{2-}} + m_{NH_4^+} m_{NO_3^-} \ell n\, a^o_{w\,NH_4^+,NO_3^-} + \left(m_{H^+} + m_{NH_4^+}\right)\left(m_{H^+,HSO_4^-} \ell n\, a^o_{w\,H^+,HSO_4^-} + \frac{9}{2} m_{NH_4^+,SO_4^{2-}} \ell n\, a^o_{w\,2H^+,SO_4^{2-}} + m_{H^+,NO_3^-} \ell n\, a^o_{w\,H^+,NO_3^-} + m_{NH_4^+,HSO_4^-} \ell n\, a^o_{w\,NH_4^+,HSO_4^-} + \frac{9}{2} m_{2NH_4^+,SO_4^{2-}} \ell n\, a^o_{w\,2NH_4^+,SO_4^{2-}} + m_{NH_4^+,NO_3^-} \ell n\, a^o_{w\,NH_4^+,NO_3^-}\right)\right] + \frac{M_w m_{SO_4^{2-}}}{10^3 I}\left(3\left(m_{H^+} + m_{NH_4^+}\right) - 2I\right)\right]$
$NH_3(g)$	$\mu^o_{NH_3(g)} + RT\ \ell n\ \frac{RTn_{NH_3(g)}}{p^o}$
$HNO_3(g)$	$\mu^o_{HNO_3(g)}\quad RT\ \ell n\ \frac{RTn_{HNO_3(g)}}{p^o}$
$H_2SO_4(g)$	$\mu^o_{H_2SO_4(g)} + RT\ \ell n\ \frac{RTn_{H_2SO_4(g)}}{p^o}$
$H_2O(g)$	$\mu^o_{H_2O(\ell)} + RT\ \ell n\ \frac{RH}{100}$

3.1 Qualitative Observations on the System

Two observations are useful in determining a priori the composition of the aerosol: (i) Sulfuric acid possesses an extremely low vapor pressure, and (ii) $(NH_4)_2SO_4$(s or aq) is the preferred form of sulfate. The second observation means that, if possible, each mole of sulfate will remove two moles of ammonia from the gas phase, and the first observation implies that the amount of sulfuric acid in the gas phase will be negligible. Based on these observations we can delineate two regimes of interest. If we let $[NH_3]$, $[SO_4^{2-}]$ and $[NO_3^-]$ denote the *total* (gas plus aqueous plus solid) concentrations of ammonia, sulfate, and nitrate, respectively, then the two cases are:

$$\text{I.} \quad [NH_3] < 2[SO_4^{2-}]$$

$$\text{II.} \quad [NH_3] > 2[SO_4^{2-}]$$

Case I. $[NH_3] < 2[SO_4^{2-}]$. In this case there is insufficient NH_3 to neutralize the sulfate. Thus, the liquid phase will be acidic. The vapor pressures of both NH_3 and H_2SO_4 will be low, and the sulfate will tend to drive the nitrate from the liquid phase. Since the NH_3 partial pressure will be low, the NH_3-HNO_3 partial pressure product will also be low, so ammonium nitrate levels will be low. This case may be summarized as follows:

Important species	Negligible species
HNO_3(g)	NH_3(g)
H^+ HSO_4^-	H_2SO_4(g)
$2H^+$ SO_4^{2-}	H^+ NO_3^-
NH_4^+ HSO_4^-	NH_4^+ NO_3^-
$2NH_4^+$ SO_4^{2-}	

After the equilibrium calculation is performed, assuming only the "important" species above are present, the "negligible" species concentrations can be estimated from

$$\ell n\ p_{H_2SO_4} = \frac{1}{RT}\left(\mu_{H^+HSO_4^-} - \mu^\circ_{H_2SO_4(g)}\right)$$

$$= \frac{1}{RT}\left(\mu_{2H^+SO_4^{2-}} - \mu^\circ_{H_2SO_4(g)}\right) \qquad (17)$$

$$\ell n\ m_{NO_3^-} = \ell n\ p_{HNO_3} - \frac{1}{RT}\left(\mu^\circ_{H^+NO_3^-} - \mu^\circ_{HNO_3(g)}\right) - \ell n\ \gamma^2_{H^+NO_3^-}\, m_{H^+} \qquad (18)$$

$$\ell n\ p_{NH_3} = \frac{1}{RT}\left(\mu_{NH_4^+HSO_4^-} - \mu^\circ_{NH_3(g)} - \mu_{H^+HSO_4^-}\right) \qquad (19)$$

The concentrations resulting from these expressions can be verified to be negligible with respect to the other species. The only species of the three above for which this may not happen is NO_3^-; if its concentration is not negligibly small, the value can be used as the next guess of an iteration.

Case II. $[NH_3] > 2[SO_4^{2-}]$. In this case there is excess ammonia, so that the liquid phase can be assumed to be fully neutralized. As a result, species containing H^+ and HSO_4^-, since the latter is proportional to that of H^+, will be present in negligible concentrations. This case may be summarized as follows:

Important species	Negligible species
$2NH^+$ SO_4^{2-}	$2H^+$ SO_4^{2-}
NH_4^+ NO_3^-	H^+ HSO_4^-
$NH_3(g)$	H^+ NO_3^-
$HNO_3(g)$	NH_4^+ HSO_4^-
	$H_2SO_4(g)$

As in Case I, the actual concentrations of the neglected species must be estimated. This estimation is somewhat more involved than in Case I, and is carried out as follows. After the simplified calculation we relax the assumptions above and allow the following three equilbria to exist:

$$H^+ + SO_4^{2-} \rightleftarrows HSO_4^-$$

$$H^+ + NH_3(g) \rightleftarrows NH_4^+$$

$$H^+ + NO_3^- \rightleftarrows HNO_3(g)$$

The last reaction is, in fact, included in the simplified calculation, but must be retained to allow the nitric acid-ammonia partial pressure product to adjust properly.

Assume that the effect of the neglected species on the activity coefficients is small. Inspection of (9) and (10) shows that this will be true if the concentrations of the neglected species are in fact small. Then define equilibrium constants for the above reactions,

$$m_{HSO_4^-} = \tilde{K}_1 \, m_{SO_4^{2-}} m_{H^+} \tag{20}$$

$$m_{NH_4^+} = \tilde{K}_2 \, n_{NH_3(g)} m_{H^+} \tag{21}$$

$$n_{HNO_3(g)} = \tilde{K}_3 \, m_{NO_3^-} m_{H^+} \tag{22}$$

$$\tilde{K}_1 = \frac{\gamma^3_{2H^+,SO_4^{2-}}}{\gamma^2_{H^+,HSO_4^-}} \exp\left(\frac{\mu^\circ_{2H^+,SO_4^{2-}} - \mu^\circ_{H^+,HSO_4^-}}{RT} \right) \tag{23}$$

$$\tilde{K}_2 = \frac{\gamma^2_{H^+,HSO_4^-} RT}{\gamma^2_{NH_4^+,HSO_4^-}} \exp\left(\frac{\mu^\circ_{H^+,HSO_4^-} - \mu^\circ_{NH_4^+,HSO_4^-}}{RT} \right) \tag{24}$$

$$\tilde{K}_3 = \frac{\gamma^2_{H^+,NO_3^-}}{RT} \exp\left(\frac{\mu^\circ_{H^+,NO_3^-} - \mu^\circ_{HNO_3(g)}}{RT} - \right) \tag{25}$$

Then, using mass balances, the concentrations of the various components can be computed for a given value of m_{H^+}. For example,

$$m_{HSO_4^-} = \tilde{K}_1 m_{H^+} \frac{\left(m_{SO_4^{2-}} + m_{HSO_4^-}\right)}{1 + \tilde{K}_1 m_{H^+}} \tag{26}$$

$$m_{SO_4^{2-}} = \frac{\left(m_{SO_4^{2-}} + m_{HSO_4^-}\right)}{1 + \tilde{K}_1 m_{H^+}} \tag{27}$$

These expressions can then be used in the electroneutrality balance to obtain an equation for m_{H^+}

$$\begin{aligned}
&(\tilde{K}_1 m_{H^+} + 2)\left(m_{HSO_4^-} + m_{SO_4^{2-}}\right)(\tilde{K}_2 m_{H^+} + 1)(\tilde{K}_3 m_{H^+} + 1) \\
&- \tilde{K}_2 m_{H^+}\left(m_{NH_4^+} + \frac{10^3}{M_w n_w} n_{NH_3(g)}\right)(\tilde{K}_1 m_{H^+} + 1)(\tilde{K}_3 m_{H^+} + 1) \\
&+ \left(m_{NO_3^-} + \frac{10^3}{M_w n_w} n_{HNO_3(g)}\right)(\tilde{K}_1 m_{H^+} + 1)(\tilde{K}_2 m_{H^+} + 1) \\
&- m_{H^+}(\tilde{K}_1 m_{H^+} + 1)(\tilde{K}_2 m_{H^+} + 1)(\tilde{K}_3 m_{H^+} + 1) = 0
\end{aligned} \tag{28}$$

where n_w, $m_{NH_4^+}$ etc. represent the values obtained from the equilibrium calculation. Equation (28) can then be solved iteratively for m_{H^+}. Knowing m_{H^+}, the concentrations of all the other species can be calculated. If any concentrations that were assumed to be negligible turn out to be non-negligible, they are included in the calculation the next time. Then, the whole process is repeated until convergence is obtained.

4. PREDICTION OF THE BEHAVIOR OF SULFATE/NITRATE/AMMONIUM AEROSOL

The nature of the model we have developed is such that, given relative humidity and temperature, the total concentration of ammonia, and the rates of generation of gaseous nitric and sulfuric acids, the quantity, composition and state of the aerosol in equilibrium with the gas phase is determined as a function of time. Ordinarily, the rates of generation of nitric and sulfuric acids can be estimated from the gas-phase chemistry component of an air quality model (Duewer et al., 1980; Seigneur et al., 1981; McRae et al. 1982; Lamb, 1982). Relative humidity and temperature are generally available, whereas the atmospheric ammonia concentration is at this time measured only in special circumstances. With the results we will present shortly we show that because of the intimate thermodynamic relationship among the ammonium salts of nitrate and sulfate, knowledge of the atmospheric ammonia level is important in being able to predict aerosol composition and quantity.

We begin this section with an examination of six hypothetical situations over a range of atmospheric conditions with respect to relative humidity, temperature and ammonia level. These situations are presented to explore the effect of relative humidity, temperature, and ammonia level on the quantity, composition and state of the atmospheric aerosol. In addition, the cases presented illustrate the capability of the equilibrium model when used to predict aerosol properties. We then turn to an analysis of the ambient aerosol data of Tanner (1983) to assess the degree to which the equilibrium hypothesis is satisfied.

4.1 Equilibrium Aerosol During Constant Production of Sulfate and Nitrate

To illustrate the use of the model and to explore the behavior of sulfate/nitrate/ammonium aerosols, we now present the results of six simulations, the conditions for which are summarized in Table 3. The general character of each simulation is that at time zero all the ammonia is present as gaseous NH_3, and sulfate and nitrate concentrations are equal to zero. At t = 0, constant sources of sulfate and nitrate are introduced as gaseous H_2SO_4 and HNO_3, Between cases 1 and 2 and cases 3 and 4 we explore the effect of a 5°K increase in temperature at 90 percent and 50 percent relative humidity, respectively. In cases 5 and 6 we examine the effect of relative humidity when there is an ammonia deficiency.

Results of the calculations will be presented as temporal plots of the aerosol constituents, both liquid and solid, over a one-hour time period. The dynamic behavior in the six cases is shown in Figures 1-6.

Cases 1 and 2. In these two cases enough ammonia is present to neutralize all the acid so the liquid phase consists of NH_4NO_3 and $(NH_4)_2SO_4$. Note that the HNO_3 partial pressure increases as the NH_3 partial pressure decreases. This behavior is especially evident in Case 2 because of the higher temperature. At 90 percent RH, the $(NH_4)_2SO_4$ immediately forms a liquid phase. This liquid phase contains some NH_4NO_3. In the absence of $(NH_4)_2SO_4$, the liquid phase would not contain any NH_4NO_3 until the NH_3-HNO_3 partial pressure product is exceeded.

Cases 3 and 4. Cases 3 and 4 contain the same total concentrations of sulfate, nitrate and ammonium as Cases 1 and 2, however the relative humidity is 50 percent as opposed to 90 percent. As a result, no liquid phase is present.* With no liquid phase to serve as a site for NH_4NO_3 condensation, no NH_4NO_3 forms

*In practice, a metastable supersaturated liquid phase may be formed. The rate at which this phase crystallizes will be determined by factors such as the amount of nuclei present for crystallization. Thus elucidating the nature of this phase is beyond the scope of this study.

Table 3. Conditions for Sulfate/Nitrate/Ammonium Simulations

Case	RH,%	T°C	$[NH_3]$,μg m^{-3}	R_{HNO_3}, μg $m^{-3}hr^{-1}$	$R_{H_2SO_4}$ μg $m^{-3}hr^{-1}$
1	90	25	20	20	30
2	90	30	20	20	30
3	50	25	20	20	30
4	50	30	20	20	30
5	90	25	5	20	30
6	50	25	5	20	30

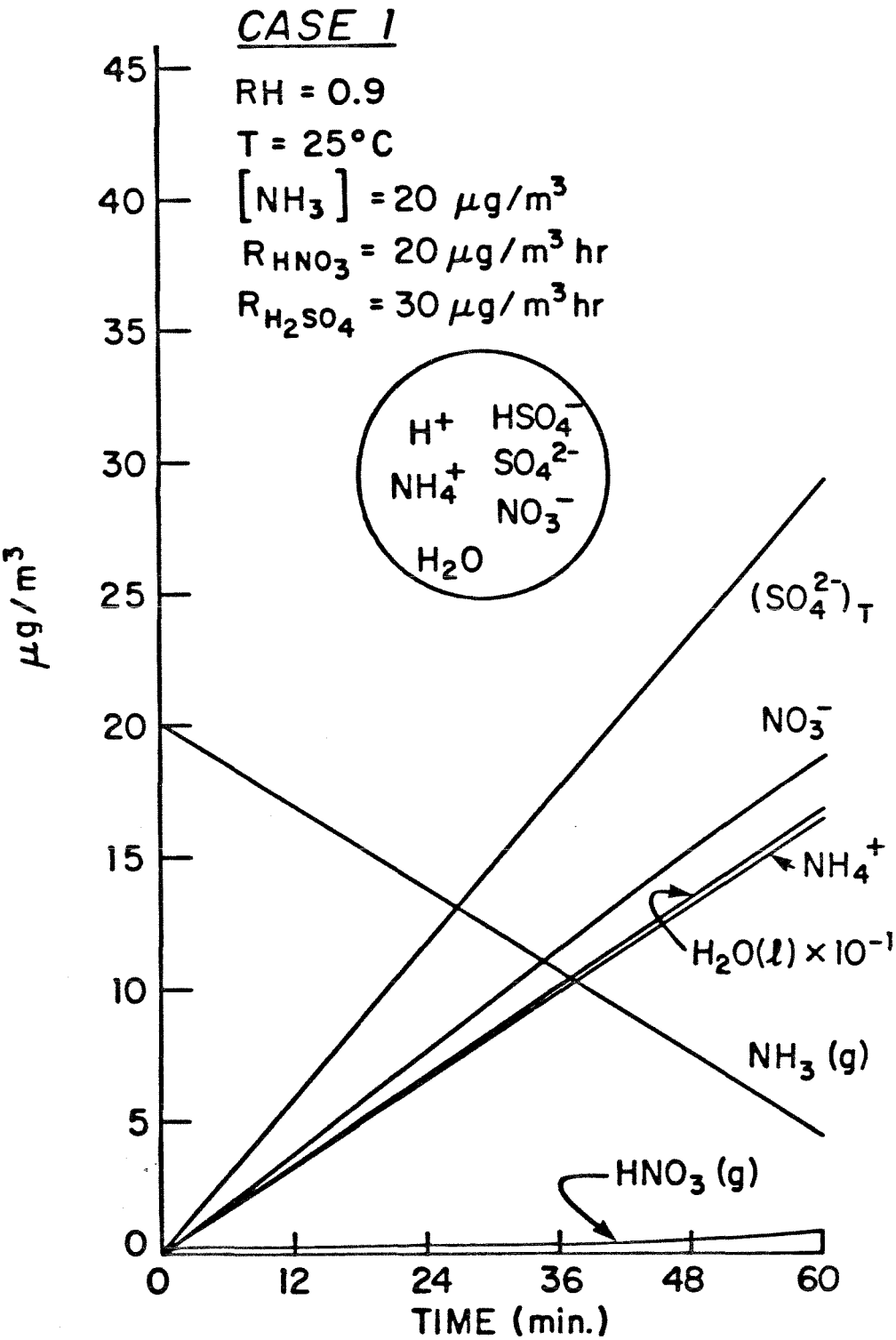

Evolution of Gaseous and Aerosol Constituents for Case 1 of Table 3. Over a one-hour simulation aerosol phase is an aqueous solution as indicated on the figure.

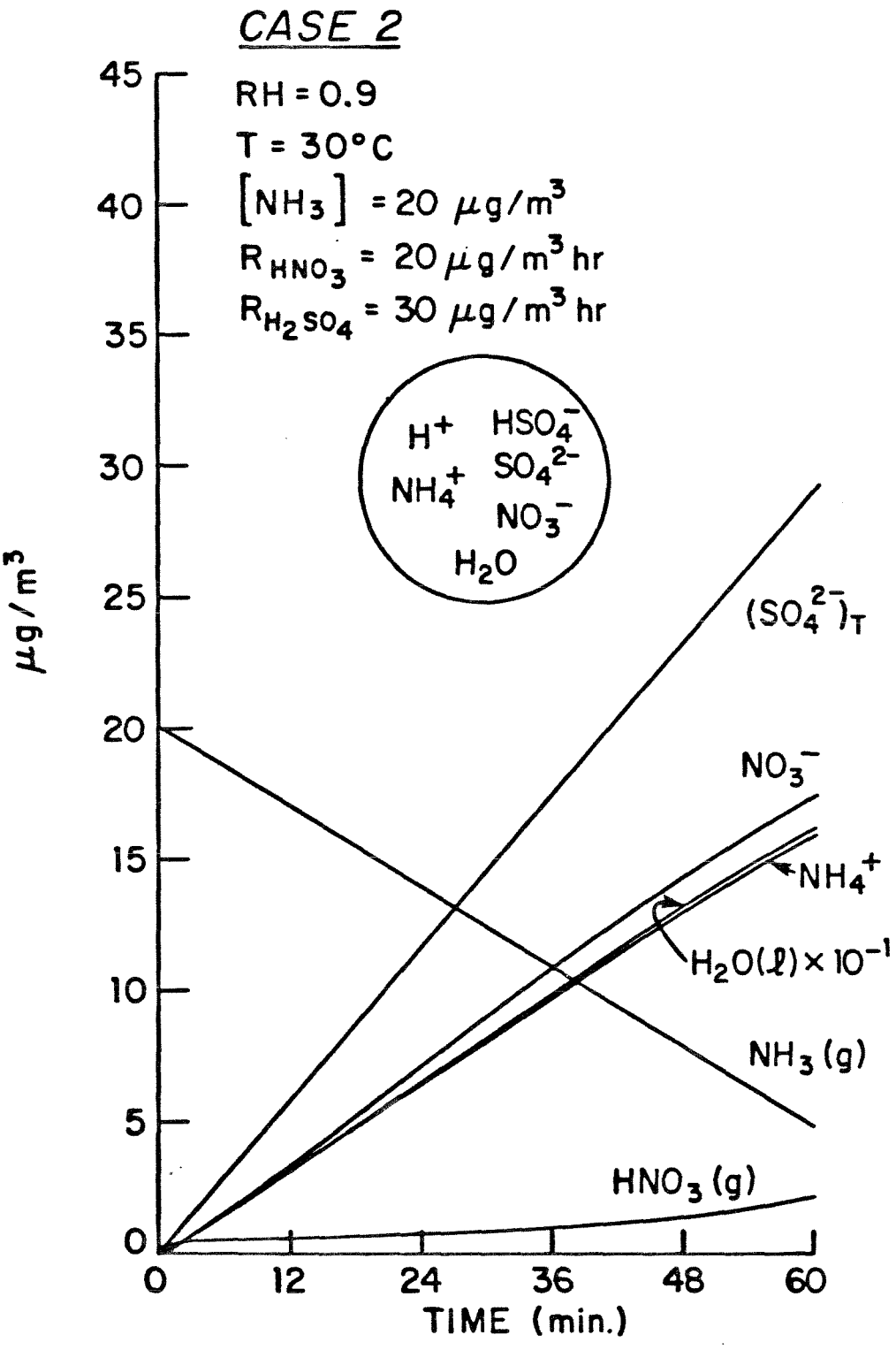

Evolution of Gaseous and Aerosol Constituents for Case 2 of Table 3. Over a one-hour simulation aerosol phase is an aqueous solution as indicated on the figure.

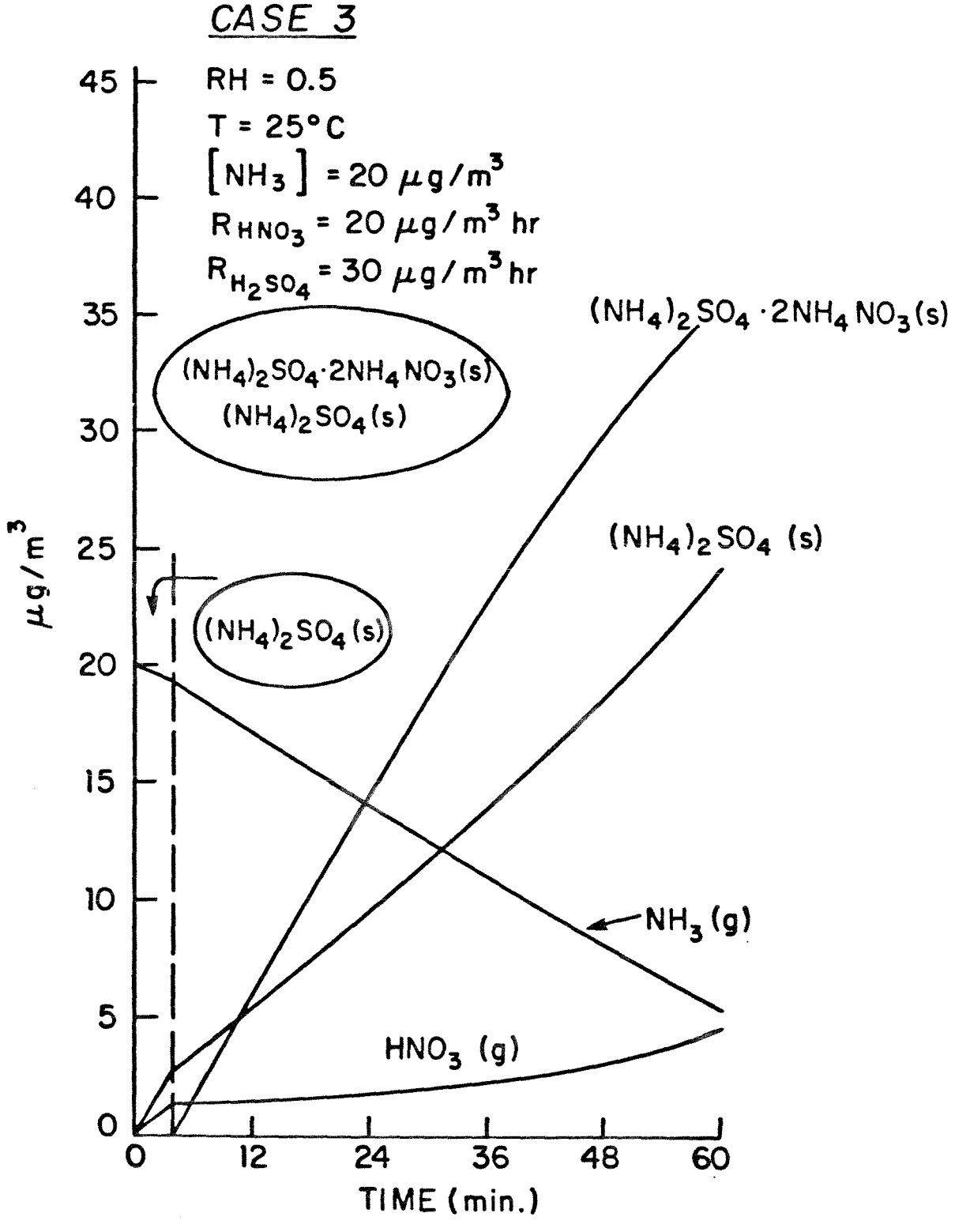

Evolution of Gaseous and Aerosol Constituents for Case 3 of Table 3. The aerosol phase starts out as solid $(NH_4)_2SO_4$, and, after about five minutes, becomes a mixture of solid $(NH_4)_2SO_4$ and $(NH_4)_2SO_4 \cdot 2NH_4NO_3$.

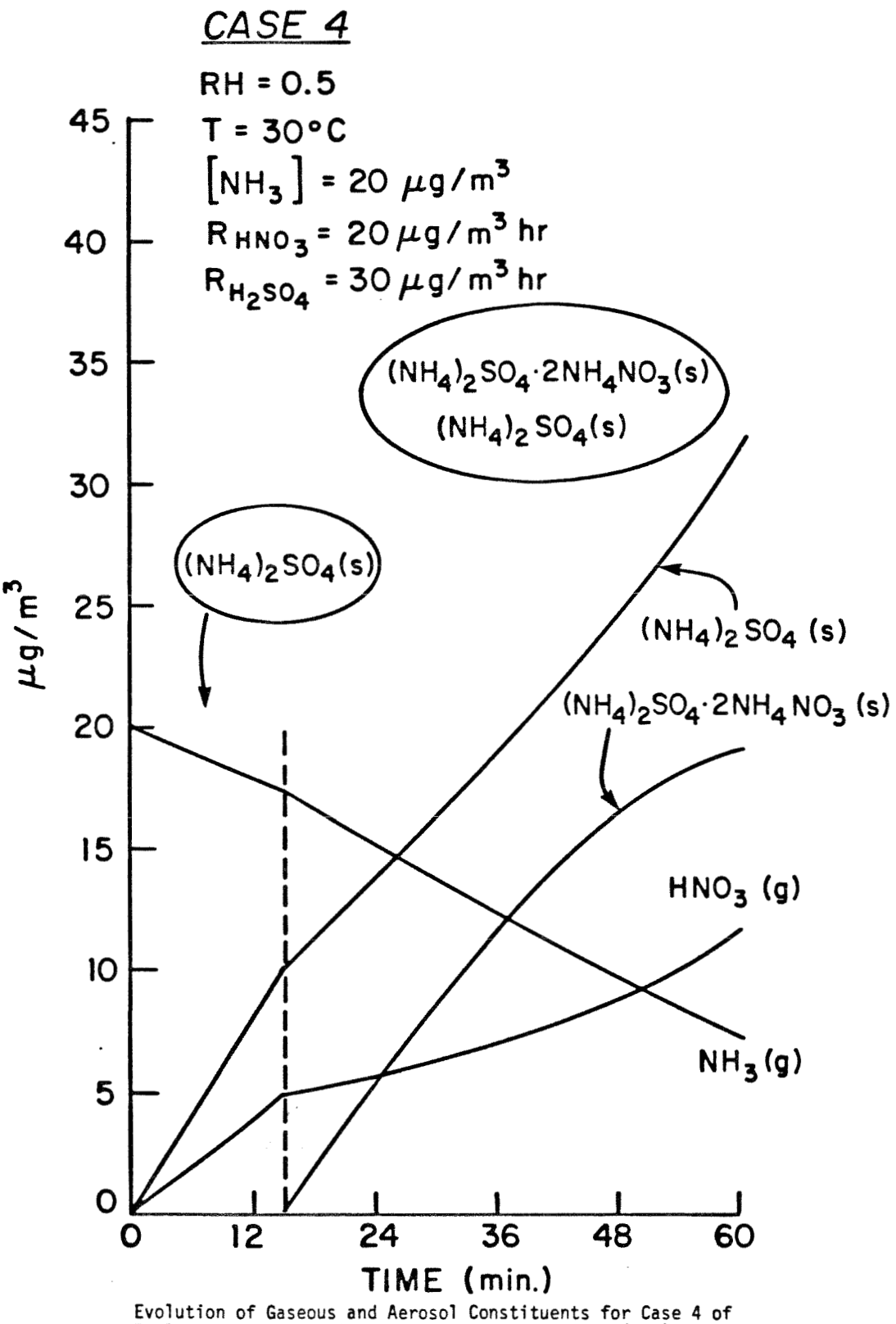

Evolution of Gaseous and Aerosol Constituents for Case 4 of Table 3. The aerosol phase starts out as solid $(NH_4)_2SO_4$, and, after about five minutes, becomes a mixture of solid $(NH_4)_2SO_4$ and $(NH_4)_2SO_4 \cdot 2NH_4NO_3$.

until the NH_3-HNO_3 partial pressure product is exceeded. After it is exceeded, solid NH_4NO_3 forms at a constant rate. However, as the NH_3 partial pressure continues to decrease, the rate of solid NH_4NO_3 formation slows. The HNO_3 partial pressure continues to increase so as to maintain the NH_3-HNO_3 partial pressure product constant.

Cases 5 and 6. The distinguishing feature of these final two cases is the low total ammonia concentration. Consequently, as the sulfate concentration increases, a point is eventually reached where the ammonia is no longer present in sufficient quantity to neutralize totally the sulfuric acid. During the course of Case 5 practically all of the NH_3 is absorbed by the liquid phase. The aqueous nitrate concentration goes through a maximum. Initially, when the NH_3 partial pressure is high, aqueous nitrate increases as HNO_3 is produced in the gas phase. However, as the NH_3 partial pressure continues to fall, the aqueous nitrate concentration also falls. There are two reasons for this behavior. First, the equilibrium constant for nitric acid is such that HNO_3 will desorb from the aqueous phase in the absence of NH_3. In addition, as the solution becomes more and more acidic due to the presence of unneutralized sulfuric acid, the nitric acid equilibrium shifts toward even more gaseous HNO_3.

Case 6 is perhaps the most interesting of the six. First, consider the behavior of the nitrate. Because of the small amount of ammonia present, no solid species containing NH_4NO_3 will be formed. Also, by the time a liquid phase forms, the partial pressure of gaseous ammonia has become extremely small. Thus, only trace amounts of aqueous NH_4NO_3 will be present. Finally, because of the low relative humidity, the liquid phase will contain concentrated sulfuric acid, and have a pH of 0.1. This high acidity will cause

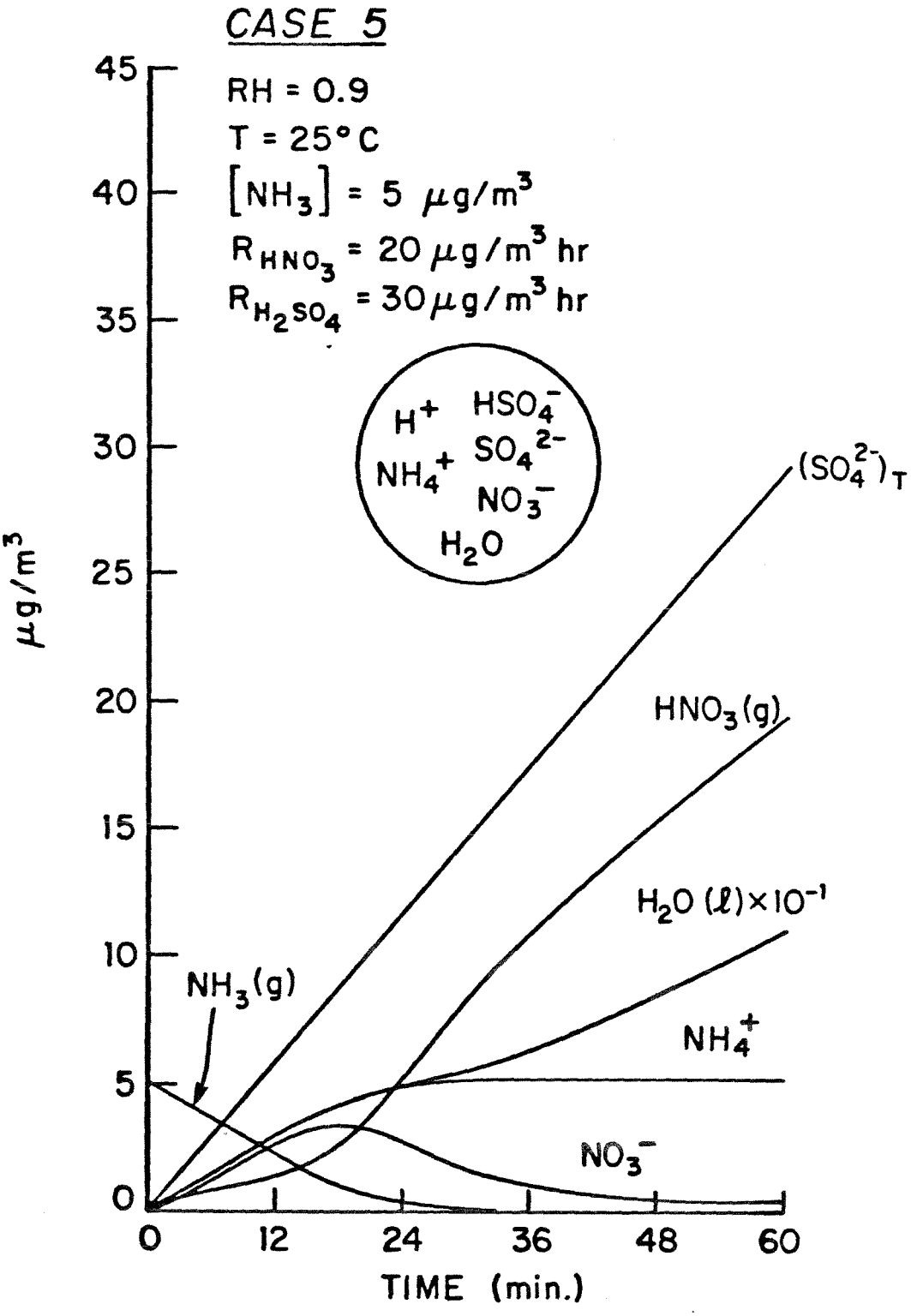

Evolution of Gaseous and Aerosol Constituents for Case 5 of Table 3. The aerosol phase is an aqueous solution as indicated on the figure.

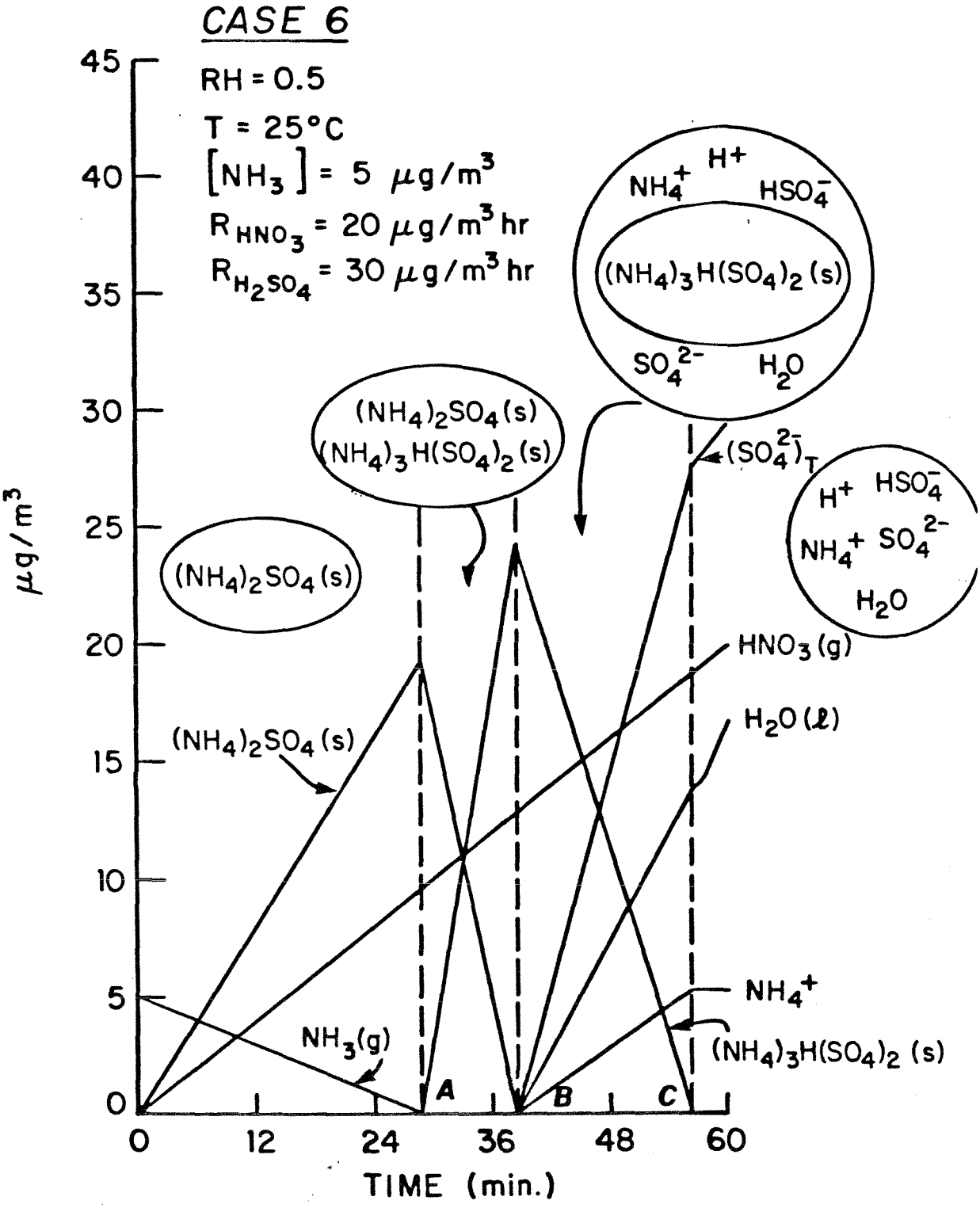

Evolution of Gaseous and Aerosol Constituents for Case 6 of Table 3. Up to point A, the aerosol phase consists of solid $(NH_4)_2SO_4$. From point A to point B, it consists of a mixture of solid $(NH_4)_2SO_4$ and solid $(NH_4)_3H(SO_4)_2$. From point B to point C, the aerosol consists of an aqueous solution surrounding solid $(NH_4)_3H(SO_4)_2$. Finally, after point C the aerosol is an aqueous solution.

the absorption of nitric acid from the gas phase to be unfavorable. As a result of all of these effects, the gas phase will be the only phase containing an appreciable amount of nitric acid.

Next, consider the behavior of the sulfate. Initially, there is excess ammonia present. Thus, as soon as sulfuric acid is introduced into the system, it will be converted to $(NH_4)_2SO_4(s)$. As more and more sulfate is added, the partial pressure of ammonia will continue to fall. Finally, at point A, letovicite, $(NH_4)_3H(SO_4)_2$, appears. Between A and B, there will be two solid phases present, letovicite and ammonium sulfate. During this time, the partial pressure of ammonia will be fixed by the equilibrium,

$$2(NH_4)_2SO_4(s) \rightleftarrows NH_3 + (NH_4)_3H(SO_4)_2(s)$$

Using values of the Gibb's free energy from Table A.1, we find that $p_{NH_3} = 2.2 \times 10^{-10}$ atm at 25°C. This corresponds to a concentration of 0.15 $\mu g/m^3$.

As the system moves from A to B, ammonium sulfate is being converted to letovicite. Finally at point B, all the ammonium sulfate has been consumed. As more sulfate is added, the partial pressure of ammonia will start to decrease again. During this time, the particle will consist solely of letovicite. After 70 seconds, the concentration of gaseous ammonia has fallen to 1.8×10^{-4} $\mu g/m^3$. At this point, a liquid phase appears. At the end of the hour, all of the letovicite has disappeared. At this point, since the relative humidity is greater than the relative humidity of deliquescence for ammonium bisulfate, the particle will be entirely liquid.

Note that if the relative humidity were less than forty percent, the relative humidity of deliquescence of ammonium bisulfate, at C, instead of a liquid phase being formed, solid ammonium bisulfate would appear. As the

simulation progressed, letovicite would be converted to ammonium bisulfate. Finally, a point D would be reached where all the letovicite was consumed and a liquid phase would appear.

4.2 Analysis of the Ambient Data of Tanner (1983)

In this section, the model developed in this work will be compared with results for ambient air obtained by Tanner (1983). These data were collected on Long Island on November 7 and 8, 1979. Tanner presented the results of two sampling runs, one of which was during the day, and the other during the night. During each of these runs, the change of temperature, relative humidity, and total masses of the various components may be approximated as linear to give the conditions used in the simulations.

The first run took place between 1000 and 1400 on November 7, 1979. The temperature remained constant at 14°C while the relative humidity fell from 70 percent to 55 percent. Total sulfate rose from 10 $\mu g/m^3$ to 11 $\mu g/m^3$ and total nitrate remained constant at 8 $\mu g/m^3$, while total ammonium fell from 5 $\mu g/m^3$ to 3 $\mu g/m^3$. Thus, initially there is excess ammonia present, with the molar ratio of total ammonium to total sulfate being 2.9. However, by the end of the run, this ratio dropped to 1.6, so that there was not enough ammonia present to neutralize totally the sulfuric acid.

According to the simulation, the condensed phase initially consists of a mixture of $(NH_4)_2SO_4$ and $(NH_4)_2SO_4 \cdot 2NH_4NO_3$. As the gas phase ammonia partial pressure falls, the nitric acid partial pressure must rise to maintain the partial pressure product for the reaction

$$(NH_4)_2SO_4 \cdot 2NH_4NO_3 \rightleftarrows (NH_4)_2SO_4 + 2NH_3(g) + 2HNO_3(g)$$

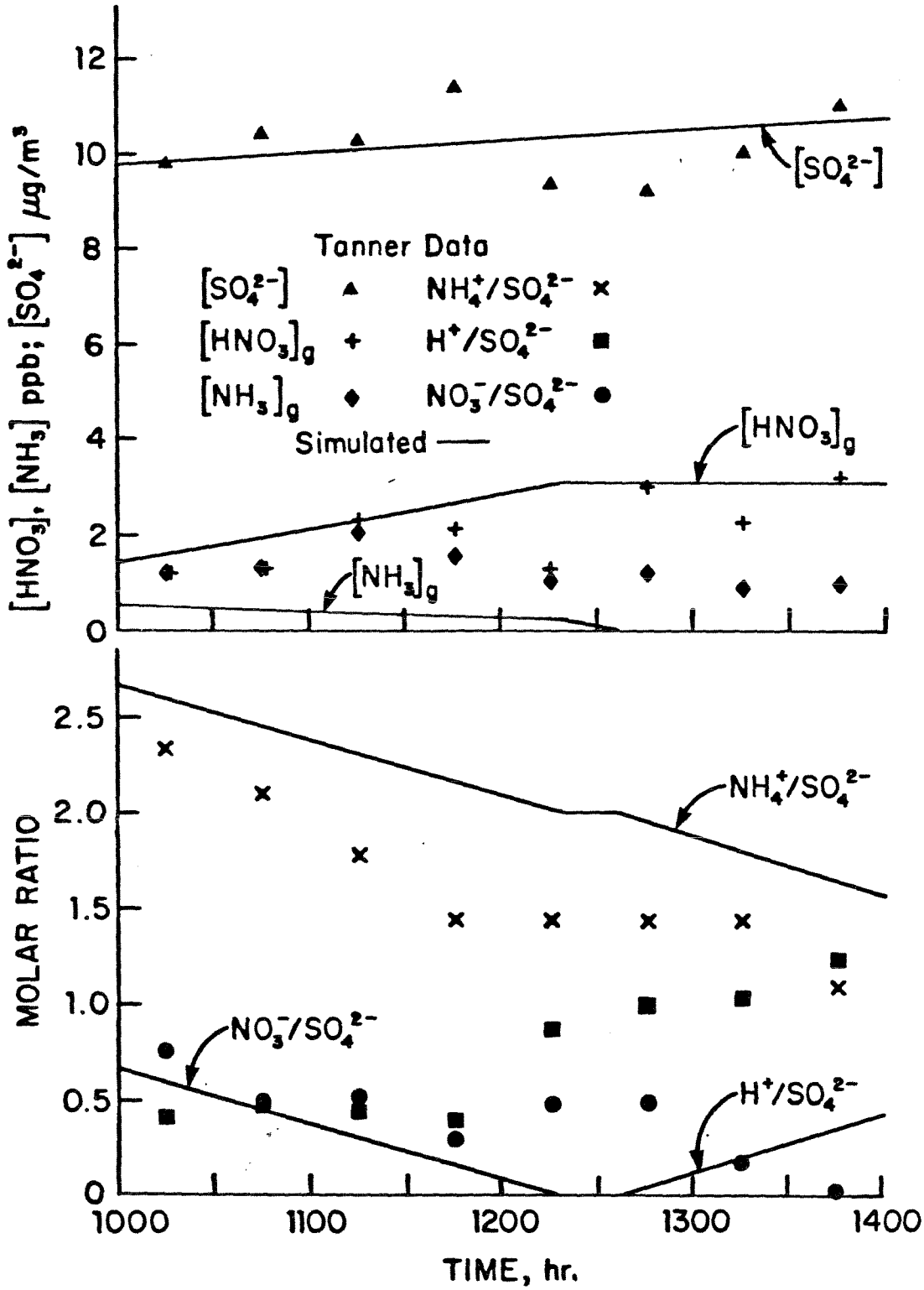

Data and Simulation of Gaseous and Aerosol Data Reported by Tanner (1983) at Brookhaven, New York. Daytime case.

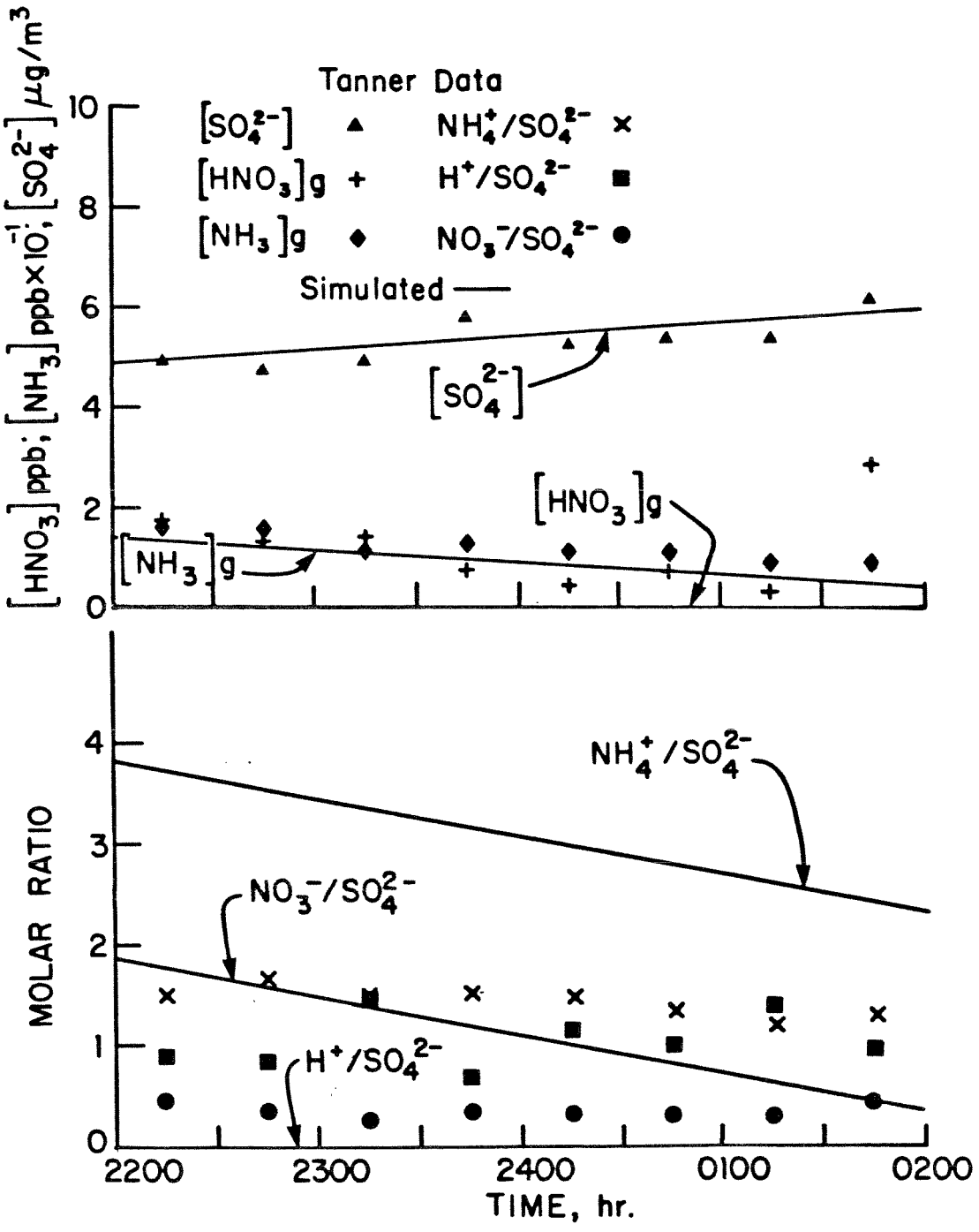

Data and Simulation of Gaseous and Aerosol Data Reported by Tanner (1983) at Brookhaven, New York. Nighttime case.

Thus, the reaction moves to the right. Finally, the point is reached where all the $(NH_4)_2SO_4 \cdot 2NH_4NO_3$ is dissociated. At this point the ammonia partial pressure continues to drop. As more sulfate is introduced, letovicite $(NH_4)_3H(SO_4)_2$ starts to form.

Note the qualitative agreement between the ambient results and the simulation. In both cases, as the ratio of total ammonium to total sulfate decreases, nitrate is forced from the condensed phase into the gas phase. In both cases, the amount of nitrate in the condensed phase eventually goes to zero, and the ratio of ammonium to sulfate in the condensed phase initially declines. However, the ratio hits a plateau, and, near the time when the nitrate has disappeared from the condensed phase, the ammonium to sulfate ratio starts to fall again. Finally, in both cases, as the ratio of total ammonium to sulfate falls, the ratio H^+/SO_4^{2-} starts to rise.

The main difference between the simulation and the data is that the ratio $[NH_3]_g H^+/NH_4^+$ is much higher for the data than the simulation. For example after 1300, for the simulation $p_{NH_3} = 3.6 \times 10^{-3}$ ppb, while values near 1 ppb were obtained experimentally. The low theoretical value is consistent with the observation that the gaseous ammonia concentration is negligible whenever the molar ratio of the total ammonium to total sulfate is less than two.

The second set of data presented by Tanner was obtained in the middle of the night, 2200 November 7, 1979 to 0200 November 8, 1979. In this case, the temperature dropped from 8.5°C to 6°C while the relative humidity remained constant at 80 percent. During this time the sulfate present increased

slightly, from 5 $\mu g/m^3$ to 6 $\mu g/m^3$, while total nitrate and ammonium fell from 6 $\mu g/m^3$ to 1.5 $\mu g/m^3$ and from 13 $\mu g/m^3$ to 5.5 $\mu g/m^3$, respectively. Thus, the molar ratio of total ammonium to sulfate fell from 15 to 5.3. That is, during the entire run, there was excess ammonia present over that which could be absorbed as ammonium nitrate and ammonium sulfate.

For the simulation, the ratio NH_4^+/SO_4^{2-} was much higher and the ratio H^+/SO_4^{2-} was much lower, than for the data. That is, given the gas phase partial pressure of ammonia, the particles observed were much more acidic than would be expected, based on the theory. Alternatively, given the particle phase, the gas phase ammonia partial pressure observed is much higher than that predicted. This disparity was noted by Tanner, who suggested several possible sources of disagreement between theory and experiment. However, as he noted, all of these factors would cause the predicted ammonia partial pressure to be even higher, thus worsening the disagreement. Thus, the source of the disparity remains unknown at present.

5. SUMMARY AND CONCLUSIONS

An equilibrum model of sulfate/nitrate/ammonium aerosol has been presented in which, given the total quantity of sulfate, nitrate and ammonia, temperature and relative humidity, the quantity, chemical composition, and physical state of the aerosol is calculated. The model can easily be integrated into a larger air quality model in the following way. At each location, or in each computational grid cell, the total quantities of sulfate and nitrate produced via gas phase chemistry are assumed to be available, together with those already in the particulate phase. In addition, temperature, relative humidity and ammonia concentration are assumed known. Given this information, the equilibrium model computes the quantity and composition of any condensed phases present. As the air quality model advances in time, the equilibrium is recalculated at each time step.

Aqueous phase sulfate formation reactions have not been considered in the present work. Their inclusion, however, is straightforward. Once the quantity and composition, namely pH, of the liquid phase has been calculated, the amount of dissolved SO_2 and the rate of its oxidation to sulfate can be computed over each time step. In addition, various physical properties such as density and refractive index, can be calculated for the aerosol.

We have not considered the role of particle surface curvature in this work. This aspect will be studied in subsequent work.

ACKNOWLEDGMENT

This work was supported by U.S. Environmental Protection Agency grant R-806844.

APPENDIX DETERMINATION OF PHYSICAL PROPERTIES

A.1 Standard State Chemical Potentials

First, we consider the determination of the standard state chemical potentials at 25°C. Most of the values required can be found in the literature, and are shown in Table A.1. However, there are four solids for which free energy data do not appear to be available, namely NH_4HSO_4, $(NH_4)_3H(SO_4)_2$, $(NH_4)_2SO_4 \cdot 3NH\ NO_3$ and $(NH_4)_2SO_4 \cdot 2NH_4NO_3$. Values of the free energy for these species must be estimated from solubility data.

Consider first $NH_4HSO_4(c)$. Tang and Munkelwitz (1977) state that a saturated solution of NH_4HSO_4 contains 74.2 weight percent NH_4HSO_4 and has a water activity of 0.397. Using the activity coefficients described below, in conjunction with equations (3)-(11), a 74.2 weight percent NH_4HSO_4 solution is calculated to have a water activity of 0.435 with NH_4^+ HSO_4^- having a chemical potential of -332.03 kcal/mol. Similarly, a 66.1 weight percent solution has a_w = 0.397 and μ = - 331.66 kcal/mole. We estimate the chemical potential of NH_4HSO_4 by taking the mean of these values, - 331.85 kcal/mol.

Similarly, Tang et al. (1978) state that a saturated solution of letovicite $(NH_4)_3H(SO_4)_2$ is 69.3 weight percent letovicite and has a water activity of 0.612. Using the same method as before, a 69.3 percent solution has a_w = 0.645, μ = - 698.68 kcal/mol and a 59.4 percent solution has a_w = 0.612, μ = - 697.18 kcal/mol. Taking the mean of these values gives μ = - 697.93 kcal/mol. Similarly, the chemical potentials of $(NH_4)_2SO_4 \cdot 3NH_4NO_3$ and $(NH_4)_2SO_4 \cdot 2NH_4NO_3$ can be estimated from the solubility data of Silcock (1979).

Next, consider the variation of the chemical potential with temperature. Integrating the van't Hoff equation gives

$$\left(\frac{\Delta\mu_o}{RT}\right)_T = \left(\frac{\Delta\mu_o}{RT}\right)_{T_o} + \frac{\Delta H_o}{R}\left(\frac{1}{T} - \frac{1}{T_o}\right) - \int_{T_o}^{T'} \frac{1}{T^{\prime 2}} \int_{T_o}^{T} \Delta C_{p_o}\, dT''\, dT' \quad (A.1)$$

where ΔH_o and $\Delta\mu_o$ are the standard enthalpy and chemical potential of formation and T_o = 298.15 K. The quantity ΔC_{p_o} represents the difference between the heat capacity of the compound and that of the elements in their standard state, e.g. for $HNO_3(g)$

Table A1 Physical Property Data at 298.15K

Species	$\frac{\Delta\mu_o}{RT}$	Ref.	$\frac{\Delta H_o}{RT}$	Ref.	$\frac{C_p}{R}$	Ref.	$\frac{\Delta C_p}{R}$ [a]
H^+ HSO_4^-	-304.925	P	-359.34	p	-16.405	B	-29.665
$2H^+$ SO_4^{2-}	-300.35	P	-366.93	p	-35.23	W	-48.49
H^+ NO_3^-	- 44.965	P	- 83.65	P	-10.42	W	-19.21
NH_4^+ HSO_4^-	-336.98	P	-413.10	P	- 6.79	C	-26.99
$2NH_4^+$ $SO_4^{2=}$	-364.46	P	-474.45	P	-16.00	W	-43.14
NH_4^+ NO_3^-	- 77.02	P	-137.41	P	- 0.805	W	-16.535
$NH_4HSO_4(s)$	-331.85	d	-413.10	e		f	0
$(NH_4)_3H(SO_4)_2(s)$	-697.93	d	-890.18	g	22.55	g	4.59
$(NH_4)_2SO_4(s)$	-364.59	P	-477.08	P	22.55	W	4.59
$NH_4NO_3(s)$	- 74.54	P	-147.82	P	16.76	W	1.03
$(NH_4)_2SO_4 \cdot 3NH_4NO_3$	-589.93	h	-920.54	i	72.83	i	7.68
$(NH_4)_2SO_4 \cdot 2NH_4NO_3$	-515.19	h	-772.72	j	56.07	j	6.65
$H_2O(\ell)$	- 95.684	P	-115.305	P	9.0556	J	3.8256
$NH_3(g)$	- 6.632	P	- 18.532	P	4.282	J	- 2.655
$HNO_3(g)$	- 29.858	J	- 54.18	J	6.415	J	- 2.375
$H_2SO_4(g)$	-264.67	J	-298.75	J	9.695	J	- 3.565
$H_2O(g)$	- 92.213	P	- 97.549	P	4.0384	W	- 1.1916
$H_2(g)$	0	k	0	k	3.468	J	
$N_2(g)$	0	k	0	k	3.503	J	
$O_2(g)$	0	k	0	k	3.533	J	
S	0	k	0	k	2.718	J	

References: P - Parker et al.
J - JANAF
W - Wagman et al.

Notes on following page

Table A1. Physical Property Data at 298.15K (Continued)

Notes:

a. Calculated from $\frac{C_p}{R}$ data.

b. Calculated by means of (20)

c. Values for $NH_4C\ell(aq)$ from Wagman et al. (1968) were used.

d. Estimated from phase data.

e. Value for $NH_4^+HSO_4^-(aq)$ was used.

f. Estimated to be zero.

g. Value for $NH_4HSO_4(s) + (NH_4)_2SO_4$ was used.

h. Estimated from phase data

i,j Values are those for $(NH_4)_2SO_4+3NH_4NO_3$ and $(NH_4)_2SO_4+2NH_4NO_3$, respectively.

k. Values which are zero by convention.

$$\Delta C_{p_o} = C_{p_{HNO_3(g)}} - \frac{1}{2} C_{p_{H_2(g)}} - \frac{1}{2} C_{p_{N_2(g)}} - \frac{3}{2} C_{p_{O_2(g)}} \qquad \text{(A-2)}$$

Neglecting the variation of C_{p_o} with temperature, (A-1) becomes

$$\left(\frac{\Delta\mu_o}{RT}\right)_T = \left(\frac{\Delta\mu_o}{RT}\right)_{T_o} + \frac{\Delta H_o}{RT_o}\left(\frac{T_o}{T} - 1\right) - \frac{\Delta C_{p_o}}{R}\left(\ell n \frac{T}{T_o} + \frac{T_o}{T} - 1\right) \qquad \text{(A-3)}$$

The various quantities required in this equation are given in Table A.1. The values of C_p for $H_2(g)$, $N_2(g)$, $O_2(g)$ are included for use in determining ΔC_{p_o}.

A.2 Aqueous Phase Activity Coefficients

Activity coefficients for the various species of interest have been given at 25°C by Stelson and Seinfeld (1982abc) and Stelson et al. (1983). These may be expressed by a function of the form

$$\ell n\gamma = \frac{-A\sqrt{I}}{1+b\sqrt{I}} + \sum_{i=1} a_i I^i \qquad \text{(A-4)}$$

where the values of A, b and the a_i for each species are given in Table A.3.

A.3 Temperature Variation of Activity Coefficients

With the exception of ammonium nitrate (Stelson and Seinfeld, 1982a), expressions for the temperature variation of activity coefficients for the system of interest here are not available in the literature. In this section we develop new expressions for the temperature dependence of the five activity coefficients required.

The activity coefficient at temperature T can be related to that at a reference temperature T_o by (Stelson et al., 1982)

Table A2

Values of the Constants in Equation A - 4

	H^+,HSO_4^-	$2H^+,SO_4^{2-}$	H^+,NO_3^-	NH_4^+,HSO_4^-	$2NH_4^+,SO_4^{2-}$	NH_4^+,NO_3^-
A	1.4460	2.0367	1.1762	1.1762	2.3525	1.1762
B	2.5384	0.6815	1.44	1.325	1.02	0.925
a_1	3.6487×10^{-1}	-2.5894×10^{-1}	2.26×10^{-1}	-4.5787×10^{-3}	-8.369×10^{-2}	-8.0010×10^{-2}
a_2	1.6614×10^{-2}	9.1128×10^{-2}	-4.722×10^{-2}	5.2712×10^{-3}	7.635×10^{-3}	2.7580×10^{-3}
a_3	-1.9585×10^{-3}	-1.7611×10^{-2}	1.656×10^{-2}	-7.0557×10^{-4}	-3.307×10^{-4}	-4.3922×10^{-5}
a_4	7.7849×10^{-5}	2.4804×10^{-3}	-2.396×10^{-3}	2.8434×10^{-5}	5.783×10^{-6}	0.0
a_5	2.7374×10^{-6}	-2.5043×10^{-4}	1.384×10^{-4}	0.0	0.0	0.0
a_6	-4.1348×10^{-7}	1.7783×10^{-5}	0.0	0.0	0.0	0.0
a_7	4.1209×10^{-10}	-8.8035×10^{-7}	0.0	0.0	0.0	0.0
a_8	1.5215×10^{-9}	2.9730×10^{-8}	0.0	0.0	0.0	0.0
a_9	-7.6288×10^{-11}	-6.5118×10^{-10}	0.0	0.0	0.0	0.0
a_{10}	1.5278×10^{-12}	8.3116×10^{-12}	0.0	0.0	0.0	0.0
a_{11}	-1.1358×10^{-14}	-4.6801×10^{-14}	0.0	0.0	0.0	0.0

$$(\ell n\ \gamma)_T = (\ell n\ \gamma)_{T_o} + \left(\frac{H-H_o}{\nu RT_o}\right)\left(\frac{T_o}{T} - 1\right) + \left(\frac{\bar{C}_p-\bar{C}_p^o}{\nu R}\right)\left(1 + \ell n\ \frac{T_o}{T} - \frac{T_o}{T}\right) \qquad (A\text{-}5)$$

where $\bar{C}_p^o$ and $\bar{C}_p$ are the partial molal heat capacities at infinite dilution and at molality m, respectively, and $(\bar{H}-\bar{H}^o)$ is the relative partial molal enthalpy difference between infinite dilution and molality m at T_o = 298.15K. The quantities $\bar{H}-\bar{H}^o$ and $\bar{C}_p-\bar{C}_p^o$ are evaluated from equations (8-2-7) and (8-4-7) in Harned and Owen (1958),

$$\bar{H} - \bar{H}^o = \phi_L + m\frac{\partial\phi_L}{\partial m} \qquad (A\text{-}6)$$

$$\bar{C}_p = \phi_{C_p} + m\frac{\partial\phi_{C_p}}{\partial m} \qquad (A\text{-}7)$$

Here, ϕ_L and ϕ_{C_p} are the relative apparent molal enthalpy and heat capacity, respectively, of the solutes at a molality m. Note that $\phi_L = -\Delta H_D$, the heat released when the solution is brought from molality m to infinite dilution. Finally,

$$\phi_{C_p} = \frac{(1000+mM_2)C_p - 1000\ C_p^o}{m} \qquad (A\text{-}8)$$

where C_p and C_p^o are the observed heat capacities of a solution of molality m and pure solvent, respectively, and M_2 is the molecular weight of the solute.

Thus, knowing the heat capacity and the heat of dilution of a solution, (A-5)-(A-8) can be used to determine the variation of the activity coefficient with temperature. The sections that follow describe the application of these equations to the system of interest.

A.3.1 Ammonium Sulfate

Values of ϕ_L were obtained by a polynomial regression of the data of Wagman et al. (1968). The result is

$$\frac{\bar{H}-\bar{H}^o}{3RT_o} = -0.1027\ I^{1/2} + 0.06245\ I \qquad \text{(A-9)}$$

Values of C_p were obtained from the data of Sukhatme and Saikhedkar (1969) giving

$$\frac{\bar{C}_p-\bar{C}^o_p}{3R} = 0.7405\ I + 1.5\times10^{-2}\ I^2 \qquad \text{(A-10)}$$

A.3.2 Ammonium Bisulfate

Since values of the thermodynamic quantities for the NH_4^+/HSO_4^- ion pair cannot be directly observed, the approach of Stelson et al. (1983) will be employed in which they will be assumed equal to those for ammonium chloride. Values for the heat of dilution of $NH_4C\ell$ were obtained from a polynomial fit of the data of Wagman et al. (1968),

$$\frac{\bar{H}-\bar{H}^o}{2RT_o} = 0.4409\ I^{1/2} - 0.5059\ I + 0.2033\ I^{3/2} - 0.0302\ I^2 \qquad \text{(A-11)}$$

Values of the $NH_4C\ell$ heat capacity were obtained from Allred and Wooley (1981) and from Epikhim et al. (1977)

$$\frac{\bar{C}_p}{2R} = 0.9168\ I^{1/2} + 0.4081\ I \qquad \text{(A-12)}$$

A.3.3 Sulfuric Acid

The H_2SO_4/H_2O system contains two ion pairs for which thermodynamic properties cannot be directly measured, H^+/HSO_4^- and H^+/SO_4^{2-}. Thus, their properties will be inferred as follows. First, γ_{H^+,HSO_4^-} will be assumed to

vary with temperature similarly to $\gamma_{H^+,C\ell^-}$. Then using heat of dilution data from Wagman (1968) and heat capacity data from Awbery (1929) for HCℓ gives

$$\frac{\bar{H}-\bar{H}^o}{2RT_o} = 0.70125\ I^{1/2} - 0.71730\ I + 0.71446\ I^{3/2} - 0.21410\ I^2 + 2.9808\times10^{-2}\ I^{5/2} - 1.5944\times10^{-3}\ I^3 \qquad \text{(A-13)}$$

$$\frac{\bar{C}_p}{2R} = 4.7706\ I^{1/2} + 0.16888\ I \qquad \text{(A-14)}$$

The equilibrium condition in the H_2SO_4/H_2O system gives the following relation (Stelson et al., 1983)

$$\frac{2Y(2+Y)}{3}\frac{dU}{dI} + \frac{(1-Y)(2+Y)}{2}\frac{dV}{dI} = -\left[\frac{n_w}{I}\ell n a_w + 1 + Y\right] + \frac{2Y(2+Y)}{3I}U + \frac{(1-Y)(2+Y)}{2I}V \qquad \text{(A-15)}$$

$$\frac{2(Y-1)}{3}\frac{dU}{dI} + \frac{9}{4}\frac{dV}{dI} = \ell n\left(\frac{K_2}{Q}\right) \qquad \text{(A-16)}$$

where

$$Q = \frac{m_H\, m_{SO_4}}{m_{HSO_4}} = \frac{(2+Y)(1-Y)I}{9Y} \qquad \text{(A-17)}$$

$$Y = \frac{m_{HSO_4}}{m_{HSO_4}+3m_{SO_4}} \qquad \text{(A-18)}$$

$$U(I) = \int_0^I \ell n\ \gamma_{H^+,HSO_4^-}\, dI' \qquad \text{(A-19)}$$

$$V(I) = \int_0^I \ell n\ \gamma_{2H^+,SO_4^{2-}}\, dI' \qquad \text{(A-20)}$$

and K_2 is the second dissociation constant for sulfuric acid.

The value of $\ell n\ \gamma_{H^+,SO_4^{2-}}$ is found as follows. The assumption that γ_{H^+,HSO_4^-} behaves like $\gamma_{H^+,C\ell^-}$ enables the values of U and dU/dI to be calculated at any I from the available HCℓ data. Then (A-15) and (A-16) can be rearranged to yield

$$\frac{2Y(2+Y)}{3}\frac{dU}{dI} + \frac{2(1-Y)(2+Y)}{9}\left[\ell n\left(\frac{K_2}{Q}\right) + \frac{2}{3}(1-Y)\frac{dU}{dI}\right]$$
$$= -\left[\frac{n_w}{I}\ell na_w + 1 + Y\right] + \frac{2Y(2+Y)}{3I}U + \frac{(1-Y)(2+Y)}{2I}V \qquad \text{(A-21)}$$

If V and I are known, (A-21) can be solved for Y. Then (A-16) can be integrated numerically to determine V(I). In doing so, one uses the data of Giauque et al. (1960) for the variation of ℓna_w with temperature and

$$\ell n\ K_2 = 4.5756 + 6.9539\left(\frac{T_o}{T} - 1\right) + 42.875\left(1 + \ell n\frac{T_o}{T} - \frac{T_o}{T}\right) \qquad \text{(A-22)}$$

from Readnour and Cobble (1969). Once $\ell n\ \gamma_{2H^+,SO_4^-}$ is known as a function of temperature, the desired quantities may be found from

$$\frac{\bar{A}-\bar{A}^o}{3R} = \frac{\partial \ell n\ \gamma}{\partial(1/T)} \qquad \text{(A-23)}$$

$$\bar{C}_p - \bar{C}_p^o = \frac{\partial}{\partial T}\left(\frac{\bar{A}-\bar{A}^o}{3R}\right) \qquad \text{(A-24)}$$

where the differentiation is performed numerically and the results are fitted by polynomials.

A.3.4 Nitric Acid

Determination of the temperaure variation of the activity coefficient for nitric acid requires a special treatment because, in the concentration range of interest, in a binary solution of nitric acid and water an appreciable fraction of the nitric acid exists in an undissociated form (Hogfelt, 1963). Thus, the stoichiometric expression must be corrected for the existence of undissociated acid.

The variation of the stoichiometric (full dissociation) activity coefficient with temperature may be calculated from the heat of dilution data of Wagman et al. (1968) and the heat capacity data of Enea et al. (1977) and Bump and Sibbit (1955).

$$\frac{\bar{H}-\bar{H}^{o}}{2RT} = 0.5943\ I^{1/2} - 1.0330\ I + 0.6378\ I^{3/2} - 0.1206\ I^{2} + 7.328\times10^{-3}\ I^{3/2} \qquad \text{(A-25)}$$

$$\frac{\bar{C}_{p}}{R} = 3.4905\ I^{1/2} - 1.1804\ I + 1.6639\ I^{3/2} - 0.5522\ I^{2} + 5.063\times10^{-2}\ I^{5/2} \qquad \text{(A-26)}$$

These expressions are then corrected for the presence of undissociated nitric acid as follows (Stelson, personal communication, 1982). The degree of dissociation $\alpha = m_{NO_3^-}/m_s$ is given by

$$\alpha = 1 - \frac{1}{m_s}\left[\frac{K_1(\gamma_s m_s)^2}{\rho\text{-}10^{-3}M_2K_1(\gamma_s m_s)^2} + \frac{K_2(\gamma_s m_s)^2 a_w}{\rho\text{-}10^{-3}K_2a_wM_2(\gamma_s m_s)^2} + \frac{a_w^3K_3(\gamma_s m_s)^2}{\rho\text{-}10^{-3}K_3a_w^3M_2\gamma_s^2m_s}\right] \qquad \text{(A-27)}$$

where γ_s and m_s are the stoichiometric activity coefficient and molality of nitric acid, respectively, ρ is the density of nitric acid and K_1, K_2 and K_3 are the equilibrium constants for the reactions

(1) $H^+ + NO_3^- \rightleftarrows HNO_3(u)$

(2) $H^+ + NO_3^- + H_2O \rightleftarrows HNO_3\cdot H_2O$

(3) $H^+ + NO_3^- + 3H_2O \rightleftarrows HNO_3\cdot 3H_2O$

where u denotes the undissociated state. The temperature variation of K_1, K_2 and K_3 can be calculated from the van't Hoff equation,

$$\frac{d\ell nK}{dt} = \frac{\Delta H}{RT_o} \tag{A-28}$$

where the enthalpy change ΔH is evaluated from the enthalpies of formation of the undissociated species (Wagman et al., 1968).

Once α has been calculated, the activity coefficient and ionic strength are found from $\gamma = \gamma_s/\alpha$ and $I = \alpha m_s$. Given the activity coefficient, the desired enthalpy difference is calculated by

$$\frac{\bar{H}-\bar{H}^o}{2RT_o} = - T_o\left(\frac{\partial \ell n\gamma}{\partial T}\right)_I \tag{A-29}$$

Using the chain rule, (A-29) becomes

$$\frac{\bar{H}-\bar{H}^o}{2RT_o} = - T_o \left[\left(\frac{\partial \ell n\gamma}{\partial T}\right)_{m_s} - \left(\frac{\partial \ell n\gamma}{\partial m_s}\right)_T \left(\frac{\partial I}{\partial m_s}\right)_T^{-1} \left(\frac{\partial I}{\partial T}\right)_{m_s} \right] \tag{A-30}$$

After evaluating the partial derivatives in (A-30) numerically, we obtain

$$\frac{\bar{H}-\bar{H}^o}{2RT_o} = 0.1499\ I^{1/2} - 3.929\times10^{-3}\ I \tag{A-31}$$

At high ionic strengths, an appreciable fraction of the nitric acid will remain undissociated. Thus, the actual ionic strength will be less than the total molality. For example, Stelson and Seinfeld (1982b) found that the maximum ionic strength of a nitric acid solution is 8.3, which occurs between 17 to 21 total nitric acid molality. As a consequence of this, it is not possible to obtain activity coefficient data for nitric acid for high ionic strengths directly. Instead data for high ionic

strengths are obtained by linearly extrapolating data for lower ionic strengths. As a result of the error inherent in the extrapolation, it was not worthwhile to develop an expression for $\bar{C}_p$ analogous to that for $\bar{H}-\bar{H}^o$.

REFERENCES

Alkezweeny A. J. (1978) Measurement of aerosol particles and trace gases in METROMEX. J. Applied Meteorology 17, 609-614.

Allred G. E. and Wooley E. M. (1981) Heat capacities of aqueous acetic acid, sodium acetate, ammonia and ammonium chloride at 283.15, 298.15 and 313.15K: ΔC_p^o for ionization of acetic acid and for dissociation of ammonium ion. J. Chem. Thermodynamics 13, 155-164.

Appel B. R., Kothny E. L., Hoffer E. M., Hidy G. M. and Wesolowski J. J. (1978) Sulfate and nitrate data from the California Aerosol Characterization Experiment (ACHEX). Environ. Sci. Technol. 12, 418-425.

Awbery J. H. (1929) *The heat capacity of certain solutions.* In International Critical Tables of Numerical Data, Physics, Chemistry and Technology, Vol. V, pp. 115-117. McGraw-Hill, New York.

Brosset C. (1978) Water-soluble sulfur compounds in aerosols. Atmospheric Environment 12, 25-28.

Bump T. R. and Sibbit W. L. (1955) Aqueous solutions of nitric acid and of sulfuric acid. Ind. Eng. Chem. 47, 1665-1670.

Charlson R. J., Covert D. S., Larson T. V. and Waggoner A. P. (1978) Chemical properties of tropospheric sulfur aerosols. Atmospheric Environment 12, 39-53.

Countess R. J., Wolff G. T. and Cadle S. H. (1980) The Denver winter aerosol: A comprehensive chemical characterization. J. Air Poll. Control Assoc. 30, 1194-1200.

Countess R. J., Cadle S. H., Groblicki P. J. and Wolff G. T. (1981) Chemical analysis of size-segregated samples of Denver's ambient particulate. J. Air Pollut. Control Assoc. 31, 247-252.

Duewer W. H., Walton J. J., Grant K. E. and Walker H. (1980) Livermore regional *air quality model (LIRAQ) transfer to EPA.* Lawrence Livermore Laboratory, Livermore, CA.

Enea O., Singh P. P., Woolley E. M., McCurdy K. S. and Hepler L. S. (1977) Heat capacities of aqueous nitric acid, sodium nitrate, and potassium nitrate at 298.15K: ΔC_p^o of ionization of water. J. Chem. Thermodynamics 9, 731-734.

Epikhim Y. A. Bazlova J. V. and Karapet'yants M. K. (1977) Changes in the volume and heat capacity in aqueous salt solutions. IV. The ammonium chloride-ammonium nitrate-water system. Zh. Fiz. Khim 51, 1150-1152.

Giauque E. W., Hornung E. W., Kunzler J. E. and Rubin T. R. (1960) The thermodynamic properties of aqueous sulfuric acid solutions and hydrates from 15 to 300°K. J. Am. Chem. Soc. 82, 62-70.

Harned H. S. and Owen B. B. (1958) The Physical Chemistry of Electrolytic Solutions, ACS Monograph Series No. 137, 3rd Edn. Reinhold Publishing Corporation, New York, Chap. 8.

Hogfelt E. (1963) The complex formation between water and strong acids. Acta. Chemico. Scandinavica 17, 785-796.

JANAF Thermochemical Tables, 2nd Edn. (1971). NSRDS-NBS 37.

Kusik C. L. and Meissner H. P. (1978) Electrolytic activity coefficients in inorganic processing. A.I.Ch.E. Symp. Ser. 173, 14-20.

Lamb R. G. (1982) A regional scale (1000 km) model of photochemical air pollution. Part I. Theoretical formulation. U.S. Environmental Protection Agency, Research Triangle Park, N.C.

Leaderer B. P. (1978) Summary of the New York summer aerosol study (NYSAS). J. Air Pollut. Control Assoc. 28, 321-327.

Macias E. S., Swicker J. O., Ouimette J. R., Hering S. V., Friedlander S. K., Cahill T. A., Kuhlmey G. A. and Richards L. W. (1981) Regional haze case studies in the Southwestern U.S. - I. Aerosol chemical composition. Atmospheric Environment 15, 1971-1986.

McRae G. J., Goodin W. R. and Seinfeld, J. H. (1982) Development of a second-generation mathematical model for urban air pollution - I. Model formulation. Atmospheric Environment 16, 679-696.

Parker V. B., Wagman D. D. and Garvin D. (1976) Selected thermochemical data compatible with the CODATA recommendations. NBSIR 75-968.

Readnour J. M. and Cobble J. W. (1969) Thermodynamic properties for the dissociation of bisulfate ion and the partial molal heat capacities of bisulfuric acid and sodium bisulfate over an extended temperature range. Inorg. Chem. 8, 2174-2182.

Russell, A. G., McRae G. J. and Cass G. R. (1983) Mathematical modeling of the formation and transport of ammonium nitrate aerosol. Atmospheric Environment 17, 949-965.

Saxena P., Seigneur C. and Peterson T. W. (1983) Modeling of multiphase atmospheric aerosols. Atmospheric Environment 17, 1315-1329.

Schwartz S. E. and Freiberg J. E. (1981) Mass-transport limitation to the rate of reaction of gases in liquid droplets: Application to oxidation of SO_2 in aqueous solutions. Atmospheric Environment 15, 1129-1144.

Seigneur C., Tesche T. W., Roth P. M. and Reid L. E. (1981) Sensitivity of a complex urban air quality model to input data. J. Applied Meteorology 20, 1020-1040.

Seinfeld J. H. (1980) Lectures in Atmospheric Chemistry. AIChE Monograph Series No. 12, American Institute of Chemical Engineers, New York.

Silcock H. L. (1979) Solubilities of Inorganic and Organic Compounds, Vol. 3 Part 2, pp. 157-159 Pergamon Press, New York.

Stelson A. W. and Seinfeld J. H. (1981) Chemical mass accounting of urban aerosol. Environ. Sci. Technol. 15, 671-679.

Stelson A. W., Friedlander S. K. and Seinfeld J. H. (1979) A note on the equilibrium relationship between ammonia and nitric acid and particulate ammonium nitrate. Atmospheric Environment 13, 369-371.

Stelson A. W. and Seinfeld J. H. (1982a) Relative humidity and temperature dependence of the ammonium nitrate dissociation constant. Atmospheric Environment 16, 983-992.

Stelson A. W. and Seinfeld J. H. (1982b) Relative humidity and pH dependence of the vapor pressure of ammonium nitrate-nitric acid solutions at 25°C. Atmospheric Environment 16, 993-1000.

Stelson A. W. and Seinfeld J. H. (1982c) Thermodynamic prediction of the water activity, NH_4NO_3 dissociation constant, density and refractive index for the NH_4NO_3-$(NH_4)_2SO_4$-H_2O system at 25°C. Atmospheric Environment 16, 2507-2514.

Stelson A. W., Bassett M. E. and Seinfeld J. H. (1983) Thermodynamic equilibrium properties of aqueous solutions of nitrate, sulfate and ammonium, in Chemistry of Particles, Fogs and Rain, J. L. Durham, ed., Ann Arbor Publ., Ann Arbor, MI

Stevens R. K., Dzubay T. G., Shaw Jr. R. W., McClenny W. A., Lewis C. W. and Wilson W. E. (1980) Characterization of aerosol in the Great Smoky Mountains. Environ. Sci. Technol. 14, 1491-1498.

South Coast Air Quality Management District (1982) Suspended particulate matter in the atmosphere of the South Coast Air Basin and Southeast Desert Areas - 1980. South Coast Air Quality Management District, El Monte, CA.

Sukhatme S. P. and Sairkhedkar N. (1969) Heat capacities of glycerol-water mixtures and aqueous solutions of ammonium sulfate ammonium nitrate and strontium nitrate. Indian J. Technol. 7, 1-4.

Tang I. N. and Munkelwitz H. R. (1977) Aerosol growth studies - III. ammonium bisulfate aerosols in a moist atmosphere. J. Aerosol Sci. 8, 321-330.

Tang I. N., Munkelwitz H. R. and Davis J. G. (1978) Aerosol growth studies - IV. phase transformation of mixed salt aerosols in a moist atmosphere. Atmospheric Environment 12, 505-511.

Tang I. N. (1980) On the equilibrium partial pressures of nitric acid and ammonia in the atmosphere. Atmospheric Environment 14, 819-828.

Tanner R. L., Marlow W. H. and Newman L. (1979) Chemical compsoition correlations of size-fractionated sulfate in New York City aerosol. Environ. Sci. Technol. 13, 75-78.

Tanner R. L., Leaderer B. P. and Spengler J. D. (1981) Acidity of atmospheric aerosols. Environ. Sci. Technol. 15, 1150-1153.

Tanner R. L. (1983) An ambient experimental study of phase equilibrium in the atmospheric system: Aerosols H^+, NH_4^+, SO_4^{2-},NO_3^- - $NH_3(g)$, $HNO_3(g)$. Atmospheric Environment 16, 2935-2942.

Wagman D. D., Evans W. H., Parker V. B., Harlow I., Baily S. M. and Schumm R. H. (1968) Selected values of chemical thermodynamic properties; tables for the first thirty-four elements in the standard order of arrangement, NBS technical note 270-3.

CHAPTER 4

ATMOSPHERIC EQUILIBRIUM MODEL OF SULFATE AND NITRATE AEROSOLS II. PARTICLE SIZE ANALYSIS

Submitted to Atmospheric Environment

ATMOSPHERIC EQUILIBRIUM MODEL OF SULFATE AND NITRATE AEROSOLS II. PARTICLE SIZE ANALYSIS*

Mark E. Bassett
and
John H. Seinfeld†

Department of Chemical Engineering
California Institute of Technology
Pasadena, California 91125

ABSTRACT

Part I of this work presented a thermodynamic equilibrium model for the quantity, composition, and physical state of atmospheric sulfate/nitrate/ammonium aerosols. In this work we extend that model to include particle size. That is, given total nitrate and ammonium levels, relative humidity and temperature, and the distribution of sulfate by particle size, we calculate the equilibrium quantity, composition, and physical state of the aerosol as a function of particle size. The model provides an explanation for the differences in observed ambient sulfate and nitrate size distributions.

*Part I of this work is Bassett and Seinfeld (1983)

†To whom correspondence should be addressed.

ATMOSPHERIC EQUILIBRIUM MODEL OF SULFATE AND NITRATE AEROSOLS II. PARTICLE SIZE ANALYSIS

1. INTRODUCTION

One of the intriguing observations from the ACHEX (Aerosol Characterization Experiment) was the disparity between the distributions of sulfate and nitrate by particle size observed in Los Angeles aerosol (Hidy et al., 1975; Appel et al., 1978). In that study, among other instruments, an impactor was used to determine the mass median diameter of sulfate and nitrate in aerosol particles at various points in the South Coast Basin. As a result, it was determined that the mass median diameter for nitrate tended to be larger than that for sulfate by up to a factor of four. To explain this observation one needs to understand why different species might tend to congregate in different regions of the aerosol particle size spectrum. The factors involved are in general a combination of kinetic and thermodynamic ones, kinetic in the sense of particles evolving due to vapors condensing from the gas phase, and thermodynamic in the sense that, at any instant of time, particles might adjust their size and composition so as to be at thermodynamic equilibrium with the gas phase.

The observation that atmospheric aerosols tend to exist at thermodynamic equilibrium with the gas phase (Stelson et al., 1979; Stelson and Seinfeld, 1982 abc; Tanner 1982) led to the development of an equilibrium model for sulfate/nitrate/ammonium aerosols by Bassett and Seinfeld (1983). In that work, hereafter referred to as Part I, a model is presented for the equilibrium composition, quantity, and state (liquid or solid) of atmospheric sulfate/nitrate/ammonium aerosols given total sulfate, nitrate, and ammonia concentrations, relative humidity and temperature. Total sulfate and nitrate levels, in terms of gaseous H_2SO_4 and HNO_3, are predictable by a gas-phase

chemical kinetic mechanism, so that the equilibrium model of Part I can be included as an aerosol module in an urban or regional air quality model. The equilibrium calculation predicts total quantity, say in $\mu g\ m^{-3}$, of each constituent, such as $(NH_4)_2SO_4$, NH_4HSO_4, NH_4NO_3, etc. but does not say anything about the sizes of the particles. The present work extends that of Part I to include particle size.

Because of the so-called Kelvin effect, the variation of vapor pressure of species in a drop with radius of the drop, the equilibrium composition of particles of different sizes will be different. The fundamental question we consider here is - Given gas-phase concentrations of sulfate, nitrate, and ammonia, relative humidity and temperature, can we calculate the equilibrium composition, quantity, and state of the aerosol *as a function of particle size?* The sulfate/nitrate/ammonium system contains one non-volatile component, namely sulfate. As a result, at equilibrium, if the size distribution of sulfate is known, the system is uniquely determined, in that the distributions of all other components by particle size is fixed. In this work we present the model that governs this situation.

2. MODEL FORMULATION

Consider a system containing a known amount of volatile species at temperature T and pressure p. Into this system is introduced a distribution of particles composed of various non-volatile species. The goal is to determine how much of each of the volatile species will condense on to each of the particles when the system reaches equilibrium. In addition, it is desired to know which of the various possible phases are present at equilibrium.

A key variable is the partial pressure of each vapor component. The partial pressure of component i is related to the total number of moles of i in the system, N_i, and to the number of moles of i in a particle, n_i, by

$$\frac{p_i}{RT} = N_i - \int_0^\infty \cdots \int_0^\infty n_i \, n(n_1, \ldots, n_s) \, dn_1 \cdots dn_s \qquad (1)$$

where $n(n_1, \ldots, n_s)\, dn_1 \ldots dn_s$ is the number of particles per unit volume having between n_j and $n_j + dn_j$ moles of species j. We note that, as a consequence of (1), the gas phase composition cannot be predicted beforehand but depends on the particles present. In other words, a total quantity N_i distributes itself between gas and particulate phases in a manner that must be determined in the solution to the overall problem.

The aerosol size distribution will be represented by the sectional approximation (Gelbard et al., 1980; Gelbard and Seinfeld, 1980). In this approach, the continuous size distribution is divided into a series of bins or sections, where the ℓth section includes all particles whose diameter d satisfies $d_{\ell-1} < d \leq d_\ell$, and where d_ℓ and $d_{\ell-1}$ are the upper and lower limits of section ℓ. Additionally, we assume that particle mass M is evenly distributed within each section, i.e. $dM/d \log_{10} d$ is constant in each section. Finally, we assume that the properties of all particles in a section are those of a particle having the average composition of all particles in the section and having a diameter $\bar{d}_\ell = (d_\ell d_{\ell-1})^{\frac{1}{2}}$. The net effect of these assumptions is to replace the continuous size distribution by a histogram.

2.1 Equilibrium Condition

The condition for chemical equilibrium in a closed system at constant T and p is that the total Gibbs free energy of the system, G, is a minimum. The Gibbs free energy is a function of T, p and n_i^ℓ, the number of moles of species i in section ℓ. Thus, the determination of the equilibrium composition is the following minimization problem

$$\min_{n_i^\ell} G(T,p,n_i^\ell)$$

subject to $n_i^\ell \geq 0$ and conservation of mass (1).

One problem with the above formulation is that the constraints arising from conservation of mass will prove awkward to handle computationally. This problem can be circumvented as follows. First, note that in the presence of the Kelvin effect, the chemical potential of a species will depend on the size of the particle in which the species is present. Thus, for example, the chemical potential of $NH_4NO_3(s)$ in the first section will be different than that in the second section. As a result, there will be a series of equilibria of the form

$$NH_3(g) + HNO_3(g) \rightleftharpoons NH_4NO_3(s, \text{ in section } \ell)$$

involving $NH_4NO_3(s)$. Assume that the reaction involving NH_3, HNO_3 and $NH_4NO_3(s)$ is reaction j. Then, let ξ_j^ℓ be the amount of $NH_4NO_3(s)$ formed in section ℓ by reaction j coming to equilibrium above that present at some arbitrary initial time, $n_{i,o}^\ell$. Then, in terms of the ξ_j^ℓ, the minimization becomes

$$\min_{\xi_j^\ell} G(T,p,\xi_j^\ell)$$

subject to

$$n_i^\ell = n_{i,o}^\ell + \sum_j \nu_{ij}\xi_j^\ell \geq 0$$

where ν_{ij} is the stoichiometric coefficient of species i in reaction j. The condition for a minimum of G is equivalent to

$$\sum_i \nu_{ij}\mu_i^\ell = 0 \qquad \text{all } j, \ell \tag{2}$$

where μ_i^ℓ is the chemical potential of species i in section ℓ.

2.2 Chemical Potentials

The chemical potential of species i in section ℓ is related to the chemical potential of species i in the bulk phase, μ_i, by the Gibbs-Thompson equation,

$$\mu_i^{\ell} - \mu_i = \frac{4\sigma \bar{V}_i}{\bar{d}_{\ell}} \tag{3}$$

where σ is the surface tension, and $\bar{V}_i$ is the molal volume of species i. Expressions for the bulk phase chemical potentials of species in the atmospheric sulfate/nitrate/ammonium system appear in Part I (Bassett and Seinfeld, 1983).

3. DETERMINATION OF THE EQUILIBRIUM

To determine the equilibrium, the system of nonlinear equations (2) must be solved numerically. The solution will be carried out by means of the global homotopy method of Keller (1978, 1982). In essence, this method allows us to construct the solution for the case with the Kelvin effect based on that obtained previously without the Kelvin effect.

The homotopy method can be described as follows. Let σ be the physically observed surface tension and σ^* be the value used in the calculation. Let $\sigma^* = \sigma\lambda$ where λ is a parameter. Then, the system of equations (2) can be rewritten as $\underset{\sim}{f}(\underset{\sim}{\xi};\lambda) = 0$ where $\underset{\sim}{\xi}$ is the vector of reaction extents. Now, the problem can be restated as follows. Find the solution of $\underset{\sim}{f}(\underset{\sim}{\xi};1) = \underset{\sim}{0}$ based on the solution to $\underset{\sim}{f}(\underset{\sim}{\xi};0) = \underset{\sim}{0}$.

An obvious way to attack this problem is by a straightforward application of Newton's method. Let $\underset{\sim}{\xi}_i$ be the value of $\underset{\sim}{\xi}$ at the end of the ith iteration. Then, let the starting point $\underset{\sim}{\xi}_0$ be the solution of $\underset{\sim}{f}(\underset{\sim}{\xi};0) = \underset{\sim}{0}$, and

$$\underset{\sim}{\xi}_{i+1} = \underset{\sim}{\xi}_i - (\underset{\sim}{f}_{\underset{\sim}{\xi}})^{-1}_{\underset{\sim}{\xi}_i} \underset{\sim}{f}(\underset{\sim}{\xi}_i;1) \tag{4}$$

where $\underset{\sim}{f}_{\underset{\sim}{\xi}} = (\partial \underset{\sim}{f}/\partial \underset{\sim}{\xi})$. The problem with this scheme is that the $\underset{\sim}{\xi}_i$'s will only approach the desired solution if the starting value of the iteration, $\underset{\sim}{\xi}_o$, is sufficiently close to the final value.

This problem can be overcome as follows. First, note that the larger the surface tension is, the greater the effect on the composition is likely to be. This means that the iteration scheme given by (4) is less likely to converge. To avoid this problem, instead of trying to go from $\lambda = 0$ to $\lambda = 1$ in one step, do it in several steps. That is, replace (4) by

$$\underset{\sim}{\xi}_{i+1} = \underset{\sim}{\xi}_i - (\underset{\sim}{f}_{\underset{\sim}{\xi}})^{-1}_{\underset{\sim}{\xi}_i} \underset{\sim}{f}(\underset{\sim}{\xi}_i;\lambda_a) \qquad (5)$$

where λ_a is between zero and one. Then, starting from $\lambda = 0$, iterate to find the solution at λ_a. Then, using the solution at λ_a as a starting value, iterate to find the solution at λ_b, and so forth, until $\lambda = 1$ is reached. Note that if the iteration fails to converge, say going from λ_a to λ_b, it is restarted from λ_a, using a smaller value of $\lambda_b - \lambda_a$.

3.1 Pseudo-arc Length Continuation

The preceding method is a powerful way to determine the equilibrium of the system for most cases. However, there are cases where the above method will break down. A simple example of this is as follows. Consider a system containing only sulfate, ammonium and water. For simplicity, assume that there is enough ammonia present so that the concentrations of all ions other than SO_4^{2-} and NH_4^+ are negligible. Then, only two equilibria are important

$$H_2O(g) \rightleftarrows H_2O\ (\ell)$$

and

$$(NH_4)_2SO_4(s) \rightleftarrows 2NH_4^+ + SO_4^{2-}$$

Using (3), the expression for the equilibrium of the first reaction is

$$\mu^{o}_{H_2O(\ell)} + RT\,\ell n a_{w_\infty} + \frac{4\sigma\lambda\bar{V}_w}{\bar{d}_\ell} = \mu^{o}_{H_2O(g)} + RT\,\ell n\, p_w/p^o \qquad (6)$$

where a_{w_∞} is the water activity without the Kelvin effect. Using the definition of relative humidity, $\frac{RH}{100} = p_w/p_w^{sat}$ where $p_w^{sat} = p^o \exp((\mu^{o}_{H_2O(g)} - \mu^{o}_{H_2O(\ell)})/RT)$ is the saturation vapor pressure of water (6) becomes

$$\ell n\, a_{w_\infty} = \ell n \frac{RH}{100} - \frac{4\sigma\lambda\bar{V}_w}{\bar{d}_\ell\, RT} \qquad (7)$$

Thus, it follows that an increase in λ is equivalent to a decrease in relative humidity. Now, consider the case where the relative humidity is exactly equal to the relative humidity of deliquescence. Then, any increase in λ, being equivalent to a decrease in RH, will cause the liquid phase to disappear totally. That is, an infinitesimal change in λ will cause a large change in $\underset{\sim}{\xi}$. Thus, $\underset{\sim}{f}(\underset{\sim}{\xi};\lambda)$ is discontinuous at this point, and the iteration scheme given by (5) will fail.

Note that this breakdown occurs because the step size is defined in terms of λ alone. That is, the step is defined to be completed when λ has changed by a given amount, irregardless of what $\underset{\sim}{\xi}$ has done in that interval. Clearly, it would be better to define the step in terms of some combination of the changes in λ and $\underset{\sim}{\xi}$. Then, in the above example, the difficulties could be circumvented by limiting the change in $\underset{\sim}{\xi}$. This is the idea behind the pseudo-arclength continuation method of Keller (1978, 1982).

This method is as follows. Start with the basic equation

$$\underset{\sim}{f}(\underset{\sim}{\xi};\lambda) = \underset{\sim}{0} \tag{8}$$

Let $\underset{\sim}{\xi} = \underset{\sim}{\xi}(s)$ and $\lambda = \lambda(s)$ where s is a new parameter. Differentiate (9) with respect to s.

$$\underset{\sim}{f}_{\underset{\sim}{\xi}} \frac{d\underset{\sim}{\xi}}{ds} + \underset{\sim}{f}_{\lambda} \left(\frac{d\lambda}{ds}\right) = 0 \tag{9}$$

where $\underset{\sim}{f}_{\lambda} = (\partial \underset{\sim}{f}/\partial\lambda)$. Thus

$$\frac{d\underset{\sim}{\xi}}{ds} = - \underset{\sim}{f}_{\underset{\sim}{\xi}}^{-1} \underset{\sim}{f}_{\lambda} \frac{d\lambda}{ds} \tag{10}$$

In addition, we will require

$$\|d\lambda/ds\|^2 + \|d\underset{\sim}{\xi}/ds\|^2 = 1 \tag{11}$$

Thus,

$$\frac{d\lambda}{ds} = \frac{\pm 1}{[1+\|\underset{\sim}{f}_{\underset{\sim}{\xi}}^{-1}\underset{\sim}{f}_{\lambda}\|^2]^{\frac{1}{2}}} \tag{12}$$

Either choice of sign in (12) satisfies (11); the proper choice will be discussed later.

The physical interpretation of the above parameterization is as follows. Let $\underset{\sim}{x} = (\underset{\sim}{\xi}^T,\lambda)^T$, the vector of unknown quantities. Now, one way to proceed is by simply solving the set of differential equations(10) and (12). If this were done, s would be the distance the curve $\underset{\sim}{x}(s)$ travels through $\underset{\sim}{x}$ space.

While it is possible to solve the set of differential equations (10) and (12), there is a simpler way to proceed. Let α be the step size. Then, define the step by (8) in conjunction with

$$\left(\frac{d\underset{\sim}{x}}{ds}\right)^T_{\underset{\sim}{x}_o} (\underset{\sim}{x} - \underset{\sim}{x}_o) = \alpha \tag{13}$$

where $\underset{\sim}{x}_o$ is the value of $\underset{\sim}{x}$ at the start of the step. Note that as α approaches zero, the lefthand side of (13) approaches the arclength along the curve $\underset{\sim}{x}(s)$. Thus, by solving (8) and (13), a method is obtained that has the advantages of arclength continuation without having to solve a differential equation.

The system of equations (8), (13) is solved as follows. To start, let

$$\underset{\sim}{x}_1 = \underset{\sim}{x}_o + \alpha\left(\frac{d\underset{\sim}{x}}{ds}\right)_{\underset{\sim}{x}_o} \tag{14}$$

The iteration is continued by

$$\underset{\sim}{\xi}_{i+1} = \underset{\sim}{\xi}_i + \delta\underset{\sim}{\xi}_i \tag{15}$$

$$\lambda_{i+1} = \lambda_i + \delta\lambda_i \tag{16}$$

where $\delta\underset{\sim}{\xi}_i$ and $\delta\lambda_i$ are found by solving

$$(\underset{\sim}{f}_{\underset{\sim}{\xi}})_i \, \delta\underset{\sim}{\xi}_i + (\underset{\sim}{f}_\lambda)_i \, \delta\lambda_i = - \underset{\sim}{f}(\underset{\sim}{\xi}_i;\lambda_i) \tag{17}$$

$$\left(\frac{d\underset{\sim}{\xi}}{ds}\right)_{\underset{\sim}{x}_o} \delta\underset{\sim}{\xi}_i + \left(\frac{d\lambda_o}{ds}\right)_{\underset{\sim}{x}_o} \delta\lambda_i = \alpha - \left(\frac{d\underset{\sim}{x}}{ds}\right)_{\underset{\sim}{x}_o} (\underset{\sim}{x}_i - \underset{\sim}{x}_o) \tag{18}$$

The sign in (12) is chosen so that

$$\left(\frac{d\underset{\sim}{x}}{ds}\right)^T_{\underset{\sim}{x}_o} \frac{d\underset{\sim}{x}}{ds} > 0 \tag{19}$$

which means that $\frac{d\underset{\sim}{x}}{ds}$ points in the same direction as $(d\underset{\sim}{x}/ds)_{\underset{\sim}{x}_o}$.

Note that if in (12), $\|\underset{\sim}{f}_{\underset{\sim}{\xi}}^{-1} \underset{\sim}{f}_\lambda\| << 1$, the iteration scheme given by (14)-(19) reduces to that given by (5).

3.2 Application to the Equilibrium Problem

In the previous section, pseudo-arclength continuation was described as it was developed by Keller (1978, 1982). However, there are some complications in the equilibrium problem that were not present in the systems treated by Keller. In particular, for the iteration described by (15)-(19) to work, $\underset{\sim}{f}$ must be continuously differentiable over the range of interest. However, this will not be true when the system undergoes a phase change. In fact, when this occurs, the number of equations in $\underset{\sim}{f}$ will, in general, change.

The situation where the dimensionality of $\underset{\sim}{f}$ changes can be handled as follows. Consider first the case where a new phase is formed. This can be handled computationally merely by increasing the number of equations being considered. The case where a solid phase disappears is less straightforward. Computationally, this case can be detected by one of the n_i^{ℓ} going negative. When this occurs, the concentration of that solid phase must be set to zero. To do this, first Gaussian elimination is performed on the matrix of stoichiometric coefficients $\underset{\sim}{\nu}$ until there is only one reaction left involving n_i^{ℓ}. Then, the equilibrium relation for this reaction is replaced by the equation $n_i^{\ell} = 0$. Then the homotopy method as described before can be used.

Note that the system (8), (13) will, in general, only be solvable by the iteration method (14)-(19) if the initial guess is sufficiently close to the solution. This means that for convergence

$$\|\underset{\sim}{f}(\underset{\sim}{\xi}_0,\lambda_0)\| \leq \varepsilon \tag{20}$$

for some value of ε. However, at a phase change, where one of the two above procedures have been used, the new equation may not be near equality. Thus, (20) may not be satisfied. This can be overcome by replacing $\underset{\sim}{f}$ with

$$\hat{\underset{\sim}{f}}(\underset{\sim}{\xi},\lambda) = \underset{\sim}{f}(\underset{\sim}{\xi},\lambda) - \frac{(\lambda-1)}{(\lambda_o-1)}\,\underset{\sim}{f}(\underset{\sim}{\xi}_o,\lambda_o) \qquad (21)$$

Note that $\underset{\sim}{\xi}_o,\lambda_o$ is a solution of $\hat{\underset{\sim}{f}}(\underset{\sim}{\xi},\lambda) = 0$. Thus, this transformation will smooth out any discontinuity in $\underset{\sim}{f}$.

4. APPLICATION TO THE ATMOSPHERIC SULFATE/NITRATE/AMMONIUM SYSTEM

We now consider the sulfate/nitrate/ammonium system. Our object is to calculate the quantity, composition, and physical state of the equilibrium aerosol as a function of particle size for several hypothetical situations. From this calculation, we wish to see if general conclusions are forthcoming concerning the particle size distribution of atmospheric water, nitrates and ammonium. Since sulfate is virtually non-volatile, it is necessary to specify the distribution of sulfate by particle size. Given that distribution, the relative humidity and temperature, and the total quantity of ammonia and nitrate present, we will determine the equilibrium size/composition distribution of the resulting aerosol.

Two additional quantities beyond those given in Part I are needed here, surface tension σ and molar volume $\bar{V}_i$. At present, there does not appear to exist a good way to predict the surface tension of an aqueous solution. Thus, we will use the value for the surface tension of water at 25°C. Since the molar volume $\bar{V}_i$ always appears as a product with σ, and since σ is to be approximated by the pure water value, we do not endeavor to develop a highly accurate expression for $\bar{V}_i$. Instead, assume that the density of the particle is constant at ρ_w, the value for pure water. The molal volume of species i is then assumed to be M_i/ρ_w, where M_i is the molecular weight of species i.

Six cases are considered, and they are summarized in Table 1. Cases 1-4 correspond to conditions at the end of 60 minutes in Cases 1, 3, 5, and 6 of Part I (Bassett and Seinfeld, 1983). Case 5 corresponds roughly to conditions in Case 6 of Part I after 40-45 minutes. The sulfate size distribution was fixed a priori to adhere to the log-normal distribution (Hegg and Hobbs, 1983)

$$\frac{dM}{d\ \ell n\ d} = \frac{2S_T}{\sqrt{3\pi}} \exp\left(-\frac{4}{3}\left(\ell n\ \frac{d}{0.3}\right)^2\right) \tag{22}$$

where S_T is the total amount of sulfate present. The size distribution is represented by five geometrically spaced sections between 0.01 μm and 3 μm, that is $(d_\ell/d_{\ell-1}) = (300)^{0.2}$

The first point of interest is a comparison of the total amounts of the species present in the aerosol phase in each of the six cases in Table 1 with and without the Kelvin effect considered. With the exception of water, there is no perceptible change in the amount of the various species when the effect of surface curvature is considered versus when it is neglected. Even in the case of water, the difference between the two situations does not exceed eight percent.

There are two reasons why the total amounts of the various species present are similar with and without the Kelvin effect. First, most of the particles present are fairly large. Second, there is a tendency for the larger particles in the distribution to control the total amounts of the various species in the aerosol phase. This effect can be explained as follows. In the smaller particles, the Kelvin effect will cause ammonium and nitrate to volatilize, raising the gas-phase partial pressures of NH_3 and HNO_3. As a result, the larger particles will absorb more ammonia and nitric acid than if the Kelvin effect is not considered. The net effect is a transfer of mass from smaller to larger particles rather than from the aerosol to the gas phase.

Table 1. Cases Considered for Analysis of Aerosol Size/Composition Distributions

Case	Total NH_3, $\mu g\ m^{-3}$	Total HNO_3, $\mu g\ m^{-3}$	Total H_2SO_4, $\mu g\ m^{-3}$	RH, %
1	20	20	30	90
2	20	20	30	50
3	5	20	30	90
4	5	20	30	50
5	5	15	20	50
6	20	20	5	50

The only species for which this argument does not hold is water. Because the amount of water vapor present is always much greater than that of the condensed water, the Kelvin effect has virtually no effect on the partial pressure of water in the system. Thus, liquid water is the only species whose concentration is altered appreciably by the inclusion of the Kelvin effect.

The effect just discussed can be seen in Figure 1, which shows the distribution of components by particle size for Case 1 of Table 1. Note that even though the third section contains more sulfate than the fourth, 14.1 vs. 13.4 $\mu g\ m^{-3}$, the fourth section has more ammonium and nitrate than the third. The molar ratio of nitrate to sulfate is 0.88 and 1.12 in sections 3 and 4, compared to 0.99 in both sections if the Kelvin effect is not considered. Also, the molar ratio of ammonium to sulfate is 2.9 in section 3 and 3.1 in section 4, compared to 3.0 without the Kelvin effect. Thus, the elevation of NH_3 and HNO_3 vapor pressures over particles in section 3 leads to a net transfer of these species to the larger particles in section 4.

Figure 2 shows the size/composition distribution in Case 2, which is identical to Case 1 except that the relative humidity is 50 percent as opposed to 90 percent. Consider the equilibrium

$$(NH_4)_2SO_4(s) + 2NH_3(g) + 2HNO_3(g) \rightleftharpoons (NH_4)_2SO_4 \cdot 2NH_4NO_3(s)$$

Using (3) and the approximations for σ and $\bar{V}_i$ gives for the change in chemical potential of this reaction

$$\Delta\mu = \Delta\mu_\infty + \frac{8\sigma}{\rho_w \bar{d}_\ell}\left(M_{NH_3} + M_{HNO_3}\right) \qquad (23)$$

where $\Delta\mu_\infty$ = the change in chemical potential when surface curvature is neglected. Thus, the smaller the particles, the more favorable the left hand side

Figure 1

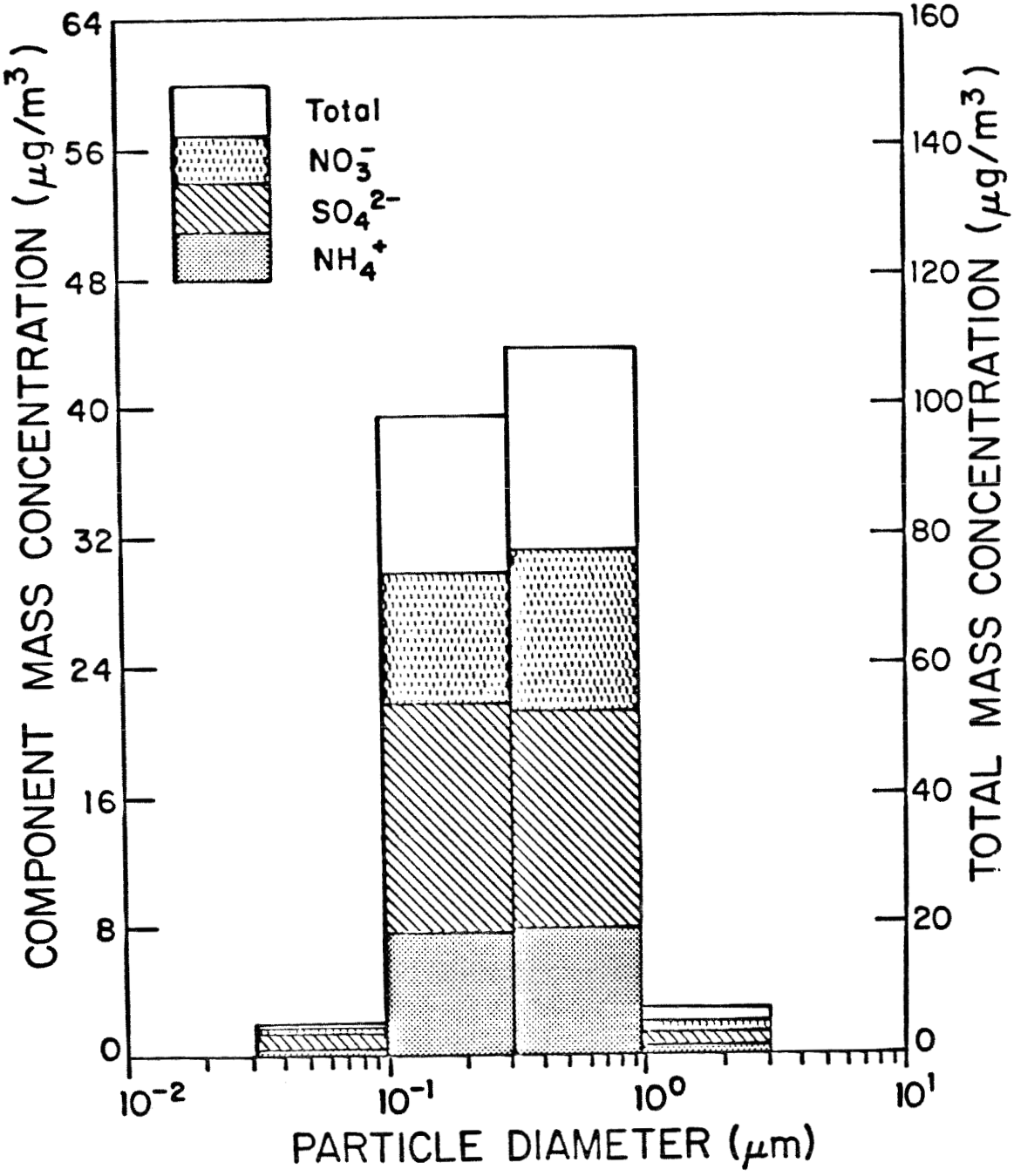

Distribution of components by particle size for Case 1 of Table 1. The sulfate size distribution is based on equation (22). The distribution of all other components is governed by chemical equilibrium.

Figure 2

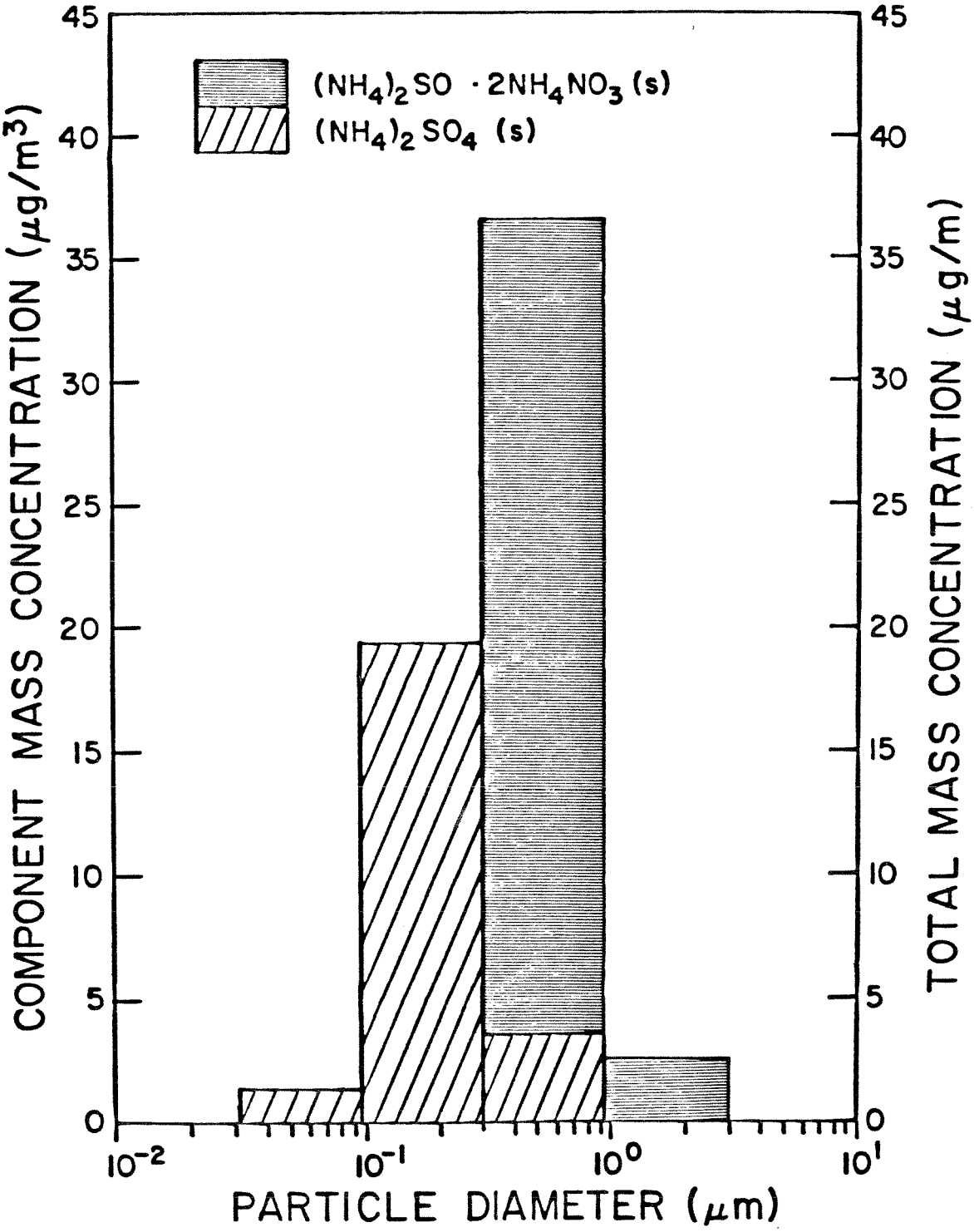

Distribution of components by particle size for Case 2 of Table 1. The sulfate size distribution is based on equation (22). The distribution of all other components is governed by chemical equilibrium.

of the reaction will become. The fourth section contains both $(NH_4)_2SO_4(s)$ and $(NH_4)_2SO_4 \cdot 2NH_4NO_3(s)$. Thus, the above reaction must be at equilibrium in this section. That means the ammonia-nitric acid partial pressure product is determined by conditions in the fourth section. In addition, the amounts of ammonia and nitric acid in the gas phase are related by stoichiometry,

$$n_{NH_3(g)} = N_{NH_3} - 2N_{H_2SO_4} - (N_{HNO_3} - n_{HNO_3(g)}) \tag{24}$$

where N_{NH_3}, $N_{H_2SO_4}$ and N_{HNO_3} are the total number of moles of ammonia, sulfate and nitrate respectively in the system. Thus, if the total amounts of sulfate, nitrate and ammonia in the system are fixed, the composition of the gas phase can be determined merely by knowing conditions in the fourth section. Once the composition of the gas phase is known, the total amounts of $(NH_4)_2SO_4(s)$ and $(NH_4)_2SO_4 \cdot 2NH_4NO_3(s)$ present can be readily calculated by a mass balance. That is, conditions in section 4 will control the total concentrations of all of the species present.

Section 4 contains particles having diameters between 0.3 and 1 μm. Because these particles are large enough so that the vapor pressure change due to surface curvature is negligible, we see why the total amounts of the aerosol species present in Case 2 do not vary as a result of the Kelvin effect.

Figures 3 and 4 shows the size/composition distributions in Cases 3 and 4, respectively. In both of these cases the molar ratio of total sulfate to nitrate to ammonium is 1:1:0.5. As a result, most of the ammonia will be in the aerosol phase. Thus, the Kelvin effect only alters in which section the ammonium ions are present rather than shifting the gas/aerosol equilibrium. With respect to aerosol nitrate, in Case 4, because of the high acidity, the

Figure 3

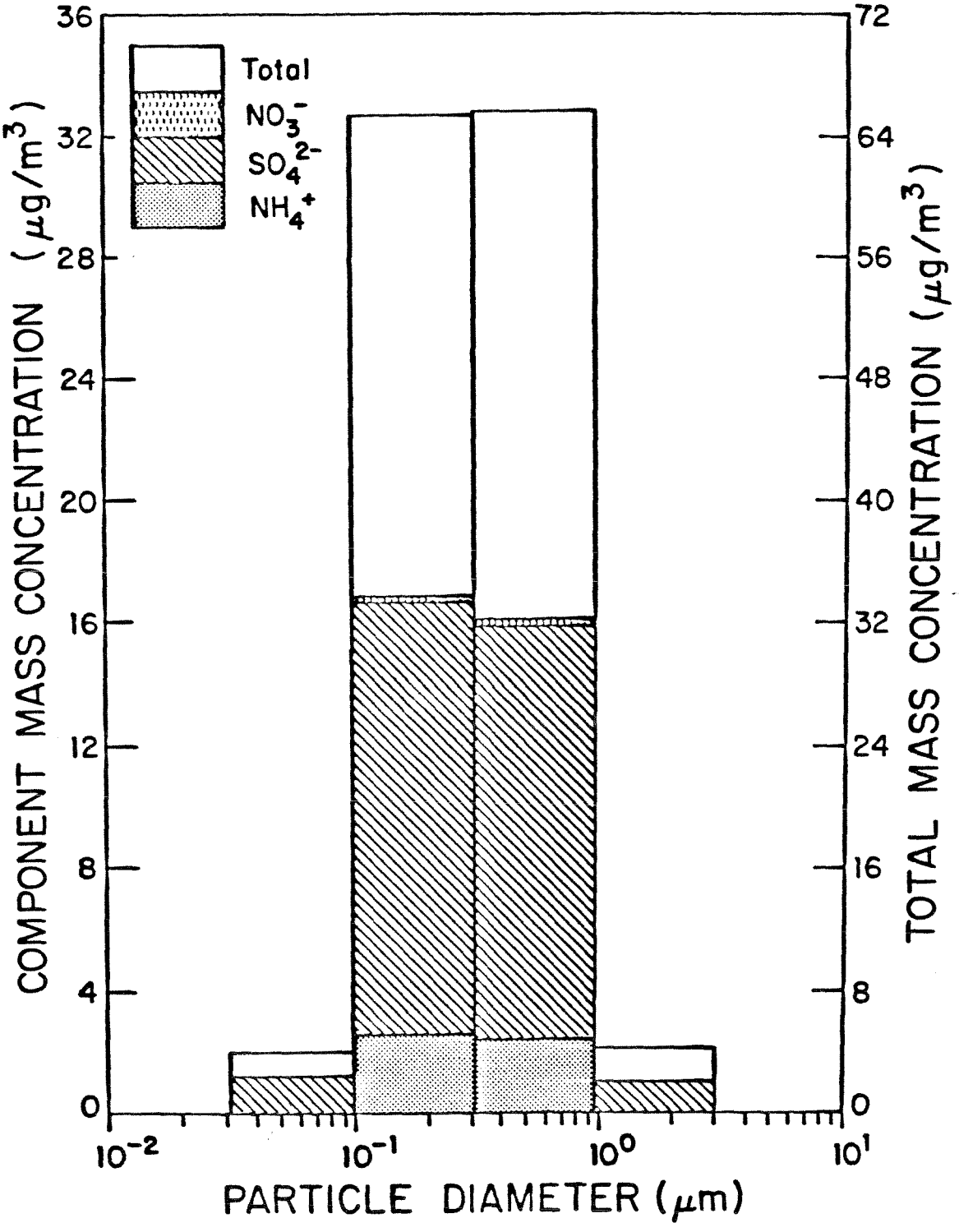

Distribution of components by particle size for Case 3 of Table 1. The sulfate size distribution is based on equation (22). The distribution of all other components is governed by chemical equilibrium.

Figure 4

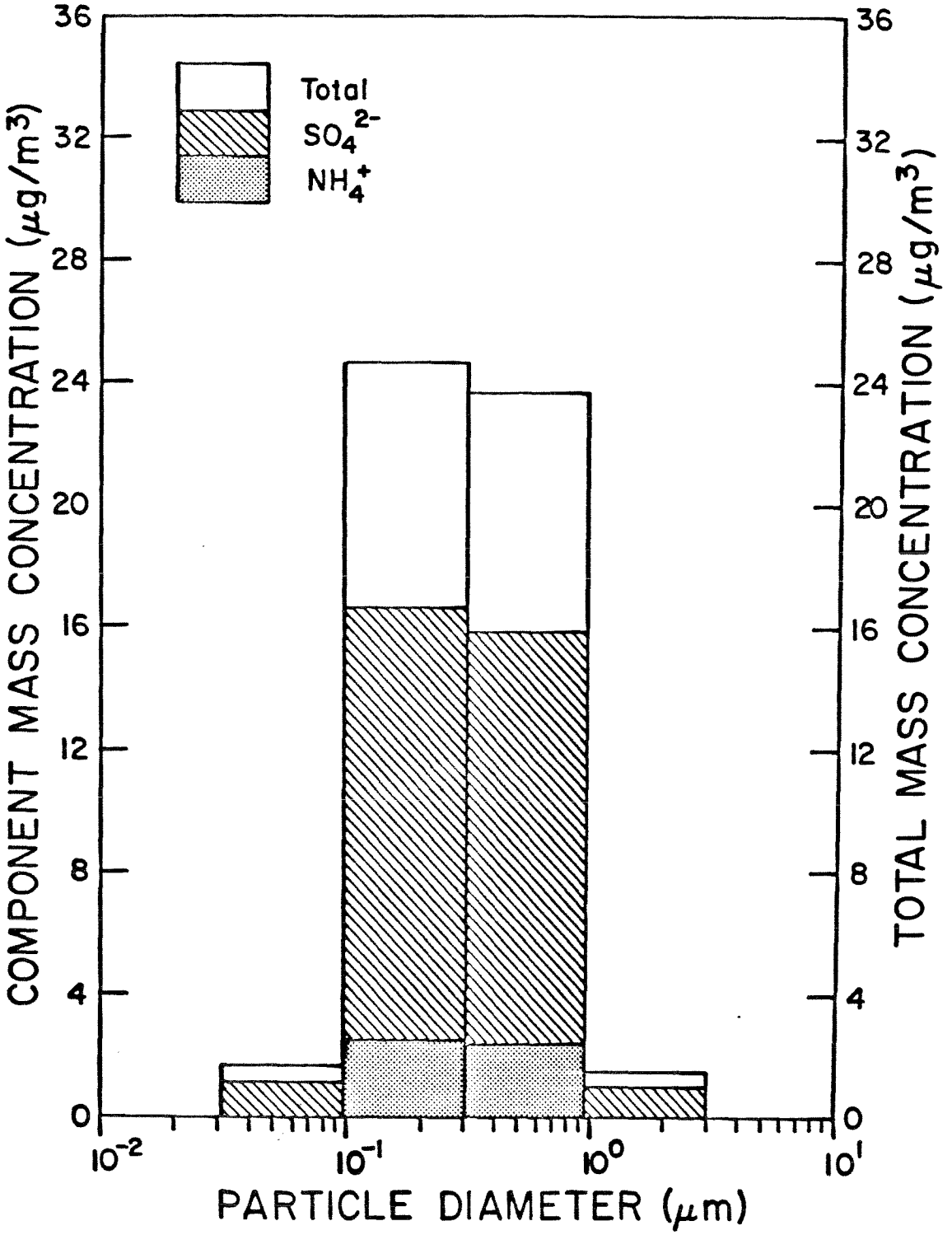

Distribution of components by particle size for Case 4 of Table 1. The sulfate size distribution is based on equation (22). The distribution of all other components is governed by chemical equilibrium.

amount of nitrate present in the liquid phase is negligible. In Case 3 there exists the same shifting effect discussed in the earlier cases. One observation of practical interest is that the Kelvin effect acts to decrease the pH of the smaller particles relative to the larger particles. In Case 3, for example, the pH of particles in sections 5 and 2 is -0.47 and -0.58, respectively, whereas the corresponding values in Case 4 are -1.28 and -1.31.

In Case 5 an argument similar to that used in Case 2 can be used to show that section 4 is the only place in the size spectrum where the reaction

$$(NH_4)_3H(SO_4)_2(s) \rightleftarrows 3NH_4^+ + H^+ + 2SO_4^{2-}$$

is not totally on one side or the other. Thus, the relative amounts of $(NH_4)_3H(SO_4)_2$ and the liquid phase are determined by conditions in the fourth section (Figure 5).

Case 6 is the only case with a phase that does not contain sulfate, namely $NH_4NO_3(s)$. The NH_4NO_3 will deposit on the largest available particles, so the large particles have a substantial amount of mass regardless of how much sulfate they contain. By an argument similar to that used in explaining Case 2, it can be shown that the conditions in the largest particles will control the amount of $NH_4NO_3(s)$ formed.

5. EFFECT OF KINETIC LIMITATIONS

The model described in the preceding sections is purely thermodynamic. That is, it assumes that all reactions go immediately to equilibrium no matter how small the driving force. This assumption will be valid when the goal is to estimate the concentration of the gas phase. This is because it often suffices to be able to say that the partial pressure of a given species is below a certain limit, say 1 ppb. However, in the results presented here, there are times when a sequence of the form

Figure 5

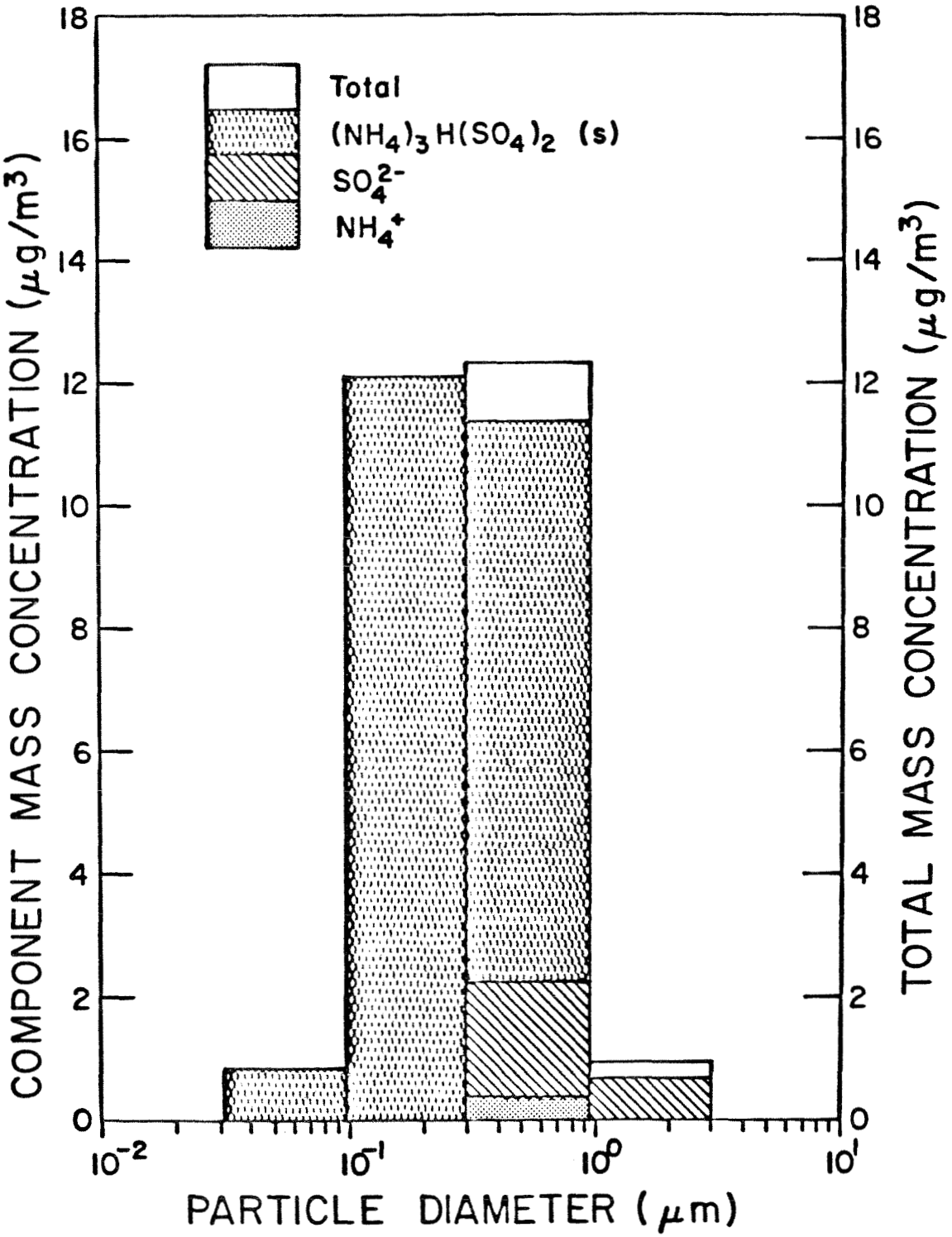

Distribution of components by particle size for Case 5 of Table 1. The sulfate size distribution is based on equation (22). The distribution of all other components is governed by chemical equilibrium.

Figure 6

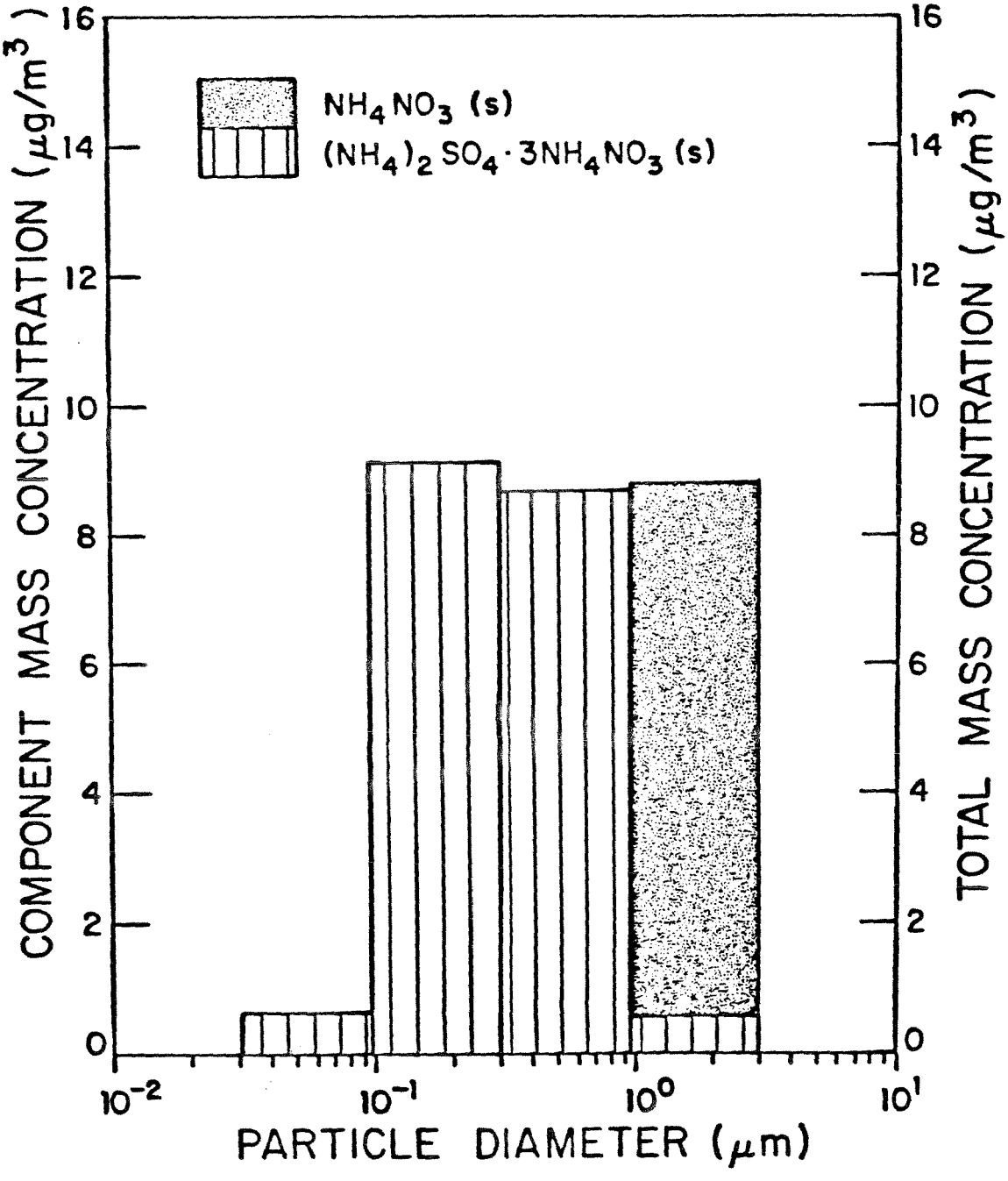

Distribution of components by particle size for Case 6 of Table 1. The sulfate size distribution is based on equation (22). The distribution of all other components is governed by chemical equilibrium.

$$A^{(\ell)} \rightleftarrows A(g) \rightleftarrows A^{(m)}$$

occurs, where $A^{(\ell)}$ and $A^{(m)}$ represent molecules of A in sections ℓ and m, respectively. Then, in the above sequence, even though the difference in the vapor pressures of $A^{(\ell)}$ and $A^{(m)}$ is small, there may be an appreciable amount of mass transferred between sections ℓ and m.

In order to analyze this effect quantitatively, consider the time constant for mass transfer given by

$$\tau_i = \frac{\rho d^2(1+\omega Kn)}{12\mathcal{D}_i(n_i - n^\circ_i)M_i} \tag{25}$$

where $\mathcal{D}_i$ and M_i are the diffusivity and molecular weight of the ith species, Kn is the Knudsen number $2\bar{\lambda}/d$ where $\bar{\lambda}$ is the mean free path, $\omega = (1.333 + 0.71\ Kn^{-1})/(1+Kn^{-1})$, and n_i and n°_i are the concentrations of species i in the gas phase, and the value at equilibrium, respectively.

There are two factors that can cause the time constant for mass transfer between sections to be large. First of all, the species being transferred could have a low vapor pressure. In this case, both n_i and n°_i will be small, so their difference will be small. As an example of this, consider case 5. Here, the vapor pressure of ammonia at equilibrium is 3.1×10^{-3} ppb. Consider the situation where a particle of letovicite with a diameter d = 0.01 μm is introduced into the system which is initially at equilibrium. Then, using (24) with $\mathcal{D}_i$ being obtained from Reid and Sherwood (1966), the value of τ_i is 13 hours.

The second factor that can cause mass transfer between sections to be small is for the particle diameter to be large. As an example of this, consider the transfer of $NH_4NO_3(s)$ between sections in case 6 via the sequence

$$NH_4NO_3(s)(\text{section } \ell) \rightleftarrows NH_3(g) + HNO_3(g) \rightleftarrows NH_4NO_3(s)(\text{section } m)$$

The Kelvin effect may be neglected in the largest section. Then, since this section is in equilibrium, the driving force for transfer from a given particle will be given by

$$(n_i - n_i^\circ) = n_i^\circ \left(\exp \frac{4\sigma V_i}{d RT} - 1 \right) \tag{24}$$

Expanding the exponential in a series gives $n_i - n_i^\circ$ inversely proportional to d. Thus, τ_i is proportional to d^3. The time constant for mass transfer between sections 4 and 5 in case 7 is found to be 35 hr.

It should be noted that the kinetic limitations arise only because the thermodynamic driving force $n_i - n_i^\circ$ is so small. Thus, in the example from case 6, the difference in vapor pressure between sections 4 and 5 was 2×10^{-2} ppb. In most calculations, one is satisfied with less accuracy in the vapor phase than this. However, in this calculation, mass transfer between sections 4 and 5 does not arise until the vapor pressure of nitric acid is within 2×10^{-2} ppb of its equilibrium value.

These kinetic limitations are most important for large particles or for species with very low vapor pressures. For species with moderate vapor pressures, and for submicron-sized particles, the thermodynamic equilibrium results given in this work show qualitatively the type of behavior that can be expected governing aerosol composition as a function of particle size.

5. SUMMARY AND CONCLUSIONS

A method has been presented for determining the equilibrium size and composition distribution of atmospheric sulfate/nitrate/ammonium aerosols. Six hypothetical cases that span a range of sulfate, nitrate, and ammonia levels and relative humidities were examined to determine how the various species are distributed according to particle size at equilibrium. Results of the calculations indicate that the effect of surface curvature on vapor pressure, the so-called Kelvin effect, *does not influence the total quantity* of aerosol species but only their distribution by particle size. The one species that constitutes an exception to this statement is water, whose quantity in the condensed state is impacted by the Kelvin effect, although differences in the amount of aerosol water with the Kelvin effect accounted for and neglected did not exceed eight percent for the cases studied here.

As a result of our analysis, we are now able to offer an explanation for observed distributions of aerosol sulfate and nitrate by particle size. Sulfate, being essentially non-volatile, will have a size distribution controlled by gas-phase diffusion and therefore will tend to accumulate in the smaller particles. Nitrate, being more volatile than sulfate, will tend to evaporate from the smaller particles and deposit on larger particles where surface curvature effects on vapor pressure are minimal.

ACKNOWLEDGMENT

This work was supported by U.S. Environmental Protection Agency grant R806844.

REFERENCES

Appel B. R., Kothny E. L., Hoffer E. M., Hidy G. M. and Wesolowski J. J. (1978) Sulfate and nitrate data from the California Aerosol Characterization Experiment (ACHEX). Environ. Sci. Technol. 12, 418-425.

Bassett M. and Seinfeld J. H. (1983) Atmospheric equilibrium model of sulfate and nitrate aerosols. Atmospheric Environment 17 XXX-XXX.

Gelbard F. and Seinfeld J. H. (1980) Simulation of multicomponent aerosol dynamics. J. Colloid Interface Sci. 78 485-501.

Gelbard F., Tambour Y. and Seinfeld J. H. (1980) Sectional representations for simulating aerosol dynamics. J. Colloid Interface Sci. 76 541-556.

Hidy G. M., Appel B. R., Charlson R. J., Clark W. E., Friedlander S. K., Hutchison D. H., Smith J. B., Suder J., Wesolowski J.J. and Whitby K. J. (1975) Summary of the California Aerosol Characterization Experiment. J. Air Pollut. Control Assoc. 25, 1106-1114.

Keller H. B. (1982) Practical procedures in path following near limit points. in Computing Methods in Applied Sciences and Engineering V, (Edited by R. Glowinski and J. L. Lions) North-Holland, Amsterdam.

Keller H. B. (1978) Global homotopies and Newton methods.in Recent Advances in Numerical Analysis (Edited by C. Deboor and G. H. Golub.) Academic Press, New York.

Reid R. C. and Sherwood T. K. (1958) The Properties of Gases and Liquids. McGraw-Hill, New York p. 281.

Stelson A. W. and Seinfeld J. H. (1982a) Relative humidity and temperature dependence of the ammonium nitrate dissociation constant. Atmospheric Environment 16 983-992.

Stelson A. W. and Seinfeld J. H. (1982b) Relative humidity and pH dependence of the vapor pressure of ammonium nitrate-nitric acid solutions at 25°C. Atmospheric Environment 16 993-1000.

Stelson A. W. and Seinfeld J. H. (1982c) Thermodynamic prediction of the water activity, NH_4NO_3 dissociation constant, density and refractive index for the NH_4NO_3-$(NH_4)_2SO_4$-H_2O system at 25°C. Atmospheric Environment 16 2507-2514.

Stelson A. W., Friedlander S. K. and Seinfeld J. H. (1979) A note on the equilibrium relationship between ammonia and nitric acid and particulate ammonium nitrate. Atmospheric Environment 13 369-371.

Tanner R. L. (1982) An ambient experimental study of phase equilibrium in the atmospheric system: aerosol H^+, NH_4^+, SO_4^{2-}, NO_3^--$NH_3(g)$, $HNO_3(g)$. Atmospheric Environment 16 2935-2942.

CHAPTER 5

EFFECT OF THE MECHANISM OF GAS-TO-PARTICLE CONVERSION ON THE EVOLUTION OF AEROSOL SIZE DISTRIBUTIONS

Published in

"Heterogeneous Atmospheric Chemistry"

D. R. Schyer, Editor

American Geophysical Union

EFFECT OF THE MECHANISM OF GAS-TO-PARTICLE CONVERSION ON THE EVOLUTION OF AEROSOL SIZE DISTRIBUTIONS

John H. Seinfeld and Mark Bassett

Department of Chemical Engineering, California Institute of Technology, Pasadena, California 91125

Abstract. The evolution of the size distribution of an aerosol undergoing growth by gas-to-particle conversion is investigated theoretically when growth occurs by any of three mechanisms, vapor phase diffusion, reaction of adsorbed vapor species on the particle surface, and reaction of dissolved vapor species in the particle volume.

Introduction

Atmospheric aerosols evolve in size by coagulation and gas-to-particle conversion. To interpret the evolution of a size spectrum it is necessary to understand the influences of these two phenomena. It has been found that aerosols in the size range 0.01 μm to 1.0 μm diameter grow principally by gas-to-particle conversion, the process by which vapor molecules diffuse to the surface of a particle and subsequently are incorporated into the particle. Considerable work has been carried out to identify the chemical pathways of incorporation of vapor species into atmospheric particles. Much of that effort has focused on elucidating gas-phase reaction mechanisms that lead to condensable vapor species such as sulfuric acid, ammonium sulfate, ammonium nitrate, and organic acids and nitrates (Hidy et al., 1980; Seinfeld, 1980), whereas additional studies have concentrated on reactions that occur on the surface of or within particles between particulate phase components such as metals and carbon, and adsorbed or absorbed vapor molecules (Judeikis and Siegel, 1973; Novakov et al., 1974; Peterson and Seinfeld, 1979, 1980; Seinfeld, 1980).

The rate-controlling step in gas-to-particle conversion may be a result of one or a combination of three mechanisms: the rate of diffusion of the vapor molecule to the surface of the particle; the rate of a surface reaction involving the adsorbed vapor molecule and the particle surface; and the rate of a reaction involving the dissolved species occurring uniformly throughout the volume of the particle. The particle growth rates that result in the three cases can be referred to as diffusion-controlled, surface reaction-controlled, and volume reaction-controlled growth, respectively. In fact, it has been suggested that information about possible chemical conversion mechanisms can be inferred from data on the evolution of an aerosol size distribution (Seinfeld and Ramabhadran, 1975; Heisler and Friedlander, 1977; Gelbard and Seinfeld, 1979; McMurry and Wilson, 1982). By calculating growth rates for particles of different sizes, the functional dependence of growth rate on particle size can be determined and compared with theoretical expressions relating particle growth rate to particle size, so-called growth laws. In this way it is possible to suggest chemical mechanisms that are consistent with the data. Carefully executed laboratory studies of this type have not yet been reported, although at least two are currently in progress.

The main object of this paper is to theoretically compare aerosol size spectra evolving by the mechanisms of diffusion-, surface reaction-, and volume reaction-controlled growth. The results will provide a basis for the interpretation of atmospheric and laboratory aerosol size spectra with respect to the governing growth mechanisms.

Growth of a Single Component Aerosol

Let $n(m,t)dm$ be the number of particles per unit volume of air having mass in the range m, $m + dm$ and let $I_m(m,t)$ be the rate of change of the mass of a particle of mass m due to gas-to-particle conversion. When the only process occurring is gas-to-particle conversion, the size distribution function $n(m,t)$ is governed by

$$\frac{\partial n}{\partial t} + \frac{\partial}{\partial m}(I_m(m,t)n) = 0 \qquad (1)$$

To study the evolution of an aerosol from an initial distribution,

$$n(m,0) = n_0(m) \qquad (2)$$

under different modes of gas-to-particle conversion requires the solution of equation (1) for the forms of $I_m(m,t)$ corresponding to the modes of conversion.

Equation (1) can be placed in dimensionless

form by defining the dimensionless time and particle mass,

$$\left.\begin{aligned} \tau &= \frac{tI_m^r}{\rho\lambda^3} \\ \mu &= \frac{m}{\rho\lambda^3} \end{aligned}\right\} \qquad (3)$$

where t is time, ρ is the density of the particle, λ is the mean free path of the air, and I_m^r is a reference value of I_m. By then defining the reference size distribution function n^r and the dimensionless growth rate, $I(\mu,\tau) = I_m(m,t)/I_m^r$, we obtain the dimensionless form of equation (1),

$$\frac{\partial N}{\partial \tau} + \frac{\partial}{\partial \mu}(I(\mu,\tau)N) = 0 \qquad (4)$$

where $N(\mu,\tau) = n(m,t)/n^r$.

The object of this work is to examine solutions of equation (4) for several forms of the growth law $I(\mu,\tau)$. In particular, three forms of I will be studied corresponding to three different rate-controlling mechanisms for gas-to-particle conversion.

Diffusion-Controlled Growth

The rate of change of the mass of a particle resulting from diffusion of vapor molecules of species A to the particle can be expressed as (Friedlander, 1977; Seinfeld, 1980)

$$I_m = \left(\frac{48\pi^2 m}{\rho}\right)^{1/3} \frac{\mathcal{D}_A M_A}{RT}(p_A - p_{A_s})f(Kn) \qquad (5)$$

where $\mathcal{D}_A$ is the molecular diffusivity of A in air, M_A is the molecular weight of A, R is the ideal gas constant, T is the absolute temperature, p_A is the partial pressure of A in the air, p_{A_s} is the vapor pressure of A just above the particle surface, and

$$f(Kn) = \frac{1 + Kn}{1 + 1.71Kn + 1.333Kn^2} \qquad (6)$$

where Kn is the Knudsen number, the ratio of the mean free path of the air λ to the particle radius r. The term f(Kn) accounts for the transition between the two limiting cases:

$$f(Kn) = \begin{cases} 1 & Kn \to 0 \quad \text{continuum limit} \\ \dfrac{3}{4Kn} & Kn \to \infty \quad \text{free molecule limit} \end{cases} \qquad (7)$$

The vapor pressure of A just above the surface can be related to the particle mass through the Kelvin equation,

$$\frac{p_{A_s}}{p_{A_0}} = \exp\left[\left(\frac{32\pi}{3}\right)^{1/3} \frac{\sigma\rho^{1/3}\bar{v}}{RTm^{1/3}}\right] \qquad (8)$$

where σ is the surface tension of the particle, $\bar{v}$ is the molar volume of condensed A, and p_{A_0} is the vapor pressure of A over a flat interface at temperature T.

We define the saturation ratio $S = p_A/p_{A_0}$ and the reference growth rate,

$$I_m^r = (48\pi^2)^{1/3} \frac{\lambda \mathcal{D}_A M_A p_{A_0}}{RT} \qquad (9)$$

Then the dimensionless growth rate corresponding to equations (5) and (8) is

$$I(\mu,\tau) = \mu^{1/3}[S(\tau) - \exp(K\mu^{-1/3})]f(Kn) \qquad (10)$$

where the dependence on time τ enters through S and where

$$K = \left(\frac{32\pi}{3}\right)^{1/3} \frac{\sigma\bar{v}}{\lambda RT} \qquad (11)$$

and

$$Kn = \left(\frac{3\mu}{4\pi}\right)^{-1/3} \qquad (12)$$

In the case of so-called perfect absorption, $p_{A_s} = 0$, and equation (10) reduces to

$$I(\mu,\tau) = \mu^{1/3} S\, f(Kn) \qquad (13)$$

The continuum and free molecule limits can be examined with reference to equation (13). We find

$$I(\mu,\tau) = \begin{cases} S\mu^{1/3} & Kn \to 0 \\ \left(\dfrac{81}{256\pi}\right)^{1/3} S\mu^{2/3} & Kn \to \infty \end{cases} \qquad (14)$$

Surface Reaction-Controlled Growth

The second case we consider is that of surface reaction-controlled growth, namely when the rate of particle growth is controlled by the rate at which adsorbed A on the particle surface is converted to another species B. Thus, we take, as the simplest representation of such a situation, the sequence,

$$A(g) \rightleftarrows A(s) \rightleftarrows B$$

where A(s) denotes an adsorbed vapor molecule A on the surface that subsequently is converted to species B.

If the concentration of adsorbed A on the sur-

face is c_s, and the rate of conversion to B is first order, with rate constant k_s, the rate of gain of particle mass due to the surface reaction is $4\pi r^2 M_B k_s c_s$. At steady state this rate must equal the rate of diffusion of molecules of A to the surface, which is given by equation (5). Thus,

$$4\pi r^2 M_B k_s c_s = \left(\frac{48\pi^2 m}{\rho}\right)^{1/3} \frac{\mathcal{D}_A M_A}{RT}(p_A - p_{A_s}) f(Kn) \tag{15}$$

Let us assume that adsorption equilibrium can be expressed by a relation of the form,

$$p_{A_0} = H_s c_s \tag{16}$$

Then c_s can be determined from equations (15), (16), and (8) as

$$c_s = \left[\left(\frac{48\pi^2 m}{\rho}\right)^{1/3} \frac{\mathcal{D}_A M_A}{RT} p_A f(Kn)\right] \left\{4\pi r^2 M_B k_s + \left(\frac{48\pi^2 m}{\rho}\right)^{1/3} \frac{\mathcal{D}_A M_A H_s}{RT} \exp\left[\left(\frac{32\pi}{3}\right)^{1/3} \frac{\sigma\rho^{1/3}\bar{v}}{RTm^{1/3}}\right] f(Kn)\right\}^{-1} \tag{17}$$

When the rate-determining step is surface reaction, the second term in the denominator of equation (17) dominates the first term and equation (17) reduces to

$$c_s \simeq \frac{p_A}{H_s} \exp\left[-\left(\frac{32\pi}{3}\right)^{1/3} \frac{\sigma\rho^{1/3}\bar{v}}{RTm^{1/3}}\right] \tag{18}$$

The corresponding rate of particle growth is

$$I_m = 4\pi r^2 M_B k_s \frac{p_A}{H_s} \exp\left[-\left(\frac{32\pi}{3}\right)^{1/3} \frac{\sigma\rho^{1/3}\bar{v}}{RTm^{1/3}}\right] \tag{19}$$

Defining the reference growth rate,

$$I_m^r = (36\pi)^{1/3} M_B k_s \frac{p_{A_0}}{H_s} \tag{20}$$

we obtain the surface reaction-controlled dimensionless growth rate as

$$I(\mu,\tau) = S\mu^{2/3} \exp(-K\mu^{-1/3}) \tag{21}$$

Volume Reaction-Controlled Growth

Finally we consider the case in which the rate of growth is controlled by the conversion of dissolved A to a second species B. The sequence can be depicted as

$$A(g) \rightleftarrows A(\ell) \rightleftarrows B(\ell)$$

If the concentration of dissolved A is c_v and the rate of conversion to B is first order, with rate constant k_v, the rate of gain of particle mass due to volume reaction is $\frac{4}{3}\pi r^3 M_B k_v c_v$. At steady state this rate must equal the rate of diffusion of molecules of A to the particle. Thus,

$$\frac{4}{3}\pi r^3 M_B c_v = \left(\frac{48\pi^2 m}{\rho}\right)^{1/3} \frac{\mathcal{D}_A M_A}{RT}(p_A - p_{A_s}) f(Kn) \tag{22}$$

As before, we assume that the equilibrium can be expressed by

$$p_{A_0} = H_v c_v \tag{23}$$

Then c_v can be determined from equations (22), (23), and (8) as

$$c_v = \left[\left(\frac{48\pi^2 m}{\rho}\right)^{1/3} \frac{\mathcal{D}_A M_A}{RT} p_A f(Kn)\right] \left\{\frac{4}{3}\pi r^3 M_B k_v + \left(\frac{48\pi^2 m}{\rho}\right)^{1/3} \frac{\mathcal{D}_A M_A H_v}{RT} \exp\left[\left(\frac{32\pi}{3}\right)^{1/3} \frac{\sigma\rho^{1/3}\bar{v}}{RTm^{1/3}}\right] f(Kn)\right\}^{-1} \tag{24}$$

When the rate-determining step is volume reaction, the second term in the denominator of equation (24) dominates the first term and equation (24) reduces to

$$c_v \simeq \frac{p_A}{H_v} \exp\left[-\left(\frac{32\pi}{3}\right)^{1/3} \frac{\sigma\rho^{1/3}\bar{v}}{RTm^{1/3}}\right] \tag{25}$$

The corresponding rate of particle growth is

$$I_m = \frac{4}{3}\pi r^3 M_B k_v \frac{p_A}{H_v} \exp\left[-\left(\frac{32\pi}{3}\right)^{1/3} \frac{\sigma\rho^{1/3}\bar{v}}{RTm^{1/3}}\right] \tag{26}$$

Defining the reference growth rate,

$$I_m^r = \lambda^3 M_B k_v \frac{p_{A_0}}{H_v} \tag{27}$$

we obtain the volume reaction-controlled dimensionless growth rate as

$$I(\mu,\tau) = S\mu \exp(-K\mu^{-1/3}) \tag{28}$$

Dimensionless Size Spectra Evolution

We now consider size spectra $N(\mu,\tau)$ corresponding to the three growth cases just devel-

TABLE 1. Dimensionless Growth Laws

Rate-Controlling Mechanism	I(μ)
Diffusion	$\mu^{1/3}[S - \exp(K\mu^{-1/3})]f(Kn)^a$
Diffusion (perfect absorption)	$\mu^{1/3} S\ f(Kn)$
Surface reaction	$S\mu^{2/3} \exp(-K\mu^{-1/3})$
Volume reaction	$S\mu \exp(-K\mu^{-1/3})$

$$^a Kn = \left(\frac{3\mu}{4\pi}\right)^{-1/3};\quad f(Kn) = \frac{1 + Kn}{1 + 1.71Kn + 1.333Kn^2}$$

oped. The initial distribution $N_0(\mu)$ was adapted from one measured in a power plant plume. (See case d in Table 3 of Eltgroth and Hobbs, 1979.) The dimensionless size distributions are presented in terms of the dimensionless mass distribution $M(\log_{10} D_p,\tau)$, where $(\rho\lambda^3)^2 n_r M(\log_{10} D_p,\tau)\, d \log_{10} D_p$ is the mass of particles having logarithm of diameter in the range ($\log_{10} D_p$, $\log_{10} D_p + d \log_{10} D_p$), where $\log_{10} D_p$ is understood as $\log_{10}(D_p/1\ \mu m)$. Thus, M is related to N by

$$M(\log_{10} D_p,\tau) = 6.9\mu^2 N(\mu,\tau) \qquad (29)$$

For the initial distribution used, the value of n_r was chosen so that the maximum value of $M(\log_{10} D_p,0)$ is 1.0. This value of n_r is $1.645 \times 10^{14}\ \mu g^{-1}\text{-}cm^{-3}$.

The dimensionless growth laws are summarized in Table 1. It is necessary to specify the parameters S and K. The saturation ratio S was set at 2.878 corresponding to a critical diameter $D_p^* = 4\sigma\bar{v}/RT\ \ln S$ of 0.01 μm for a sulfuric acid/water aerosol at 25°C. The Kelvin parameter K is then equal to 0.1282. Since S is taken as independent of time τ, the growth laws I are functions of μ only.

Figure 1 shows the evolution of the dimensionless mass distribution at τ = 0, 0.2, 0.4, and 0.6 for case (1), diffusion-controlled growth with perfect absorption. We see that the smaller particles grow proportionally faster than the larger ones. The dependence of I on particle diameter gradually shifts from D_p^2 for the smallest particles (free molecule regime) to D_p for the largest particles (continuum regime), as indicated in equation (14).

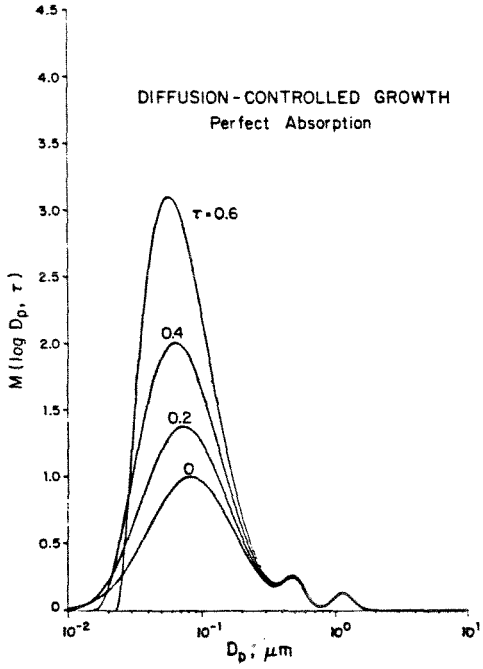

Fig. 1. Dimensionless mass distribution for diffusion-controlled growth with perfect adsorption.

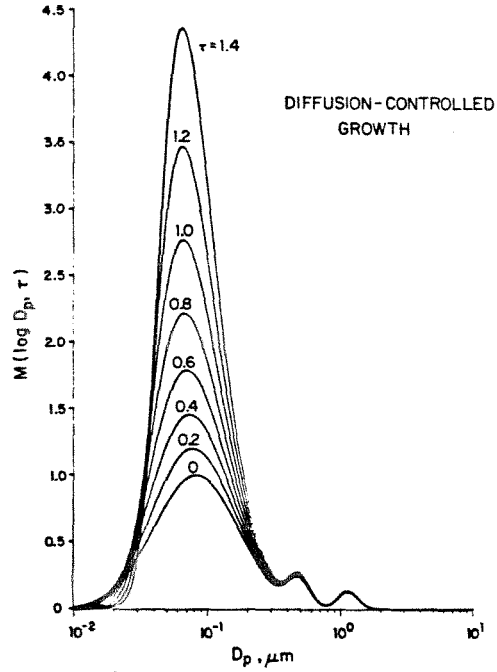

Fig. 2. Dimensionless mass distribution for diffusion-controlled growth.

In case (2), diffusion-controlled growth with a non-zero vapor pressure over the particle surface, as shown in Figure 2, addition of a vapor pressure leads to a much slower growth of the smaller particles than in case (1) in Figure 1. This, in turn, reduces the tendency of the major mode in the mass distribution to steepen. To understand why this is so consider equation (10) which may be expressed in terms of D_p^* as

$$I = \alpha D_p \left[S - \exp(K/\alpha D_p^*) \exp \frac{K(D_p^* - D_p)}{\alpha D_p^* D_p} \right] f(Kn) \quad (30)$$

where $\alpha = (\pi/6)^{1/3}\lambda - 1$. Now consider a particle of diameter close to D_p^*, i.e., for which $(D_p/D_p^* - 1) << \alpha D_p/K$. Then the second exponential in equation (30) can be expanded to give

$$I = \frac{KS(D_p - D_p^*)}{D_p^*} f(Kn) \quad (31)$$

Thus, particles close to the critical diameter grow at a rate proportional to $(D_p - D_p^*)$. This

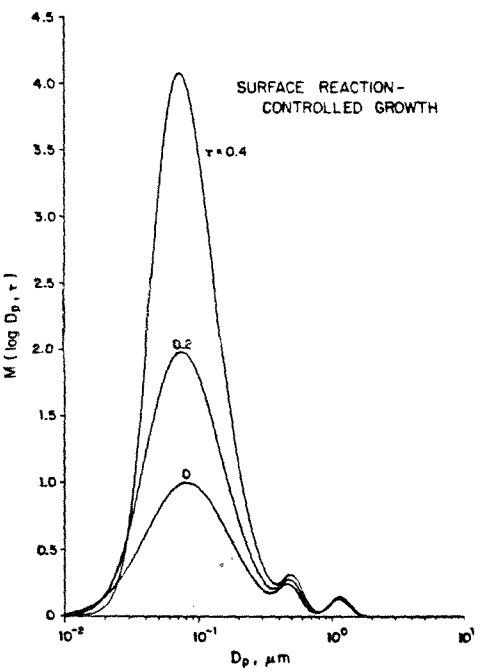

Fig. 3. Dimensionless mass distribution for surface reaction-controlled growth.

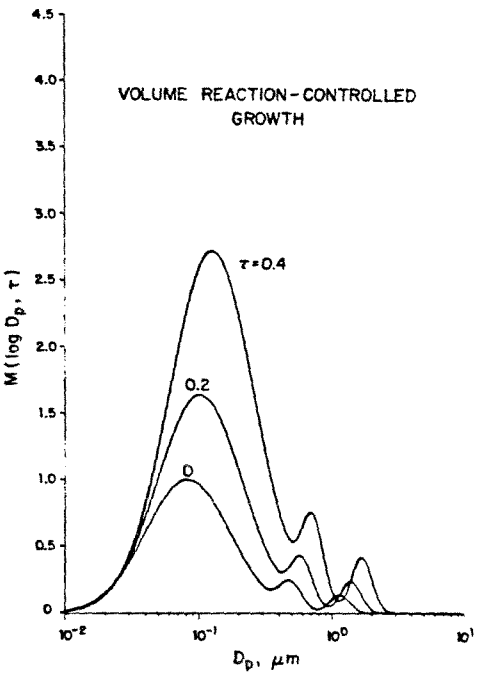

Fig. 4. Dimensionless mass distribution for volume reaction-controlled growth.

situation can be contrasted with that in case (1) in which $I \sim D_p^2$.

Figures 3 and 4 show the evolution of the dimensionless mass distribution in cases (3) and (4), surface and volume reaction-controlled growth, respectively. In the case of surface reaction-controlled growth (Figure 3), we note that the large particles, for which the Kelvin effect is negligible, grow at a rate proportional to D_p^2. Recall that in diffusion-controlled growth the smallest particles also grow at a rate proportional to D_p^2. The larger particles growing by diffusion grow at a rate proportional to D_p. Thus, we expect that of two continuum regime particles, one growing by diffusion and one by surface reaction, the particle growing by surface reaction does so at a greater rate. When gas-to-particle conversion occurs by volume reaction, large particles grow at a rate proportional to D_p^3. Thus, these particles grow more rapidly than in either diffusion or surface reaction cases.

In Figure 5, the distributions from all three mechanisms at $\tau = 0.4$ are shown, providing a summary of the effects previously mentioned. With the current non-dimensionalization, the surface reaction is faster than diffusional

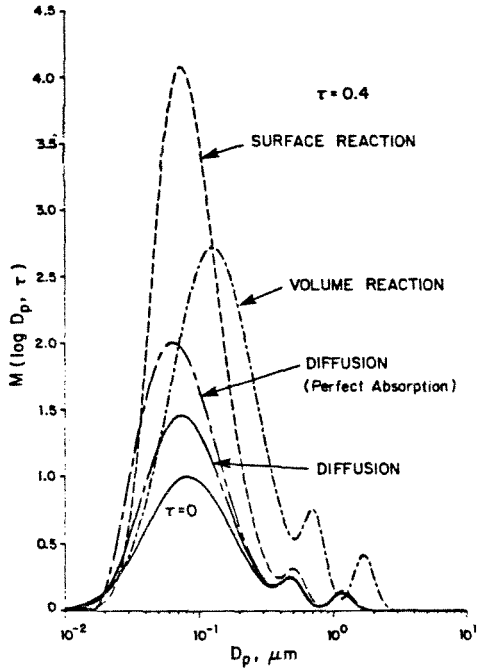

Fig. 5. Dimensionless mass distributions for the three growth mechanisms at $\tau = 0.4$.

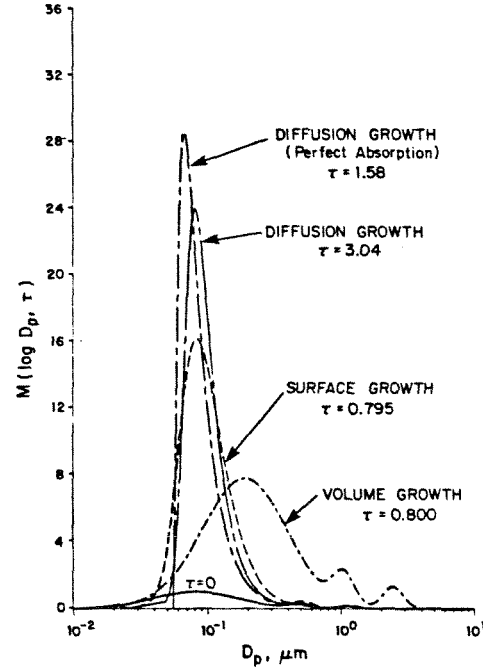

Fig. 6. Dimensionless mass distributions for the three growth mechanisms when the ratio of mass added by gas-to-particle conversion to initial mass is 7.

growth. However, with a different non-dimensionalization, diffusional growth could be faster.

The location of the main peak provides an indication of the relative importance of the growth of small and large particles. For the volume reaction case, where the ratio of large particle growth to small particle growth is the greatest, the particle diameter at which the peak is located is the greatest. On the other hand, for diffusional growth with no vapor pressure, where the growth of small particles is the most important, the particle diameter at which the peak is located is smaller than for any of the other cases.

Application to Identification of Growth Mechanism

The results of the previous section indicate that the mechanism of growth of an aerosol can be inferred from the evolution of its size spectrum. Figure 6 shows three size distributions at times when the total mass added to the particulate phase is the same (seven times the initial aerosol mass). Thus, the different size distributions are solely the result of the manner in which the different mechanisms distribute mass among the different particle sizes. This approach is useful, because in general, there may be uncertainties in the parameters needed to relate τ to t.

The distribution for the volume reaction case has significantly more large particles than any other. Thus, it should be fairly easy to distinguish experimentally between a volume reaction and the other mechanisms. On the other hand, it would probably be difficult to distinguish between the surface reaction case and diffusion growth without a vapor pressure. It would probably be impossible to distinguish experimentally between diffusion growth with a vapor pressure and a surface reaction.

Acknowledgement. This work was supported by U. S. Environmental Protection Agency grant R806844.

References

Eltgroth, M. W., and P. V. Hobbs, Evolution of particles in the plumes of coal-fired power

plants - II. A numerical model and comparisons with field measurements, Atmos. Environ., 13, 953-976, 1979.

Friedlander, S. K., Smoke, Dust and Haze: Fundamentals of Aerosol Behavior, Wiley, New York, 1977.

Gelbard, F., and John H. Seinfeld, Exact solution of the general dynamic equation for aerosol growth by condensation, J. Colloid Interface Sci., 68, 173-183, 1979.

Heisler, S. L., and S. K. Friedlander, Gas-to-particle conversion in photochemical smog; Growth laws and mechanisms for organics, Atmos. Environ., 11, 158-168, 1977.

Hidy, G. M., P. K. Mueller, D. Grosjean, B. R. Appel, and J. J. Wesolowski, The Character and Origins of Smog Aerosols, Wiley, New York, 1980.

Judeikis, H. S., and S. Siegel, Particle catalyzed oxidation of atmospheric pollutants, Atmos. Environ., 7, 619-631, 1973.

McMurry, P. H., and J. C. Wilson, Growth laws for the formation of secondary ambient aerosols: Implications for chemical conversion mechanisms, Atmos. Environ., 16, 121-134, 1982.

Novakov, T., C. S. Chang, and A. B. Harker, Sulfates as pollution particles: Catalytic formation on carbon (soot) particles, Science, 186, 256-261, 1974.

Peterson, T. W., and John H. Seinfeld, Calculation of sulfate and nitrate levels in a growing, reacting aerosol, AIChE J., 25, 831-838, 1979.

Peterson, T. W., and John H. Seinfeld, Heterogeneous condensation and chemical reaction in droplets - Application to the heterogeneous atmospheric oxidation of SO_2, Adv. Environ. Sci. Technol., 10, 125-180, 1980.

Seinfeld, J. H., Lectures in Atmospheric Chemistry, AIChE Monogr. Ser. 12, Am. Inst. Chem. Eng., New York, 1980.

Seinfeld, J. H., and T. E. Ramabhadran, Atmospheric aerosol growth by heterogeneous condensation, Atmos. Environ., 9, 1091-1097, 1975.

CHAPTER 6

MATHEMATICAL MODEL FOR MULTICOMPONENT AEROSOL FORMATION AND GROWTH IN PLUMES

Published in Atmospheric Environment 15, 2395-2406

MATHEMATICAL MODEL FOR MULTICOMPONENT AEROSOL FORMATION AND GROWTH IN PLUMES*

MARK BASSETT
Department of Chemical Engineering, California Institute of Technology, Pasadena, California 91125, U.S.A.

FRED GELBARD
Department of Chemical Engineering, Massachusetts Institute of Technology, Cambridge, Mass. 02139, U.S.A.

and

JOHN H. SEINFELD
Department of Chemical Engineering, California Institute of Technology, Pasadena, California 91125, U.S.A

(*First received* 10 *September* 1980 *and in final form* 21 *January* 1981)

Abstract—Description of the evolution of the size and chemical composition of aerosols in plumes is fundamental to the ability to predict visibility impairment. Previously it has only been possible to predict changes in aerosol size distributions in plumes. In this work the first model for predicting both size and chemical composition evolution of plume aerosols is presented. Coagulation, homogeneous particle formation, heterogeneous condensation, and particulate phase chemical equilibria and kinetics are explicitly included. The model is based on a sectional representation of the size-composition spectrum and computation is easy to implement. This model holds promise to be a standard component of all plume visibility calculations that require plume aerosol size and composition information.

NOMENCLATURE

a_i	activity of species i, mol (kg water)$^{-1}$ except a_w which is dimensionless
a_y, a_z	plume dispersion parameters
A	cross-sectional area of plume, m^2
b_y, b_z	plume dispersion parameters
c_i	molality of species i, mol (kg water)$^{-1}$
$C[n, n]$	net rate of change of n by coagulation, $(\mu g)^{-s} m^{-3} s^{-1}$
D	particle diameter, μm
D_l	particle diameter at the upper limit of section l, μm
D_{l-1}	particle diameter at the lower limit of section l, μm
$\mathscr{D}_B$	Brownian diffusivity, m^2 s^{-1}
$\mathscr{D}$	molecular diffusivity, m^2 s^{-1}
I_i	rate of change of component i in a particle due to condensation, g s^{-1}
$k_i(M)$	mass transfer coefficient of species i to a particle of mass M, $\mu g\, s^{-1}\, atm^{-1}$
k_g	first-order rate constant for gas-phase SO_2 oxidation, s^{-1}
$\overline{k_{li}}$	mean mass transfer coefficient for species i in section l, defined by (A.32), atm^{-1} s^{-1}
k_{pj}	mass transfer coefficient for species j to a particle with mass M_p defined by (A.33), atm^{-1} s^{-1}
K	equilibrium constant (see Table 1)
K_{ii}	turbulent eddy diffusivity in coordinate direction i, m^2 s^{-1}
Kn	Knudsen number, $2\lambda/D$
m	number of sections
m_i	mass of component i in a particle, μg
M	total mass in a particle, μg
M_i	molecular weight of species i, g mol^{-1}
n	size-composition density function, $(\mu g)^{-s} m^{-3}$
N	total aerosol number density, m^{-3}
p_i	partial pressure of species i in gas phase, atm
p_{io}	partial pressure of species i in gas phase in equilibrium with the particle composition, atm
p_{lio}	partial pressure of species i in gas phase in equilibrium with the mean particle composition of section l, atm
q_l	average mass concentration in section l, $\mu g\, m^{-3}$
Q_l	total aerosol mass in section l, $\mu g\, m^{-3}$
Q_{li}	total aerosol mass of species i in section l, $\mu g\, m^{-3}$
r_{li}	rate constant for species i in section l, from $(dm_i/dt) = r_{li}M$, s^{-1}
R_i	rate of change of component i in a particle due to intra-particle chemical reaction, $\mu g\, s^{-1}$
R.H.	relative humidity, %
s	number of components in the particulate phase
S	rate of introduction of particles, $(\mu g)^{-s} m^{-3} s^{-1}$
t	time, sec
t'	plume travel time, $x_1/\bar{u}_1$, s
$\mathbf{u}$	velocity of air (u_1, u_2, u_3), m s^{-1}
$\hat{\mathbf{u}}$	generalized velocity in phase space
w_s	setting velocity of a particle, m s^{-1}
$\mathbf{x}$	spatial position vector (x_1, x_2, x_3), m
y_i	gas-phase mixing ratio of species i, ppm
z	charge on a species

Greek

α_i	coefficients in heterogeneous rate expression, $i = 1, 2, 3$
$^1\overline{\beta}_{ijk}$	intra-sectional coagulation coefficient, defined by (A.34), m$^3\, \mu g^{-1}\, s^{-1}$
$^2\overline{\beta}_{ij}$	inter-sectional coagulation coefficient, defined by (A.35), m$^3\, \mu g^{-1}\, s^{-1}$

* Paper presented at the Symposium on Plumes and Visibility: Measurements and Model Components. Grand Canyon, Arizona, U.S.A. 10–14 November 1980.

$\beta(U, M)$	coagulation coefficient for particle with masses U and M, $m^3 s^{-1}$
γ_z	activity coefficient for species with charge z
Δ_l	$\ln(M_l/M_{l-1})$
ε	fractional error
ζ	ratio of the mass of sulfate to the total mass of a particle
θ	conditional function used in (A.26)
λ	mean free path of air, μm
σ_y, σ_z	standard deviations of plume dimensions, m
χ	total molality of HSO_4^-, SO_4^{2-}, and Mn^{2+}, mol(kg water)$^{-1}$
ω	$(1.333 + 0.71 Kn^{-1})/(1 + Kn^{-1})$

Symbols

$\bar{}$	time average (except for $\bar{k}_{ii}$ which is a sectional average)
$'$	fluctuating quantity
$\langle\ \rangle$	plume cross-sectional average.

1. INTRODUCTION

A mathematical model for visibility impairment from either plume blight or regional haze must contain three ingredients: (1) a treatment of the advection and diffusion of gases and particles; (2) a routine for calculating visual range given the atmospheric gas and aerosol concentrations, viewing angle, solar angle, etc.; and (3) a description of the gas–particle dynamics, including the evolution of aerosol size and chemical composition. Items (1) and (2) have received considerable attention in visibility and other models. The major missing aspect in all current visibility models is a detailed treatment of the gas–aerosol dynamics. What is usually done is to specify the aerosol characteristics on the basis of empirical observations rather than to simulate them from first principles. However this approach provides little insight into the governing mechanisms. The object of this paper is to develop and present a model based on first principles for the dynamics of atmospheric aerosol size and chemical composition and to apply the model to predict aerosol size and composition as a function of downwind distance in a plume in which SO_2 is being converted homogeneously and heterogeneously to sulfate aerosol.

Prediction of the effect of changes in primary gaseous and particulate emission levels on particulate air quality necessitates the development of mathematical models that include aerosol processes and gas-to-particle conversion. Aerosols that do not change properties once in the atmosphere may be treated from a modeling point of view as inert gaseous species, with due attention to wet and dry deposition. As long as the aerosols do not interact or grow in the atmosphere, their size distribution is altered only through these removal processes which may be accounted for in a straightforward manner. However, most atmospheric aerosols do interact and grow by gas-to-particle conversion and thus more sophisticated approaches must be adopted. The prediction of both aerosol size and composition is the ultimate goal of aerosol modeling efforts and is the issue addressed in this paper.

Although there exists a large number of reported ambient aerosol size distributions (Willeke *et al.*, 1974; Willeke and Whitby, 1975; Hidy, 1975; Whitby, 1978) as well as efforts to characterize various atmospheric aerosol size distributions by empirical relationships, such as by sums of log-normal distributions, observed atmospheric aerosol size spectra and aerosol compositions have not been predicted *a priori*. The reason for this is twofold. First, until recently it has not been possible to solve the general dynamic equation governing a coagulating multicomponent aerosol, even without considering gas-to-particle conversion, sources, or removal mechanisms (Gelbard and Seinfeld, 1980). Second, the size distribution and chemical composition of typical primary aerosols are not adequately known, and the major secondary species and their chemical and physical routes of incorporation into particles have yet to be completely identified. Even though not enough is known about the chemistry and physics of individual particles to support predictions of the evolution of complex atmospheric aerosols, it is now possible to attempt to explain the nature of atmospheric aerosol size distributions and to begin to develop mathematical models capable of relating primary gaseous and particulate emissions to ambient aerosol size and chemical composition distributions. The model presented in this work will predict aerosol size distribution and composition given inputs of gas- and particulate-phase chemistry and primary particle emissions. Based on the model, light scattering calculations which incorporate both particle size and chemical composition effects can be used for visibility predictions.

In section 2 we present the basic equations governing the multicomponent sectional plume model. The detailed derivation of the model is given in Appendix A2. The discussion in Section 2 is aimed at describing the essential assumptions needed to obtain the model and describing the physical significance of each of its terms. In essence, the model represents a temporally (turbulent), spatially, and size/composition-averaged form of the fundamental aerosol conservation equation. Section 3 is devoted to an application of the model to a plume aerosol. All phenomena that might be expected to be important in a plume are included in the example, primarily as a means of illustrating the features of the model. The case considered consists of a power plant plume aerosol containing an aqueous solution of $MnSO_4$ that evolves due to absorption of SO_2 followed by liquid-phase catalytic oxidation, coagulation, and gas-to-particle conversion of sulfuric acid vapor generated by gas-phase oxidation of SO_2.

2. MULTICOMPONENT AEROSOL DYNAMICS

Gelbard and Seinfeld (1980) have developed a general method for simulating the evolution of the distribution of chemical species with respect to aerosol particle size. The physical phenomena included are: (1)

coagulation; (2) intra-particle chemical reaction; (3) gas-to-particle conversion and (4) particle sources and removal mechanisms. Thus, for the first time a technique is available for computation of not only the evolving size distribution but also the variation of chemical composition with particle size. In Appendix A1 and A2, a detailed extension of the multicomponent sectional technique developed by Gelbard and Seinfeld (1980) is presented for a plume aerosol. Therefore, only an outline of the logic used to develop the plume model follows.

Consider for the moment a spatially homogeneous aerosol in which particle size is characterized by a single variable M, particle mass, which is conserved during coagulation and intra-particle chemical reactions. By dividing the entire particle size domain into m contiguous arbitrarily sized sections and defining Q_l as the total mass of aerosol per unit volume of fluid in section l at time t we have, by definition,

$$Q_l = \sum_{i=1}^{s} Q_{li}, \tag{1}$$

where Q_{li} is the mass of component i in section l, and s is the total number of components in the particulate phase. M_{l-1} and M_l will denote the masses of the smallest and largest particles, respectively, in section l. Note that M_0 is arbitrary and the upper bound of section $l-1$ is equal to the lower bound of section l for $l = 2, 3, \ldots, m$. The model derived in this work describes Q_{li} in a plume.

A detailed model of Q_{li} as a three-dimensional, time-dependent function would clearly be the most comprehensive approach available. However, such a model would probably be of limited use due to: (1) the scarcity of detailed aerosol and meteorological data needed to justify such a complicated approach and (2) the excessive computational requirements of such a detailed model. Furthermore, much insight can be gained by using a steady state, spatially and temporally averaged plume model that does not have the above shortcomings. Thus, in the proposed one-dimensional, steady state model Q_{li} is determined in an expanding puff traveling with a mean wind velocity.

The summary of the approximations used to obtain the model is:

1. Neglect Brownian diffusion for bulk transport of particles.
2. Time-average and neglect terms containing temporal fluctuations for coagulation and condensation.
3. Spatially average in the x_2–x_3 plane for a plume traveling in the x_1-direction.
4. All particles within a section are approximated as being uniformly distributed with respect to the logarithm of $(D/1\ \mu m)$ (where D is the particle diameter).
5. All particles within a section are approximated as being of uniform composition in component i ($i = 1, 2, \ldots, s$) given by Q_{li}/Q_l.

Note that by temporally and spatially averaging, the only coordinate upon which Q_{li} depends is x_1, the distance downwind from the plume source. Therefore, one can define "a plume time" $t' = x_1/\bar{u}_1$, where $\bar{u}_1$ is the mean speed in the x_1-direction. The set of ms differential equations governing Q_{li} is*

$$\frac{dQ_{li}}{dt} = \underbrace{\left[\overline{k_{li}}(\langle \bar{p}_i \rangle - p_{lio}) + r_{li}\right] Q_l}_{\text{(A)}}$$

$$\underbrace{-\left[\sum_{j=1}^{s}\left(k_{qj}(\langle \bar{p}_i \rangle - p_{lio}) + r_{lj}\Delta_q^{-1}\right)Q_{qi}\right]\Bigg|_{q=l-1}^{q=l}}_{\text{(B)}}$$

$$+ \underbrace{\tfrac{1}{2}\sum_{j=1}^{l}\sum_{k=1}^{l}\left({}^1\overline{\beta}_{ljk}\, Q_{ji}\, Q_k + {}^1\overline{\beta}_{lkj}\, Q_{ki}\, Q_j\right)}_{\text{(C)}}$$

$$\underbrace{- Q_{li}\sum_{j=1}^{m} {}^2\overline{\beta}_{lj}\, Q_j}_{\text{(D)}} \underbrace{- Q_{li}\frac{1}{A}\frac{dA}{dt'}}_{\text{(E)}} + \underbrace{\langle \overline{S_{li}} \rangle}_{\text{(F)}} \tag{2}$$

$$l = 1, 2, \ldots, m$$
$$i = 1, 2, \ldots, s.$$

Term A represents the net rate of addition of the i-th component to section l by the heterogeneous condensation of vapor molecules onto particles within section l and by aerosol-phase chemical reactions occurring in particles of section l. Term B represents the net rate of change of Q_{li} by condensation and aerosol-phase chemical reaction due to the growth of particles in section l-1 into section l and to the growth of particles in section l into section $l+1$. As a particle grows by condensation of vapor or as a result of chemical reactions, it may eventually leave its section, while, at the same time, some of those in the lower section may grow into that section. Thus, together, terms A and B represent the net rate of change of component i in section l from intra-section processes and growth between sections.

Terms C and D represent the effects of coagulation. Term C represents the rate of addition of particles to section l resulting from all collisions involving particles in sections lower than and including section l itself. Term D accounts for the rate of removal of component i from section l due to the collision of particles in section l with those of all other sections.

Term E represents the effect of dilution of the plume. Finally, term F represents the rate of addition of mass of component i to section l by sources. In the plume situation, the original source of particles appears as an initial condition on (2),

$$Q_{li}(t'_o) = Q^0_{li}, \tag{3}$$

and $\langle \overline{S_{li}} \rangle = 0$ for all sections l, except possibly for $l = 1$ if new particle formation by nucleation is occurring as a source of fresh particles into the first section. (It is assumed by this statement that if homogeneous

* All symbols are defined in Appendixes, A.1 and A.2 and in the Nomenclature section.

nucleation is occurring, the particles so formed would be of a size such that they would fall within the first section. This assumption is, of course, not necessary; fresh particles can be added to any section through specification of $\langle \overline{S_{li}} \rangle$.)

Equation (2) is the result of a careful accounting of all aerosol processes that add or remove mass of a component from a section on the particle size domain. The particular form of (2) is that for the plume cross-section averaged sectional concentrations, as indicated by the spatial averaging brackets, $\langle\ \rangle$. The coefficients $\overline{k_{li}}$ and k_{pj} are determined based on the gas-to-particle conversion processes occurring, whereas r_{li} depends on heterogeneous reactions that are taking place. The term $A^{-1}\,dA/dt$ is determined by the rate of expansion of the plume.

To illustrate the application of the multicomponent sectional model we now consider predicting the evolution of a power plant plume aerosol. The example we will present is, for the most part, hypothetical. With the introduction of a new model such as that just described it is important that the first application be an example that is carefully defined and for which the calculations may be repeated by others interested in using the model. In the example that follows we have endeavored to include all important phenomena that influence a plume aerosol. The initial aerosol size distribution is taken from the plume field data reported by Eltgroth and Hobbs (1979). The composition of the initial aerosol is assumed to be an aqueous $MnSO_4$ solution, for which an empirical expression is available for the rate of oxidation of dissolved SO_2 to sulfate. All parameters that need to be specified are set at atmospherically relevant values. Thus, while the calculation does not correspond to an actual plume, each element of the model is treated realistically so that application to an actual field situation in which the particles consist of aqueous solutions follows from that presented here.

3. APPLICATION TO POWER PLANT PLUME AEROSOL

We consider the problem of predicting the evolution of the aerosol size and composition distribution in a power plant plume. Upon emission from the stack, we assume that the primary aerosol consists of an aqueous $MnSO_4$ solution and that the gas contains SO_2. As the plume is carried downwind and disperses, the SO_2 is both absorbed by the plume aerosol particles and converted to H_2SO_4 vapor by gas-phase chemistry. In the particles, the dissolved SO_2 is catalytically oxidized to sulfate (SO_4^{2-}), while, at the same time, the sulfuric acid vapor molecules from the vapor phase SO_2 oxidation are absorbed by the particles. Particle growth occurs due to the water vapor pressure lowering effect of the sulfate formed in the particles. The ambient relative humidity and temperature are assumed to be known, as is the background concentration of NH_3. It is desired to predict the distribution of all the dissolved aerosol species with particle size as a function of downwind distance.

Although the specific conditions of our example do not correpond to those of a particular plume, they have been chosen to reflect as closely as possible the situation in an actual plume. Only the gas-phase conversion of SO_2 to H_2SO_4 will not be treated in detail, as this step is only of peripheral interest to the model. In particular, the gas-phase oxidation of SO_2 is treated as first-order in SO_2, with the rate of formation of H_2SO_4 vapor given by

$$\frac{dp_{H_2SO_4}}{dt'} = k_g p_{SO_2}. \tag{4}$$

It is necessary to specify the following parameters to exercise the model: $\overline{k_{li}}$ = the section average coefficient for gas-to-particle conversion of component i; $\langle \overline{p}_i \rangle$ = the mean partial pressure of each condensing component; p_{lio} = the partial pressure of component i in equilibrium with the particles in section l; r_{li} = the rate constant for production of component i by intraparticle chemical reaction in section l; ${}^1\overline{\beta}_{ijk}$, ${}^2\overline{\beta}_{ij}$ = the sectional coagulation coefficients; and $(1/A)\,(dA/dt')$ = the rate of plume expansion. In addition, the number of species, s, and the number m and locations of the sections must be specified.

Physically, the plume aerosol consists of aqueous droplets containing $MnSO_4$, in the amount specified as initially present, together with the other components that result from the dissolution of SO_2, NH_3 and H_2SO_4 in the droplets. The time needed for equilibrium to be established between the gas and liquid phases is much shorter than that for coagulation or formation of sulfuric acid. Therefore, all the liquid-phase compositions, except those of Mn^{2+} and SO_4^{2-}, are determined by equilibrium with the gas phase. That is, once the concentrations of Mn^{2+} and SO_4^{2-} are specified, the entire composition of the particle is fixed through chemical equilibrium. As a result, Mn^{2+} and SO_4^{2-} are the only two components for which the multicomponent sectional equations are needed, i.e. $s=2$. The calculation proceeds as if the particles consist solely of Mn^{2+} and SO_4^{2-}, although the particles are considerably more complex, and the parameters listed above must be determined on the basis of the actual particle composition. The dependent variables in the model are Q_{l1} and Q_{l2}, where 1 refers to manganese and 2 to sulfate.

The gas-phase species are SO_2, NH_3, H_2O and H_2SO_4. The ammonia and water concentrations are assumed uniform and constant. The SO_2 concentration decreases with distance due to plume dilution and conversion to H_2SO_4. The production of sulfuric acid vapor is described by (4). The droplet-phase concentrations of SO_2, NH_3 and H_2O are those in equilibrium with their prevailing gas-phase concentrations. Transport of sulfuric acid vapor to the par-

ticles occurs by diffusion, the mass transfer coefficient of which is given by (Fuchs and Sutugin, 1971)*

$$k_2 = \frac{2\pi D\mathscr{D}}{(1+\omega Kn)}\frac{M_{SO_4}}{RT}, \tag{5}$$

where $\omega = (1.333 + 0.71\,Kn^{-1})/(1 + Kn^{-1})$. $\overline{k_{li}}$ and k_{li} can be calculated from (A.33) and (A.34). The absorption of H_2SO_4 is irreversible, so $p_{lio} = 0$.

An expression for the rate of the Mn-catalyzed oxidation of dissolved SO_2 to sulfate has been given by Wadden *et al.* (1974),

$$\frac{d[H_2SO_4]}{dt} = \frac{[MnSO_4](\alpha_1 y_{SO_2} - \alpha_2[H^+][HSO_4^-])}{\alpha_3 + y_{SO_2}}, \tag{6}$$

where [ ] represents concentrations in moles ℓ^{-1}, y is concentration in ppm, $\alpha_1 = 2.025\,min^{-1}$, $\alpha_2 = 4.254$ (moles $\ell^{-1})^{-2}$ (ppm min^{-1}), and $\alpha_3 =$ 200 ppm. Converting (6) to the units used here, we have

$$R_2 = \frac{m_1 M_{SO_4}}{M_{Mn}}\left[\frac{\alpha_1 y_{SO_2} - \alpha_2[H^+][HSO_4^-]}{\alpha_3 + y_{SO_2}}\right]. \tag{7}$$

To obtain an expression for r_{2l}, we write (7) as $R_2 = r_{2l}M$. Assuming all particles in a section have the same composition, $m_1 = (Q_{l1}/Q_l)M$, from which

$$r_{2l} = \frac{Q_{l1}}{Q_l}\frac{M_{SO_4}}{M_{Mn}}\left[\frac{\alpha_1 y_{SO_2} - \alpha_2[H^+][HSO_4^-]}{\alpha_3 + y_{SO_2}}\right]. \tag{8}$$

The most involved aspect of the model application is the calculation of the sectional coagulation coefficients, ${}^1\bar{\beta}_{ijk}$ and ${}^2\bar{\beta}_{ij}$. Assuming the coagulation coefficient depends only on the volumes of the two particles, once the volumes of the particles are specified, ${}^1\bar{\beta}_{ijk}$ and ${}^2\bar{\beta}_{ik}$ can be determined from (A.34) and (A.35). In this work the Fuchs–Phillips expression for the Brownian coefficient $\beta(U, M)$ is used (Sitarski and Seinfeld, 1977). To calculate these coefficients it is necessary to relate the masses of Mn^{2+} and SO_4^{2-} to the volume of the particle. Relating the concentrations of manganese and sulfate to the size of the particle requires information on the complete particle composition that can be determined by imposing the condition that all species except Mn^{2+} and SO_4^{2-} be at their equilibrium concentrations.

The equilibrium computation is carried out as follows. At any time t', the total masses of manganese and sulfate, Q_{l1} and Q_{l2}, are known in each section l. A basic assumption of the approach is that all particles in a section have identical composition. Knowing Q_{l1} and Q_{l2}, we also know their ratio, Q_{l1}/Q_{l2}. The equilibrium constants required are given in Table 1. In the equilibrium calculation for each section there are three equations involving the three unknown quantities, I (ionic strength), $c_{SO_4^{2-}}$, and c_{H^+} (molalities of sulfate and H^+). (The molality of manganese can be used instead of that for sulfate since given the ratio Q_{l1}/Q_{l2}, only one of these two quantities is considered as unknown.) The three equations are those for the ionic strength, the water activity, and electroneutrality.

The ionic strength is related to the species molalities by (Denbigh, 1971)

$$I = \frac{1}{2}\sum_i c_i z_i^2, \tag{9}$$

where z_i is the charge on species i.

The water vapor equilibrium is expressed by (Stokes and Robinson, 1966)

$$1 = \sum \frac{c_i}{c_{bi}(a_w)}, \tag{10}$$

where c_{bi} is the molality of a binary solution of the i-th component and water at the same water activity a_w.

We assume that the effect of sulfite on water activity is the same as sulfate. Then, the droplet may be treated as a mixture of $MnSO_4$, $(NH_4)_2SO_4$ and H_2SO_4, and (10) may be solved for $\chi = c_{SO_4^{2-}} + c_{HSO_4^-} + c_{Mn^{2+}}$ as

$$\chi = \left[1 + \frac{1}{2}\left(\frac{1}{c_{bH_2SO_4}} - \frac{1}{c_{b(NH_4)_2SO_4}}\right)p_{NH_3}K_{ha}\left(a_w + \frac{K_{1a}c_{H^+}}{K_w}\right) - \frac{a_w}{c_{bH_2SO_4}}\left(p_{SO_2}K_{hs}\left(1 + \frac{K_{1s}}{\gamma_+\gamma_-c_{H^+}}\left(1 + \frac{K_{2s}\gamma_-}{\gamma_+\gamma_-c_{H^+}}\right)\right)\right)\right]\left[(1-\zeta)\left(\frac{1}{c_{bMnSO_4}} - \frac{1}{c_{bH_2SO_4}}\right) + \frac{\zeta}{c_{bH_2SO_4}}\right]^{-1}, \tag{11}$$

where $\zeta = (c_{SO_4^{2-}} + c_{HSO_4^-})/\chi$ and where the activity coefficients are approx. by (Davis, 1938)

$$\log \gamma_z = -\phi z^2\left(\frac{\sqrt{I}}{1+\sqrt{I}} - 0.2I\right). \tag{12}$$

γ_z is the activity coefficient for an ion with a charge z. For the system considered here $\phi = 0.5085$.

The condition of electroneutrality leads to

$$0 = -\frac{1}{c_{H^+}}\frac{a_w}{\gamma_+\gamma_-}\left[K_w + p_{SO_2}K_{hs}K_{1s}\right] - \frac{2p_{SO_2}K_{hs}K_{1s}K_{2s}a_w}{\gamma_+^2\gamma_{2-}c_{H^+}^2} + c_{H^+} + \frac{p_{NH_3}K_{ha}K_{1a}c_{H^+}}{K_w} + \chi\left[(2-4\zeta) + \frac{\gamma_{2-}\gamma_+\zeta c_{H^+}}{K_{ds}\gamma_- + \gamma_{2-}\gamma_+c_{H^+}}\right]. \tag{13}$$

The ionic strength relation (9) can be written as

$$0 = 2I - \left[\frac{a_w}{\gamma_+\gamma_-c_{H^+}}(K_w + p_{SO_2}K_{hs}K_{1s}) + \frac{4p_{SO_2}K_{hs}K_{1s}K_{2s}a_w}{\gamma_+^2\gamma_{2-}c_{H^+}^2}\right.$$

* Since "component" 2 is sulfate, only the molecular weight of sulfate, M_{SO_4}, is needed in (5). The hydrogen atoms are automatically determined by the equilibrium calculation.

Table 1. Equilibrium constants for the aqueous SO_2-NH_3 system*

Reaction	Equilibrium constant†	Value @ 298 K
$H_2O \rightleftarrows H^+ + OH^-$	$K_w = \frac{a_{H^+} a_{OH^-}}{a_w}$	1.008×10^{-14} (mol kg^{-1})^2
$SO_2(g) + H_2O \rightleftarrows SO_2 \cdot H_2O$	$K_{hs} = \frac{a_{SO_2 \cdot H_2O}}{p_{SO_2} a_w}$	1.231 mol kg^{-1} atm^{-1}
$SO_2 \cdot H_2O \rightleftarrows H^+ + HSO_3^-$	$K_{1s} = \frac{a_{H^+} a_{HSO_3^-}}{a_{SO_2 \cdot H_2O}}$	1.717×10^{-2} mol kg^{-1}
$HSO_3^- \rightleftarrows H^+ + SO_3^{2-}$	$K_{2s} = \frac{a_{H^+} a_{SO_3^{2-}}}{a_{HSO_3^-}}$	6.0139×10^{-8} mol kg^{-1}
$NH_3(g) + H_2O \rightleftarrows NH_3 \cdot H_2O$	$K_{ha} = \frac{a_{NH_3 \cdot H_2O}}{p_{NH_3} a_w}$	57.46 mol kg^{-1} atm^{-1}
$NH_3 \cdot H_2O \rightleftarrows NH_4^+ + OH^-$	$K_{1a} = \frac{a_{NH_4^+} a_{OH^-}}{a_{NH_3 \cdot H_2O}}$	1.798×10^{-5} mol kg^{-1}
$HSO_4^- \rightleftarrows SO_4^{2-} + H^+$	$K_{ds} = \frac{a_{H^+} a_{SO_4^{2-}}}{a_{HSO_4^-}}$	1.014×10^{-2} mol kg^{-1}

* Reference: Wagman *et al.* (1968)
† Water activity a_w = R.H./100, where R.H. is the relative humidity in %.

$$+\frac{p_{NH_3} K_{ha} K_{1a} c_{H^+}}{K_w} + c_{H^+} + \left(4 - \frac{3c_{H^+}\gamma_{2-}\gamma_{+}\zeta}{\gamma_{2-}\gamma_{+} c_{H^+} + K_{ds}\gamma_{-}}\right)\chi\Bigg]. \quad (14)$$

Equations (13) and (14) may be solved iteratively as follows. First, values of c_{H^+} and I are assumed. Using the assumed value of I, the activity coefficients may be calculated from (12). The values of c_{H^+} and I are determined by iterating on (13) and (14).

The total mass of the particle is now available since the masses of Mn^{2+} and SO_4^{2-} are known together with their molalities. Finally, the volume of the particle can be calculated from

$$V = \frac{\left(\frac{10^3}{\rho_w} + \sum_i c_i v_i\right) M}{\zeta \chi M_{SO_4} + (1-\zeta)\chi M_{Mn}}, \quad (15)$$

where v_i is the molal volume of the i-th component. Values of v_i were calculated from data in International Critical Tables (1928), Klotz and Eckert (1942) and Lindstrom and Wirth (1969).

4. RESULTS OF PLUME SIMULATION

Figures 1–7 show the results of the calculations performed. In each figure the component mass concentrations are referred to the left-hand ordinate. The component mass concentrations are indicated by the shaded regions on each bar representing a section. The difference between the mass represented by the shaded regions and the total mass is that of water. In all cases, water comprises at least three-fifths of the mass of each section. Ten sections ($m = 10$) were used in the computations*. The sections were selected according to $D_0 = 0.01\ \mu m$, $D_{10} = 5\ \mu m$ and $D_i/D_{i-1} = 1.86$.

* Results similar to those presented here were obtained using 20 sections.

Figure 1 shows the assumed "initial" size-composition distribution at 1 km. The "initial" distribution was chosen based on data reported by Eltgroth and Hobbs (1979) for the Centralia plume on 22 September, 1977 (entry (d) of Table 3 of that work). In addition, we have assumed that the initial plume aerosol consists of an aqueous solution of $MnSO_4$ in equilibrium with a relative humidity of 90%. This relative humidity was taken to be constant over the length of the plume. A uniform background concen-

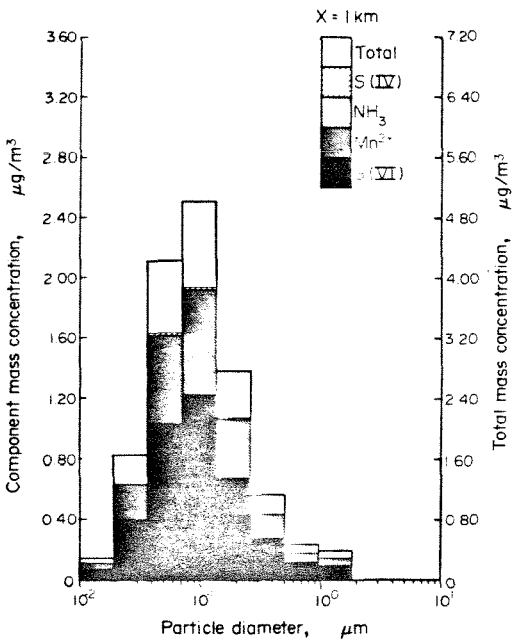

Fig. 1. Aerosol mass distribution at a distance of 1 km from the source. S(IV) refers to the total concentration of sulfur in oxidation state four, i.e. $SO_2 \cdot H_2O$, HSO_3^- and SO_3^{2-}. S(VI) refers to the total concentration of sulfur in oxidation state six, i.e. SO_4^{2-} and $HSO_4^- \cdot NH_3$ refers to the total concentration of $NH_3 \cdot H_2O$ and NH_4^+.

tration of NH_3 of 0.05 ppm was assumed. At 1 km, the concentration of SO_2 in the plume was taken to be 1.2 ppm. As the plume is diluted, the SO_2 concentration is reduced accordingly. (Sulfur dioxide is also depleted by gas-phase conversion to sulfuric acid and by absorption into the particles.)

Three cases were studied:

(i) Case 1 (Figs 2–3): no reactions, coagulation, dilution.

(ii) Case 2 (Figs 4–5): liquid-phase reaction only, coagulation, dilution.

(iii) Case 3 (Figs 6–7): all phenomena included; gas- and liquid-phase reactions, coagulation, dilution.

In each case, the size-composition distributions at 2 and 10 km downwind are shown. A common feature of each of the three cases is the depletion of the two lowest sections ($D_0 = 0.01\,\mu m$, $D_1 = 0.0186\,\mu m$, $D_2 = 0.0346\,\mu m$) due to coagulation with larger particles. Because we have not assumed that homogeneous nucleation is occurring, there is no source of fresh particles to replenish the two lower sections.

Case 1 shows the effects of coagulation and dilution on the size distribution. No reactions were assumed to be occurring. Section 4, centered around 0.1 μm dia., initially has the highest mass concentration. As the plume is carried downwind, dilution reduces the mass concentrations in all sections equally. Dilution is accounted for by the term $A^{-1}\mathrm{d}A/\mathrm{d}t'$. This term can be specified based on the conventional σ_y and σ_z parameters for the Gaussian plume equation. In this work, the Pasquill-Gifford (P–G) σ_y and σ_z parameters for neutral conditions were used. If the plume area A is taken as proportional to the product, $\sigma_y\sigma_z$, then

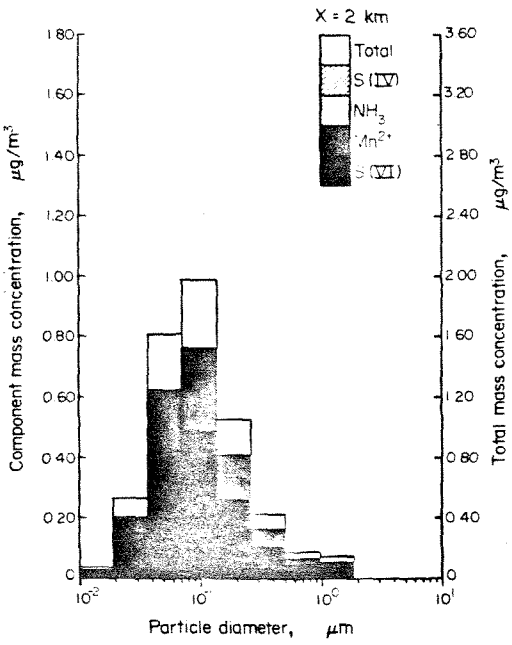

Fig. 2. Aerosol mass distribution at a distance of 2 km from the source resulting from coagulation and dilution of the distribution of Fig. 1.

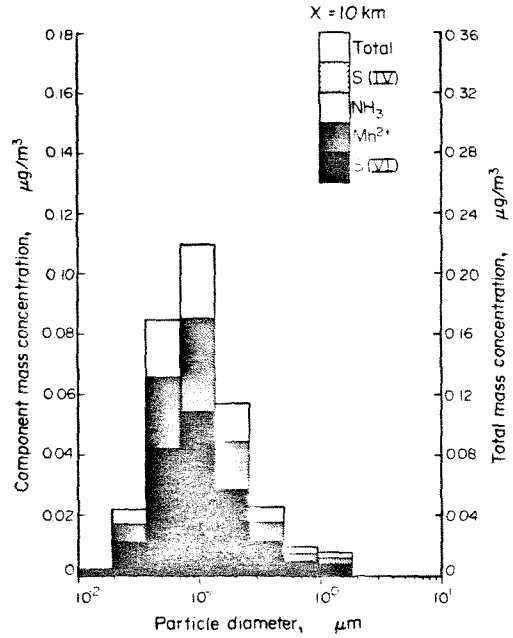

Fig. 3. Aerosol mass distribution at a distance of 10 km from the source resulting from coagulation and dilution of the distribution of Fig. 1.

$$\frac{1}{A}\frac{\mathrm{d}A}{\mathrm{d}t'} = \frac{1}{\sigma_y\sigma_z}\left[\sigma_y\frac{\mathrm{d}\sigma_z}{\mathrm{d}t'} + \sigma_z\frac{\mathrm{d}\sigma_y}{\mathrm{d}t'}\right]. \tag{16}$$

Fitting functions of the form, $\sigma_y = a_y(t')^{b_y}$ and $\sigma_z = a_z(t')^{b_z}$ to the P–G neutral curves, we obtain

$$\frac{1}{A}\frac{\mathrm{d}A}{\mathrm{d}t'} = \frac{1.4}{t'}. \tag{17}$$

From 1 to 10 km, the plume is diluted by a factor of 25.

The size distribution evolution in Figs 1–3 can be explained on the basis of the combined effects of dilution and coagulation. Particles in sections 1 and 2 are continually depleted through coagulation with those in higher sections. Conversely, the other sections gain mass by the same process. This effect is greatest for the smallest sections. For example, from 1 to 10 km, coagulation reduces the amount of mass in the first section by a factor of almost three. On the other hand, for the sixth section coagulation adds less than 1% of the final mass. Dilution simply lowers all concentrations equally whereas coagulation produces a shift toward the upper end of the spectrum.

Figures 4 and 5 show the mass distributions at 2 and 10 km when the manganese catalyzed liquid-phase oxidation of dissolved SO_2 is occurring, in addition to coagulation and dilution. In each section, the rate of formation of sulfate, expressed as a percentage of the total particle mass, depends only on the internal concentrations. Since the internal concentrations are initially equal for all sections, an equal percentage of the total mass of each section is added as sulfate with downwind distance. Thus, for example, at 2 km, the SO_4^{2-}, Mn^{2+}, NH_4^+, etc. fractions of the total mass of

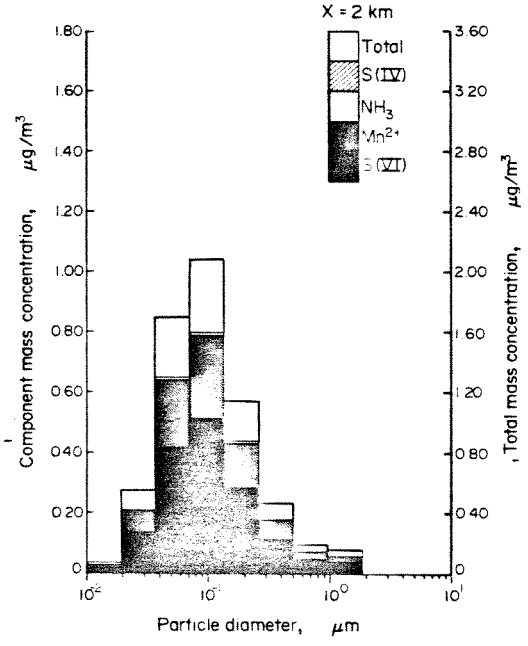

Fig. 4. Aerosol mass distribution at a distance of 2 km from the source resulting from coagulation, dilution, and liquid-phase oxidation of dissolved SO_2.

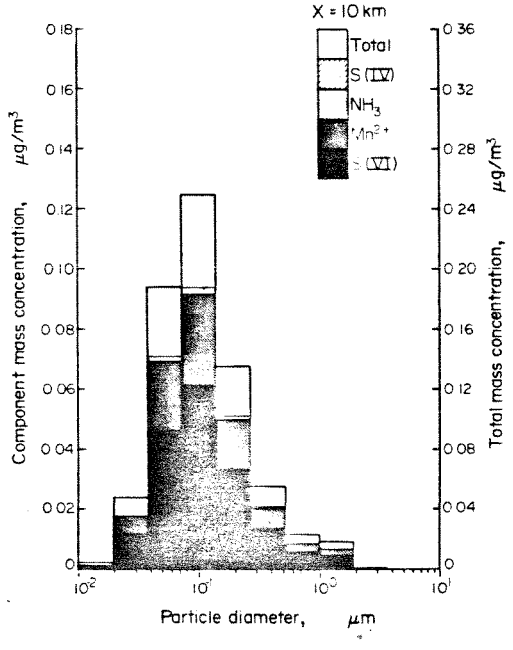

Fig. 5. Aerosol mass distribution at a distance of 10 km from the source resulting from coagulation, dilution, and liquid-phase oxidation of dissolved SO_2.

each section are equal. The values of these fractions change with downwind distance but remain uniform across the sections. At the rate of sulfate formation predicted by (7), the quantity of sulfate formed in each section is not large enough to alter substantially the total mass distributions from Case 1. For example, at

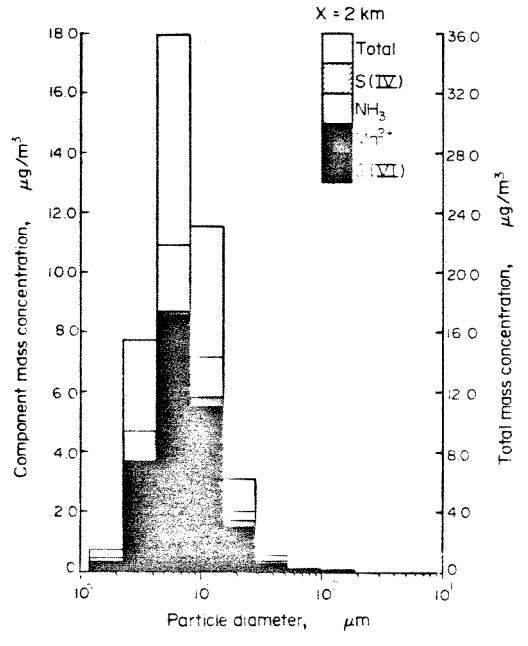

Fig. 6. Aerosol mass distribution at a distance of 2 km from the source resulting from coagulation, dilution, liquid-phase oxidation of dissolved SO_2, and gas-to-particle conversion of H_2SO_4 vapor formed by gas-phase oxidation of SO_2.

10 km, particles in Section 4 contain approximately 0.008 $\mu g\,m^{-3}$ of sulfate,* as compared to a total mass concentration in Section 4 of about 0.24 $\mu g\,m^{-3}$.

Case 3 (Figs. 6 and 7) includes all the phenomena of interest. Gas-phase oxidation of SO_2 to H_2SO_4 is now assumed to occur, with a first-order rate constant $k_g = 0.05\,h^{-1}$. The sulfuric acid vapor is absorbed by the particles, directly contributing sulfate to that being formed in the liquid-phase by the manganese catalyzed oxidation. We note that for the specific parameters of our study, this gas-phase oxidation rate dominates that in the liquid phase. For example, at 10 km, particles in Section 4 contain about 10 $\mu g\,m^{-3}$ of sulfate, as compared with about 0.008 $\mu g\,m^{-3}$ in the previous case. Because of the hygroscopicity of sulfate, a large amount of water is associated with the particles. Thus, the total mass concentration of particles in Section 4 in this case is about 40 $\mu g\,m^{-3}$, as compared with 0.24 $\mu g\,m^{-3}$ in Case 2. When the sulfate is being added by gas-to-particle conversion, more sulfate per unit mass is added to the smaller particles.

Recall that sections are defined in terms of M, the total mass of metal and sulfate, rather than in terms of particle diameter. Thus, as the composition of a section changes, its boundaries, expressed in terms of particle diameter may change. This happens in Fig. 6. From 1 km to 2 km a large amount of sulfate from the gas phase is deposited on the drop. Thus, the main

* This sulfate refers to that formed by reaction beyond that present initially as $MnSO_4$.

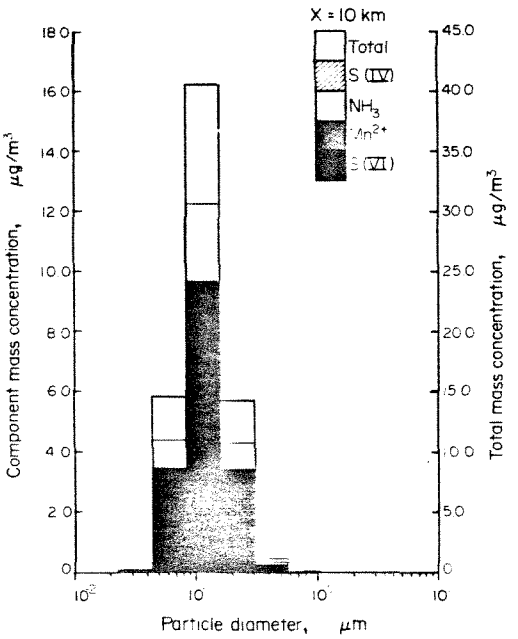

Fig. 7. Aerosol mass distribution at a distance of 10 km from the source resulting from coagulation, dilution, liquid-phase oxidation of dissolved SO_2, and gas-to-particle conversion of H_2SO_4 vapor formed by gas-phase oxidation of SO_2.

component changes from $MnSO_4$ to $(NH_4)_2SO_4$. As a result of this change, for a given amount of metal plus sulfate, the droplet has a larger diameter. Note, for example, that the lower boundary of the first section becomes larger than 0.01 μm.

The ratio of sulfate added to the particles by gas-to-particle conversion to that produced by heterogeneous reaction decreases as particle diameter increases. Thus, even though on an overall basis, for the particular set of parameters chosen here, the gas-phase oxidation of SO_2 is more important than that in the liquid phase, internal reaction dominates the rate of sulfate production in large particles.

The rate of liquid-phase sulfate formation is second-order overall, being proportional to the product, $y_{SO_2}Q_l$. (If y_{SO_2} greatly exceeds 200 ppm, the value of α_3 in the rate expression (6), the rate becomes independent of y_{SO_2}. In the situation considered here, SO_2 concentrations are well below this value.) On the other hand, the homogeneous conversion of SO_2 to H_2SO_4 is first-order. As the plume is diluted, the rate of the heterogeneous reaction is quenched relative to that of the first-order reaction, a phenomenon that has been discussed in detail by Freiberg (1978) and Schwartz and Newman (1978). As a result, the particle size at which homogeneous and heterogeneous sulfate production mechanisms are roughly equal increases with downwind distance.

5. CONCLUSIONS

A model for computing the size-composition distribution of plume aerosols has been presented and applied to a hypothetical, yet realistic, example of a power plant plume aerosol. The evolution of the aerosol size and composition distribution averaged across the plume has been calculated as a function of down wind distance. Upon emission, the aerosol was assumed to consist of aqueous droplets of $MnSO_4$. During transport downwind and dilution, the plume particles interact by coagulation and grow due to liquid-phase catalytic oxidation of dissolved SO_2 and gas-to-particle conversion of sulfuric acid vapor formed by the gas-phase oxidation of SO_2. Based on the work of Gelbard and Seinfeld (1980), the model consists of a set of ordinary differential equations for Q_{li}, the mass of component i in section l, where the aerosol size spectrum has been segmented into m sections ($l = 1, 2, \ldots, m$). The set of ordinary differential equations is solved by standard methods. The model presented in this work has the unique capability of simulating both the aerosol size and composition distributions and therefore can be used as an aerosol dynamics component of detailed plume models.

Acknowledgement—This work was supported by U.S. Environmental Protection Agency grant R806844. The research reported in this paper made use of computational facilities funded through grants from the Camille and Henry Dreyfus Foundation and the National Science Foundation (Grant No. CHE78-20235). Fred Gelbard was supported by NIEHS grant 5P30-ES02109-03 under the Center for Health Effects of Fossil Fuels Utilization of the Harvard—MIT Division of Health Sciences and Technology and the Energy Laboratory.

REFERENCES

Davies C. W. (1938) The extent of dissociation of salts in water. Part VIII. *J. chem. Soc.* 2093–2098.

Denbigh K. (1971) *The Principles of Chemical Equilibrium*, Cambridge University Press, Cambridge, pp. 312.

Eltgroth M. W. and Hobbs P. V. (1979) Evolution of particles in the plumes of coal-fired power plants—II. A numerical model and comparisons with field measurements. *Atmospheric Environment* **13**, 953–976.

Freiberg J. (1978) Conversion limit and characteristic time of SO_2 oxidation in plumes. *Atmospheric Environment* **12**, 339–347.

Fuchs N. A. and Sutugin A. G. (1971) High dispersed aerosols. In *Topics in Current Aerosol Research* Vol. 2, p. 35. (Edited by G. M. Hidy and J. R. Brock). Pergamon Press, Oxford.

Gelbard F. and Seinfeld J. H. (1980) Simulation of multicomponent aerosol dynamics. *J. Colloid Interface Sci.* **78**, 485–501.

Hidy G. M. (1975) Summary of the California Aerosol Characterization Experiment. *J. Air Pollut. Control Ass.* **25**, 1106–1114.

International Critical Tables (1928) First Edition, **3**, 56, 60, 68.

Klotz J. M. and Eckert C. F. (1942) The apparent molal volumes of aqueous solutions of sulfuric acid at 25°. *J. Am. chem. Soc.* **64**, 1878–1880.

Lindstrom R. E. and Wirth H. E. (1969) Estimation of the bisulfate ion dissociation in solutions of sulfuric acid and sodium bisulfate. *J. phys. Chem.* **73**, 218–223.

Schwartz S. E. and Newman L. (1978) Processes limiting the oxidation of sulfur dioxide in stack plumes. *Envir. Sci. Technol.* **12**, 67–73.

Seinfeld J. H. and Ramabhadran T. E. (1975) Atmospheric aerosol growth by heterogeneous condensation. *Atmospheric Environment* **9**, 1091–1097.

Sitarski M. and Seinfeld J. H. (1977) Brownian coagulation in the transition regime. *J. Colloid Interface Science* **61**, 261–271.

Stokes R. H. and Robinson R. A. (1966) Interactions in aqueous nonelectrolyte solutions. I. Solute–solvent equilibria. *J. phys. chem.* **70**, 2126–2131.

Wadden R. A., Quon J. E. and Hulburt H. M. (1974). A model of a growing coagulating aerosol. *Atmospheric Environment* **8**, 1009–1028.

Wagman D. D. *et al.* (1968) Selected values of chemical thermodynamic properties. NBS Technical Note 270–3.

Whitby K. T. (1978) The physical characteristics of sulfur aerosols. *Atmospheric Environment* **12**, 135–139.

Willeke K. and Whitby K. T. (1975) Atmospheric aerosols: size distribution interpretation. *J. Air Pollution Control Ass.* **25**, 529–534.

Willeke K., Whitby K. T., Clark W. E. and Marple V. A. (1974) Size distributions of Denver aerosols—A comparison of two sites. *Atmospheric Environment* **8**, 609–633.

APPENDIX A1: MODEL DEVELOPMENT

Derivation of the equation governing the mean aerosol size-composition distribution function in a plume from a continuous point source

Let M denote the total mass of a particle. Let m_i be the mass of the i-th component in the particle. Let $\mathbf{m} = (m_1, \ldots, m_{s-1})$, where the particle has s components. Note that m_s has been omitted from the $\mathbf{m}$ vector, because it is fixed once the rest of the m_i's are given, i.e.,

$$\sum_{i=1}^{s} m_i = M. \tag{A.1}$$

Then, let $n(\mathbf{m}, M, \mathbf{x}, t)\, dm_1 \ldots dm_{s-1}\, dM$ be the number of particles having total mass M in the range $[M, M+dM]$, mass of component i, m_i in the range $[m_i, m_i + dm_i]$, $i = 1, 2, \ldots, s-1$, at location $\mathbf{x}$ at time t. The rate of change of n is

$$\left.\frac{\partial n}{\partial t}\right|_{\text{total}} = \left.\frac{\partial n}{\partial t}\right|_{\text{drifting}} + \left.\frac{\partial n}{\partial t}\right|_{\text{coagulation}} + \left.\frac{\partial n}{\partial t}\right|_{\text{sources}} + \left.\frac{\partial n}{\partial t}\right|_{\text{Brownian diffusion}} \tag{A.2}$$

Using the divergence theorem in $s+3$ dimensions, the drifting term is

$$\left.\frac{\partial n}{\partial t}\right|_{\text{drifting}} = -\hat{\nabla}\cdot(n\hat{\mathbf{u}}), \tag{A.3}$$

where

$$\hat{\nabla} = \left[\frac{\partial}{\partial m_1}, \frac{\partial}{\partial m_2}, \ldots \frac{\partial}{\partial m_{s-1}}, \frac{\partial}{\partial M}, \frac{\partial}{\partial x_1}, \frac{\partial}{\partial x_2}, \frac{\partial}{\partial x_3}\right],$$

$$\hat{\mathbf{u}} = \left[\frac{\partial m_1}{\partial t}, \frac{\partial m_2}{\partial t}, \ldots \frac{\partial m_{s-1}}{\partial t}, \frac{\partial M}{\partial t}, u_1, u_2, u_3 - w_s\right].$$

Here, $\mathbf{u} = (u_1, u_2, u_3)$ is the velocity of the air and $w_s = w_s(M)$ is the settling velocity.

Let $R_i(\mathbf{m}, M)$ and $I_i(\mathbf{m}, M, \mathbf{x}, t)$ represent the net rate of change of component i in a particle due to intra-particle chemical reaction and condensation, respectively. Note that I_i is the rate of condensation minus that of evaporation. Then

$$\frac{\partial m_i}{\partial t} = I_i + R_i, \tag{A.4}$$

and

$$\frac{\partial M}{\partial t} = I_T + R_T, \tag{A.5}$$

where

$$I_T = \sum_{i=1}^{s} I_i, \tag{A.6}$$

$$R_T = \sum_{i=1}^{s} R_i. \tag{A.7}$$

The coagulation term in (A.2) may be written as

$$\left.\frac{\partial n}{\partial t}\right|_{\text{coagulation}} = \frac{1}{2}\int_0^M \int_0^\infty \cdots \int_0^\infty \beta(U, M-U) n(\xi, U, \mathbf{x}, t) \times n(m-\xi, M-U, \mathbf{x}, t)\, d\xi\, dU - \int_0^\infty \cdots \int_0^\infty \beta(U, M) n(\xi, U, \mathbf{x}, t) \times n(\mathbf{m}, M, \mathbf{x}, t)\, d\xi\, dU, \tag{A.8}$$

where $\beta(U, M)$ is the coagulation coefficient for particles with masses U and M. Note that $n(\mathbf{m}, U, \mathbf{x}, t) = 0$ if

$$U < \sum_{i=1}^{s-1} m_i.$$

Because of this condition, the limits on the integrals in (A.8) can be extended from $-\infty$ to ∞ as n is zero whenever any of the m_i's are negative.

The Brownian diffusion term in (A.2) is given by

$$\left.\frac{\partial n}{\partial t}\right|_{\substack{\text{Brownian}\\ \text{diffusion}}} = \mathscr{D}_B \sum_{i=1}^{3} \frac{\partial^2 n}{\partial x_i^2}, \tag{A.9}$$

where $\mathscr{D}_B$ is the Brownian diffusivity. However, transport by Brownian diffusion is negligible compared with that of turbulent diffusion, and this term can be neglected. Finally, let $S(\mathbf{m}, M, \mathbf{x}, t)$ represent the source term in (A.2).

We now time average (A.2) and use an overbar to denote the average values. Let $C[n, n]$ denote the coagulation term of (A.8). Time averaging gives

$$\frac{\partial \bar{n}}{\partial t} = -\sum_{i=1}^{s-1} \frac{\partial}{\partial m_i}(\bar{I}_i \bar{n} + \overline{I_i' n'} + R_i \bar{n}) - \frac{\partial}{\partial M}\left[\sum_{i=1}^{s}(\bar{I}_i \bar{n} + \overline{I_i' n'} + R_i \bar{n})\right] - \sum_{i=1}^{3} \frac{\partial}{\partial x_i}(\bar{u}_i \bar{n} + \overline{u_i' n'}) + C[\bar{n}, \bar{n}] + \overline{C[n', n']} + \bar{S} + \frac{\partial}{\partial x_3} w_s \bar{n}. \tag{A.10}$$

In general, I_i can be expressed as

$$I_i = k_i(M)(p_i - p_{io}), \tag{A.11}$$

where $k_i(M)$ is a mass transfer coefficient, $p_i = p_i(\mathbf{x}, t)$ is the partial pressure of species i in the bulk fluid, and p_{io} is the partial pressure of i just above the particle surface in equilibrium with that in the droplet.

We will assume that the stochastic coagulation term is small compared to the mean coagulation rate,

$$C[\bar{n}, \bar{n}] \gg \overline{C[n', n']},$$

and that the turbulent species fluxes can be represented by eddy diffusivities,

$$\overline{\frac{\partial}{\partial x_i} u_i' n'} = -K_{ii} \frac{\partial \bar{n}}{\partial x_i}.$$

Seinfeld and Ramabhadran (1975) considered the stochastic condensation term, $\overline{I_i' n'}$, and showed that this term is generally negligible compared with $\bar{I}_i \bar{n}$, and it will henceforth be neglected here.

Using these assumptions in (A.10) gives

$$\frac{\partial \bar{n}}{\partial t} = -\sum_{i=1}^{s-1} \frac{\partial}{\partial m_i}\left[k_i(M)(\bar{p}_i - p_{io})\bar{n} + R_i \bar{n}\right] - \frac{\partial}{\partial M}\left[\sum_{i=1}^{s}\left(k_i(M)(\bar{p}_i - p_{io})\bar{n} + R_i \bar{n}\right)\right] - \sum_{i=1}^{3} \frac{\partial}{\partial x_i}\left(\bar{u}_i \bar{n} - K_{ii}\frac{\partial \bar{n}}{\partial x_i}\right) + C[\bar{n}, \bar{n}] + \bar{S} + \frac{\partial}{\partial x_3} w_s \bar{n}. \tag{A.12}$$

This is the general equation governing the mean aerosol size-composition density function in the atmosphere.

We wish to apply this equation to typical plume geometries. Define the plume cross-sectional averages,

$$\langle \bar{p}_i \rangle = \frac{1}{A} \int\int \bar{p}_i(x_1, x_2, x_3)\, dx_2 dx_3, \qquad (A.13)$$

$$\langle \bar{n} \rangle = \frac{1}{A} \int\int \bar{n}(\mathbf{m}, M, \mathbf{x}, t)\, dx_2 dx_3, \qquad (A.14)$$

where $A = A(x_1)$ is the cross-sectional area of the plume at downwind distance x_1.

We now average (A.12) across the cross-section of the plume. In general, R_i will be independent of $\mathbf{x}$ so

$$\frac{1}{A} \int\int R_i \bar{n}\, dx_2 dx_3 = R_i \langle \bar{n} \rangle. \qquad (A.15)$$

It will be assumed that*

$$\frac{1}{A} \int\int \bar{p}_i \bar{n}\, dx_2 dx_3 = \langle \bar{p}_i \rangle \langle \bar{n} \rangle. \qquad (A.16)$$

Consider next the advection term. Assume that both $\bar{u}_2$ and $\bar{u}_3$ are zero. Further, assume that $\bar{u}_1$ is constant across the plume. The advection term becomes

$$\bar{u}_1 \frac{1}{A} \frac{\partial}{\partial x_1} \int\int \bar{n}\, dx_2 dx_3 = \left(\bar{u}_1 \frac{\partial}{\partial x_1} \langle \bar{n} \rangle \right) + \bar{u}_1 \langle \bar{n} \rangle \frac{1}{A} \frac{dA}{dx_1}. \qquad (A.17)$$

Next, we consider the turbulent diffusion term. It is customary to neglect the x_1-term (the "slender plume approximation"). Choose the region of integration so that the gradients of $\langle \bar{n} \rangle$ vanish at the boundaries. Thus, the entire turbulent diffusion term vanishes from the spatially averaged equation.

For the coagulation term, assume that†

$$\langle C[\bar{n}, \bar{n}] \rangle = C[\langle \bar{n} \rangle, \langle \bar{n} \rangle]. \qquad (A.18)$$

Let $\langle \overline{S} \rangle$ represent the cross sectional average of the source term and neglect the settling term (restricting our analysis to aerosols of dia. 1 μm and smaller.)

We are interested in steady state conditions. However, in the case of a plume, x_1 and "time" are related, so we can define a new "time" variable, $t' = x_1/\bar{u}_1$. Note that t' is the time a parcel of fluid has been in the plume.

Thus, (A.12) becomes for a continuous plume,

$$\frac{\partial \langle \bar{n} \rangle}{\partial t'} = -\sum_{i=1}^{s-1} \frac{\partial}{\partial m_i} \left[k_i(M) \left(\langle \bar{p}_i \rangle - p_{io} \right) \langle \bar{n} \rangle + R_i \langle \bar{n} \rangle \right] - \frac{\partial}{\partial M} \left[\sum_{i=1}^{s} \left\{ k_i(M) \left(\langle \bar{p}_i \rangle - p_{io} \right) \langle \bar{n} \rangle + R_i \langle \bar{n} \rangle \right\} \right] - \langle \bar{n} \rangle \frac{1}{A} \frac{dA}{dt'} + C[\langle \bar{n} \rangle, \langle \bar{n} \rangle] + \langle \overline{S} \rangle. \qquad (A.19)$$

* The error introduced by this assumption can be estimated by assuming Gaussian profiles for both p and n. The fractional error is defined as $\varepsilon = \langle \bar{p}_i \bar{n} \rangle - \langle \bar{p}_i \rangle \langle \bar{n} \rangle / \langle \bar{p}_i \bar{n} \rangle$. If the area A is selected to include 75% of the plume mass, $\varepsilon = 0.13$. If A is chosen to include 80% of the plume mass, $\varepsilon = 0.17$.

† The error introduced by this assumption can be estimated from a typical plume cross-sectional profile for total aerosol number density, $N(\text{cm}^{-3})$. The fractional error is given by $\varepsilon = (\langle N^2 \rangle - \langle N \rangle \langle N \rangle / \langle N^2 \rangle)$. For example, using the distribution from Fig. 19 of Eltgroth and Hobbs (1979), ε was found to be 0.07.

APPENDIX A.2: DERIVATION OF THE SECTIONAL EQUATIONS

The numerical solution of (A.19) poses a difficult problem. If the size spectrum is divided into a set of sections, over each of which the particle composition is assumed to be uniform, then (A.19) can be converted to a set of ordinary differential equations that are easy to solve and implement.

To sectionalize (A.19), multiply (A.19) by m_i and integrate over M from M_{l-1} to M_l and over all $\mathbf{m}$. Let‡

$$Q_{li} = \int_{M_{l-1}}^{M_l} \int_{-\infty}^{\infty} \cdots \int_{-\infty}^{\infty} m_i \langle \bar{n} \rangle\, d\mathbf{m}\, dM, \qquad (A.20)$$

$$Q_l = \int_{M_{l-1}}^{M_l} \int_{-\infty}^{\infty} \cdots \int_{-\infty}^{\infty} M \langle \bar{n} \rangle\, d\mathbf{m}\, dM, \qquad (A.21)$$

$$\langle \overline{S}_{li} \rangle = \int_{M_{l-1}}^{M_l} \int_{-\infty}^{\infty} \cdots \int_{-\infty}^{\infty} m_i \langle \overline{S} \rangle\, d\mathbf{m}\, dM. \qquad (A.22)$$

Consider the first term of (A.19). After multiplying by m_i and integrating, it is of the form

$$\int_{M_{l-1}}^{M_l} \int_{-\infty}^{\infty} \cdots \int_{-\infty}^{\infty} m_i \frac{\partial}{\partial m_j} f_j\, d\mathbf{m}\, dM = \begin{cases} 0 & i \neq j \\ -\int_{M_{l-1}}^{M_l} \int_{-\infty}^{\infty} \cdots \int_{-\infty}^{\infty} f_i\, d\mathbf{m}\, dM & i = j. \end{cases} \qquad (A.23)$$

Similarly, the second summation becomes

$$\int_{-\infty}^{\infty} \cdots \int_{-\infty}^{\infty} m_i \sum_{i=1}^{s} (k_i(M)(\langle \bar{p}_i \rangle - p_{io}) \langle \bar{n} \rangle + R_i \langle \bar{n} \rangle)\, d\mathbf{m} \Big|_{M_{l-1}}^{M_l}. \qquad (A.24)$$

Consider the coagulation term $C[\langle \bar{n} \rangle, \langle \bar{n} \rangle]$,

$$\int_{M_{l-1}}^{M_l} \int_{-\infty}^{\infty} \cdots \int_{-\infty}^{\infty} m_i C[\langle \bar{n} \rangle, \langle \bar{n} \rangle]\, d\mathbf{m}\, dM = \frac{1}{2} \int_{-\infty}^{\infty} \cdots \int_{-\infty}^{\infty} m_i \beta(U, M-U) \langle \bar{n}(\mathbf{m}-\xi, M-U, t') \rangle \times \langle \bar{n}(\xi, U, t') \rangle\, d\xi\, d\mathbf{m}\, dU\, dM + \int_{M_{l-1}}^{M_l} \int_{0}^{\infty} \int_{-\infty}^{\infty} \cdots \int_{-\infty}^{\infty} m_i \beta(U, M) \langle \bar{n}(\xi, U) \rangle \langle \bar{n}(\mathbf{m}, M) \rangle\, d\xi\, d\mathbf{m}\, dU\, dM. \qquad (A.25)$$

In the first integral, change variables. Let $\zeta = \mathbf{m} - \xi$ and $W = M - U$. Introduce the function defined by

$$\theta(\text{condition}) = \begin{cases} 1 & \text{if the condition is true} \\ 0 & \text{otherwise.} \end{cases}$$

With the above substitutions, (A.19) becomes

$$\frac{dQ_{li}}{dt'} = \int_{M_{l-1}}^{M_l} \int_{-\infty}^{\infty} \cdots \int_{-\infty}^{\infty} [k_i(M)(\langle \bar{p}_i \rangle - p_{io}) \langle \bar{n} \rangle + R_i \langle \bar{n} \rangle]\, d\mathbf{m}\, dM - \int_{-\infty}^{\infty} \cdots \int_{-\infty}^{\infty} m_i \sum_{j=1}^{s} [k_j(M) \times (\langle \bar{p}_j \rangle - p_{jo}) \langle \bar{n} \rangle + R_j \langle \bar{n} \rangle]\, d\mathbf{m} \Big|_{M_{l-1}}^{M_l} + \frac{1}{2} \sum_{j=1}^{l} \sum_{k=1}^{l} \int_{M_{j-1}}^{M_j} \int_{M_{k-1}}^{M_k}$$

‡ Notational consistency would dictate that Q_{li} be written as $\langle \overline{Q}_{li} \rangle$, denoting both temporal and spatial averaging. For simplicity, we neglect the overbar and brackets on Q_{li} and Q_l.

$$\times \int_{-\infty}^{\infty} \cdots \int_{-\infty}^{\infty} (\zeta_i + \xi_i)\beta(U, W)\theta$$
$$\times (M_{l-1} < U + W < M_l)$$
$$\cdot \langle \bar{n}(U, \xi, t') \rangle \langle \bar{n}(W, \zeta, t') \rangle \, d\xi \, d\zeta \, dW dU$$
$$- \sum_{j=1}^{\infty} \int_{M_{l-1}}^{M_l} \int_{M_{j-1}}^{M_j} \int_{-\infty}^{\infty} \cdots \int_{-\infty}^{\infty} m_i \beta(U, M)$$
$$\times \langle \bar{n}(\xi, U, t') \rangle \langle \bar{n}(\mathbf{m}, M, t') \rangle \, d\xi \, d\mathbf{m} \, dU \, dM$$
$$- Q_{li} \frac{1}{A} \frac{dA}{dt'} + \langle \overline{S}_{li} \rangle. \qquad \text{(A.26)}$$

In the above equation, the first term on the right represents the total mass of i added to particles within the section by condensation and reaction. The second term represents the change in i due to growth into or out of section l.

In order to put (A.26) into closed form, it is necessary to know the behavior of $\langle \bar{n}(M, m) \rangle$ as a function of M. Unfortunately, the only quantity that is known in a given section is the average value of $\langle \bar{n} \rangle$ in that section. Since particle mass, rather than the number of particles, is conserved, it will be assumed that particle mass, not number, is uniformly distributed. In addition, since experimental data are usually plotted against the logarithm of particle diameter, it will be assumed that particle mass in a section is evenly distributed in terms of the logarithm of diameter. The curve for the actual mass distribution is approximated by a horizontal line, $M(dN/d\log D) = q_l(t)$*, in each section, where $q_l(t)$ is the average mass concentration in the section. In terms of $\langle \bar{n} \rangle$, this becomes

$$M \langle \bar{n}(M, m) \rangle = q_l(t) \frac{d}{dM} \log D. \qquad \text{(A.27)}$$

Using (A.27) in (A.21) gives

$$Q_l(t) = q_l(t) \log \frac{D_l}{D_{l-1}}, \qquad \text{(A.28)}$$

where D_l is the particle diameter corresponding to M_l. Using (A.27) in (A.28) gives

$$\langle \bar{n}(m, M) \rangle = \frac{Q_l}{M^2 \Delta_l}, \qquad \text{(A.29)}$$

where $\Delta_l = \ln \dfrac{M_l}{M_{l-1}}$.

* Througout this paper, $\log D$ is used as a shorthand notation for $\log(D/1\ \mu m)$.

Assuming that the composition of all particles within a section is uniform, we have

$$\int_{M_{l-1}}^{M_l} \int_{-\infty}^{\infty} \cdots \int_{-\infty}^{\infty} k_i(M) p_{io} \langle \bar{n} \rangle \, d\mathbf{m} \, dM = p_{lio}$$
$$\times \int_{M_{l-1}}^{M_l} \int_{-\infty}^{\infty} \cdots \int_{-\infty}^{\infty} k_i(M) \langle \bar{n} \rangle \, d\mathbf{m} \, dM. \qquad \text{(A.30)}$$

where p_{lio} is the value of p_{io} evaluated at the mean particle mass and composition of section l. We express the rate of heterogeneous reaction R_i as $r_{li}M$ in evaluating the second term in the integrand of (A.26).

The second term in (A.26) is to be evaluated between the upper and lower limits of the l-th section. There is some ambiguity about how the values at the limits related to the Q_{li}, which are averages over the entire section. As mentioned previously, this term represents the effect of particles growing into the next larger section. This rate will be determined by the conditions in the section the particles are leaving. Thus, the upper and lower limits of this term will be evaluated using quantities in the l-th and $(l-1)$-th sections, respectively.

With these assumptions, (A.26) becomes

$$\frac{dQ_{li}}{dt'} = [\overline{k}_{li}(\bar{p}_i - p_{lio}) + r_{li}] Q_l$$
$$- \left[\sum_{j=1}^{s} \left(k_{qj}(\langle \bar{p}_i \rangle - p_{lio}) + r_{lj} \Delta_q^{-1} \right) Q_{qi} \right]_{p=l-1}^{p=l}$$
$$+ \frac{1}{2} \sum_{j=1}^{l} \sum_{k=1}^{l} ({}^1\overline{\beta}_{ljk} Q_{ji} Q_k + {}^1\overline{\beta}_{lkj} Q_{ki} Q_j)$$
$$- Q_{li} \sum_{j=1}^{m} {}^2\overline{\beta}_{lj} Q_j - Q_{li} \frac{1}{A} \frac{dA}{dt'} + \langle \overline{S}_{li} \rangle, \qquad \text{(A.31)}$$

where

$$\overline{k}_{li} = \int_{M_{l-1}}^{M_l} \frac{k_i(M)}{M^2 \Delta_l} dM, \qquad \text{(A.32)}$$

$$k_{qj} = \frac{k_j(M_q)}{M \Delta_q}, \qquad \text{(A.33)}$$

$${}^1\overline{\beta}_{ijk} =$$
$$\int_{M_{j-1}}^{M_j} \int_{M_{k-1}}^{M_k} \frac{\beta(U, M)\theta(M_{l-1} < U + M \leq M_l)}{U^2 M \Delta_j \Delta_k} dU \, dM, \qquad \text{(A.34)}$$

$${}^2\overline{\beta}_{lk} = \int_{M_{l-1}}^{M_l} \int_{M_{j-1}}^{M_j} \frac{\beta(U, M)}{U^2 M \Delta_l \Delta_j} dU \, dM. \qquad \text{(A.35)}$$

CHAPTER 7

SUMMARY AND CONCLUSIONS

Summary and Conclusions

A study has been made of atmospheric aerosols. This study has involved modeling both the thermodynamics and kinetics of these aerosols.

In the thermodynamic study, correlations were developed for the chemical potentials present in the sulfate/nitrate/ammonium/water system. The behavior obtained using these correlations was checked against experimental data. The agreement was good. These correlations can easily be extended to deal with more complex systems.

Then, using these correlations, a computer code was written to predict the equilibrium behavior of the system. This code accepts as inputs the total concentrations of sulfate, nitrate and ammonia, as well as the temperature and relative humidity. It then outputs the amount of aerosol present, its composition, and physical state (liquid or solid). This program was tested over a range of conditions, and the results were discussed.

The next step was to extend these results to the case where the effect of particle curvature on vapor pressure, the so-called Kelvin effect, is important. As a result, it was determined that, except for water, the impact of the Kelvin effect on the total composition of the aerosol is negligible. Even in the case of water, for the cases studied, the change in the total amount of water present caused by including the Kelvin effect was less than eight percent. However, the Kelvin effect did alter the composition of the smaller particles relative to the larger ones. Specifically, it tends to shift ammonium and nitrate from the smaller particles to the larger ones. This explains why nitrate tends to be found in larger particles than sulfate (Appel et al., 1978).

The second area covered in this study is aerosol kinetics. First of all, a study was made of the case where coagulation is not important. As a result of this study, it was shown that the evolution of an aerosol distribution can be used to infer the mechanism of sulfate production.

Then, a model was developed for the evolution of aerosol size and chemical composition by coagulation and condensation of one or more gaseous species and by aerosol-phase chemical reaction. This model uses the sectional method. In addition, it also includes simplified thermodynamics.

The most important result of this study was the development of two large computer codes to predict the thermodynamics of the atmospheric sulfate/nitrate/ammonium/water system. These programs have been tested under a wide variety of conditions. They can be incorporated into larger codes simulating the kinetics of the system.

APPENDIX A

ATMOSPHERIC EQUILIBRIUM MODEL OF SULFATE, NITRATE AND AMMONIUM AEROSOLS

PROGRAM USER'S MANUAL

ATMOSPHERIC EQUILIBRIUM MODEL OF SULFATE, NITRATE AND AMMONIUM AEROSOLS

PROGRAM USER'S MANUAL

Mark E. Bassett
Department of Chemical Engineering
California Institute of Technology
Pasadena, California 91125

Prepared for

U.S. Environmental Protection Agency
Research Triangle Park, N.C. 27711

Under

Cooperative Agreement R806844

Kenneth L. Demerjian
Program Director

INTRODUCTION

This report describes a computer program for calculating the equilibrium in a system containing the following components:

liquid phase: NH_4^+, H^+, HSO_4^-, SO_4^{2-}, NO_3^-, H_2O

solid phases: NH_4HSO_4, $(NH_4)_3H(SO_4)_2$, $(NH_4)_2SO_4$
NH_4NO_3, $(NH_4)_2SO_4 \cdot 2NH_4NO_3$
$(NH_4)_2SO_4 \cdot 3NH_4NO_3$

gas phase: NH_3, HNO_3, H_2SO_4, H_2O

This system consists of 13 chemical equilibria involving 17 species (Table 1). Which of the possible equilibria are relevant in a given situation depends on which of the species are present. The specification of the system is completed by four mass balance relations for the total quantities of NH_3, HNO_3, H_2SO_4 and H_2O. The program determines the chemical equilibrium operationally by solving a set of nonlinear algebraic equations. Exactly which equations must be solved is something which must be determined during the course of the calculation.

The quantities determined by the program are the 17 concentrations:

$$n_{H^+,HSO_4^-},\ n_{2H^+,SO_4^{2-}},\ n_{H^+,NO_3^-},\ n_{NH_4^+,HSO_4^-},\ n_{2NH_4^+,SO_4^{2-}},\ n_{NH_4^+,NO_3^-},$$

$$n_{NH_4HSO_4(s)},\ n_{(NH_4)_3H(SO_4)_2(s)},\ n_{(NH_4)_2SO_4(s)},$$

$$n_{NH_4NO_3(s)},\ n_{(NH_4)_2SO_4\cdot 2NH_4NO_3(s)},\ n_{(NH_4)_2SO_4\cdot 3NH_4NO_3(s)},$$

$$n_{H_2O(\ell)},\ n_{NH_3(g)},\ n_{HNO_3(g)},\ n_{H_2SO_4(g)},\ n_{H_2O(g)}$$

where n_i is the concentration of species i in $\mu mol/m^3$ of air. The actual calculation is carried out in terms of the molalities

$$m_i = 10^3 \, n_i/(M_w n_{H_2O(\ell)})$$

where M_w is the molecular weight of water.

DEFINITION OF THE PROBLEM

The basic condition for equilibrium is that the total Gibbs free energy G_T of the system should be a minimum. Thus, the problem is

$$\min_{n_i} G_T \tag{1}$$

subject to: a) conservation of mass

b) $n_i \geq 0$ all i

The problem can be simplified by introducing ξ, the vector of extents of reaction, such that n_i can be expressed as

$$n_i = n_{io} + \sum_j \nu_{ij}\xi_j \tag{2}$$

where n_{io} is the initial value of n_i, and ν is the matrix of stoichiometric coefficients. The use of the extents of reaction automatically satisfies conservation of mass. The reactions are chosen as shown in Table 1. Note that the i-th reaction is associated with the formation of n_i from the gas phase components.

In general, the solution to the minimization problem (1) will lie on one or more of the constraints (b). That is, not all of the possible species will be present. For example, by the Gibbs phase rule, at most two of the six possible solid phases will be present at one time. The criterion for when $n_i = 0$ for some i in the solution is that the change in G_T must be positive whenever n_i is formed. For a species for which n_i is positive,

the change in G_T whenever an infinitesimal amount of n_i is formed must be zero. Thus, the criteria for equilibrium become

$$g_i = 0 \qquad \text{for } n_i > 0 \tag{3}$$

$$g_i \geq 0 \qquad \text{for } n_i = 0 \tag{4}$$

where $g_i = (\partial G_T/\partial \xi_i) = \Sigma\, \nu_{ji}\mu_j$. Thus, it follows that there are two parts to the calculation. First, it must be determined for which species n_i is zero. Then, the system of equations (3) must be solved for the remaining species.

Explicit expressions for the g_i for the system of interest are given in Table 2. Note that for the liquid phase species, g_i depends on the ionic strength I. However, ionic strength is only defined when there is a liquid phase present. This problem is resolved by requiring that there always be a certain minimum amount of water present, chosen small enough not to significantly affect the calculation of the composition of the other phases.

NUMERICAL SOLUTION OF THE EQUILIBRIUM PROBLEM

The equilibrium determination problem is divided into two parts. First, the amount of water in the liquid phase is assumed. An iteration is then performed to find the equilibrium concentrations of all the other species. Since the amount of liquid water present is the natural scale for the problem, considering it as known makes this calculation easier to perform. The water activity obtained is then compared with the relative humidity, and the amount of water present is adjusted accordingly. This second step is the solution of one equation in one variable, for which there are standard routines. A flow diagram for the solution is shown in Figure 1.

Table 1. Chemical Reactions Occurring in the Sulfate/Nitrate/Ammonium System

Reaction	Equilibrium constant expression	Equilibrium constant value
$H_2SO_4(g) \rightleftarrows H^+ + HSO_4^-$	$\frac{\gamma^2_{H^+,HSO_4^-} m_{H^+} m_{HSO_4^-}}{p_{H_2SO_4}}$	$3.038\times10^{17} \exp\left[60.59\left(\frac{T_o}{T}-1\right)+26.1\left(1+\ln\frac{T_o}{T}-\frac{T_o}{T}\right)\right] mol^2kg^{-2}atm^{-1}$
$H_2SO_4(g) \rightleftarrows 2H^+ + SO_4^{2-}$	$\frac{\gamma^3_{2H^+,SO_4^{2-}} m^2_{H^+} m_{SO_4^{2-}}}{p_{H_2SO_4}}$	$3.131\times10^{15} \exp\left[68.18\left(\frac{T_o}{T}-1\right)+44.925\left(1+\ln\frac{T_o}{T}-\frac{T_o}{T}\right)\right] mol^3kg^{-3}\ atm^{-1}$
$HNO_3(g) \rightleftarrows H^+ + NO_3^-$	$\frac{\gamma^2_{H^+,NO_3^-} m_{H^+} m_{NO_3^-}}{p_{HNO_3}}$	$3.638\times10^{6} \exp\left[29.47\left(\frac{T_o}{T}-1\right)+16.835\left(1+\ln\frac{T_o}{T}-\frac{T_o}{T}\right)\right] mol^2kg^{-2}\ atm^{-1}$
$NH_3(g) + H_2SO_4(g) \rightleftarrows NH_4^+ + HSO_4^-$	$\frac{\gamma^2_{NH_4^+,HSO_4^-} m_{NH_4^+} m_{HSO_4^-}}{p_{NH_3} p_{H_2SO_4}}$	$3.339\times10^{28} \exp\left[95.818\left(\frac{T_o}{T}-1\right)+20.77\left(1+\ln\frac{T_o}{T}-\frac{T_o}{T}\right)\right] mol^2kg^{-2}\ atm^{-2}$
$2NH_3(g) + H_2SO_4(g) \rightleftarrows 2NH_4^+ + SO_4^{2-}$	$\frac{\gamma^3_{2NH_4^+,SO_4^{2-}} m^2_{NH_4^+} m_{SO_4^{2-}}}{p^2_{NH_3} p_{H_2SO_4}}$	$3.782\times10^{37} \exp\left[138.636\left(\frac{T_o}{T}-1\right)+34.265\left(1+\ln\frac{T_o}{T}-\frac{T_o}{T}\right)\right] mol^3kg^{-2}\ atm^{-2}$
$NH_3(g) + HNO_3(g) \rightleftarrows NH_4^+ + NO_3^-$	$\frac{\gamma^2_{NH_4^+,NO_3^-} m_{NH_4^+} m_{NO_3^-}}{p_{NH_3} p_{HNO_3}}$	$3.999\times10^{17} \exp\left[64.698\left(\frac{T_o}{T}-1\right)+11.505\left(1+\ln\frac{T_o}{T}-\frac{T_o}{T}\right)\right] mol^2kg^{-2}\ atm^{-2}$
$NH_3(g) + H_2SO_4(g) \rightleftarrows NH_4HSO_4(S)$	$\frac{1}{p_{NH_3} p_{H_2SO_4}}$	$1.975\times10^{26} \exp\left[95.818\left(\frac{T_o}{T}-1\right)-6.22\left(1+\ln\frac{T_o}{T}-\frac{T_o}{T}\right)\right] atm^{-2}$

Table 1. Chemical Reactions Occurring in the Sulfate/Nitrate/Ammonium System (Continued)

Reaction	Equilibrium constant expression	Equilibrium constant value
$2NH_3(g) + 2H_2SO_4(g) \rightleftarrows (NH_4)_3H(SO_4)_2(S)$	$\frac{1}{P_{NH_3}^3 P_{H_2SO_4}^2}$	$3.776\times10^{64} \exp\left[237.084\left(\frac{T_o}{T} - 1\right) - 19.685\left(1 + \ln\frac{T_o}{T} - \frac{T_o}{T}\right)\right] atm^{-5}$
$2NH_3(g) + H_2SO_4(g) \rightleftarrows (NH_4)_2SO(S)$	$\frac{1}{P_{NH_3}^2 P_{H_2SO_4}}$	$4.307\times10^{37} \exp\left[141.266\left(\frac{T_o}{T} - 1\right) - 13.456\left(1 + \ln\frac{T_o}{T} - \frac{T_o}{T}\right)\right] atm^{-3}$
$NH_3(g) + HNO_3(g) \rightleftarrows NH_4NO_3(S)$	$\frac{1}{P_{NH_3} P_{HNO_3}}$	$3.349\times10^{16} \exp\left[75.108\left(\frac{T_o}{T} - 1\right) - 6.06\left(1 + \ln\frac{T_o}{T} - \frac{T_o}{T}\right)\right] atm^{-2}$
$5NH_3(g) + 3HNO_3(g) + H_2SO_4(g) \rightleftarrows (NH_4)_2SO_4 \cdot 3NH_4NO_3(S)$	$\frac{1}{P_{NH_3}^5 P_{HNO_3}^3 P_{H_2SO_4}}$	$9.035\times10^{87} \exp\left[366.59\left(\frac{T_o}{T} - 1\right) - 31.645\left(1 + \ln\frac{T_o}{T} - \frac{T_o}{T}\right)\right] atm^{-9}$
$4NH_3(g) + 2HNO_3(g) + H_2SO_4(g) \rightleftarrows (NH_4)_2SO_4 \cdot 2NH_4NO_3(s)$	$\frac{1}{P_{NH_3}^4 P_{HNO_3}^2 P_{H_2SO_4}}$	$2.209\times10^{71} \exp\left[291.482\left(\frac{T_o}{T} - 1\right) - 25.585\left(1 + \ln\frac{T_o}{T} - \frac{T_o}{T}\right)\right] atm^{-7}$
$H_2O(g) \rightleftarrows H_2O(\ell)$	$\frac{a_w}{\frac{RH}{100}}$	1.

Table 2. Explicit Equilibrium and Mass Balance Relations for the Sulfate/Nitrate/Ammonium System

$$g_1 = \ln m_{H^+} m_{HSO_4^-} + \frac{1}{I}\left[\left(m_{H^+} + m_{HSO_4^-}\right) \ln \gamma^o_{H^+,HSO_4^-} + \frac{9}{4} m_{SO_4^{2-}} \ln \gamma^o_{2H^+,SO_4^{2-}} + m_{NO_3^-} \ln \gamma^o_{H^+,NO_3^-} + m_{NH_4^+} \ln \gamma^o_{NH_4^+,HSO_4^-}\right] - \ln \frac{RTn_{H_2SO_4(g)}}{p^o} - \left[40.255 + 60.59\left(\frac{T_o}{T} - 1\right) + 26.1\left(1 + \ln \frac{T_o}{T} - \frac{T_o}{T}\right)\right]$$

$$g_2 = \ln m^2_{H^+} m_{SO_4^{2-}} + \frac{1}{I}\left[2 m_{HSO_4^-} \ln \gamma^o_{H^+,HSO_4^-} + \frac{9}{4}\left(m_{H^+} + 2 m_{SO_4^{2-}}\right) \ln \gamma^o_{2H^+,SO_4^{2-}} + 2 m_{NO_3^-} \ln \gamma^o_{H^+,NO_3^-} + \frac{9}{4} m_{NH_4^+} \ln \gamma^o_{2NH_4^+,SO_4^{2-}}\right] - \ln \frac{RTn_{H_2SO_4(g)}}{p^o} - \left[35.680 + 68.18\left(\frac{T_o}{T} - 1\right) + 44.925\left(1 + \ln \frac{T_o}{T} - \frac{T_o}{T}\right)\right]$$

$$g_3 = \ln m_{H^+} m_{NO_3^-} + \frac{1}{I}\left[m_{HSO_4^-} \ln \gamma^o_{H^+,HSO_4^-} + \frac{9}{4} m_{SO_4^{2-}} \ln \gamma^o_{2H^+,SO_4^{2-}} + \left(m_{H^+} + m_{NO_3^-}\right) \ln \gamma^o_{H^+,NO_3^-} + m_{NH_4^+} \ln \gamma^o_{NH_4^+,NO_3^-}\right] - \ln \frac{RTn_{HNO_3}}{p^o} - \left[15.107 + 29.47\left(\frac{T_o}{T} - 1\right) + 16.835\left(1 + \ln \frac{T_o}{T} - \frac{T_o}{T}\right)\right]$$

$$g_4 = \ln m_{NH_4^+} m_{HSO_4^-} + \frac{1}{I}\left[\left(m_{NH_4^+} + m_{HSO_4^-}\right) \ln \gamma^o_{NH_4^+,HSO_4^-} + \frac{9}{4} m_{SO_4^{2-}} \ln \gamma^o_{2NH_4^+,SO_4^{2-}}\right.$$

Table 2. Explicit Equilibrium and Mass Balance Relations for the Sulfate/Nitrate/Ammonium System (Continued)

$$g_4 \text{ (Continued)} \quad + m_{NO_3^-} \ln \gamma^o_{NH_4^+,NO_3^-} + m_{H^+} \ln \gamma^o_{H^+,HSO_4^-} \Big] - \ln \frac{R^2T^2 n_{HN_3(g)} n_{H_2SO_4(g)}}{(P^o)^2}$$

$$- \left[65.678 + 95.818\left(\frac{T_o}{T} - 1\right) + 20.77\left(1 + \ln \frac{T_o}{T} - \frac{T_o}{T}\right)\right]$$

$$g_5 = \ln m^2_{NH_4^+} m_{SO_4^{2-}} + \frac{1}{I}\left[2 m_{HSO_4^-} \ln \gamma^o_{NH_4^+,HSO_4^-} + \frac{9}{4}\left(m_{NH_4^+} + 2 m_{SO_4^{2-}}\right) \ln \gamma^o_{2NH_4^+,SO_4^{2-}}\right.$$

$$\left. + 2 m_{NO_3^-} \ln \gamma^o_{NH_4^+,NO_3^-} + \frac{9}{4} m_{H^+} \ln \gamma^o_{2H^+,SO_4^{2-}}\right] - \ln \frac{R^3T^3 n^2_{NH_3(g)} n_{H_2SO_4(g)}}{(P^o)^3}$$

$$- \left[86.526 + 138.636\left(\frac{T_o}{T} - 1\right) + 34.265\left(1 + \ln \frac{T_o}{T} - \frac{T_o}{T}\right)\right]$$

$$g_6 = \ln m_{NH_4^+} m_{NO_3^-} + \frac{1}{I}\left[m_{HSO_4^-} \ln \gamma^o_{NH_4^+,HSO_4^-} + \frac{9}{4} m_{SO_4^{2-}} \ln \gamma^o_{2NH_4^+,SO_4^{2-}}\right.$$

$$\left. + m_{H^+} \ln \gamma^o_{H^+,NO_3^-} + \left(m_{NH_4^+} + m_{NO_3^-}\right) \ln \gamma^o_{NH^+NO_3^-}\right] - \ln \frac{R^2T^2 n_{NH_3(g)} n_{HNO_3(g)}}{(P^o)^2}$$

$$- \left[40.530 + 64.698\left(\frac{T_o}{T} - 1\right) + 11.505\left(1 + n \frac{T_o}{T} - \frac{T_o}{T}\right)\right]$$

$$g_7 = - \ln \frac{R^2T^2 n_{NH_3(g)} n_{H_2SO_4(g)}}{(P^o)^2}$$

$$- 60.548 - 95.818\left(\frac{T_o}{T} - 1\right) + 6.22\left(1 + \ln \frac{T_o}{T} - \frac{T_o}{T}\right)$$

$$g_8 = - \ln \frac{R^5T^5 n^3_{NH_3(g)} n^2_{H_2SO_4(g)}}{(P^o)^5} - 148.694 - 237.084\left(\frac{T_o}{T} - 1\right)$$

$$+ 19.685\left(1 + \ln \frac{T_o}{T} - \frac{T_o}{T}\right)$$

Table 2. Explicit Equilibrium and Mass Balance Relations for the Sulfate/Nitrate/Ammonium System (Continued)

$$g_9 = -\ln \frac{R^3T^3 n^2_{NH_3(g)} n_{H_2SO_4(g)}}{(P^o)^3} - 86.656 - 141.266\left(\frac{T_o}{T} - 1\right)$$

$$+ 13.465\left(1 + \ln\frac{T_o}{T} - \frac{T_o}{T}\right)$$

$$g_{10} = -\ln \frac{R^2T^2 n_{NH_3(g)} n_{HNO_3(g)}}{(P^o)^2} - 38.05 - 75.108\left(\frac{T_o}{T} - 1\right)$$

$$+ 6.06\left(1 + \ln\frac{T_o}{T} - \frac{T_o}{T}\right)$$

$$g_{11} = -\ln \frac{R^9T^9 n^5_{NH_3(g)} n^3_{NHO_3(g)} n_{H_2SO_4(g)}}{(P^o)^9} - 202.526 - 366.59\left(\frac{T_o}{T} - 1\right)$$

$$+ 31.645\left(1 + \ln\frac{T_o}{T} - \frac{T_o}{T}\right)$$

$$g_{12} = -\ln \frac{R^7T^7 n^4_{NH_3(g)} n^2_{H_3NO_3(g)} n_{H_2SO_4(g)}}{(P^o)^7} - 164.276 - 291.482\left(\frac{T_o}{T} - 1\right)$$

$$+ 25.585\left(1 + \ln\frac{T_o}{T} - \frac{T_o}{T}\right)$$

$$g_{13} = \frac{1}{2I^2}\left[m_{H^+} m_{HSO_4^-} \ln a^o_{w\,H^+,HSO_4^-} + 9\left(m_{H^+} - m_{2H^+,SO_4^{2-}}\right) m_{SO_4^{2-}} \ln a^o_{w\,2H^+,SO_4^{2-}}\right.$$

$$\left. + m_{H^+} m_{NO_3^-} \ln a^o_{w\,H^+,NO_3^-} + m_{NH_4^+} m_{HSO_4^-} \ln a^o_{w\,NH_4^+,HSO_4^-}\right.$$

Table 2. Explicit Equilibrium and Mass Balance Relations for the Sulfate/Nitrate/Ammonium System (Continued)

g_{13} (continued)

$$+ 9\left(m_{NH_4^+} - m_{2NH_4^+,SO_4^{2-}}\right) m_{SO_4^{2-}} \ln a^o_{w\,2NH_4^+,SO_4^{2-}} + m_{NH_4^+} m_{NO_3^-} \ln a^o_{w\,NH_4^+,NO_3^-}$$

$$+ \left(m_{H^+} + m_{NH_4^+}\right)\left(m_{H^+,HSO_4} \ln a^o_{w\,H^+,HSO_4^-} + \frac{9}{2} m_{2H^+,SO_4^{2-}} \ln a^o_{w\,2H^+,SO_4^{2-}}\right.$$

$$+ m_{H^+,NO_3^-} \ln a^o_{w\,H^+,NO_3^-} + m_{NH_4^+,HSO_4^-} \ln a^o_{w\,NH_4^+,HSO_4^-} + \frac{9}{2} m_{2NH_4^+,SO_4^{2-}} \ln a^o_{w\,2NH_4^+,SO_4^{2-}}$$

$$\left. + m_{NH_4^+,NO_3^-} \ln a^o_{w\,NH_4^+,NO_3^-}\right)\Bigg] + \frac{M_w m_{SO_4^{2-}}}{10^3 I}\left(3\left(m_{H^+} + m_{NH_4^+}\right) - 2I\right)$$

$$- \ln \frac{RH}{100}$$

$$(n_{NH_3})_T = n_{NH_4^+} + n_{NH_4HSO_4(s)} + 3n_{(NH_4)_3H(SO_4)_2(s)} + 2n_{(NH_4)_2SO_4(s)}$$

$$+ n_{NH_4NO_3(s)} + 5n_{(NH_4)_2SO_4\cdot 3NH_4NO_3} + 4n_{(NH_4)_2SO_4\cdot 2NH_4NO_3} + n_{NH_3(g)}$$

$$(n_{HNO_3})_T = n_{NO_3^-} + n_{NH_4NO_3(s)} + 3n_{(NH_4)_2SO_4\cdot 3NH_4NO_3(s)} + 2n_{(NH_4)_2SO_4\cdot 2NH_4NO_3}$$

$$+ n_{HNO_3(g)}$$

$$(n_{H_2SO_4})_T = n_{HSO_4^-} + n_{SO_4^{2-}} + n_{NH_4HSO_4(s)} + 2n_{(NH_4)_3H(SO_4)_2(s)}$$

$$+ n_{(NH_4)_2SO_4(s)} + n_{(NH_4)_2SO_4\cdot 3NH_4NO_3(s)} + n_{(NH_4)_2SO_4\cdot 2NH_4NO_3(s)}$$

$$(n_{H_2O})_T = n_{H_2O(\ell)} + n_{H_2O(g)}$$

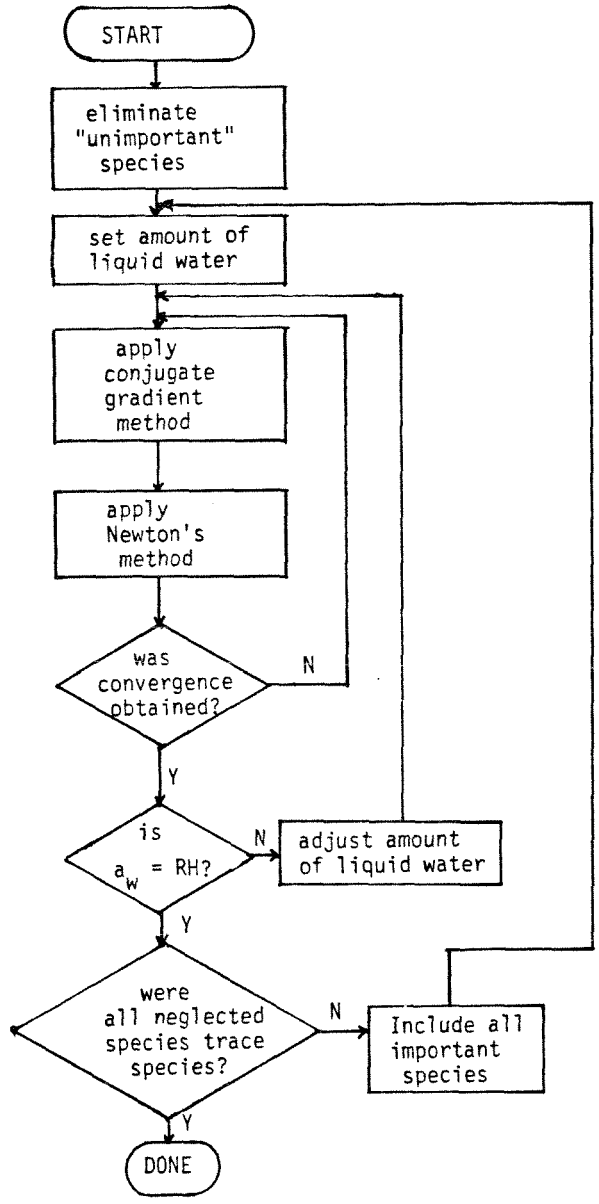

Figure 1. Flow Diagram of Equilibrium Calculation

In the first part of the calculation the equations are solved using a combination of two optimization methods. Initially, the conjugate gradient method is used to minimize the expression for the total Gibbs free energy. This method has the advantage that each step is guaranteed to decrease the total Gibbs free energy of the system, and thus will improve even a poor starting guess. The second method, used when the minimum is approached, is Newton's method.

The conjugate gradient method may be summarized as follows. Let $\underset{\sim}{g} = \nabla G_T$ i.e. $g_j = \sum_i \nu_{ij}\mu_i$. That is, the components of $\underset{\sim}{g}$ are given in Table 2. Let superscripts represent the values obtained at the end of each iteration. Let $H^\circ = I$, the identity matrix. Then, for each step, k, proceed as follows.

1. set $\hat{\underset{\sim}{s}}^k = - H^k \underset{\sim}{g}^k$

2. find α a scalar such that

$$(\hat{\underset{\sim}{s}}^k)^T \underset{\sim}{g}(\underset{\sim}{\xi}^k + \alpha\hat{\underset{\sim}{s}}^k) = 0$$

3. let $\underset{\sim}{s}^k = \alpha\hat{\underset{\sim}{s}}^k$

4. update

$$H^{k+1} = H^k + \frac{\underset{\sim}{s}^k(\underset{\sim}{s}^k)^T}{(\underset{\sim}{s}^k)^T\underset{\sim}{y}} - \frac{(H^k\underset{\sim}{y}^k)(H^k\underset{\sim}{y}^k)^T}{(\underset{\sim}{y}^k)^T H^k\underset{\sim}{y}^k}$$

$$\underset{\sim}{\xi}^{k+1} = \underset{\sim}{\xi}^k + \underset{\sim}{s}^k$$

where

$$\underset{\sim}{y}^k = \underset{\sim}{g}^{k+1} - \underset{\sim}{g}^k$$

This procedure is repeated for k = 0,... 12, and then restarted using $H^\circ = I$. However, in practice, before k reaches 12, the method will have converged sufficiently to allow the second method to be used.

At each step, the quantity $\underset{\sim}{g}^T\underset{\sim}{s}$ is checked to make sure that it is negative, i.e. that the step is headed downhill. If it is not, the method is restarted from k = 0.

Step 2 requires further explanation. This requires finding α such that $\underset{\sim}{g}$ is orthogonal to $\hat{\underset{\sim}{s}}^k$ at $\underset{\sim}{\xi}^k + \alpha\hat{\underset{\sim}{s}}^k$. This is done as follows. First, find α_M, the largest number such that $\underset{\sim}{\xi}^k + \alpha\hat{\underset{\sim}{s}}^k$ is still in the feasible region. Define

$$f(\alpha) = (\hat{\underset{\sim}{s}}^k)^T \underset{\sim}{g}(\underset{\sim}{\xi}^k + \alpha\hat{\underset{\sim}{s}}^k)$$

Compute $f(\alpha_M)$. If $f(\alpha_M) < 0$, the algorithm is trying to leave the feasible region, so use $\alpha = \alpha_M$. If $f(\alpha_M) > 0$, then it is known that $f(0) < 0$ by construction, and $f(\alpha_M) > 0$. Thus two values which bracket the root are known. There are standard routines to find the zero of f in this case

Occasionally, it will occur that $\alpha_M = 0$. This usually means that a species has been included in the calculation which should not have been. That is, a species which should actually be handled by (4) had been treated by (3). Thus, this reaction must be removed from the set of reactions which are being treated by (3).

The procedure for eliminating reactions is as follows. First, the reactions which are trying to consume n_i are found. These are the reactions for which $\sum_j \nu_{ij} s_j$ is negative. If there is only one such reaction, a flag is set signifying that this reaction is no longer to be included in the calculation. Then, a new value of α_M is calculated and the calculation proceeds as before.

Suppose there are several reactions which consume n_i. Then, the one which benefits least from consuming n_i is found. That is, j is found such that g_j/ν_{ij} is a minimum. This reaction is then forced to run in reverse to provide n_i to the other reactions. Mathematically, this is done by performing Gaussian elimination on ν so that $\nu_{ik} = 0$ for $k \neq j$. In addition, the same operations are performed on $\underset{\sim}{s}$ and on the rows and columns of H. Then, the inverse elimination is performed on $\underset{\sim}{\xi}$. After this, a flag is set signifying that the jth reaction has been dropped. Finally α_M is recalculated, and the calculation proceeds as before.

When reactions are dropped as above, some provision must be made to check when they should be reinstated. This is done as follows. Every time the conjugate gradient method is restarted, or convergence is suspected, all dropped reactions are reinstated. If the excluded reactions were the proper ones, all of the reinstated reactions will immediately be dropped again.

The second method used is Newton's method. Near the solution, this method will converse in fewer functional evaluations than the conjugate gradient method. However, far from the correct answer, there is no guarantee that each step will be better than the last one. This is especially true if incorrect species have been included in the calculation.

The evaluation of F, the Jacobian of G, is done numerically, using finite differences to approximate derivatives. However, care must be taken that the number of reactions included does not exceed the number permitted by the Gibbs phase rule. If it does, all of the reactions will not be linearly independent. In this case F will be singular.

There are two situations when the phase rule can be violated. The first results from including too many reactions involving the liquid phase. Consider the system with no solid phases present. There are five basic species present-H^+, NH_3, SO_4^{2-}, NO_3^-, H_2O. In addition, there is one restriction, electroneutrality. Fixing T and P leaves only four degrees of freedom. This may be understood by noting that an equimolar mixture of H^+, NH_4^+, HSO_4^-, and NO_3^- may be considered as

$$\underset{1}{H^+}\ \underset{}{HSO_4}\ \ \underset{6}{NH_4^+}\ NO_3^- \quad \text{or} \quad \underset{3}{H^+}\ NO_3^-\ \ \underset{4}{NH_4^+}\ HSO_4^-$$

Thus,

$$\mu_1 + \mu_6 = \mu_3 + \mu_4$$

Similarly,

$$\mu_2 + 2\mu_6 = \mu_5 + 2\mu_3$$

A second way that the Gibbs phase rule can be violated is by the existence of too many solid phases. For example, there are six possible solid phases involving only three species.

A third possible problem is that the Jacobian can be ill-conditioned. In this case, even though the problem itself is well posed, roundoff error can cause the Jacobian to become singular. As an example of this behavior, consider the hypothetical system

$$A_{(g)} + B_{(g)} \rightleftarrows C_{(s)}$$

$$2A_{(g)} + B_{(g)} \rightleftarrows D_{(s)}$$

Let $[A] = 10^{-3}$, $[B] = 1$. Then, the Jacobian becomes

$$F = \frac{1}{RT}\begin{bmatrix} \frac{1}{[A]} + \frac{1}{[B]} & \frac{2}{[A]} + \frac{1}{[B]} \\ \frac{2}{[A]} + \frac{1}{[B]} & \frac{4}{[A]} + \frac{1}{[B]} \end{bmatrix} = \frac{1}{RT}\begin{bmatrix} 1001 & 2001 \\ 2001 & 4001 \end{bmatrix}$$

If only three significant figures are returned

$$F = \frac{10^3}{RT}\begin{bmatrix} 1 & 2 \\ 2 & 4 \end{bmatrix}$$

which is singular.

Note that the problem arises because the chemical potential of A varies more rapidly than that for B as the compositions are changed. Thus, the term relating to the chemical potential of A masked the term relating to the chemical potential of B. This can be overcome by rewriting the equations

$$A_{(g)} + B_{(g)} \rightleftarrows C_{(s)}$$

$$D_{(s)} + B_{(g)} \rightleftarrows 2C_{(s)}$$

All three of these problems, ill-conditioned Jacobians, and two violations of the phase rule are dealt with by the following method. First of all, A is found such that

$$A^T = B\nu$$

$$B = \begin{bmatrix} \tilde{B} & 0 \\ 0 & I \end{bmatrix}$$

$$\tilde{B} = \begin{bmatrix} 1 & 2 & 1 & 0 & 0 & 0 \\ 0 & 0 & 0 & 1 & 2 & 1 \\ 1 & 0 & 0 & 1 & 0 & 0 \\ 0 & 1 & 0 & 0 & 1 & 0 \\ 0 & 0 & 1 & 0 & 0 & 1 \end{bmatrix}$$

The ultimate goal is to separate as much as possible species where $\partial\mu_i/\partial n_i$ is large from those where it is not. In order to do this, it is first necessary to determine for which species $\partial\mu_i/\partial n_i$ is large. That is, the species will be ordered in terms of $(\partial\mu_i/\partial n_i)$. First of all, for solids, $(\partial\mu_i/\partial n_i) = 0$. Thus, these species go to the back of the list. Since the ordering need only be approximate, it will be assumed that for gases and liquids $(\partial\mu_i/\partial n_i) = RT/n_i$, the value for gases. Thus, gaseous and aqueous species will be ranked in order of increasing n_i.

The next step is to do the actual rewriting of the equations. This is done as follows. First, take the first species in the order described above. Then, a reaction containing that species is selected. If there is no such reaction which has not been selected in an earlier step, the procedure is started over using the next species on the list. If there is such a reaction Gaussian elimination is used on the rows of A until there is only one reaction involving that species. This procedure is then followed for each species in order until only solid species remain.

Consider the resulting situation. By construction, each of the reactions which have been selected contain a species present in no other reaction. Thus, the Jacobian of the system containing these reactions will be non-singular. By construction, the remaining reactions contain no species which are composition dependent. These reactions are then allowed to run to completion. They are then eliminated as described in the section on the conjugate gradient method.

PROGRAM USE

The program is called as follows:

CALL EQUIL (W, RH, T, CONC, IFLAG)

Where W, RH, T and IFLAG are the inputs and CONC is the output. The various input and output variables are defined in Table 3.

SAMPLE CALCULATION

Consider the following sample problem which is Case 6 of Bassett and Seinfeld (1983).

$T = 25°C$

$RH = 50\%$

$([NH_3]_T)_o = 5\ \mu g/m^3$ $\qquad R_{NH_3} = 0$

$([HNO_3]_T)_o = 0$ $\qquad R_{HNO_3} = 20\ \mu g/m^3\ hr$

$([H_2SO_4]_T)_o = 0$ $\qquad R_{H_2SO_4} = 30\ \mu g/m^3\ hr$

$0 < t < 1\ hr$

where R_{NH_3}, R_{HNO_3} and $R_{H_2SO_4}$ are the rates at which the corresponding species are introduced.

The program to solve this problem is as follows

```
      IMPLICIT DOUBLE PRECISION (A-H, O-Z)
      DIMENSION PLT(61 ,16), W(3), CONC(15)
C     PLT is the array used to store the results of the calculation
C
C     W, CONC are the arguments for the subroutine
      DO 2  I = 2,61
C     each time through this loop advances the
C       solution one time step
      TIME = (I-1)/60.
C     TIME is the time in hours
        T = 298.15
        RH = 0.500
        W(1) = 5.00
        W(2) = 20.00*TIME
        W(3) = 30.00*TIME
```

Table 3. Subroutine Arguments

Input Variables

Name	Type	Description
W	Double Precision array W(3)	Total mass concentrations of the various constituents $\mu g/m^3$ W(1) total NH_3 W(2) total HNO_3 W(3) total H_2SO_4
RH	Double Precision scalar	Relative humidity fraction $0 \leq RH \leq 1.$
T	Double Precision scalar	temperature °K
IFLAG	Integer scalar	Flag IFLAG ≠ 0 use results of last step as starting value for this step IFLAG = 0 generate a new starting value for this step

Output Variables

Name	Type	Description
CONC	Double Precision array CONC(15)	Mass concentrations of the species at equilibrium $\mu g/m^3$
		CONC(1) H^+
		CONC(2) NH_4^+
		CONC(3) HSO_4^-
		CONC(4) SO_4^{2-}
		CONC(5) NO_3^-
		CONC(6) $(NH_4)_2H(SO_4)_2(s)$
		CONC(7) $NH_4HSO_4(s)$
		CONC(8) $(NH_4)_2SO_4(s)$
		CONC(9) $NH_4NO_3(s)$
		CONC(10) $(NH_4)_2SO_4 \cdot 3NH_4NO_3(s)$
		CONC(11) $(NH_4)_2SO_4 \cdot 2NH_4NO_3(s)$
		CONC(12) $H_2O(\ell)$
		CONC(13) $NH_3(g)$
		CONC(14) $HNO_3(g)$
		CONC(15) $H_2SO_4(g)$

```
C     Calculate the inputs to the program
      CALL EQUIL (W,RH,T,CONC, ISTART)
C     call the equilibrium routine
      ISTART=1
C     Set ISTART ≠ 0
C     Thus, the first time through, the program
C     will generate a starting guess.  After
C     this, it will use the results of
C     the last step as the starting value
C     for the next step

      PLOT (I,1) = 60. *TIME
      DO 2 J-2,16
2     PLOT(I,J) = CONC(J-1)
C     Store the results in the array PLT for
C     later output
C     OUTPUT THE RESULTS
      WRITE (96,900)
900   FORMAT (58X,'Test case'//T44,'Concentrations ( 1.D-6 g/',
     A      'm**3 of air)'/'  time',T13,'H+',T20,'NH4+',T27,
     B      'HSO4-',T35,'SO4-2',T44,'NO3-',T49,'(NH4)3H(SO4)2',
     C      T64,'(NH4)2SO4',T74,'NH4NO3',
     D      2(' (NH4)2SO4'),1X,'H2O(l)',1X,'NH3(g)',1X,
     E      'HNO3(g)',T123,'H2SO4(g)'/'(min)',T58,'NH4HSO4',T81,
     F      '*3NH4NO3',1X,' *2NH4NO3'/1X,132('-'))
      WRITE (96,901) ((PLT(II,JJ),JJ=I,16),II=1,61
901   FORMAT(16F8.4)
      STOP
      END
```

The output from this program is shown in Table 3.

INTERFACE WITH A CELL MODEL

The equilibrium model described here interfaces with a cell model as follows. At the start of each step, the total amounts of NH_3, HNO_3 and H_2SO_4 are known from the results of the last step. In addition, the temperature and relative humidity are assumed known from meteorological data. Using these as inputs, the equilibrium program can then be used to calculate the resulting concentration of aerosol, its composition, and physical state. These can then, in turn, be used to calculate various rate constants, such as rates of dry deposition. Knowing these, the cell model can then be used to integrate the system, to find the total amounts of the various species present at the end of the time step.

Table 4. Output From Sample Program

Concentrations (1.D-6 g/m**3 of air)

time (min)	H+	NH4+	HSO4-	SO4-2	NO3-	(NH4)HSO4(s)	NH4HSO4	(NH4)2SO4	NH4NO3	(NH4)2SO4 *1NH4NO3	(NH4)2SO4 *2NH4NO3	H2O(l)	NH3(g)	HNO3(g)	H2SO4(g)
0.0000	0.0000	0.0000	0.0000	0.0000	0.0000	0.0000	0.0000	0.0000	0.0000	0.0000	0.0000	0.0000	5.0000	0.0000	0.0000
1.0000	0.0000	0.0000	0.0000	0.0000	0.0000	0.0000	0.0000	0.6738	0.0000	0.0000	0.0000	0.0000	4.8263	0.3333	0.0000
2.0000	0.0000	0.0000	0.0000	0.0000	0.0000	0.0000	0.0000	1.3475	0.0000	0.0000	0.0000	0.0000	4.6526	0.6667	0.0000
3.0000	0.0000	0.0000	0.0000	0.0000	0.0000	0.0000	0.0000	2.0212	0.0000	0.0000	0.0000	0.0000	4.4790	1.0000	0.0000
4.0000	0.0000	0.0000	0.0000	0.0000	0.0000	0.0000	0.0000	2.6948	0.0000	0.0000	0.0000	0.0000	4.3053	1.3333	0.0000
5.0000	0.0000	0.0000	0.0000	0.0000	0.0000	0.0000	0.0000	3.3685	0.0000	0.0000	0.0000	0.0000	4.1317	1.6667	0.0000
6.0000	0.0000	0.0000	0.0000	0.0000	0.0000	0.0000	0.0000	4.0422	0.0000	0.0000	0.0000	0.0000	3.9580	2.0000	0.0000
7.0000	0.0000	0.0000	0.0000	0.0000	0.0000	0.0000	0.0000	4.7159	0.0000	0.0000	0.0000	0.0000	3.7844	2.3333	0.0000
8.0000	0.0000	0.0000	0.0000	0.0000	0.0000	0.0000	0.0000	5.3895	0.0000	0.0000	0.0000	0.0000	3.6107	2.6667	0.0000
9.0000	0.0000	0.0000	0.0000	0.0000	0.0000	0.0000	0.0000	6.0632	0.0000	0.0000	0.0000	0.0000	3.4370	3.0000	0.0000
10.0000	0.0000	0.0000	0.0000	0.0000	0.0000	0.0000	0.0000	6.7369	0.0000	0.0000	0.0000	0.0000	3.2634	3.3333	0.0000
11.0000	0.0000	0.0000	0.0000	0.0000	0.0000	0.0000	0.0000	7.4106	0.0000	0.0000	0.0000	0.0000	3.0897	3.6667	0.0000
12.0000	0.0000	0.0000	0.0000	0.0000	0.0000	0.0000	0.0000	8.0842	0.0000	0.0000	0.0000	0.0000	2.9161	4.0000	0.0000
13.0000	0.0000	0.0000	0.0000	0.0000	0.0000	0.0000	0.0000	8.7579	0.0000	0.0000	0.0000	0.0000	2.7424	4.3333	0.0000
14.0000	0.0000	0.0000	0.0000	0.0000	0.0000	0.0000	0.0000	9.4316	0.0000	0.0000	0.0000	0.0000	2.5687	4.6667	0.0000
15.0000	0.0000	0.0000	0.0000	0.0000	0.0000	0.0000	0.0000	10.1053	0.0000	0.0000	0.0000	0.0000	2.3951	5.0000	0.0000
16.0000	0.0000	0.0000	0.0000	0.0000	0.0000	0.0000	0.0000	10.7790	0.0000	0.0000	0.0000	0.0000	2.2214	5.3333	0.0000
17.0000	0.0000	0.0000	0.0000	0.0000	0.0000	0.0000	0.0000	11.4526	0.0000	0.0000	0.0000	0.0000	2.0478	5.6667	0.0000
18.0000	0.0000	0.0000	0.0000	0.0000	0.0000	0.0000	0.0000	12.1263	0.0000	0.0000	0.0000	0.0000	1.8741	6.0000	0.0000
19.0000	0.0000	0.0000	0.0000	0.0000	0.0000	0.0000	0.0000	12.8000	0.0000	0.0000	0.0000	0.0000	1.7005	6.3333	0.0000
20.0000	0.0000	0.0000	0.0000	0.0000	0.0000	0.0000	0.0000	13.4737	0.0000	0.0000	0.0000	0.0000	1.5268	6.6667	0.0000
21.0000	0.0000	0.0000	0.0000	0.0000	0.0000	0.0000	0.0000	14.1473	0.0000	0.0000	0.0000	0.0000	1.3531	7.0000	0.0000
22.0000	0.0000	0.0000	0.0000	0.0000	0.0000	0.0000	0.0000	14.8210	0.0000	0.0000	0.0000	0.0000	1.1794	7.3333	0.0000
23.0000	0.0000	0.0000	0.0000	0.0000	0.0000	0.0000	0.0000	15.4947	0.0000	0.0000	0.0000	0.0000	1.0058	7.6667	0.0000
24.0000	0.0000	0.0000	0.0000	0.0000	0.0000	0.0000	0.0000	16.1684	0.0000	0.0000	0.0000	0.0000	0.8322	8.0000	0.0000
25.0000	0.0000	0.0000	0.0000	0.0000	0.0000	0.0000	0.0000	16.8420	0.0000	0.0000	0.0000	0.0000	0.6585	8.3333	0.0000
26.0000	0.0000	0.0000	0.0000	0.0000	0.0000	0.0000	0.0000	17.5157	0.0000	0.0000	0.0000	0.0000	0.4848	8.6667	0.0000
27.0000	0.0000	0.0000	0.0000	0.0000	0.0000	0.0000	0.0000	18.1894	0.0000	0.0000	0.0000	0.0000	0.3112	9.0000	0.0000
28.0000	0.0000	0.0000	0.0000	0.0000	0.0000	0.0000	0.0000	18.8631	0.0000	0.0000	0.0000	0.0000	0.1375	9.3333	0.0000
29.0000	0.0000	0.0000	0.0000	0.0000	0.0000	0.7297	0.0000	18.7566	0.0000	0.0000	0.0000	0.0000	0.0142	9.6667	0.0000
30.0000	0.0000	0.0000	0.0000	0.0000	0.0000	3.2508	0.0000	16.7356	0.0000	0.0000	0.0000	0.0000	0.0142	10.0000	0.0000
31.0000	0.0000	0.0000	0.0000	0.0000	0.0000	5.7718	0.0000	14.7146	0.0000	0.0000	0.0000	0.0000	0.0142	10.3333	0.0000
32.0000	0.0000	0.0000	0.0000	0.0000	0.0000	8.2929	0.0000	12.6935	0.0000	0.0000	0.0000	0.0000	0.0142	10.6667	0.0000
33.0000	0.0000	0.0000	0.0000	0.0000	0.0000	10.8139	0.0000	10.6725	0.0000	0.0000	0.0000	0.0000	0.0142	11.0000	0.0000
34.0000	0.0000	0.0000	0.0000	0.0000	0.0000	13.3350	0.0000	8.6515	0.0000	0.0000	0.0000	0.0000	0.0142	11.3333	0.0000
35.0000	0.0000	0.0000	0.0000	0.0000	0.0000	15.8560	0.0000	6.6304	0.0000	0.0000	0.0000	0.0000	0.0142	11.6667	0.0000
36.0000	0.0000	0.0000	0.0000	0.0000	0.0000	18.3771	0.0000	4.6094	0.0000	0.0000	0.0000	0.0000	0.0142	12.0000	0.0000
37.0000	0.0000	0.0000	0.0000	0.0000	0.0000	20.8981	0.0000	2.5884	0.0000	0.0000	0.0000	0.0000	0.0142	12.3333	0.0000
38.0000	0.0000	0.0000	0.0000	0.0000	0.0000	23.4192	0.0000	0.5674	0.0000	0.0000	0.0000	0.0000	0.0142	12.6667	0.0000
39.0000	0.0000	0.1796	0.9731	0.0731	0.0000	23.7748	0.0000	0.0000	0.0000	0.0000	0.0000	0.0000	0.4710	0.0022	13.0000	0.0000
40.0000	0.0001	0.4739	2.4251	0.6610	0.0000	22.0305	0.0000	0.0000	0.0000	0.0000	0.0000	0.0000	1.2424	0.0022	13.3333	0.0000
41.0000	0.0001	0.7681	3.9472	0.0989	0.0000	20.6861	0.0000	0.0000	0.0000	0.0000	0.0000	0.0000	2.0139	0.0022	13.6667	0.0000
42.0000	0.0002	1.0623	5.4592	0.1961	0.0000	19.3420	0.0000	0.0000	0.0000	0.0000	0.0000	0.0000	2.7854	0.0022	14.0000	0.0000
43.0000	0.0002	1.3566	6.9712	0.1746	0.0000	17.9978	0.0000	0.0000	0.0000	0.0000	0.0000	0.0000	3.5568	0.0022	14.3333	0.0000
44.0000	0.0003	1.6508	8.4832	0.2125	0.0000	16.6535	0.0000	0.0000	0.0000	0.0000	0.0000	0.0000	4.3283	0.0022	14.6667	0.0000
45.0000	0.0004	1.9451	9.9953	0.2503	0.0000	15.3092	0.0000	0.0000	0.0000	0.0000	0.0000	0.0000	5.0997	0.0022	15.0000	0.0000
46.0000	0.0004	2.2393	11.5073	0.2882	0.0000	13.9650	0.0000	0.0000	0.0000	0.0000	0.0000	0.0000	5.8712	0.0022	15.3333	0.0000
47.0000	0.0005	2.5335	13.0193	0.3261	0.0000	12.6208	0.0000	0.0000	0.0000	0.0000	0.0000	0.0000	6.6427	0.0022	15.6667	0.0000
48.0000	0.0005	2.8278	14.5313	0.3639	0.0000	11.2765	0.0000	0.0000	0.0000	0.0000	0.0000	0.0000	7.4141	0.0022	16.0000	0.0000
49.0000	0.0006	3.1220	16.0434	0.4018	0.0000	9.9323	0.0000	0.0000	0.0000	0.0000	0.0000	0.0000	8.1856	0.0022	16.3333	0.0000
50.0000	0.0007	3.4162	17.5554	0.4397	0.0000	8.5880	0.0000	0.0000	0.0000	0.0000	0.0000	0.0000	8.9570	0.0022	16.6667	0.0000
51.0000	0.0007	3.7105	19.0674	0.4776	0.0000	7.7438	0.0000	0.0000	0.0000	0.0000	0.0000	0.0000	9.7285	0.0022	17.0000	0.0000
52.0000	0.0008	4.0047	20.5794	0.5154	0.0000	5.8995	0.0000	0.0000	0.0000	0.0000	0.0000	10.5000	0.0022	17.3333	0.0000
53.0000	0.0008	4.2989	22.0915	0.5533	0.0000	4.0553	0.0000	0.0000	0.0000	0.0000	0.0000	11.2714	0.0022	17.6667	0.0000
54.0000	0.0009	4.5932	23.6035	0.5912	0.0000	2.2110	0.0000	0.0000	0.0000	0.0000	0.0000	12.0429	0.0022	18.0000	0.0000
55.0000	0.0009	4.8874	25.1155	0.6290	0.0000	0.3668	0.0000	0.0000	0.0000	0.0000	0.0000	12.8144	0.0022	18.3333	0.0000
56.0000	0.0010	5.1817	26.6276	0.6669	0.0000	0.5225	0.0000	0.0000	0.0000	0.0000	0.0000	13.5859	0.0022	18.6666	0.0000
57.0000	0.0010	5.2760	27.7709	0.6911	0.0000	0.0000	0.0000	0.0000	0.0000	0.0000	0.0000	14.1064	0.0013	19.0000	0.0000
58.0000	0.0010	5.2960	28.5197	0.7097	0.0000	0.0000	0.0000	0.0000	0.0000	0.0000	0.0000	14.7497	0.0005	19.3333	0.0000
59.0000	0.0010	5.2960	29.0817	0.7237	0.0000	0.0000	0.0000	0.0000	0.0000	0.0000	0.0000	15.7074	0.0003	19.6667	0.0000
60.0000	0.0010	5.2960	29.5026	0.7342	0.0000	0.0000	0.0000	0.0000	0.0000	0.0000	0.0000	16.7214	0.0002	20.0000	0.0000

References

Bassett, M. E. and Seinfeld, J. H. (1983) Atmospheric equilibrium model of sulfate and nitrate aerosols. Submitted to Atmospheric Environment.

APPENDIX B

ATMOSPHERIC EQUILIBRIUM MODEL OF SULFATE AND NITRATE AEROSOLS II. PARTICLE SIZE ANALYSIS

PROGRAM USER'S MANUAL

Introduction

This report describes a computer program for calculating the equilibrium in a system containing the following components

liquid phase: NH_4^+, H^+, HSO_4^-, SO_4^{2-}, NO_3^-, H_2O

solid phases: NH_4HSO_4, $(NH_4)_3H(SO_4)_2$
NH_4NO_3, $(NH_4)_2SO_4$, $(NH_4)_2SO_4 \cdot 2NH_4NO_3$
$(NH_4)_2SO_4 \cdot 3NH_4NO_3$

gas phase: NH_3, HNO_3, H_2O

This calculation takes into account the effect of surface curvature on the particles, the so-called Kelvin effect. The strength of the effect depends on the radius of the particles. Thus, it is necessary to take into account the particle size distribution. This is done using the sectional method. In this method, all particles whose diameters lie in a given range are assumed to have the same equilibrium properties. These ranges of particle sizes are referred to as sections. Since the chemical potential depends on particle diameter, the same species in two different sections must be treated as if it were two different species. Thus, for example, $NH_4NO_3(s)$ in section ℓ must be treated as being different from $NH_4NO_3(s)$ in section m. Thus, the system contains $10\,N_s$ equilibria involving $12\,N_s+3$ different species, where N_s is the number of sections used. Which of the possible equilibria are relevant in a given situation depends on which of the species are present. In each section, there will be the electroneutrality condition, and, since H_2SO_4 is assumed to be non-volatile, a mass balance on sulfate. In addition, there will be three mass balance relations for the total quantities of NH_3, HNO_3, and H_2O in the system.

The program determines the chemical equilibrium operationally by solving a set of nonlinear algebraic equations. Exactly which equations must be solved is something which must be determined during the course of the calculation.

The quantities determined by the program are the $12N_s+3$ concentrations

$$n^{\ell}_{H^+},\ n^{\ell}_{NH_4^+},\ n^{\ell}_{HSO_4^-},\ n^{\ell}_{SO_4^{2-}},\ n^{\ell}_{NO_3^-},$$

$$n^{\ell}_{NH_4HSO_4(s)},\ n^{\ell}_{(NH_4)_3H(SO_4)_2(s)},\ n^{\ell}_{(NH_4)_2SO_4(s)},$$

$$n^{\ell}_{NH_4NO_3(s)},\ n^{\ell}_{(NH_4)_2SO_4\cdot 2NH_4NO_3(s)},\ n^{\ell}_{(NH_4)_2SO_4\cdot 3NH_4NO_3(s)}$$

$$n^{\ell}_{H_2O(\ell)} \qquad n_{NH_3(g)} \qquad n_{HNO_3(g)} \qquad n_{H_2O(g)}$$

where n_i^{ℓ} is the concentration of species i in particles having diameters d between $d_{\ell-1}$ and d_{ℓ} in $\mu mol/m^3$ of air. The actual calculation is carried out in terms of the molalities

$$m_i^{\ell} = 10^3\ n_i^{\ell}/(M_w\ n^{\ell}_{H_2O(\ell)})$$

where M_w is the molecular weight of water.

Definition of the Problem

The condition for chemical equilibrium in a closed system at constant T and p is that the total Gibbs free energy of the system G be a minimum. Thus, the problem is

$$\min_{n_i^{\ell}} G(T,p,n_i^{\ell})$$

subject to $n_i^{\ell} \geq 0$ and conservation of mass.

One problem with the above formulation is that the constraints arising from conservation of mass will prove awkward to handle computationally. This problem can be circumvented as follows. As mentioned before, the chemical potential of a given species will depend on the diameter of the particle in which the species is present. Thus, for example, for $NH_4NO_3(s)$, there will be a series of equilibria of the form

$$NH_3(g) + HNO_3(g) \rightleftarrows NH_4NO_3(s, \text{ in section } \ell)$$

Assume that the reaction involving $NH_3(g)$, $HNO_3(g)$ and $NH_4NO_3(s)$ is reaction j. Then, let ξ_j^ℓ be the amount of $NH_4NO_3(s)$ formed in section ℓ above that present at some arbitrary initial time, $n_{i,0}^\ell$. Then, the minimization becomes

$$\min_{\xi_j^\ell} G$$

subject to

$$n_i^\ell = n_{i,0}^\ell + \sum_j \nu_{ij}\xi_j^\ell \geq 0 \qquad (1)$$

where ν is the matrix of stoichiometric coefficients.

In general, not all of the species will be present at equilibrium. For example, by the Gibbs phase rule, at most two of the six possible solid phases will be present at one time. The criterion for when $n_i^\ell = 0$ for some i and ℓ at equilibrium is that the change in G must be positive whenever an infinitesimal amount of n_i^ℓ is formed. For a species which is present at equilibrium, the change in G whenever an infinitesimal amount of n_i^ℓ is formed must be zero. Thus, the criteria for equilibrium are

$$g_i^\ell = 0 \text{ for } n_i^\ell > 0 \tag{2}$$

$$g_i^\ell \geq 0 \text{ for } n_i^\ell = 0 \tag{3}$$

where $g_i^\ell = (\partial G/\partial \xi_k^\ell) = \sum_j \nu_{jk}\mu_k^\ell$ where the k-th reaction involves the formation of species i. Thus, there are two parts to the calculation. First, it must be determined for which species n_i^ℓ is zero. Then, the system of equations (2) must be solved for the remaining species.

Evaluation of Chemical Potentials

Values for the bulk phase chemical potentials have been given previously (Bassett and Seinfeld, 1983) and will not be repeated here. The effect of surface curvature on the chemical potential is estimated as follows. First, assume that all particles in section ℓ behave as if they had a diameter $\bar{d}_\ell = (d_{\ell-1}d_\ell)^{\frac{1}{2}}$ where $d_{\ell-1}$ and d_ℓ are the lower and upper limits of the ℓ-th section, respectively. Then, by the Gibbs-Thompson equation

$$\mu_i^\ell - \mu_i = \frac{4\sigma\bar{v}_i}{\bar{d}_\ell} \tag{4}$$

where μ_i is the bulk phase chemical potential of species i, σ is the surface tension, and $\bar{v}_i$ is the molal volume of species i.

Currently, there does not appear to be a good way available to calculate σ for aqueous mixtures. Thus, the value for pure water will be used. As a result of this approximation, it is not worthwhile to develop complex methods for computing $\bar{v}_i$. Instead, it will be approximated assuming that the density of the particle is that of pure water, ρ_w. Then,

$$\bar{v}_i = \frac{M_i}{\rho_w} \tag{5}$$

where M_i is the molecular weight of species i.

Finally, note that evaluation of the liquid phase chemical potentials requires knowledge of the liquid phase concentrations. However, these quantities are only defined when there is a liquid phase present. Thus, it will be necessary to require that there always be a certain minimum amount of water present, chosen small enough not to significantly affect the calculation of the composition of the other phases.

Method of Solution

To determine the equilibrium, the system of nonlinear equations (2) must be solved numerically. In solving this system, the solution for the case without surface tension, determined by the program EQUIL, will be used as a starting value. Thus, the problem is to construct the solution for the case with the Kelvin effect from the solution for the case without the Kelvin effect. This is done using the homotopy method of Keller (1978, 1982). For details of solving the case without the Kelvin effect, see "Atmospheric Equilibrium Model of Sulfate, Nitrate and Ammonium Aerosols, Program Users Manual."

A. Homotopy Method

The homotopy method can be described as follows. Let σ be the physically observed surface tension, and let σ^* be the value used in the calculation. Let $\sigma^* = \sigma\lambda$ where λ is a parameter. Then, the system of equations (2) can be rewritten as $\underset{\sim}{f}(\underset{\sim}{\xi},\lambda) = \underset{\sim}{0}$ where $\underset{\sim}{\xi}$ is the vector of extents of reaction. Now, the problem is to find the solution of $\underset{\sim}{f}(\underset{\sim}{\xi},1) = \underset{\sim}{0}$ based on the solution of $\underset{\sim}{f}(\underset{\sim}{\xi},0) = \underset{\sim}{0}$

An obvious way to attack this problem is by a straightforward application of Newton's method. Let $\underset{\sim}{\xi}_i$ be the value of $\underset{\sim}{\xi}$ at the end of the i-th iteration. Then, let the starting point $\underset{\sim}{\xi}_0$ be the solution of $\underset{\sim}{f}(\underset{\sim}{\xi},0) = \underset{\sim}{0}$, and

$$\underset{\sim}{\xi}_{i+1} = \underset{\sim}{\xi}_i - \left(\underset{\sim}{f}_{\underset{\sim}{\xi}}\right)^{-1}_{\underset{\sim}{\xi}_i} \underset{\sim}{f}(\underset{\sim}{\xi}_i,1) \tag{6}$$

where $\underset{\sim}{f}_{\underset{\sim}{\xi}} = (\partial \underset{\sim}{f}/\partial \underset{\sim}{\xi})$. The problem with this scheme is that it will only converge to the desired solution if $\underset{\sim}{\xi}_0$ is sufficiently close to the final value.

This problem can be overcome as follows. First, note that the larger the surface tension is, the larger the effect on the composition is likely to be. This means that the iteration given by (6) is less likely to converge. To avoid this problem, instead of trying to go from $\lambda = 0$ to $\lambda = 1$ in one step, do it in several steps. That is, replace (6) by

$$\underset{\sim}{\xi}_{i+1} = \underset{\sim}{\xi}_i - \left(\underset{\sim}{f}_{\underset{\sim}{\xi}}\right)^{-1}_{\underset{\sim}{\xi}_i} \underset{\sim}{f}(\underset{\sim}{\xi}_i,\lambda_a) \tag{7}$$

where λ_a is between zero and one. Then, starting from $\lambda = 0$, iterate to find the solution at λ_a. Then, using the solution at λ_a as a starting value, iterate to find the solution at λ_b and so forth until $\lambda = 1$ is reached.

The preceding method is a powerful way to determine the equilibrium of the system for most cases. However, there are cases where the above method will break down. A simple example of this is as follows. Consider a system containing only sulfate, ammonium and water. For simplicity, assume that there is enough ammonia present so that the concentrations of

all ions other than SO_4^{2-} and NH_4^+ are negligible. Then, only two equilibria are important

$$H_2O(g) \rightleftarrows H_2O(\ell)$$

and

$$(NH_4)_2SO_4(s) \rightleftarrows 2NH_4^+ + SO_4^{2-}$$

Using (4), the expression for the equilibrium of the first reaction is

$$\mu^\circ_{H_2O(\ell)} + RT\ \ell n\ a_{w_\infty} + \frac{4\sigma\lambda\bar{v}_w}{\bar{d}_\ell} = \mu^\circ_{H_2O(g)} + RT\ \ell n\ p_w/p^\circ \qquad (8)$$

where a_{w_∞} is the water activity without the Kelvin effect. Using the definition of relative humidity, $RH/100 = p_w/p_w^{sat}$ where $p_w^{sat} = p^\circ \exp((\mu^\circ_{H_2O(g)} - \mu^\circ_{H_2O(\ell)})/RT)$ is the saturation vapor pressure of water, (8) becomes

$$\ell n\ a_{w_\infty} = \ell n\ \frac{RH}{100} - \frac{4\sigma\lambda\bar{v}_w}{\bar{d}_\ell\ RT} \qquad (9)$$

Thus, it follows that an increase in λ is equivalent to a decrease in relative humidity. Now consider the case where the relative humidity is exactly equal to the relative humidity of deliquescence. Then, any increase in λ, being equivalent to a decrease in relative humidity will cause the liquid phase to disappear completely. That is, an infinitesimal change in λ will cause a large change in $\underset{\sim}{\xi}$. Thus, $\underset{\sim}{f}(\underset{\sim}{\xi},\lambda)$ is discontinuous at this point, and the iteration scheme given by (7) will fail.

Note that this breakdown occurs because the step size is defined in terms of λ alone. That is, the step is defined to be over when λ has changed by a given amount, irregardless of the change in $\underset{\sim}{\xi}$. Clearly, it

would be better to define the step in terms of some combination of the changes in λ and $\underset{\sim}{\xi}$. Then, in the preceding example, the difficulties could be overcome by only letting $\underset{\sim}{\xi}$ change by a small amount. This is the idea behind the pseudo-arclength continuation method of Keller (1978, 1982).

This method is as follows. Start with the basic equation

$$\underset{\sim}{f}(\underset{\sim}{\xi},\lambda) = \underset{\sim}{0} \tag{10}$$

Let $\underset{\sim}{\xi} = \underset{\sim}{\xi}(s)$ and $\lambda = \lambda(s)$ where s is a new parameter. Differentiate (10) with respect to s

$$\underset{\sim}{f}_{\underset{\sim}{\xi}} \frac{d\underset{\sim}{\xi}}{ds} + \underset{\sim}{f}_{\lambda} \frac{d\lambda}{ds} = \underset{\sim}{0} \tag{11}$$

where $\underset{\sim}{f}_{\lambda} = (\partial \underset{\sim}{f}/\partial\lambda)$. Thus

$$\frac{d\underset{\sim}{\xi}}{ds} = - \underset{\sim}{f}_{\underset{\sim}{\xi}}^{-1} \underset{\sim}{f}_{\lambda} \frac{d\lambda}{ds} \tag{12}$$

In addition, we will require

$$\|d\lambda/ds\|^2 + \|d\underset{\sim}{\xi}/ds\|^2 = 1 \tag{13}$$

Thus

$$\frac{d\lambda}{ds} = \frac{\pm 1}{[1+\|\underset{\sim}{f}_{\underset{\sim}{\xi}}^{-1}\underset{\sim}{f}_{\lambda}\|^2]^{\frac{1}{2}}} \tag{14}$$

Either choice of sign in (14) satisfies (13), the proper choice will be discussed later.

The physical interpretation of the above parameterization is as follows. Let $\underset{\sim}{x} = (\underset{\sim}{\xi}^T, \lambda)^T$ the vector of unknown quantities. Now, one way to proceed is by solving the set of differential equations (12), (14). If this were done, s would be the distance the curve $\underset{\sim}{x}(s)$ travels through $\underset{\sim}{x}$ space.

While it is possible to solve the system (12), (14) there is a method which avoids the necessity of solving a set of differential equations. Let α be the step size. Then the method is defined by (10) in conjunction with

$$\left(\frac{d\underset{\sim}{x}}{ds}\right)^T_{\underset{\sim}{x}_o} (\underset{\sim}{x}-\underset{\sim}{x}_o) = \alpha \tag{15}$$

where $\underset{\sim}{x}_o$ is the value of $\underset{\sim}{x}$ at the start of the step. Note that as α approaches zero, the lefthand side of (15) approaches the arclength along the curve $\underset{\sim}{x}(s)$. Thus, by solving (10) and (15), a method is obtained which has the advantages of arclength continuation without having to solve a differential equation.

The system (10), (15) is solved as follows. To start, let

$$\underset{\sim}{x}_1 = \underset{\sim}{x}_o + \alpha \left(\frac{d\underset{\sim}{x}}{ds}\right)_{\underset{\sim}{x}_o} \tag{16}$$

The iteration is continued by

$$\underset{\sim}{\xi}_{i+1} = \underset{\sim}{\xi}_i + \delta\underset{\sim}{\xi}_i \tag{17}$$

$$\lambda_{i+1} = \lambda_i + \delta\lambda_i \tag{18}$$

where $\delta\underset{\sim}{\xi}_i$ and $\delta\lambda_i$ are found by solving

$$(\underset{\sim}{f}_{\underset{\sim}{\xi}})_i \; \delta\underset{\sim}{\xi}_i + (\underset{\sim}{f}_{\lambda})_i \; \delta\lambda_i = - \underset{\sim}{f}(\underset{\sim}{\xi}_i, \lambda_i) \tag{19}$$

$$\left(\frac{d\underset{\sim}{\xi}}{ds}\right)_{\underset{\sim}{x}_o} \delta\underset{\sim}{\xi}_i + \left(\frac{d\lambda}{ds}\right)_{\underset{\sim}{x}_o} \delta\lambda_i = \alpha - \left(\frac{d\underset{\sim}{x}}{ds}\right)_{\underset{\sim}{x}_o} (\underset{\sim}{x}_i - \underset{\sim}{x}_o) \tag{20}$$

The sign in (14) is chosen so that

$$\left(\frac{d\underset{\sim}{x}}{ds}\right)^T_{\underset{\sim}{x}_o} \left(\frac{d\underset{\sim}{x}}{ds}\right) > 0 \tag{21}$$

which means that $\frac{d\underset{\sim}{x}}{ds}$ points in the same direction as $(d\underset{\sim}{x}/ds)_{\underset{\sim}{x}_o}$.

Note that if in (14), $\| \underset{\sim}{f}^{-1}_{\underset{\sim}{\xi}} \underset{\sim}{f}_{\lambda} \| \ll 1$, the iteration scheme given by (16)-(21) reduces to that given by (7).

B. Application to the Equilibrium Problem

In the preceding section, a method of solving the system of equations (2) is described. However, as mentioned before, it is necessary to check to make sure that the right equations are included in the system (2). This is done as follows. At the end of each step, a check is made to see that (3) is still satisfied for the species having $n_i^{\ell} = 0$. If there is a species having $n_i^{\ell} = 0$, but not satisfying (3), i.e. g_i^{ℓ} changed sign during the last step, the concentration of that species is allowed to become positive. This is done by including the corresponding reaction in (2).

In addition to the above check, each n_i^{ℓ} is checked to make sure it is non-negative. If it is negative, the following procedure is used. First, Gaussian elimination is performed on the matrix of stoichiometric

coefficients until there is only one reaction involving n_i^ℓ. Then, the equilibrium relation for this reaction is replaced by the equation $n_i^\ell = 0$.

Note that the system (10), (15) will, in general, only be solvable by the iteration method (16)-(21) if the initial guess is sufficiently close to the solution. This means that for convergence

$$\|\underset{\sim}{f}(\underset{\sim}{\xi}_0,\lambda_0)\| \leq \varepsilon \tag{22}$$

for some value of ε. However, when the system has been altered by one of the above procedures, the new system may not be near equality. Thus, (22) may not be satisfied. This can be overcome by replacing $\underset{\sim}{f}$ with

$$\hat{\underset{\sim}{f}}(\underset{\sim}{\xi},\lambda) = \underset{\sim}{f}(\underset{\sim}{\xi},\lambda) - \frac{(\lambda-1)}{(\lambda_0-1)}\,\underset{\sim}{f}(\underset{\sim}{\xi}_0,\lambda_0) \tag{23}$$

Note that $\underset{\sim}{\xi}_0$, λ_0 is a solution of $\hat{\underset{\sim}{f}}(\underset{\sim}{\xi},\lambda) = 0$. Thus, this transformation will smooth out any discontinuities in $\underset{\sim}{f}$.

C. Choice of Step Size

A key element in the preceding calculation is the choice of step size, α. This is chosen as follows. First of all a tentative value of α is chosen based on the results of the last step. Then $\underset{\sim}{x}_1$ is computed using (16), and the corresponding values of n_i^ℓ are determined. If n_i^ℓ is non-positive for some gas or liquid phase component, the value of α used was too large. Then, the value of α must be adjusted as follows. First, find α_M, the largest value of α such that n_i^ℓ is non-negative for all liquid and gas phase species. Then, restart the calculation from the previous value of $\underset{\sim}{x}_0$ using $\alpha = 0.9\,\alpha_M$

If all the n_i^{ℓ} are positive for gaseous and liquid phase species the calculation proceeds as follows. Calculate $\underset{\sim}{x}_2$ using (17)-(20). Then, find

$$R = \|\underset{\sim}{f}(\underset{\sim}{\xi}_2,\lambda_2)\| / \|\underset{\sim}{f}(\underset{\sim}{\xi}_1,\lambda_1)\| \tag{24}$$

If R is greater than or equal to one, the calculation is diverging, halve α and start over from $\underset{\sim}{x}_0$. Similarly, if at some point after $\underset{\sim}{x}_2$ is calculated, n_i^{ℓ} is non-positive for a liquid or gas phase species, halve α and start over from $\underset{\sim}{x}_0$.

If R is less than one, iterate to convergence. Then, the value of α for the next step is determined as follows. First, note that this method is quadratically convergent. Thus, for small α, $\|\underset{\sim}{f}(\underset{\sim}{\xi}_1,\lambda_1)\|$ and $\|\underset{\sim}{f}(\underset{\sim}{\xi}_2,\lambda_2)\|$ are proportional to α^2 and α^4, respectively. Thus, R is proportional to α^2. The idea is to make R for the next step equal to some desired value , say 0.2. To do this, let

$$\alpha_N = \alpha\left(\frac{\varepsilon}{R}\right)^{\frac{1}{2}}$$

where α_N is the value of α for the next step. However, there will be limits placed on how much α can change between steps. Specifically, the initial value used for the next step, $\tilde{\alpha}$ is given by

$$\tilde{\alpha} = \begin{cases} \frac{\alpha}{2} & \alpha_N < \frac{\alpha}{2} \\ \alpha_N & \frac{\alpha}{2} \leq \alpha_N \leq 2\alpha \\ 2\alpha & 2\alpha < \alpha_N \end{cases}$$

Alternate Use of the Homotopy Method

The parameter λ can be used to change other quantities besides surface tension. For example, let $[HNO_3]$, $[NH_3]$ and $[H_2SO_4]$ denote the total amounts of nitrate, ammonia, and sulfate, respectively in the system. Then, the effect on the equilibrium compositions of a change in total mass present and in the relative humidity can be determined by letting

$$[HNO_3] = [HNO_3]_o + \lambda \Delta[HNO_3]$$

$$[NH_3] = [NH_3]_o + \lambda \Delta[NH_3]$$

$$[H_2SO_4] = [H_2SO_4]_o + \lambda \Delta[H_2SO_4]$$

$$RH = RH_o + \lambda \Delta RH$$

where the subscript o denotes the initial value, and Δ denotes a change. This will probably be the best way of using the program inside a larger regional model.

Program Use

The program is called as follows:

```
CALL KEQUIL(W, RAT, CONCS, RHS, D, CONC, RH, T, IFLAG)
```

where W, RAT, CONCS, RHS, D, RH, T, AND IFLAG are inputs, and CONC is the output. The various input and output variables are defined in Table 1.

Other Requirements

When compiling the file KEQUIL.FOR, the user's default directory must contain the file NS.PAR containing the single FORTRAN statement

```
PARAMETER (NS=XX)
```

where XX is the number of sections to be used. Note that this means KEQUIL.FOR must be recompiled whenever NS is changed.

Sample Calculation

Consider the following sample problem.

T = 25°C

RH = 90%

$[NH_3]$ = 20 μg/m^3

$[HNO_3]$ = 20 μg/m^3

$[H_2SO_4]$ = 30 μg/m^3

sulfate distribution

$$\frac{dS}{d\ell nd} = \frac{2[H_2SO_4]}{\sqrt{3\pi}} \exp\left(-\frac{4}{3}\left(\ell n \frac{d}{0.3}\right)^2\right)$$

sectional boundaries

5 sections, d_o = 0.01 μm $(d_\ell/d_{\ell-1})$ = $(300)^{0.2}$

The program to solve this problem is as follows

```
      IMPLICIT DOUBLE PRECISION(A-H,O-Z)
      INCLUDE 'NS.PAR'
C        NS.PAR IS A FILE WHICH DEFINES THE VALUE OF NS - THE NUMBER
C        OF SECTIONS IN THE CALCULATION
      DIMENSION CONC(14*NS),CONCS(14*NS),W(3),RAT(NS),D(NS+1)
      DATA W/2*20.DO,30.DO/,DZ/0.3DO/
      DATA RH/.9DO/,T/298.15DO/,IFLAG/1/
      FN(X)=0.500*ERF(SIG*LOG(X/DZ))
C        INITIALIZE THE VARIOUS VARIABLES USED IN THE CALCULATION
      SIG=2.DO/SORT(3.DO)
      D(1)=1.D-2
      FCT=300.DO**(1.DO/NS)
      DO 10 I=1,NS
      D(I+1)=FCT*D(I)
10    RAT(I)= FN(D(I+1))-FN(D(I))
C        CALL THE EQUILIBRIUM ROUTINE
      CALL KEQUIL(W,RAT,CONCS,RHS,D,CONC,RH,T,IFLAG)
C        OUTPUT THE RESULTS
      WRITE(96,900)
900   FORMAT(58X,'Test case'//T44,'Concentrations ( 1.d-6 g/m**3 ',
     A          ' of air )',/' section',T13,'H+',T20,'NH4+',T27,'HSO4-',
     B          T35,'SO4-2',T44,'NO3-',T49,'(NH4)3H(SO4)2',T64,
     C          '(NH4)2SO4',T74,'NH4NO3',2(' (NH4)2SO4'),1X,'H2O(l)',
     D          1X,'NH3(g)',1X,'HNO3(g)'/T58,'NH4HSO4',T81,'*3NH4NO3',
     E          2X,'*2NH4NO3'/1X,(125('-')))
```

```
      WRITE(96,901) (LL,(CONC(14*(LL-1)+II),II=1,14),LL=1,NS)
901   FORMAT((I4,4X,14F8.4))
      STOP
      END
```

A sample output from this program is given in Table 2.

Table 1. Subroutine Arguments

Input variables

Name	Type	Description
W	Double Precision array W(3)	Total mass concentrations of the various constituents $\mu g/m^3$ W(1) total NH_3 W(2) total HNO_3 W(3) total H_2SO_4
RAT	Double Precision array RAT(NS[1])	Relative amount of sulfate in each section[2]
CONCS	Double Precision array CONCS(14 NS)	Starting value for iteration for IFLAG=2
RHS	Double Precision scalar	Relative humidity for the last step for IFLAG=2
D	Double Precision array D(NS+1)	Sectional boundaries i.e. d_ℓ, μm
RH	Double Precision scalar	Relative humidity fraction $0 < RH < 1$
T	Double Precision scalar	Temperature K
IFLAG	Integer Scalar	Flag IFLAG=1 - no starting data is available IFLAG=2 The results from a previous calculation are to be used as the starting value for this run. Requires CONCS and RHS, the values of the output variable and the relative humidity respectively at the last step.
	Output Variable	
CONC	Double Precision Array CONC(14 NS)	Mass concentrations of the species at equilibrium $\mu g/m^3$. CONC(14(L-1)+I) is the concentration of species I in section L

Table 1. Subroutine Arguments (continued)

Output Variable

Name	Type		Description
CONC (continued)	Double Precision Array CONC(14 NS) (continued)	I	species
		1	H^+
		2	NH_4^+
		3	HSO_4^-
		4	SO_4^{2-}
		5	NO_3^-
		6	$(NH_4)_3H(SO_4)_2(s)$
		7	$NH_4HSO_4(s)$
		8	$(NH_4)_2SO_4(s)$
		9	$NH_4NO_3(s)$
		10	$(NH_4)_2SO_4 \cdot 3NH_4NO_3(s)$
		11	$(NH_4)_2SO_4 \cdot 2NH_4NO_3(s)$
		12	$H_2O(\ell)$
		13	$NH_3(g)$[3]
		14	$HNO_3(g)$[3]

Notes

[1]NS is the number of sections used.

[2]The amount of sulfate in each section is automatically normalized to give the proper total.

[3]The gas phase concentrations appear only in the last two elements of CONC.

Table 2. Output from the Sample Calculation

Test case

section	Concentrations (1.d-6 g/m**3 of air) H+	NH4+	HSO4-	SO4-2	NO3-	(NH4)3H(SO4)2 NH4HSO4	(NH4)2SO4	NH4NO3	(NH4)2SO4 *3NH4NO3	(NH4)2SO4 *2NH4NO3	H2O(l)	NH3(g)	HNO3(g)
1	0.0000	0.0001	0.0000	0.0003	0.0000	0.0000	0.0000	0.0041	0.0000	0.0000	0.0000	0.0005	0.0000	0.0000
2	0.0000	0.4318	0.0133	0.9752	0.2180	0.0000	0.0000	0.0000	0.0000	0.0000	0.0000	2.6203	0.0000	0.0000
3	0.0003	7.3814	0.1442	13.9629	7.2717	0.0000	0.0000	0.0000	0.0000	0.0000	0.0000	61.5252	0.0000	0.0000
4	0.0003	8.0510	0.1234	13.3191	10.4198	0.0000	0.0000	0.0000	0.0000	0.0000	0.0000	78.1008	0.0000	0.0000
5	0.0000	0.5409	0.0075	0.8393	0.7721	0.0000	0.0000	0.0000	0.0000	0.0000	0.0000	5.5620	4.5107	1.0147

References

Keller H.B. (1982) Practical procedures in path following near limit points. in Computing Methods in Applied Science and Engineering, V (Edited by R. Glowinski and J. L. Lions.) North-Holland, Amsterdam.

Keller H.B. (1978) Global homotopies and Newton methods in Recent Advances in Numerical Analysis (Edited by C. Deboor and G. H. Golub.) Academic Press, New York.